Probabilistic Accident Consequence Uncertainty Analysis

A Joint Report Prepared by U.S. Nuclear Regulatory Commission and Commission of European Communities

Dispersion and Deposition Uncertainty Assessment

Volume 2 Appendices A and B

A/2

AVAILABILITY NOTICE

Availability of Reference Materials Cited in NRC Publications

Most documents cited in NRC publications will be available from one of the following sources:

1. The NRC Public Document Room, 2120 L Street, NW., Lower Level, Washington, DC 20555-0001

2. The Superintendent of Documents, U.S. Government Printing Office, P O Box 37082, Washington, DC 20402-9328

3. The National Technical Information Service, Springfield, VA 22161-0002

Although the listing that follows represents the majority of documents cited in NRC publications, it is not intended to be exhaustive.

Referenced documents available for inspection and copying for a fee from the NRC Public Document Room include NRC correspondence and internal NRC memoranda; NRC bulletins, circulars, information notices, inspection and investigation notices; licensee event reports; vendor reports and correspondence; Commission papers; and applicant and licensee documents and correspondence.

The following documents in the NUREG series are available for purchase from the Government Printing Office: formal NRC staff and contractor reports, NRC-sponsored conference proceedings, international agreement reports, grantee reports, and NRC booklets and brochures. Also available are regulatory guides, NRC regulations in the *Code of Federal Regulations*, and *Nuclear Regulatory Commission Issuances*.

Documents available from the National Technical Information Service include NUREG-series reports and technical reports prepared by other Federal agencies and reports prepared by the Atomic Energy Commission, forerunner agency to the Nuclear Regulatory Commission.

Documents available from public and special technical libraries include all open literature items, such as books, journal articles, and transactions. *Federal Register* notices, Federal and State legislation, and congressional reports can usually be obtained from these libraries.

Documents such as theses, dissertations, foreign reports and translations, and non-NRC conference proceedings are available for purchase from the organization sponsoring the publication cited.

Single copies of NRC draft reports are available free, to the extent of supply, upon written request to the Office of Administration, Printing and Mail Services Section, U.S. Nuclear Regulatory Commission, Washington, DC 20555-0001.

Copies of industry codes and standards used in a substantive manner in the NRC regulatory process are maintained at the NRC Library, Two White Flint North, 11545 Rockville Pike, Rockville, MD 20852-2738, for use by the public. Codes and standards are usually copyrighted and may be purchased from the originating organization or, if they are American National Standards, from the American National Standards Institute, 1430 Broadway, New York, NY 10018-3308.

DISCLAIMER NOTICE

This report was prepared as an account of work sponsored by an agency of the United States Government. Neither the United States Government nor any agency thereof, nor any of their employees, makes any warranty, expressed or implied, or assumes any legal liability or responsibility for any third party's use, or the results of such use, of any information, apparatus, product, or process disclosed in this report, or represents that its use by such third party would not infringe privately owned rights.

NUREG/CR-6244
EUR 15855EN
SAND94-1453
Vol. 2

Probabilistic Accident Consequence Uncertainty Analysis

Dispersion and Deposition Uncertainty Assessment

Appendices A and B

Manuscript Completed: November 1994
Date Published: January 1995

Prepared by
F. T. Harper
Sandia National Laboratories, USA

S. C. Hora
University of Hawaii at Hilo, USA

M. L. Young
Sandia National Laboratories, USA

L. A. Miller
Sandia National Laboratories, USA

C. H. Lui
U.S. Nuclear Regulatory Commission, USA

M. D. McKay
Los Alamos National Laboratory, USA

J. C. Helton
Arizona State University, USA

L. H. J. Goossens
Delft University of Technology
The Netherlands

R. M. Cooke
Delft University of Technology
The Netherlands

J. Pasler-Sauer
Research Center, Karlsruhe
Germany

B. Kraan
Delft University of Technology
The Netherlands

J. A. Jones
National Radiological Protection Board
United Kingdom

Prepared for

Division of Systems Technology
Office of Nuclear Regulatory Research
U.S. Nuclear Regulatory Commission
Washington, DC 20555-0001
NRC Job Code L2294

Commission of the European Communities
DG XII and XI
200, rue de la Loi
B-1049 Brussels
CEC Contract Numbers F13P-Ct92-0023 and 93-ET-001

Publication no. EUR 15855 EN of the
Commission of the European Communities,
Dissemination of Scientific and Technical Knowledge Unit,
Directorate-General Telecommunications, Information Market and
Exploitation of Research
Luxembourg

c ESCE-EEC-EAEC, Brussels-Luxembourg, 1994

LEGAL NOTICE

Neither the Commission of the European Communities nor any person acting on behalf of the Commission is responsible for the use which might be made of the following information.

Abstract

The development of two new probabilistic accident consequence codes, MACCS and COSYMA, was completed in 1990. These codes estimate the risks presented by nuclear installations based on postulated frequencies and magnitudes of potential accidents. In 1991, the US Nuclear Regulatory Commission (NRC) and the Commission of the European Communities (CEC) began a joint uncertainty analysis of the two codes. The ultimate objective of the joint effort was to develop credible and traceable uncertainty distributions for the input variables of the codes. As a first step, a feasibility study was conducted to determine the efficacy of evaluating a limited phenomenological area of consequence calculations (atmospheric dispersion and deposition parameters) and to determine whether the technology exists to develop credible uncertainty distributions on the input variables for the codes. Expert elicitation was identified as the best technology available for developing a library of uncertainty distributions for the selected consequence parameters.

The study was formulated jointly and was limited to the current code models and to physical quantities that could be measured in experiments. The elicitation procedure was devised from previous US and EC studies with refinements based on recent experience. Elicitation questions were developed, tested, and clarified. Sixteen internationally recognized experts from nine countries were selected using a common set of selection criteria. Probability training exercises were conducted to establish ground rules and set the initial boundary conditions. Experts developed their distributions independently. Results were processed with an equal weighting aggregation method, and the aggregated distributions were processed into code input variables. To validate the distributions generated for the wet deposition input variables, samples were taken from these distributions and propagated through the wet deposition code model. Resulting distributions closely replicated the aggregated elicited wet deposition distributions. To validate the distributions generated for the dispersion code input variables, samples were taken from the distributions and propagated through the Gaussian plume model (GPM) implemented in the MACCS and COSYMA codes. Resulting distributions were found to well replicate aggregated elicited dispersion distributions consistent with the GPM assumptions.

Valuable information was obtained from the elicitation exercise. Project teams from the NRC and CEC cooperated successfully to develop and implement a unified process for the elaboration of uncertainty distributions on consequence code input parameters. Formal expert judgment elicitation proved valuable for synthesizing the best available information. Distributions on measurable atmospheric dispersion and deposition parameters were successfully elicited from experts involved in the many phenomenological areas of consequence analysis.

Contents

Contents v

Preface vii

Acknowledgments ix

Appendix A.1 Expert Rationales, Unprocessed Deposition Data A-1
- Expert A A-1
- Expert B A-37
- Expert C A-61
- Expert D A-81
- Expert E A-95
- Expert F A-109
- Expert G A-137
- Expert H A-155

Appendix A.2 Expert Rationales, Unprocessed Dispersion Data A-169
- Expert I A-169
- Expert J A-183
- Expert K A-197
- Expert L A-215
- Expert M A-225
- Expert N A-237
- Expert O A-251
- Expert P A-271

Appendix B Short Biographies of Dispersion and Deposition Experts B-1

Preface

This volume is the second of a three-volume document that summarizes a joint project conducted by the US Nuclear Regulatory Commission and the Commission of European Communities to assess uncertainties in the MACCS and COSYMA probabilistic accident consequence codes. These codes were developed primarily for making estimates of the risks presented by nuclear reactors based on postulated frequencies and magnitudes of potential accidents. This three-volume document reports on an ongoing project intended to assess uncertainty in the MACCS and COSYMA offsite radiological consequence calculations for hypothetical nuclear power plant accidents. A panel of 16 experts was formed to compile credible and traceable uncertainty distributions for the dispersion and deposition code input variables that affect offsite radiological consequence calculations. The expert judgment elicitation procedure and its outcomes are described in these volumes.

Volume II contains two appendices. Appendix A contains (1) the rationales for the dispersion and deposition data provided by the 16 experts who participated in the elicitation process and (2) the tabulated elicited information from the experts. Appendix B contains short biographies of the 16 experts.

Volume I of this document includes a complete description of the joint consequence uncertainty study. Volume III contains six appendices that describe in greater detail the specific methodologies used by the atmospheric dispersion and deposition panels.

Acknowledgments

The authors would like to acknowledge all the participants in the expert judgment elicitation process, in particular the dispersion and deposition expert panels. While we wrote and edited the report, organized the process, and processed the results, the experts provided the technical content that is the foundation of this report. Dr. Detlof von Winterfeldt is acknowledged for his contribution as elicitor in several expert sessions.

The authors would also like to express their thanks for the support and fruitful remarks from Dr. G. N. Kelly (CEC/DG XII), Dr. R. Serro (CEC/DG XI), and Dr. J. Glynn (USNRC).

We would also like to acknowledge several institutes that facilitated the collection of unpublished experimental information used in the probabilistic training and evaluation of the dispersion and deposition experts. The authors want to thank Dr. T. Mikkelsen and coworkers at Riso and the Danish Center for Atmospheric Research, Denmark; Dr. R. Brown at British Gas, UK; Dr. B. Jolliffe at NPL Teddington, UK; Dr. G. Deville-Cavelin at IPSN/Cadarache, France; Dr. P. Berne at IPSN/Grenoble, France; Dr. Y. Belot at IPSN/Fontenay-aux-Roses, France; Dr. J. Duyzer at TNO/Delft, The Netherlands; and Dr. J. Slanina at ECN/Petten, The Netherlands.

The authors also greatly appreciate the technical assistance of Ms. Ina Bos of Delft University of Technology, The Netherlands; the support of Ms. Darla Tyree and Ms. Judy Jones of Sandia National Laboratories, USA.; and the extensive assistance and guidance provided by Tim Peterson of Tech Reps, Inc., in the preparation of this report.

This report is written under the following contracts:

Contract No. L2294, United States Nuclear Regulatory Commission, Office of Nuclear Regulatory Research, Division of Safety Issue Resolution.

Contract No. F13P-Ct92-0023, Commission of European Communities, Directorate-General for Science, Research and Development, XII Radiation Research.

Contract No. 93-ET-001, Commission of European Communities, Directorate-General of Environment, Nuclear Safety and Civil Protection, XI-A-1 Radiation Protection.

APPENDIX A

Experts' Rationales

Unprocessed Data

A.1 Expert Rationales, Unprocessed Deposition Data

The Case Structures for the deposition expert panel are presented in Volume III Appendix F of this document.

Expert A

Introduction

The deposition velocity is the mass transfer boundary condition at the air-surface interface in atmospheric diffusion and transport models. The dry deposition velocity idea is assumed applicable to describe rates of gas and particle removal to all surfaces, rough or smooth, and vertical or horizontal. Chamberlain and Chadwick[4] defined the deposition velocity as the ratio of the deposition flux divided by the airborne pollutant concentration per unit volume at some height above the deposition surface. The deposition velocity is often reported in units of either cm/s or m/s. The maximum range of reported deposition velocities is about five orders of magnitude from 10^{-5} to 1 m/s, or 10^{-3} to 10^{2} cm/s (Sehmel).[8,9,11]

Expressed here is the author's rationale for opinions of deposition velocities for large area surfaces. The NRC/CEC Program considers the dry deposition velocity, v_d, as the ratio of the rate of deposition of radioactivity to the ground [Bq/(s m^2)] to the air concentration at one meter height (Bq/m^3), and has units of m/s. The program requests opinions on the median, 0.05 quantile, and 0.95 quantile for dry deposition velocities, and the 0 and 100% bounds of the distributions.

It is emphasized that it stretches and exceeds predictive capabilities to predict accurately the median. Uncertainties to be meaningful in the 0.05 and 0.95 quantile and the 0 and 100 percent bounds also stretch and exceed predictive capabilities based on experimental results.

The agreed upon constraints for the rationale with the Sandia program manager (Fred Harper) are 1) rationale are to be based upon data known to the author, and 2) new theories or ideas are not to be developed for the rationale. Since the program is based on current knowledge, the rationale for estimates is based on prior publications by the author.

Deposition Parameters to be Addressed

The Joint NRC/CEC Consequence Uncertainty Program (program) requests opinions on elicitation questions for dry deposition velocities for general and specific surface types (the case structure and elicitation variable) and particle and gas properties.

Generic Surfaces for Elicitation Questions

Generic surface types are urban, meadow, forest and human skin. The urban surface type consists of buildings and concrete. The meadow surface type includes bare soil, freshly cut grass, pasture, and crops such as harvestable corn. The forest surface type includes any type of trees including deciduous and evergreen varieties. Human skin refers to skin that might be exposed to a passing plume. The only initial condition is the average wind speed. Wind speeds are 2 and 5 m/s at 10 m height.

For general surface types, the program requests opinions on hourly average dry deposition velocities as the airborne plume traverses across general surface types. The program requests dry deposition velocities for elemental iodine, methyl iodide, and particles in indicated diameter ranges.

Table A-1 shows the diameters of interest for estimating dry deposition velocities. A program constraint is that particle size corresponds to spherical particles of unit density (1 g/cm^3).

Table A-1. Particle diameters of interest for general surfaces

Indicated Particle Diameter (μm)	Range Assumed for Indicated Particle Diameter (μm)
0.1	0.05 to 0.2
0.3	0.2 to 0.5
1.0	0.5 to 2.0
3.0	2.0 to 5.0
10.0	5.0 to 15.0

Specific Surfaces for Elicitation Questions

Dry deposition velocities for specific surface types are under the general heading of meadow: moorland/peatland, heather and grass, and grassland. The program considers two specific surfaces.

The first surface is moorland/peatland with vegetation consisting of 40 cm high tussocks and old dry grass partly filling the spaces between the tussocks and underlain by a wet peat layer. The wind speed is 5 m/s at 5 m height. Surface roughness is 5 ± 1 cm. Particle sizes are 0.55, 0.7, 0.9, 1.2, and 1.6 μm.

The second surface is heather and green grass, with vegetation only partly covering the soil. The wind speed is 5 m/s at 5 m height. Surface roughness is 4.5 ± 1.5 cm. Particle sizes are 0.55, 0.7, 0.9, 1.2, 1.6, 2.32, 3.2, and 4.2 μm.

General Caveats for Rationale

Deposition velocities requested by the Joint USNRC/CEC Uncertainty program are not conventional values reported in the literature, but grouped values. The program requests opinions from panel members for dry deposition velocities that might apply to the generic surface types considered by the program.

The uncertainties in predicting dry deposition velocities are large. Further refinements in averaging deposition velocities for surface variations within one mile increments (in transport models used by the program) are considered a second order effect compared to uncertainties in predicting dry deposition velocities.

There is no general correlation to predict dry deposition velocities based on field measurements of dry deposition velocities. The author prefers measurements of dry deposition velocities, not dry deposition velocities inferred by application of diffusion and transport models to interpret field results. The author cautions the use of inferred dry deposition velocities that depend on the diffusion and transport model used. There is not an obvious way to apply deposition velocities inferred from one transport and diffusion model to different transport and diffusion models.

The rationale emphasizes the prediction of dry deposition velocities as a function of particle diameter (and iodine) as requested of the panel members. Rationale considers the empirical predictive model developed by Sehmel and Hodgson.[14,15] The model is based on experimental evaluation of surface mass transfer within the 1 cm above deposition surfaces in wind tunnel dry deposition experiments. Diffusion equations are used to adjust the concentration reference height from 1 cm to 1 m.

Assuming surface variation and dry deposition velocities can be calculated for an area average surface, the grouped dry deposition values, $v_{Grouped}$, are hourly averages that might be estimated by the expression

$$V_{GROUPED} = \sum_i \sum_j A_i V_{dij} / \sum_i A_i \qquad (1)$$

where

A_i = surface within area of type i

V_{dj} = dry deposition velocity of species j over deposition surface i.

An assumption is that variation caused by changes in airflow between different surfaces can be neglected.

For a surface type i, the dry deposition velocity, v_{dj}, is dependent on the particle size distribution and airborne concentrations, C_j. For an aerosol with a polydispersed particle size distribution (real aerosols), the average dry deposition velocity to surface i is

$$V_{di} = \sum K_j C_j / \sum C_j \qquad (2)$$

where K_j = dry deposition velocity for a monodispersed particle of size j

C_j = airborne concentration of particle size j.

Uncertainties in grouped dry deposition values might be comparable to uncertainties in transport and diffusion codes to predict accurately airborne concentrations. Neither describe the effects of non-uniform surfaces on dry deposition velocities and airborne concentration.

Experimental Dry Deposition Velocities

The rationale is based on field data for iodine and particle deposition, and predictions of particle deposition as a function of particle size made from an empirical model based on dry deposition velocities measured in wind tunnel experiments. Literature values from field experiments of dry deposition velocities for iodine and particles were summarized by Sehmel.[8,9,10,11] Predictions of dry deposition velocities of particles as a function of particle size are based on Sehmel.[14,15,16]

Dry Deposition Velocities for Iodine Measured in Field Experiments

Dry deposition velocities for iodine summarized by Sehmel[8,9,10,11] range from 0.02 to 26 cm/s. Figure A-1 shows dry deposition velocity data for iodine arranged according to the maximum deposition velocity reported in each field experiment.

Deposition velocities for iodine show a wide range even for the same types of deposition surface. This wide range is most evident for grass surfaces. Although a 1 cm/s deposition velocity is often assumed for gases, Figure A-1 shows that 1 cm/s may have an uncertainty range from about 10^{-2} to 10 cm/s. Evidence exists that deposition velocities for gases may also depend on atmospheric stability (Bunch; Whelpdale and Shaw).[2,18]

Dry Deposition Velocities for Methyl Iodide Measured in Field Experiments

Table A-2 lists dry deposition velocities for iodine summarized by Sehmel.[8,9,11] Deposition velocities for methyl iodide are less than one percent of that for molecular iodine. For grass surfaces, the deposition velocities range from 10^{-4} to 10^{-2} cm/s.

Dry Deposition Velocities of Particulates Measured in Field Experiments

Particle dry deposition velocities for particles and various deposition surfaces in field experiments were summarized by Sehmel.[8,9,10,11] In Figure A-2, dry deposition velocities are organized graphically as a function of particle diameter. The reference numbers refer to references given in Sehmel.[8,9] Dry deposition velocities range over five orders of magnitude, a minimum of 10^{-3} cm/s to a maximum of 180 cm/s.

Figure A-2 shows ranges of deposition velocities for each set of experimental conditions as a function of particle diameter range. The dashed lines are for field experiments with the wider particle size distributions (more polydispersed). In contrast, the solid lines are for experiments with narrower particle size distributions. The data show the following:

- the deposition velocities in any individual experiment range over several orders of magnitude
- a minimum deposition velocity is approximately 10^{-3} cm/s for particle diameters in the range of 0.1 to 1 μm diameter.

The range of experimental deposition velocities for each field experiment is presented rather than an "average" deposition velocity. Ranges emphasize the experimental uncertainties in many dry deposition field experiments and in our ability to predict accurately dry deposition velocities.

The development of generalized deposition velocity predictors based on these field experiments have been hindered in part because experimental variables were not adequately controlled or reported (i.e., often the particle size distribution was either not known or not reported). Data from these field-determined deposition velocities have limited value to develop generalized deposition velocity predictors.

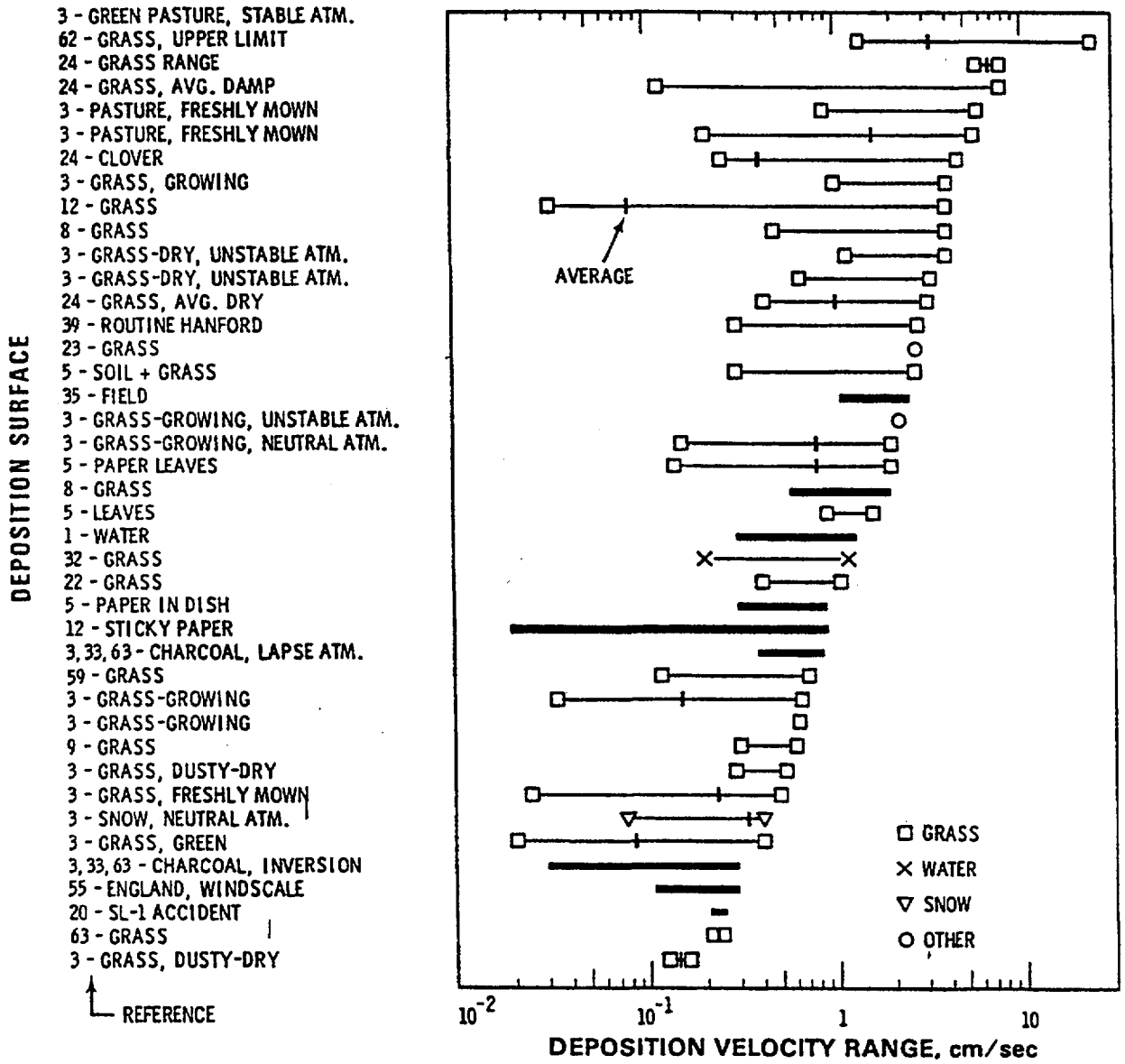

Figure A-1. Deposition velocities for iodine.

Dry Deposition Velocities Measured in Wind Tunnel Experiments

Sehmel and Hodgson's[14,15] empirical model to predict particle dry deposition velocities is based on wind tunnel measurements of dry deposition velocities for monodispersed particles (single sized particles) onto five different surfaces. Table A-3 shows the ranges of experimental conditions in these wind tunnel experiments. Particle density was 1.5 g/cm^3. All experiments were for near isothermal conditions, about 70°F (20°C).

Airborne concentrations were measured at a height of 1 cm above the deposition surface in order to define the dry deposition velocity at 1 cm height (this allows evaluation of the surface mass transfer resistance below a height of 1 cm). The deposition velocity, K, is defined as

$$K_1 = -\frac{N}{C}. \qquad (3)$$

In this case, the concentration, C, is for monodispersed particles, with concentration measured 1 cm above the deposition surface.

Table A-2. Dry deposition velocities for methyl iodide

Deposition Surface	Deposition Velocity (cm/s)	Reference
Pasture grass	1.4×10^{-4} to 2.4×10^{-3}	Atkins et al.[1]
Activated charcoal fallout plate	0.12	Bunch[2]
Mixed pasture grass	10^{-4} to 10^{-2}	Bunch[2]
Grass	0.9 per cent of that for molecular iodine	Heinemann et al.[6]
Mixed pasture grass	less than 0.05 per cent of that for molecular iodine	Zimbrick and Voilleque[19]

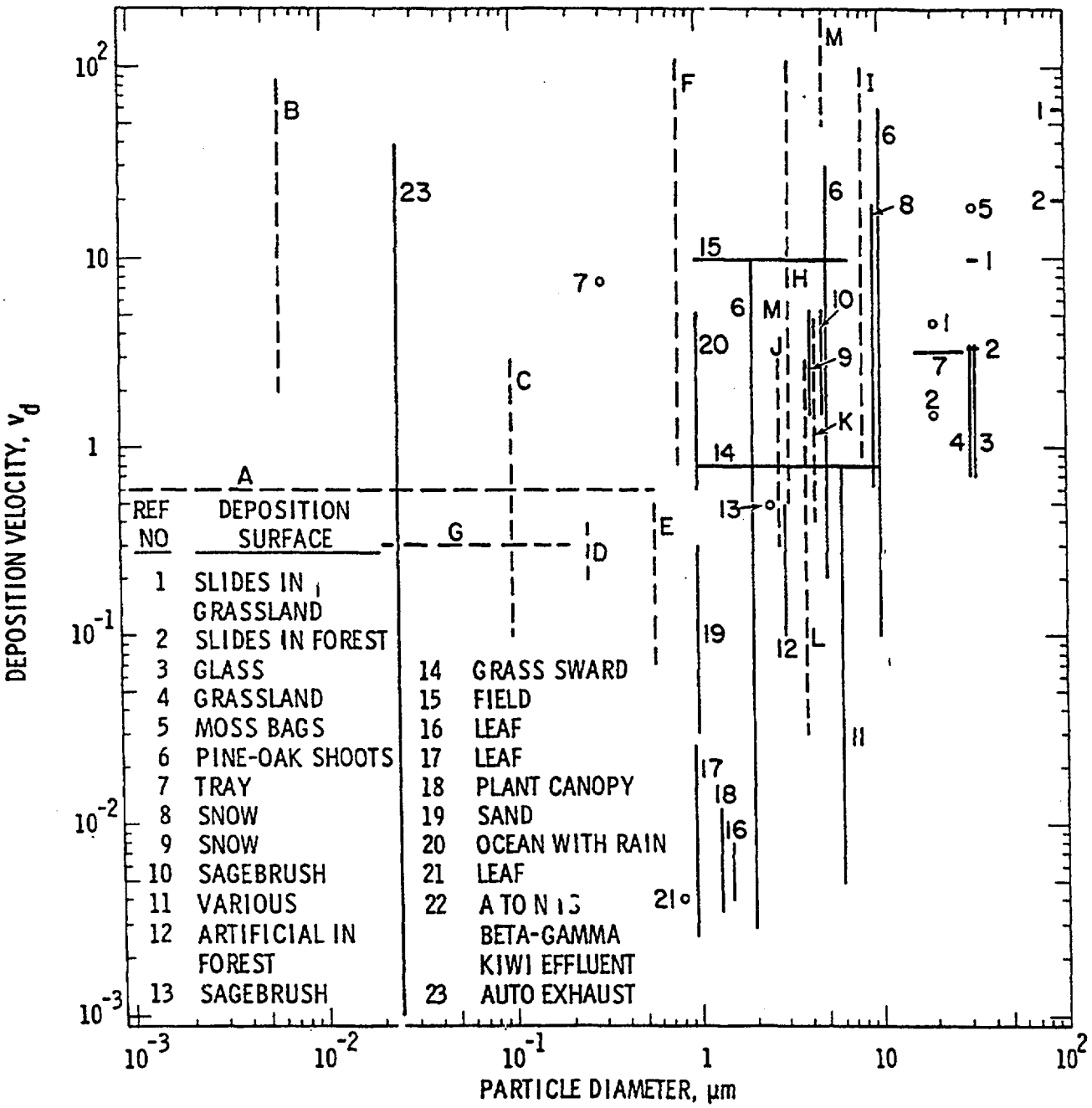

Figure A-2. Particle deposition velocities measured in the field; numbers refer to references—cited data in Sehmel and Hodgson.[15]

Deposition velocities to a small canopy were determined also in wind tunnel experiments (Sehmel and Hodgson).[13,14,15] The canopy was an artificial tree foliage vetch 9 cm high. The artificial tree foliage vetch was 23 cm by 30 cm. Trees were mounted in a rectangular array with eight downwind rows of six trees. Tree spacing was 3.8 cm. The polyethylene trees were 7 to 9 high with a maximum crown width of 4 to 6 cm. Each crown had eight branches located around the central trunk, and the tree trunk extended approximately 2 cm below the crown.

Experiments in the wind tunnel indicated nonuniform particle deposition in the tree vetch, i.e., edge effects in the transition from no trees to trees. Figure A-3 shows average deposition velocities for trees and the support plate. Depending upon particle diameter and wind speed, the front row of trees usually had either more or less deposition than downwind rows. Since particle penetration to the entire plate was significant, deposition velocities for each row could not be calculated. Deposition velocity curves show different patterns than those for the simpler surfaces. At a wind speed of 2 m/s approaching the trees, a minimum deposition velocity occurs at about 1 to 2 μm for the trees. (Wind speed was measured upwind and at a 6 cm height, which was approximately the height of the tree crown mid-plane.) In contrast, simpler surfaces exhibit minima in the particle diameter range from 0.1 to 1 μm. For a 13 m/s wind speed approaching the trees, deposition velocities are nearly constant for all particle diameters studied. Again, in contrast, deposition velocities for 2 μm compared to larger particles would be significantly less for a simpler surface.

Table A-3. Experimental range of variables in wind tunnel experiments

Deposition Surface		Range of Variables		
Type	Dimensions (cm)	Particle Diameter (μm)	Friction Velocity, u_* (cm/s)	Roughness Height, z_0 (cm)
Brass shim stock	smooth surface	0.03 to 28	11 to 73	0.004
Artificial grass	0.7 cm high	0.03 to 28	19 to 144	0.12 to 0.40
Gravel	0.5 to 1.5 diameter	0.03 to 26	22 to 133	0.13 to 0.18
Water	Wave height to 2.5 cm	0.03 to 29	11 to 122	0.001 to 0.002
Gravel	3.8 to 5.1 diameter	0.03 to 28	15 to 107	0.3 to 0.6

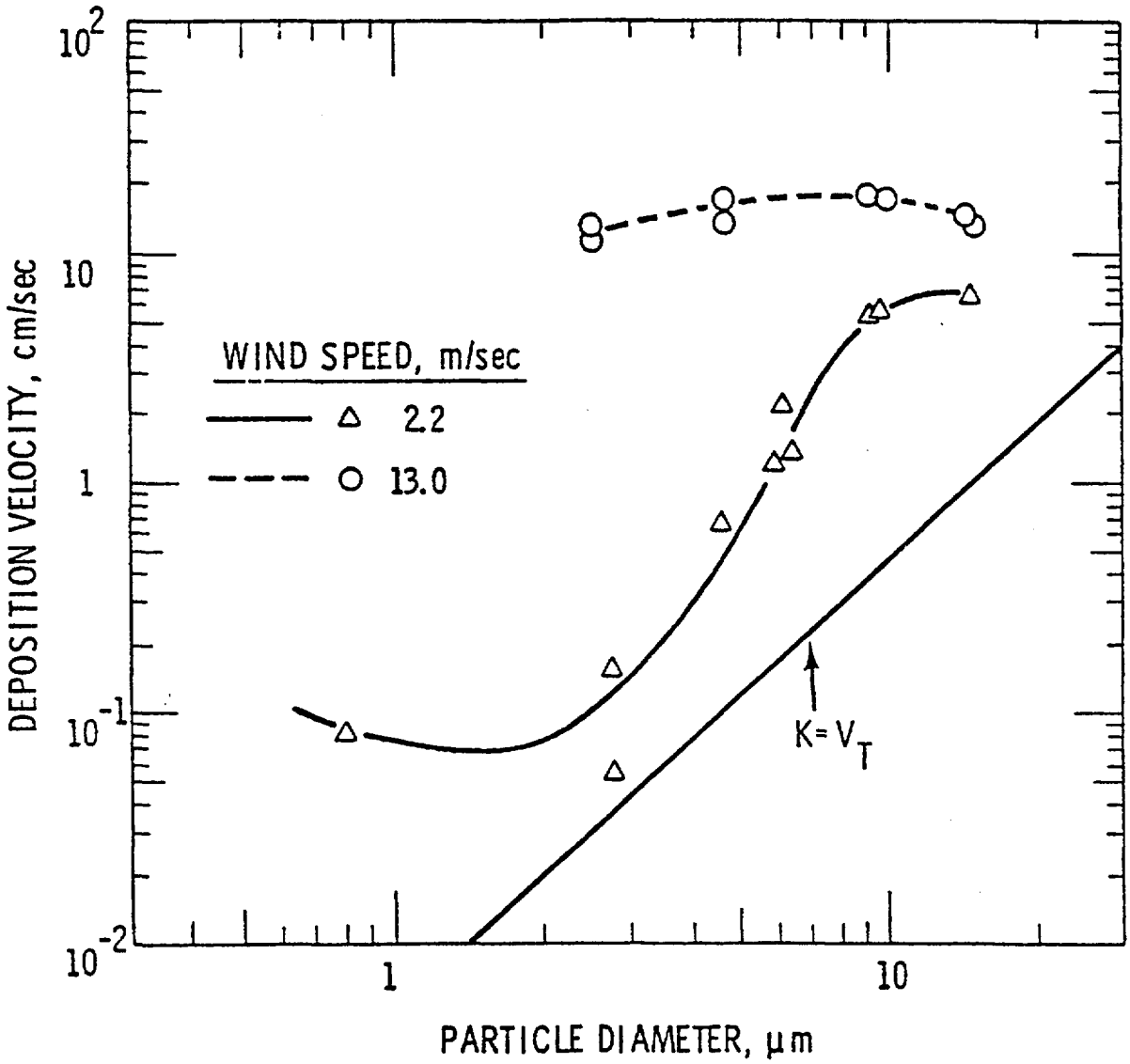

Figure A-3. Deposition velocities to a canopy of plastic trees 9 cm high.

Comparison of Field and Wind Tunnel Dry Deposition Velocities

After understanding that field deposition experiments have large uncertainties, it is encouraging that deposition velocity predictions based on wind tunnel experiments to determine particle deposition (Sehmel and Hodgson)[14,15] are in the same range as those determined in field experiments.

A field experiment (Sehmel et al.)[17] supports the validity of the deposition velocity model. The test aerosol had a mass medium diameter of about 0.7 μm, but the size distribution showed that 3 percent of the particles were greater than 4.5 μm diameter. The predicted deposition velocity of 0.17 cm/s compared favorably with the experimental measurement of 0.21 cm/s across a surface vegetated with sage brush. (The friction velocity was 24 cm/s and the roughness height was 0.4 cm.)

Description of Predictive Dry Deposition Model

Sehmel and Hodgson[13,14,15] describe an empirical model to predict deposition velocities that is used as a basis of the rationale to estimate dry deposition velocities for general and specific surfaces.

The deposition flux is described by a one-dimensional, steady-state continuity equation Basic assumptions are that particles diffuse at a constant flux from a uniform concentration of particles, that a relationship for eddy diffusivity can be determined, that the effect of gravity can be described by the terminal settling velocity, that particle agglomeration does not occur, and that particles are retained by the deposition surface.

A three-box conceptual model is used to describe the overall deposition process. In each box, particle transport is described by:

Box 1 — The atmospheric turbulent layer in which the transfer processes are best described by micrometeorological eddy diffusivity. (The model assumes that this distance is from 1 cm to 1 m above the deposition surface.)

Box 2 — A layer just above and just within the vegetative canopy or surface elements in which the transfer processes are modified by the presence or structure of the canopy or surface.

Box 3 — A layer (occupied by the canopy or surface elements) in which the final transfer process is expressed by surface mass transfer coefficients, where the interaction between the surface material and airborne particles is important. (The model assumes that this distance is within 1 cm of the deposition surface.)

A relatively large data base exists in the meteorological literature to calculate the diffusional resistance in boxes 1 and 2. The more significant unknown is the surface resistance in box 3. Surface resistance in box 3 was experimentally investigated in wind tunnel experiments (in which dry deposition velocities were evaluated. Results were correlated and predicted based on the following model.

Deposition velocity, K, predictions are based on a one-dimensional, steady-state continuity equation that describes particle deposition. The deposition flux to a surface is described by

$$N = -(\epsilon + D)\frac{dC}{dz} - V_t C \ , \qquad (4)$$

in which v_t is the absolute value of the terminal settling velocity.

The model predicts deposition velocities from a dimensionless integral form of Equation (4):

$$-\int_{C_z}^{0} \frac{U_* dC}{N + v_t C} = \int_{z_{c,z}^+}^{r^+} \frac{dz^+}{\epsilon/\nu + D/\nu} = IR \qquad (5)$$

in which ε is the particle eddy diffusivity, D is the Brownian diffusivity, ν is the kinematic viscosity of air, u_* is the friction velocity, $z^+ = zu_*/\nu$ is the dimensionless distance above the surface, and v_t is the particle terminal settling velocity. Integration limits are that particle concentration is C_z at a reference height of z cm and that particle concentration is zero at a dimensionless particle radius, r^+, from the deposition surface.

The integral involving diffusion is an integral resistance, abbreviated as *IR* in the following text (*IR* is a negative value). Since *IR* contains the dimensionless eddy diffusivity, ε/ν and Brownian diffusivity, the resistance integral quantifies only diffusional resistance between the integration limits. The integral, *IR*, can be subdivided into

$$IR = \int_{z_{cz}}^{z^+_{1-2}} \frac{dz^+}{\epsilon/\nu + D/\nu} + \int_{z^+_{1-2}}^{z^+_{2-3}} \frac{dz^+}{\epsilon/\nu + D/\nu} + IR_3 \quad (6)$$

where the first integral (in Box 1) is IR_1 and the second integral (in Box 2) is IR_2. The limit, z^+_{1-2}, is the height at which boxes 1 and 2 interface. Similarly, boxes 2 and 3 interface at z^+_{2-3}. These integrals are evaluated after a relationship between deposition velocity and integral resistance (IR) is shown.

The deposition velocity is obtained from an integrated form of Equation (4) for the deposition flux, N,

$$N = \frac{V_t C_z \alpha}{1 - \alpha} \quad (7)$$

in which

$$\alpha = \exp(-V_t \frac{IR}{U_*}) \ . \quad (8)$$

Now the deposition velocity is defined in terms of the reference concentration, C_z, at z cm height.

$$K_z = -\frac{N}{C_z} . \quad (9)$$

Thus, the deposition velocity at height z is

$$K_z = -\frac{v_t}{1 - \frac{1}{\alpha}} . \quad (10)$$

As shown by Equation (10), the lower limit of predicted deposition velocities is v_t. The reason for this lower limit is that if the diffusional resistance were large (IR is a negative number), α would approach infinity and $1/\alpha$ would approach zero. As diffusional resistance became relatively less, the deposition velocity becomes increasingly greater than the gravitational settling velocity.

From the above equation, the integral resistance (IR) is related to a simple resistance R (1/K) by,

$$R = \frac{1}{K} = \frac{1 - \exp(\frac{V_t}{U_*} IR)}{V_t} . \quad (11)$$

Surface Resistance Correlation

Surface integral resistances (IR_3) were evaluated from wind tunnel determined deposition velocities (Sehmel et al.[16]). Experimentally, deposition velocities, K_1, correspond to a box 3 integral resistance. Values of IR_3 were evaluated from the K_1's by using the expression

$$IR_3 = \frac{u_*}{v_t} \ln(1 - \frac{v_t}{K_1}) . \quad (12)$$

Subsequently, least squares techniques were used (Sehmel and Hodgson[14,15]) to determine a dimensionless correlation, except for one dimensional term, for predicting IR_3.

The correlation is based on dry deposition velocity data for nonreentrainment conditions, for five surfaces and a total of 180 experiments in the wind tunnel. The unweighted correlation for the integral mass transfer resistance, IR_3, is

$$\begin{aligned} IR_3 = -exp\{&-408.728 \\ &+[\ln(Sc)]\left[17.8583 - 0.03638\ln(\frac{d}{Z_0})\right] \\ &+[\ln(\tau^+)]\ \left[-14.336 - 0.3441\ln(\tau^+)\right. \\ &\left.+0.37444\ln(\frac{d}{Z_0}) - 0.410321\ln(\frac{D}{Z_0 u_*})\right] - 12.7830\ln d\}^* \end{aligned} \quad (13)$$

After the best data fit was obtained (a multiple correlation coefficient of 0.93 with all terms statistically significant at the 99% level), some deposition velocity predictions were made. However for particle diameters below about 5 x 10^{-2} µm, deposition velocity predictions did not increase with decreasing particle diameter. An increase should be caused by increased Brownian diffusion rates for smaller particles. The relatively few experimental data points in the minimum deposition velocity range were not sufficiently weighted (all points were equally weighted) in the data fit.

The dimensionless correlation was redetermined by a weighted least squares technique. The weight was the natural logarithm of the reciprocal of particle diameter in cm. Thus the weight of a 0.03 µm diameter particle was 2.2 times the weight of a 30 µm diameter particle.

The weighted correlation for the integral mass transfer resistance, IR_3, is

$$IR_3 = -exp\{-378.051 + 16.498\ln(Sc) + [\ln\tau^+]\left[-11.8178 - 0.28628\ln\tau^+ + 0.32262\ln(\frac{d}{Z_0}) - 0.33850\ln(\frac{D}{z_0 u_*}\right] - 12.8044\ln d\} \quad (14)$$

The multiple correlation coefficient was 0.92 and the group [lnSc][ln(d/z_o)] was omitted in order to have all coefficients statistically significant at the 99% level.

In both equations the dimensionless relaxation time, τ^+, was calculated for a particle density of 1.5 g/cm^3. Since experimental observations have not been made for other particle densities, the surface integral resistance IR_3 is assumed independent of particle density and is calculated for a particle density of 1.5 g/cm^3.

Roughness Height and Friction Velocity

To predict deposition velocities, the model requires estimates of the aerodynamic surface roughness height, z_o, and air friction velocity, u.. Aerodynamic surface roughness is about 0.15 of the vegetation and physical roughness height (Plate).[7] This simple relationship does not attempt to describe change in surface roughness that occur as wind speed changes, like a field of long grass becoming smooth during high wind speeds.

The aerodynamic surface roughness, z_o, and friction velocity, u_*, are calculated empirically from the air velocity profile above a relatively smooth ground surface by using the expression

$$u = \frac{U^*}{k}\ln\frac{z+Z_0}{Z_0} \quad (15)$$

where u is the measured velocity, z is the measured height above ground, and k is von Kármán's constant of 0.4 (Businger et al.).[3] For a surface of greater geometric roughness, the height is adjusted to a zero-displacement plane, d, within the canopy. In this case, the relationship is

$$u = \frac{U_*}{k}\ln\frac{z-d}{Z_0}. \quad (16)$$

In applying these equations to experimental velocity data as a function of height, the quantities d and z_o are adjusted until straight lines are obtained on semi-log paper. Thus, these d and z_o values have no physical meaning other than an empirical data fit. Often d is about ¾ of the canopy height while z_o might range from 10^{-4} to 10^2 cm (flat plate with d = 0 to a forest with d = 7 m). Similarly, the friction velocity might be a few percent of the average air velocity.

Table A-4 shows aerodynamic surface roughness of different surfaces along with calculated friction velocities from Equation (14). (The zero plane displacement was not used because it was not included in the dimensionless predictors for dry deposition velocities.) Friction velocities correspond to wind speeds listed for general (some) and specific surfaces for the elicitation questions.

Model Predictions

Deposition velocity predictors for large vegetative canopies are expected to be even more complex than predictors developed for simple surfaces in wind tunnel experiments. Also, dry deposition velocities should be a function of other parameters and variables including leaf area index and atmospheric stability. Sehmel and Hodgson[14,15] predicted deposition velocities, k_{1m}, as a function of particle diameter from 10^{-2} to 100 μm, of friction velocities from 10 to 200 cm/s, of aerodynamic roughness heights from 10^{-3} to 10 cm, of particle densities from 1 to 11.5 g/cm^3, and of atmospheric stabilities for Obukhov's lengths from -10 to +10 m (unstable and stable atmospheres, respectively). Predictions indicate that deposition velocities can range over several orders of magnitude from about 10^{-3} up to 10 cm/s. Moreover, they increase as roughness height increases, usually as friction velocity increases and they are nearly independent of atmospheric stability.

Caveats in using the model are that results are reasonably valid for the range of variables investigated. In addition, predictions were made by extrapolation beyond the range of variables investigated. Although the extrapolations show general trends as observed in field experiments, the extrapolations are not based on experimental observations.

The model can predict dry deposition velocities for most variables except increased surface area within the deposition surface canopy. Prediction procedures cannot describe the effects of foliage density on deposition velocities or particle penetration through the foliage to the underlying surface. Consequently, penetration results and foliar deposition velocities are needed to improve deposition velocity models.

Table A-4. Friction velocities for general and specific surfaces

Surface	z_0 (cm)	For Wind Speed of 2 m/s at 10 m u_*[1] (m/s)	For Wind Speed of 5 m/s at 10 m u_*[1] (m/s)	For Wind Speed of 5 m/s at 5 m u_*[1] (m/s)
Smooth mud flats, ice	0.001	0.058	0.145	0.152
Smooth snow on short grass	0.005	0.066	0.164	0.174
Smooth sea	0.02	0.074	0.185	0.197
Level desert	0.03	0.077	0.192	0.206
Snow surface, lawn to 1 cm	0.1	0.087	0.217	0.235
Mown grass				
1.5 cm	0.2	0.094	0.235	0.256
3.0 cm	0.7	0.110	0.275	0.304
To 5 cm grass	1	0.116	0.289	0.322
	2	0.129	0.322	0.362
To 60 cm grass	4	0.145	0.362	0.414
	9	0.170	0.424	0.496
Fully grown root crops	14	0.187	0.467	0.555
Moorland/peatland	4	0.145	0.362	0.414
with 40 cm tussocks	5	0.151	0.377	0.433
	6	0.156	0.390	0.451
Heather and green grass	3	0.138	0.344	0.390
partly covering the soil	4.5	0.148	0.370	0.424
	6	0.156	0.390	0.451

[1] Friction velocity is reported here in units of m/s. In contrast, the integral resistance correlation to predict dry deposition velocities uses u* with units of cm/s

The following text addresses dry deposition velocities predicted using the dimensionless integral correlation, the weighted correlation in Equation (14). The ground surface area was used as the deposition surface area for these calculations. The total canopy surface area is greater than on the underlying ground surface.

General aspects of dry deposition velocity predictions will

be considered. Afterward, dry deposition velocities predicted as a function friction velocity are shown in a series of figures.

Overview of Model Predictions

Model predictions indicate the functional dependency of deposition velocity on the several controlling parameters. For a concentration reference height of 1 m and a constant friction velocity of 30 cm/s, Figure A-4 shows predicted deposition velocities, k_{1m}, as a function of aerodynamic surface roughness and particle density.

Predicted deposition velocities are greater than the particle's gravitational settling velocity, i.e.,

$$K_{1-m} \leq V_t. \qquad (17)$$

The gravitational settling velocity increases proportionally with particle density and the square of particle diameter.

Only in the particle diameter range from about 0.1 to 1 μm is the deposition velocity nearly constant for a selected surface roughness, particle density, and friction velocity. For particle diameters larger than about 1 μm, deposition velocities increase because of an increase in eddy diffusion and gravitational settling. For large particles, deposition velocities approach their respective gravitational settling velocity.

Predicted deposition velocities for small particles are dependent upon Brownian diffusion near the deposition surface. For particle diameter less than about 0.1 μm, the effects of Brownian diffusion cause deposition velocities to increase with decreasing particle diameter. The left portion of Figure A-4 shows lower limits for deposition velocities calculated from only Brownian diffusion below and from atmospheric diffusion and Brownian diffusion above heights of 0.01 and 1 cm. For the calculation, the IR_3 term was replaced by

$$IR_s = -\int_{z_{lcm}}^{a=0^+} \frac{dz^+}{D/\nu} \qquad (18)$$

to account for mass transfer only by Brownian diffusion next to the deposition surface.

Diffusion in a stable atmosphere was assumed from the indicated height to 1 m. These lower limits are a function of each distance across which Brownian diffusion transports particles. When the controlling diffusion distance was decreased from 1 cm to 0.01 cm near to the deposition surface (the interface between boxes 2 and 3), the lower limit for deposition velocities increased by nearly two orders of magnitude.

Figure A-4 also shows upper limits for dry deposition velocities (Sehmel; Sehmel and Hodgson).[8,9,14,15] For these calculations the surface resistance to mass transfer within 1 cm of the surface was assumed to be zero. For this case, the IR_3 term on the right side Equation (6) was assumed to be zero. Deposition velocities were calculated by including only atmospheric diffusion and gravity settling between 1 cm and 1 m. For particle diameters less than 1 μm, this upper limit is nearly constant and decreases from 1.1 cm/s at 1 μm to 1.08 cm/s at 10^{-3} μm. For particle diameters greater than 2 μm, deposition velocities approach their respective terminal settling velocity.

Integral Resistances At Elevated Heights;

Most deposition velocity predictions are for a stable atmosphere. Other predictions by Sehmel and Hodgson[14,15] indicate instability to increase the value of the predicted deposition velocity. The increase is small compared to the effects of particle diameter, friction velocity and aerodynamic surface roughness.

Resistance integrals IR_1 and IR_2 for heights greater that 1 cm were evaluated using Equation (6) and atmospheric diffusion correlations for stable, neutral and unstable conditions (Businger et al.).[3] An assumption in the calculation was an equality of particle eddy diffusivity and eddy diffusivity of air momentum. Since these correlations do not include any canopy effect on eddy diffusivity, IR_1 and IR_2 were combined into a single resistance integral. The combined resistance integral was calculated from 1 cm up to 1 m, and added to IR_3 (Equation 14) to predict deposition velocities K_{1-m}, for a 1 m reference concentration height.

Integral Resistance Ranges

The surface resistance in box 3 usually controls overall mass transfer. Predictions were made for the surface mass transfer resistance integral within 1 cm of the deposition surface, IR_3, and compared with atmospheric diffusional resistances. Atmospheric diffusional resistances were calculated from the integrals in Equation (6) by assuming Brownian diffusion was zero and an equality between particle and air momentum diffusivity (Sehmel and Hodgson).[12]

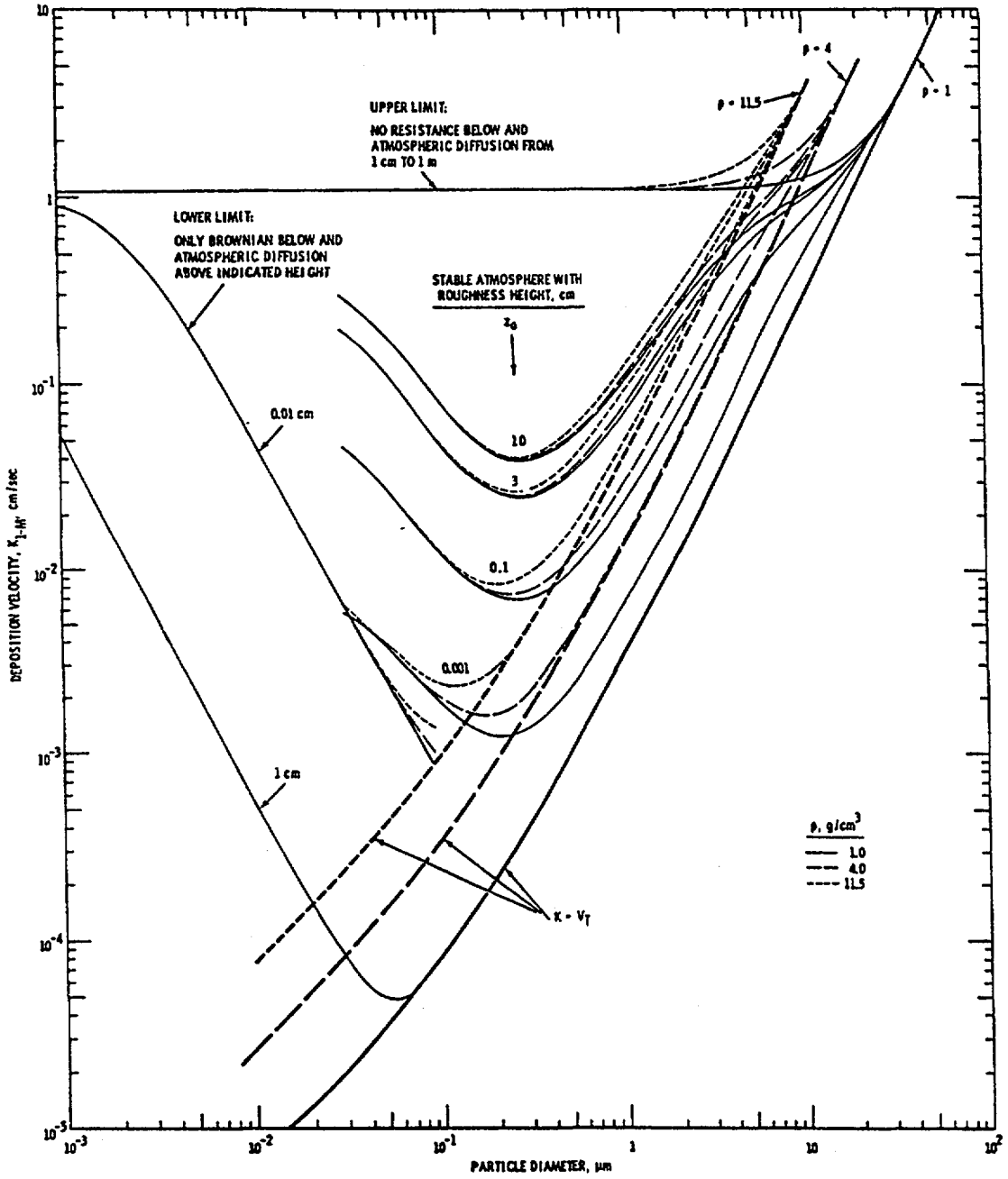

Figure A-4. Predicted deposition velocities at 1 m height for $u_* = 30$ cm/s and particle densities of 1, 4, and 11.5 g/cm³.

Figure A-5 shows predicted atmospheric resistances as a function of height and stability. Since eddy diffusion is least in stable atmospheres, mass transfer resistance integrals were largest for stable atmospheres. The largest shown is -30. For unstable atmospheres, mass transfer resistance integrals were least. For atmospheric instability, the largest resistance integral is -15.5. By contrast, in magnitude, IR_3 surface resistance integrals ranged from -1 to -10^5.

Deposition Velocity as Function of Height and Atmospheric Stability

Predicted deposition velocities were calculated from the IR_3 correlation of Equation (14) and integral resistances above 1 cm, to 1 m, and to 10 m (from Figure A-5).

Figure A-6 shows predicted deposition velocities at each height for both unstable and stable atmospheres. The upper bound for each height is for an unstable atmosphere with Obukhov's length equal to -10 m, while the lower bound is for a stable atmosphere with Obukhov's length equal to +10m. Predicted deposition velocities show a minor influence of atmospheric stability on deposition. The bounds merge into one indistinguishable line for reference heights of 1 and 10 cm. Between particle diameters from about 10^{-1} to 1 μm, all predictions are nearly identical. Consequently in this range, curves are shown only for reference heights of 1 cm and 10 m. All predicted deposition velocities are greater than particle terminal settling velocities indicated by the $K = v_t$ curve for no flow conditions and a particle density of 1.0 g/cm^3.

Deposition velocities with a 1 cm reference concentration height are shown as an upper curve. As expected from increased mass transfer resistance, deposition velocities for larger reference concentration heights are always less than for a 1 cm reference concentration height. For particle diameters less than about 6 μm, deposition velocities are almost insensitive to changes in reference concentration height.

The relative resistance above 1 cm becomes increasingly controlling as particle diameters increase above about 6 μm. For these particle diameters, deposition velocities are larger for a 1 cm reference height than for reference heights from 10 cm to 10 m. This sensitivity appears less pronounced at 1 m and above. Due to this insensitivity, a 1 m reference height was selected for presentation in the following deposition velocity figures. It is fortunate that deposition velocities are relatively insensitive to height at 1 m since field experiments and atmospheric transport and diffusion models have often used a similar height.

Predicted Deposition Velocities for a 1 Meter Reference Height

Figures A-7 through A-12 show deposition velocities at $K_{1\text{-}m}$ predicted as a function of particle diameter from 10^{-2} to 100 μm, friction velocities from 10 to 200 cm/s, roughness height from 10^{-3} to 10 cm, and particle density from 1 to 11.5 g/cm^3 (Sehmel and Hodgson).[14,15] Predictions indicate deposition velocities vary several orders of magnitude from about 10^{-3} to 10 cm/s and increase with an increase in roughness height and usually with an increase in friction velocity. Within each figure are curves that illustrate the influence on deposition velocities of particle densities of 1, 4, and 11.4 g/cm^3 and roughness heights of 10^{-3}, 10^{-1}, 3, and 10 cm. In all cases, predicted deposition velocities are greater than the particle terminal settling velocity.

Deposition velocities are independent of particle density for small particles where Brownian diffusion controls mass transfer. Brownian diffusion is controlling mass transfer in the particle size region in which the three density curves merge for particle diameters less than about 0.1 μm.

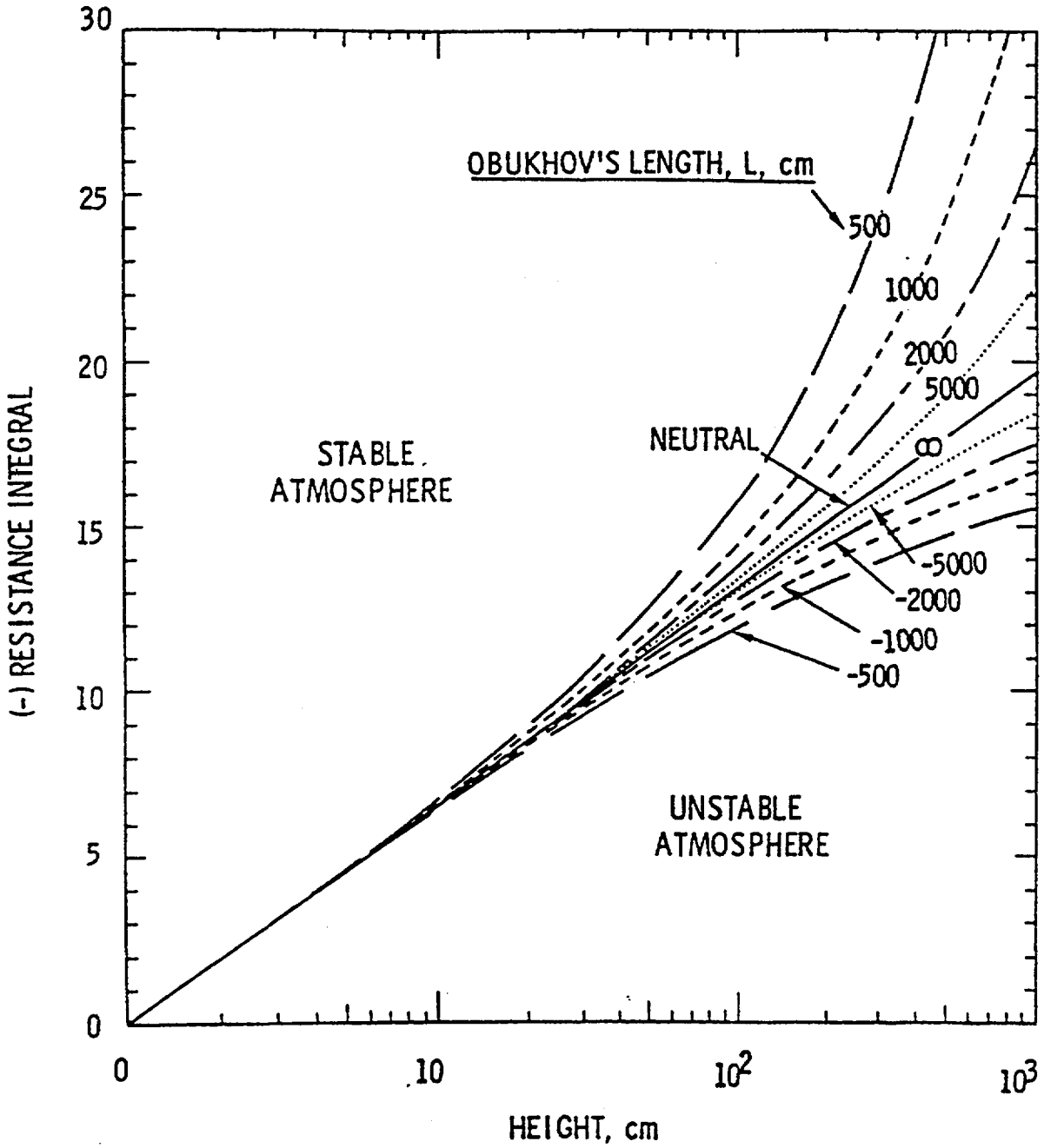

Figure A-5. Resistance integral from 1 cm to indicated height.

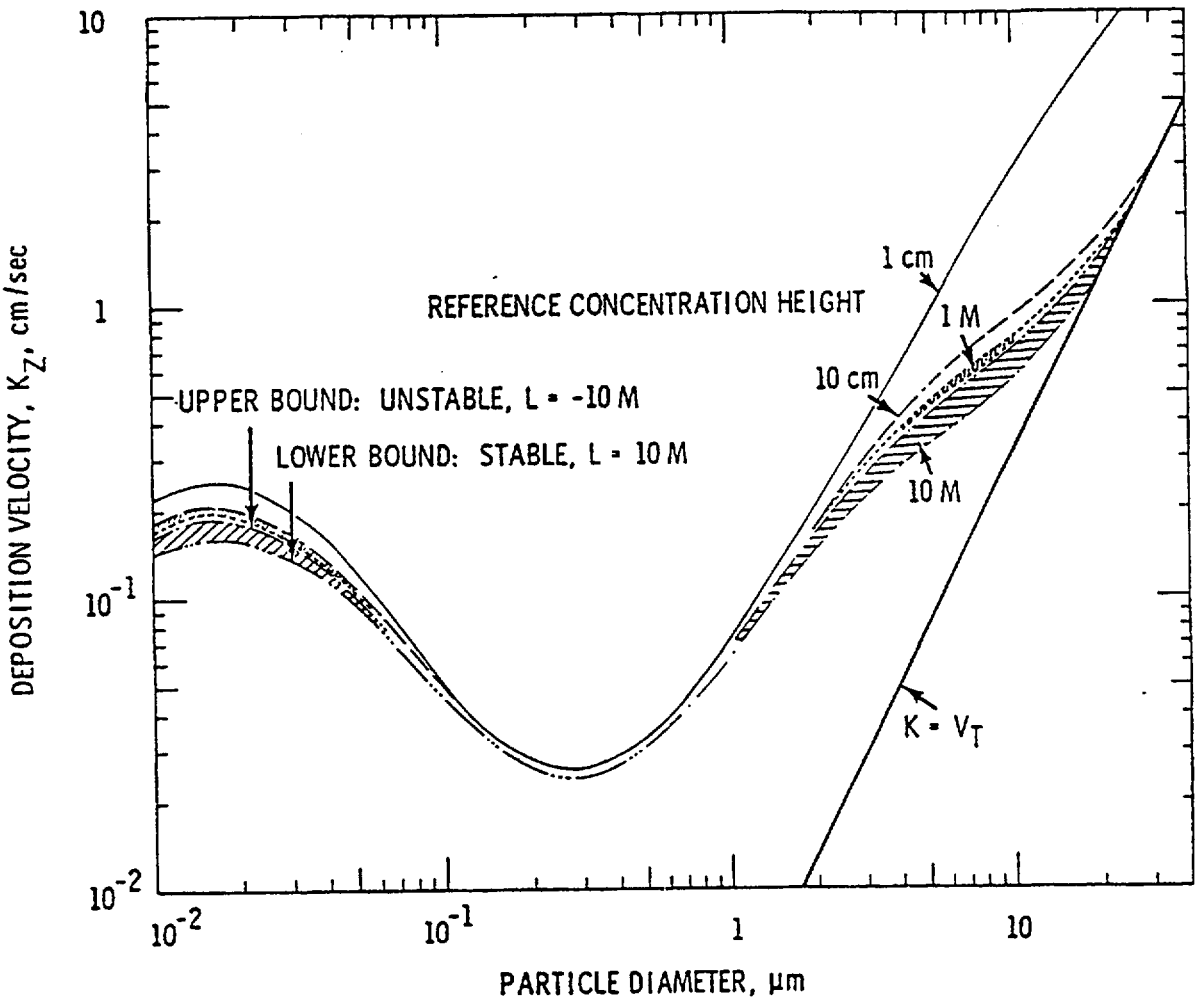

Figure A-6. Predicted deposition velocities at indicated height for $u_* = 20$ cm/s, $z_0 = 3.0$ cm and particle density of 1.0 g/cm^3.

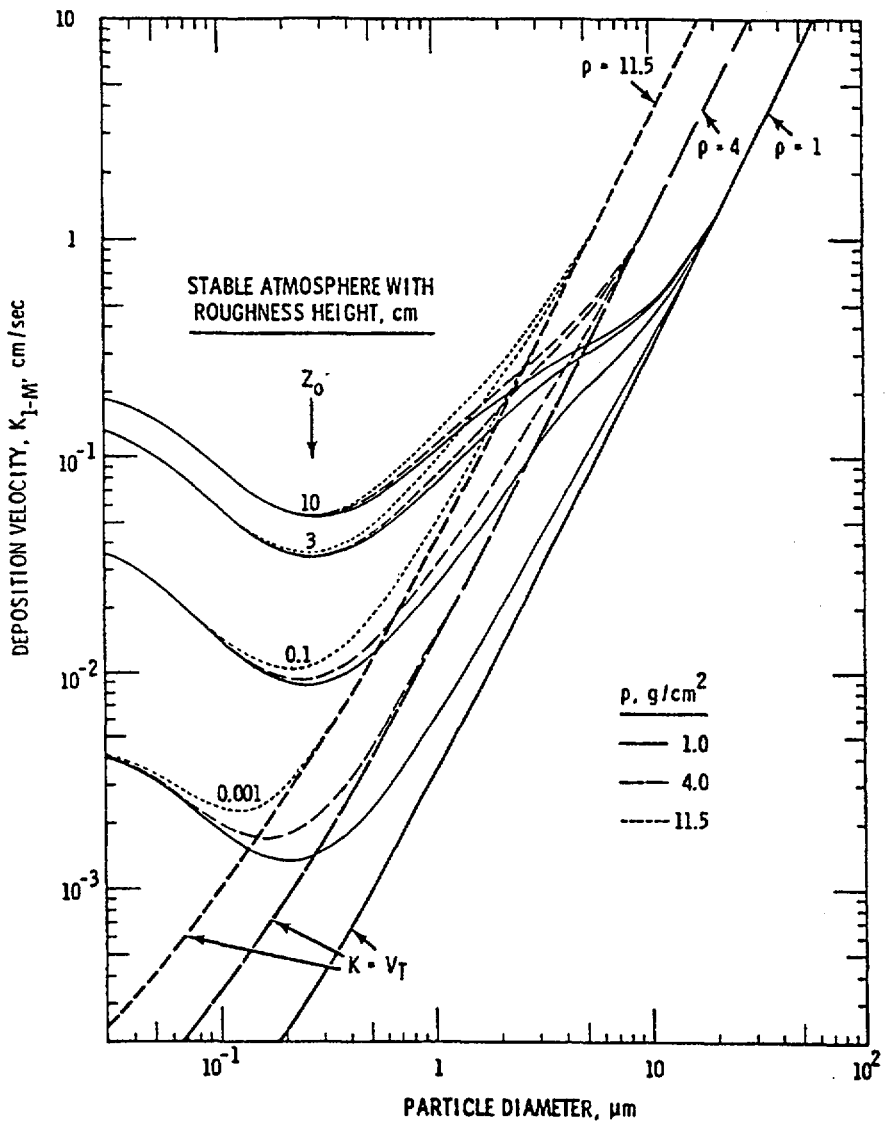

Figure A-7. Predicted deposition velocities at 1M for $u_* = 10$ cm/s and particle densities of 1, 4, and 11.5 g/cm³.

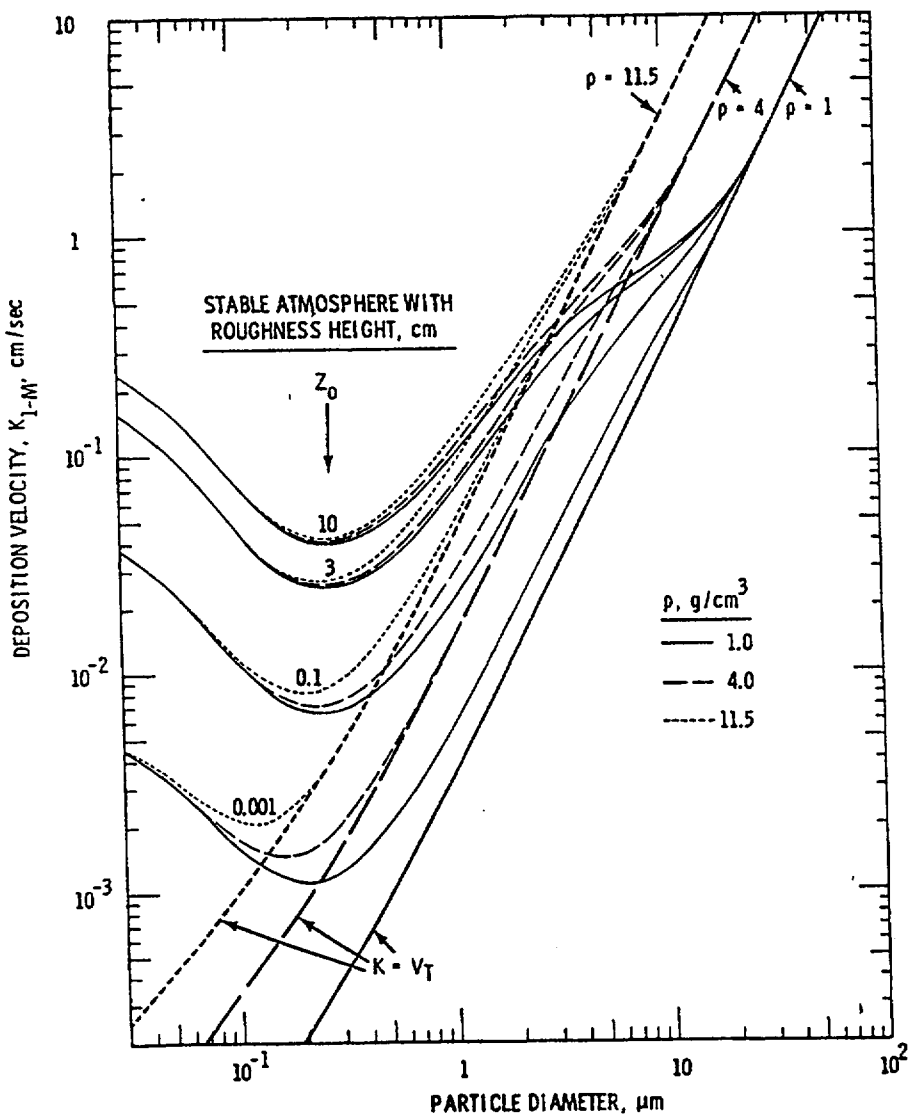

Figure A-8. Predicted deposition velocities at 1M for $u_* = 20$ cm/s and particle densities of 1, 4, and 11.5 g/cm^3.

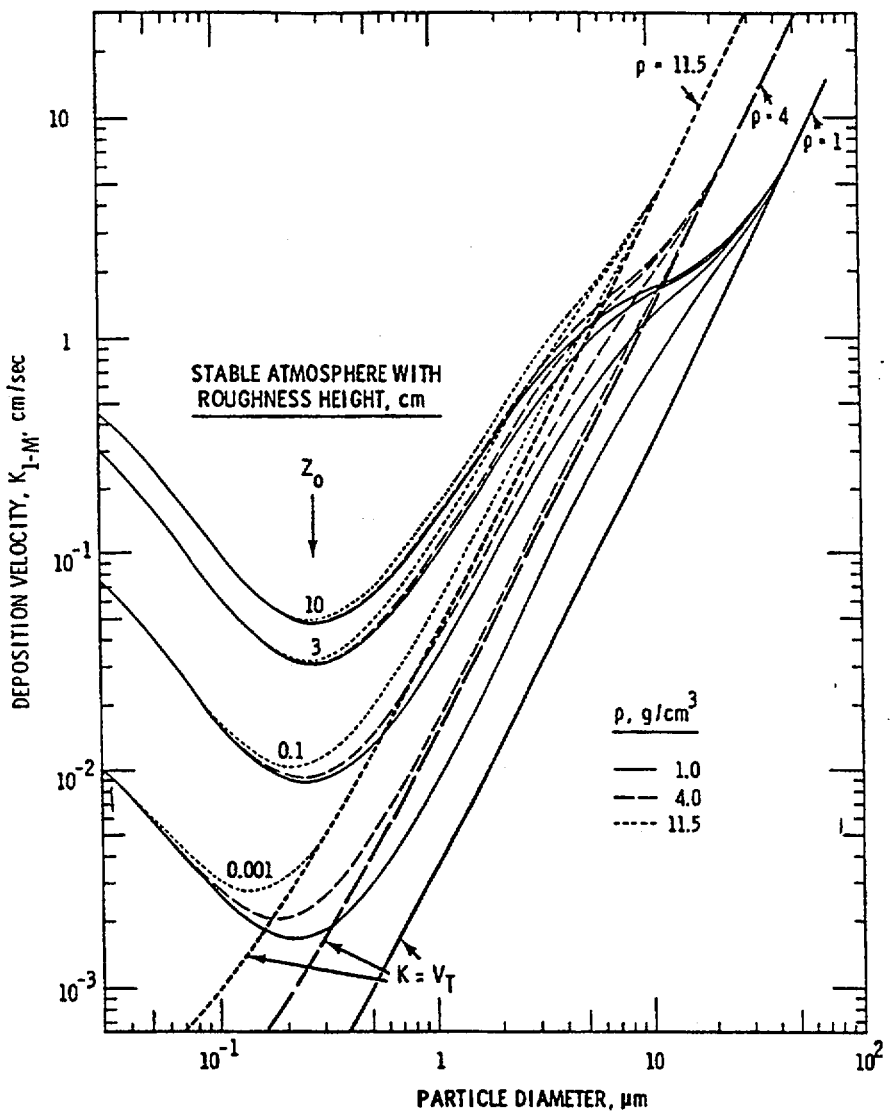

Figure A-9. Predicted deposition velocities at 1M for u. = 50 cm/s and particle densities of 1, 4, and 11.5 g/cm³.

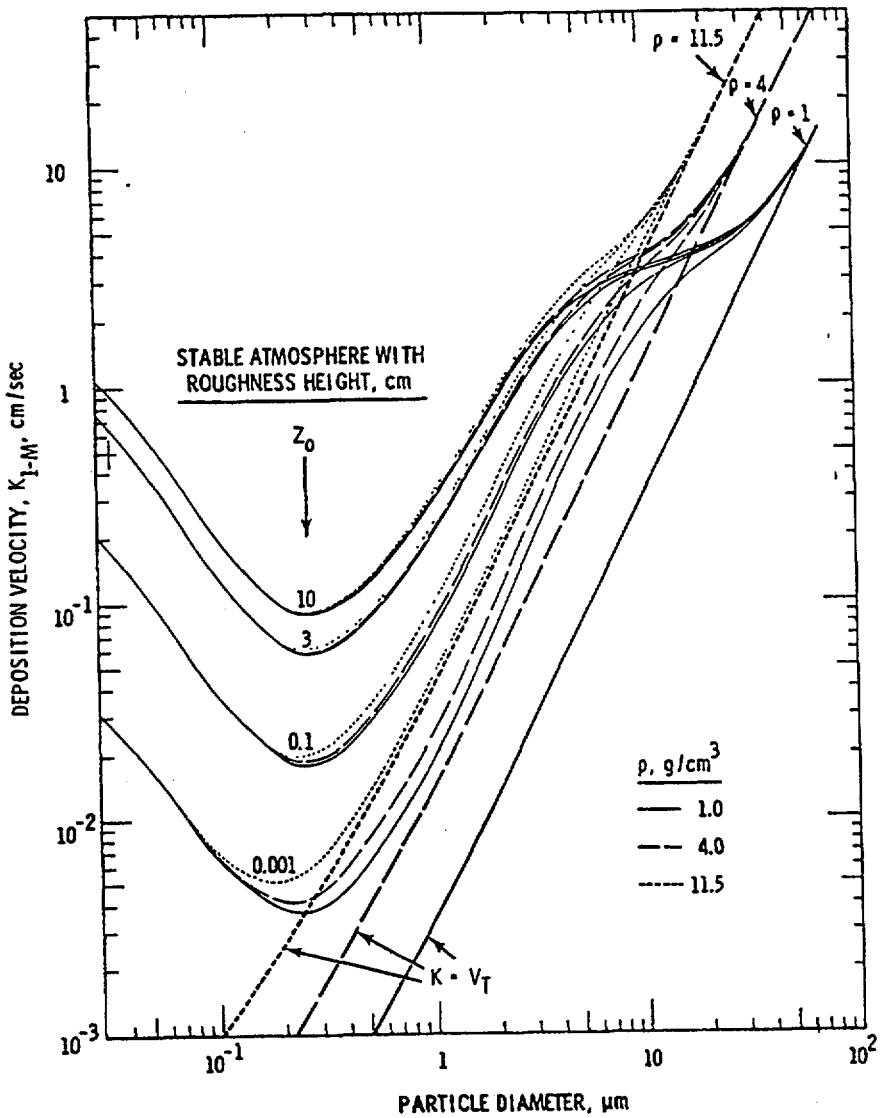

Figure A-10. Predicted deposition velocities at 1M for $u_* = 100$ cm/s and particle densities of 1, 4, and 11.5 g/cm³.

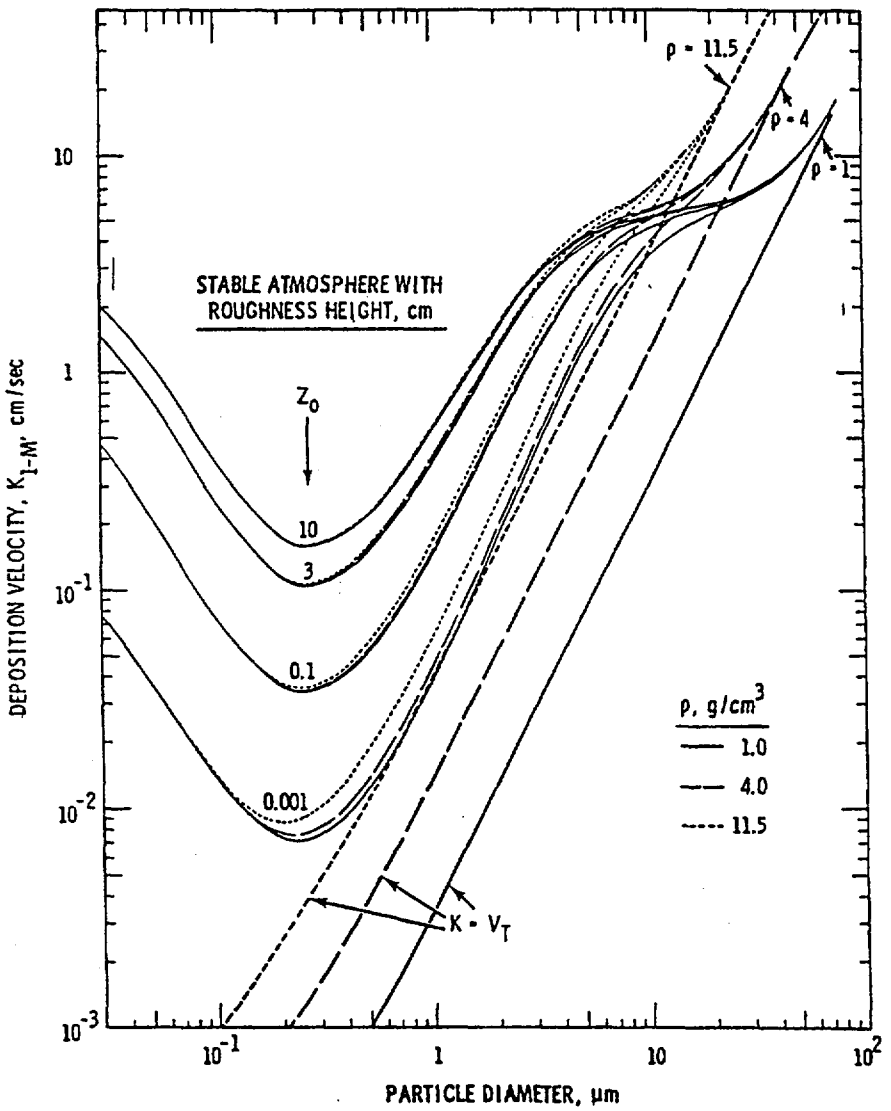

Figure A-11. Predicted deposition velocities at 1M for $u_* = 150$ cm/s and particle densities of 1, 4, and 11.5 g/cm³.

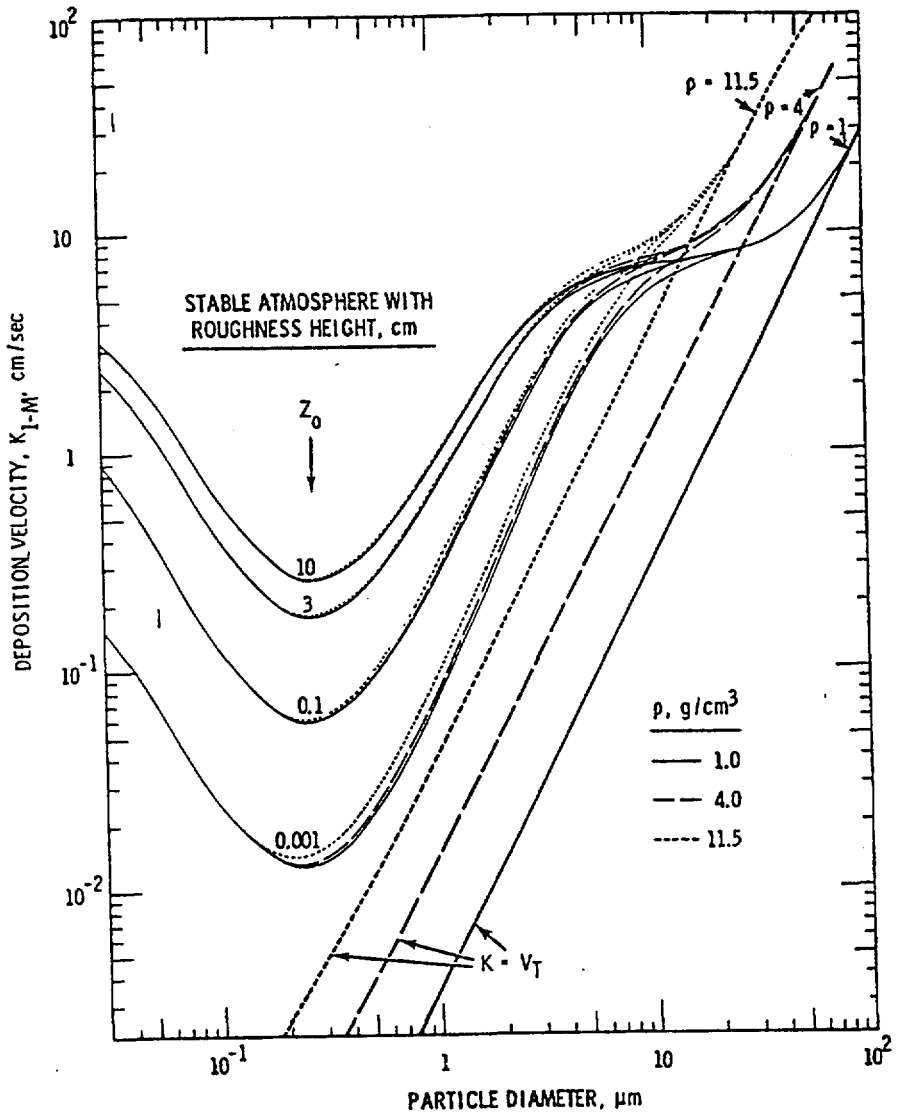

Figure A-12. Predicted deposition velocities at 1M for u. = 200 cm/s and particle densities of 1, 4, and 11.5 g/cm³.

Nomenclature

a	=	particle radium, cm
C	=	airborne concentration of monodispersed particles, cm^{-3}
d	=	particle diameter, cm
D	=	Brownian diffusion coefficient cm^2/s, (see Equation 19)
IR	=	Integral mass transfer resistance next to surface, dimensionless
k	=	Boltzmann's constant, 1.32×10^{-16} erg/(molecule °K)
p	=	pressure, cm of mercury (76.0 cm used)
Sc	=	Schmidt number, υ/D
T	=	temperature, °K (296°K used)
u_*	=	friction velocity, cm/s
v_t	=	monodispersed particle gravity settling velocity, cm/s
z_o	=	aerodynamic surface roughness, cm
z^+	=	dimensionless height, zu_*/u
μ	=	air viscosity, g/(cm·s), [1.78×10^{-4} g/(cm·s) used]
u	=	kinematic viscosity, μ/ρ
r	=	air density, g/cm^3, (1.2×10^{-3} g/cm^3 used)
r_p	=	particle density, g/cm^3 (1.5 g/cm^3 used)
t^+	=	dimensionless relaxation time,

$$\frac{\rho_p d^2}{18\mu}\frac{u_*^2}{\nu}10^{-8}$$

The Brownian diffusivity was calculated (Davies)[5] from

$$D = \frac{kT}{6\pi\mu a}\left\{1 + \frac{10^{-4}}{pa}[6.32 + 2.01\exp(-2190pa)]\right\} \quad (19)$$

Deposition Tables

Units of velocity are in cm/s; N/A = not provided by expert; unkn = unknown

DD-A: Dry deposition velocity of aerosols - Wind Speed at 2m/s					
PARTICLE SIZE	**QUANTILE**	**URBAN**	**MEADOW**	**FOREST**	**HUMAN SKIN**
0.10μ	**0%**	2.00E-02	2.00E-02	2.00E-02	2.00E-02
	5%	3.00E-02	2.50E-02	3.00E-02	3.00E-02
	50%	7.00E-01	1.80E-01	7.00E-01	3.60E-01
	95%	1.00E+01	2.00E+00	1.00E+01	1.00E+01
	100%	N/A	N/A	N/A	N/A
0.30μ	**0%**	6.00E-03	6.00E-03	6.00E-03	6.00E-03
	5%	9.00E-03	8.00E-03	1.40E-02	7.00E-03
	50%	2.80E-01	7.50E-02	2.80E-01	2.00E-02
	95%	8.00E+00	8.00E-01	8.00E+00	8.00E+00
	100%	N/A	N/A	N/A	N/A
1.00μ	**0%**	4.00E-03	4.00E-03	4.00E-03	4.00E-03
	5%	7.00E-03	6.00E-03	7.00E-03	5.00E-03
	50%	9.00E-01	2.80E-01	9.00E-01	8.00E-02
	95%	1.00E+01	2.80E+00	1.00E+01	1.00E+01
	100%	N/A	N/A	N/A	N/A
3.00μ	**0%**	5.00E-02	5.00E-02	5.00E-02	5.00E-02
	5%	8.00E-02	7.00E-02	8.00E-02	6.00E-02
	50%	4.00E+00	1.60E+00	4.00E+00	6.00E-01
	95%	3.00E+01	1.60E+01	3.00E+01	3.00E+01
	100%	N/A	N/A	N/A	N/A
10.00μ	**0%**	4.00E-01	4.00E-01	4.00E-01	4.00E-01
	5%	5.00E-01	5.00E-01	5.30E-01	5.00E-01
	50%	7.00E+00	4.10E+00	7.00E+00	2.40E+00
	95%	1.00E+02	1.00E+01	1.00E+02	1.00E+02
	100%	N/A	N/A	N/A	N/A

DD-B: Dry deposition velocity of aerosols - Wind Speed at 5m/s					
PARTICLE SIZE	QUANTILE	URBAN	MEADOW	FOREST	HUMAN SKIN
0.10μ	0%	2.00E-02	2.00E-02	2.00E-02	2.00E-02
	5%	3.00E-02	3.00E-02	3.00E-02	2.00E-02
	50%	7.00E-01	4.20E-01	7.00E-01	1.30E-01
	95%	1.00E+01	4.00E+00	1.00E+01	1.00E+01
	100%	N/A	N/A	N/A	N/A
0.30μ	0%	6.00E-03	6.00E-03	6.00E-03	6.00E-03
	5%	4.00E-03	8.00E-03	9.00E-03	8.00E-03
	50%	2.80E-01	1.80E-01	2.80E-01	6.00E-02
	95%	8.00E+00	1.80E+00	8.00E+00	8.00E+00
	100%	N/A	N/A	N/A	N/A
1.00μ	0%	4.00E-03	4.00E-03	4.00E-03	4.00E-03
	5%	7.00E-03	7.00E-03	7.00E-03	6.00E-03
	50%	9.00E-01	6.50E-01	9.00E-01	2.30E-01
	95%	1.00E+01	6.50E+00	1.00E+01	1.00E+01
	100%	N/A	N/A	N/A	N/A
3.00μ	0%	5.00E-02	5.00E-02	5 00E-02	5.00E-02
	5%	8.00E-02	7.00E-02	8.00E-02	7.00E-02
	50%	4.00E+00	2.00E+00	4.00E+00	2.00E+00
	95%	3.00E+01	2.00E+01	3.00E+01	3.00E+01
	100%	N/A	N/A	N/A	N/A
10.00μ	0%	4.00E-01	4.00E-01	4.00E-01	4.00E-01
	5%	5.30E-01	5.30E-01	5.30E-01	5.20E-01
	50%	7.00E+00	6.50E+00	7.00E+00	6.00E+00
	95%	1.00E+02	6.50E+01	1.00E+02	1.00E+02
	100%	N/A	N/A	N/A	N/A

DD-C: Dry deposition velocity of elemental iodine - Wind Speed at 2 and 5m/s					
WIND SPEED	QUANTILE	URBAN	MEADOW	FOREST	HUMAN SKIN
2.m/s	0%	2.00E-02	2.00E-02	2.00E-02	2.00E-02
	5%	5.00E-02	5.00E-02	5.00E-02	5.00E-02
	50%	5.00E-01	5.00E-01	5.00E-01	5.00E-01
	95%	7.00E+00	7.00E+00	7.00E+00	7.00E+00
	100%	2.00E+00	2.00E+00	2.00E+00	2.00E+00
5.m/s	0%	2.00E-02	2.00E-02	2.00E-02	2.00E-02
	5%	5.00E-02	5.00E-02	5.00E-02	5.00E-02
	50%	5.00E-01	5.00E-01	5.00E-01	5.00E-01
	95%	7.00E+00	7.00E+00	7.00E+00	7.00E+00
	100%	2.00E+00	2.00E+00	2.00E+00	2.00E+00

DD-D: Dry deposition velocity of methyl iodide - Wind Speed at 2 and 5m/s					
WIND SPEED	QUANTILE	URBAN	MEADOW	FOREST	HUMAN SKIN
2.m/s	0%	N/A	N/A	N/A	N/A
	5%	1.00E-04	1.00E-04	1.00E-04	1.00E-04
	50%	1.00E-03	1.00E-03	1.00E-03	1.00E-03
	95%	1.00E-02	1.00E-02	1.00E-02	1.00E-02
	100%	N/A	N/A	N/A	N/A
5.m/s	0%	N/A	N/A	N/A	N/A
	5%	1.00E-04	1.00E-04	1.00E-04	1.00E-04
	50%	1.00E-03	1.00E-03	1.00E-03	1.00E-03
	95%	1.00E-02	1.00E-02	1.00E-02	1.00E-02
	100%	N/A	N/A	N/A	N/A

DD-E-1: Dry deposition velocity of aerosols on Moorland/Peatland Surface		
PARTICLE SIZE	**QUANTILE**	
0.55μ	**0%**	5.00E-03
	5%	8.00E-03
	50%	3.10E-01
	95%	1.00E+01
	100%	N/A
0.70μ	**0%**	4.50E-03
	5%	7.00E-03
	50%	4.50E-01
	95%	1.10E+01
	100%	N/A
0.90μ	**0%**	4.00E-03
	5%	7.00E-03
	50%	6.50E-01
	95%	1.20E+01
	100%	N/A
1.20μ	**0%**	6.00E-03
	5%	1.00E-02
	50%	1.10E+00
	95%	1.40E+01
	100%	N/A
1.60μ	**0%**	8.00E-03
	5%	1.40E-02
	50%	1.50E+00
	95%	1.80E+01
	100%	N/A

DD-E-2: Dry deposition velocity of aerosols on Heather/Green Grass Surface		
PARTICLE SIZE	**QUANTILE**	
0.55μ	**0%**	5.00E-03
	5%	8.00E-03
	50%	3.10E-01
	95%	1.00E+01
	100%	N/A
0.70μ	**0%**	4.50E-03
	5%	7.00E-03
	50%	4.50E-01
	95%	1.10E+01
	100%	N/A
0.90μ	**0%**	4.00E-03
	5%	7.00E-03
	50%	6.50E-01
	95%	1.20E+01
	100%	N/A
1.20μ	**0%**	6.00E-03
	5%	1.00E-02
	50%	1.10E+00
	95%	1.40E+01
	100%	N/A
1.60μ	**0%**	8.00E-03
	5%	1.40E-02
	50%	1.50E+00
	95%	1.80E+01
	100%	N/A

DD-E-2: Dry deposition velocity of aerosols on Heather/Green Grass Surface (continued)		
PARTICLE SIZE	QUANTILE	
2.30μ	0%	3.00E-02
	5%	4.70E-01
	50%	2.90E+00
	95%	3.00E+01
	100%	N/A
3.20μ	0%	4.00E-02
	5%	6.30E-02
	50%	4.00E+00
	95%	5.00E+01
	100%	N/A
4.20μ	0%	8.00E-02
	5%	1.20E-01
	50%	5.50E+00
	95%	6.00E+01
	100%	N/A

DD-F: Dry deposition velocity of aerosols on Grassland Surface		
PARTICLE SIZE	QUANTILE	
1.0μ	0%	4.00E-03
	5%	5.00E-03
	50%	6.70E-02
	95%	1.00E+01
	100%	N/A

WD-A: Elemental iodine—fraction removed by rain ($1\text{-}f_w$)							
Rainfall/ Time	Wind Speed	Quantile	$1\text{-}f_w$	Rainfall/ Time	Wind Speed	Quantile	$1\text{-}f_w$
.3mm/hr	unkn	0%	N/A	2.mm/hr	unkn	0%	N/A
		5%	N/A			5%	N/A
		50%	N/A			50%	N/A
		95%	N/A			95%	N/A
		100%	N/A			100%	N/A
.075mm/ 10min	10 m/s	0%	N/A	.05mm/ 10min	unkn	0%	N/A
		5%	N/A			5%	N/A
		50%	N/A			50%	N/A
		95%	N/A			95%	N/A
		100%	N/A			100%	N/A
.17mm/ 10min	5 m/s	0%	N/A	.17mm/ 10 min	14 m/s	0%	N/A
		5%	N/A			5%	N/A
		50%	N/A			50%	N/A
		95%	N/A			95%	N/A
		100%	N/A			100%	N/A
0.23mm/ 10min	12 m/s	0%	N/A	.5mm/ 10min	unkn	0%	N/A
		5%	N/A			5%	N/A
		50%	N/A			50%	N/A
		95%	N/A			95%	N/A
		100%	N/A			100%	N/A
.33mm/ 10min	unkn	0%	N/A	1.0mm/ 10min	14 m/s	0%	N/A
		5%	N/A			5%	N/A
		50%	N/A			50%	N/A
		95%	N/A			95%	N/A
		100%	N/A			100%	N/A

WD-A: Elemental iodine—fraction removed by rain ($1\text{-}f_w$) (continued)			
Rainfall/Time	**Wind Speed**	**Quantile**	$1\text{-}f_w$
1.67mm/ 10 min	**unkn**	**0%**	N/A
		5%	N/A
		50%	N/A
		95%	N/A
		100%	N/A

WD-B: Methyl iodide—fraction removed by rain (Wind Speed=unknown)		
Rainfall/Time	**Quantile**	$1\text{-}f_w$
.3mm/hr	**0%**	N/A
	5%	N/A
	50%	N/A
	95%	N/A
	100%	N/A
2.mm/hr	**0%**	N/A
	5%	N/A
	50%	N/A
	95%	N/A
	100%	N/A
.05mm/10 min	**0%**	N/A
	5%	N/A
	50%	N/A
	95%	N/A
	100%	N/A
.33mm/10 min	**0%**	N/A
	5%	N/A
	50%	N/A
	95%	N/A
	100%	N/A

WD-B: Methyl iodide—fraction removed by rain (Wind Speed=unknown) (continued)		
Rainfall/Time	**Quantile**	**$1-f_w$**
1.67mm/10 min	**0%**	N/A
	5%	N/A
	50%	N/A
	95%	N/A
	100%	N/A

WD-C: Fraction of aerosols removed by rain						
PARTICLE SIZE	**QUANTILE**	**Rainfall: .3mm/hr**	**Rainfall: 2.mm/hr**	**Rainfall: .05mm/10 min**	**Rainfall: .33mm/10 min**	**Rainfall: 1.67mm/10 min**
0.10μ	**0%**	N/A	N/A	N/A	N/A	N/A
	5%	N/A	N/A	N/A	N/A	N/A
	50%	N/A	N/A	N/A	N/A	N/A
	95%	N/A	N/A	N/A	N/A	N/A
	100%	N/A	N/A	N/A	N/A	N/A
0.30μ	**0%**	N/A	N/A	N/A	N/A	N/A
	5%	N/A	N/A	N/A	N/A	N/A
	50%	N/A	N/A	N/A	N/A	N/A
	95%	N/A	N/A	N/A	N/A	N/A
	100%	N/A	N/A	N/A	N/A	N/A
1.00μ	**0%**	N/A	N/A	N/A	N/A	N/A
	5%	N/A	N/A	N/A	N/A	N/A
	50%	N/A	N/A	N/A	N/A	N/A
	95%	N/A	N/A	N/A	N/A	N/A
	100%	N/A	N/A	N/A	N/A	N/A
10.00μ	**0%**	N/A	N/A	N/A	N/A	N/A
	5%	N/A	N/A	N/A	N/A	N/A
	50%	N/A	N/A	N/A	N/A	N/A
	95%	N/A	N/A	N/A	N/A	N/A
	100%	N/A	N/A	N/A	N/A	N/A

References

1. Atkins, D.H.F., R.C. Chadwick, and A.C. Chamberlain, "Deposition of Radioactive Methyl Iodide to Vegetation," *Health Physics*, 13:91-92, 1967.

2. Bunch, D.F., ed., "Controlled Environmental Radioiodine Tests, Progress Report No. 3," IDO-12063, Idaho Operations Office, USAEC, available National Technical Information Service, U.S. Dept. of Commerce, Springfield, VA, January 1968.

3. Businger, J.A., et al., "Flux-Profile Relationships in the Atmospheric Surface Layer," *Journal of Atmospheric Science*, 28:181-189, 1971.

4. Chamberlain, A.C., and R.C. Chadwick, "Deposition of Airborne Radioiodine Vapor," *Nucleonics*, 8:22-25, 1953.

5. Davies, C.N., ed., *Aerosol Science*, Academic Press, New York, p. 408, 1966.

6. Heinemann, K., et al., "Studies on the Deposition and Release of Iodine on Vegetation," ORNL-tr-4313, available National Technical Information Service, U.S. Dept. of Commerce, Springfield, VA, April 1967.

7. Plate, E.J., "Aerodynamic Characteristics of Atmospheric Boundary Layers," TID-25465, available National Technical Information Service, U.S. Dept. of Commerce, Springfield, VA, 1971.

8. Sehmel, G.A., "Particle and Gas Deposition· A Review," PNL-SA-7584, Pacific Northwest Laboratory, Richland, WA, 1979.

9. Sehmel, G.A., "Particle and Gas Dry Deposition: A Review," *Atmospheric Environment*, 14:983-1011, 1980.

10. Sehmel, G.A., "Deposition and Resuspension," (D. Randerson, ed.), *Atmospheric Science and Power Production*, DOE/TIC-27601, Technical Information Center, Office of Scientific and Technical Information, United States Department of Energy, Oak Ridge, TN, pp. 533-583, 1984.

11. Sehmel, G.A., "Dry Deposition Velocities", PNL-SA-12156, Pacific Northwest Laboratory, Richland, WA, March 1984.

12. Sehmel, G.A., and W.H. Hodgson, "Predicted Dry Deposition Velocities," *Proceedings of the Atmosphere-Surface Exchange of Particulate and Gaseous Pollutants (1974)*, Energy Research and Development Administration Symposium Series 38, CONF-740921-13, National Technical Information Service, U.S. Department of Commerce, Richland, WA, pp. 399-422, 1986.

13. Sehmel, G.A., and W.H. Hodgson, "Particle Deposition and Penetration Through Vegetation Canopies from Wind Tunnel Experiments," *Pacific Northwest Laboratory Annual Report for 1975: Atmospheric Sciences*, BNWL-2000-3, Pacific Northwest Laboratory, Richland, WA, pp. 86-89, March 1976.

14. Sehmel, G.A., and W.H. Hodgson, "A Model for Predicting Dry Deposition of Particles and Gases to Environmental Surfaces," PNL-SA-6721, Pacific Northwest Laboratory, Richland, WA, 1978.

15. Sehmel, G.A., and W.H. Hodgson, "A Model for Predicting Dry Deposition of Particles and Gases to Environmental Surfaces," (W. Licht, ed.), *Implications of the Clean Air Amendments of 1977 and of Energy Considerations for Air Pollution Control*, Symposium Series No. 196, American Institute of Chemical Engineers, New York, pp. 218-230, 1980.

16. Sehmel, G.A., et al., "Particle Deposition and Penetration Through Vegetation Canopies from Wind Tunnel Experiments, *Pacific Northwest Laboratory Annual Report for 1975: Atmospheric Sciences*, BNWL-2000-3, Pacific Northwest Laboratory, Richland, WA, March 1976.

17. Sehmel, G.A., et al., "Dry Deposition Processes," *Pacific Northwest Laboratory Annual Report for 1972: Atmospheric Sciences*, BNWL-1751-1, Pacific Northwest Laboratory, Richland, WA, pp. 43-49, April 1973.

18. Whelpdale, D.M. and R.W. Shaw, "Sulfur Dioxide Removal by Turbulent Transfer Over Grass, Snow, and Water Surfaces", *Tellus*, XXVI: 196-205, 1974.

19. Zimbrick, J.D., and P.G. Voilleque, "Controlled Environmental Radioiodine Tests at the National Reactor Testing Station, 1967 Cert Progress Report," Progress Report No. 4, IDO-12065, AEC Operations Office, Idaho Falls, ID, January 1969.

Attachment A

Estimation of Dry Deposition Velocities for Methyl Iodide

The dry deposition velocity for methyl iodide is given as a percentage of the dry deposition velocity for iodine for two references in Table A-2 of the main text. The purpose of this appendix is to use the percentages to estimate the dry deposition velocity for methyl iodide. Results are shown in Table A.

Table A. Dry deposition velocities for methyl iodide compared to iodine

Deposition Surface	Deposition Velocity (cm/s)	Reference
Grass		Heinemann et al.[6]
	Iodine	
Grass	0.12 to 8.0	
Dry, average	0.3 to 2.8	
Damp, average	0.9 to 6.3	
Clover	1.0 to 4.2	
	Methyl iodide	
Grass	0.9 percent of that for molecular iodine	
	0.9 percent of 0.12 to 8.0 implies range from 1×10^{-3} to 7×10^{-2}	
Mixed pasture grass		Zimbrick and Voilleque[19]
	Iodine	
	2.1 to 2.4	
	Methyl iodide	
	less than 0.05 percent of that for molecular iodine	
	Implies less than 1×10^{-3}	

Expert B

Dry Deposition

The dry deposition velocity, v_d, was originally defined by Chamberlain and Chadwick[6] for both gases and particles as the ratio of the deposition flux, F_d, and the airborne concentration, c, at a reference height, z_{ref}:

$$v_d = \frac{-F_d}{c(z_{ref})} \tag{1}$$

The flux is negative when net transport is downward. The minus sign in Equation (1) is necessary to yield a positive dry deposition velocity when the flux is negative. In this project, v_d is defined to be the ratio of the rate of deposition of radioactivity to the ground (Bq/s/m^2) to the air concentration at 1 m height (Bq/m^3).

Our approach to quantifying the uncertainties of dry deposition predictions is to emphasize the results of field experiments. We chose to give greater attention to field measurements than wind tunnel studies, and to those taken on natural surfaces rather than those using surrogate surfaces. Wind tunnel studies have shown good agreement with field data on smooth surfaces, but are less appropriate for rough surfaces. Surrogate surfaces have been criticized because they disturb airflow (e.g., bucket collectors) and are not representative of the surface of interest.[36]

If the dry deposition velocity is known for a certain particle size, v_d can be estimated for other particle sizes. Fernandez de la Mora and Friedlander[12] showed that the mass transfer coefficient k for particle deposition in boundary layer flows is given by:

$$\frac{kd_P}{D} = \psi(\mu) \tag{2}$$

where D is the diffusion coefficient and

$$\mu = \left(\frac{d_P}{R}\right) Re^{1/2} Sc^{1/3} = \left(\frac{d_P}{R}\right) Pe^{1/3} Re^{1/6} \tag{3}$$

R is a characteristic length of the collecting element, $Re = u_\infty R/\nu$ is the Reynolds number, $Sc = \nu/D$ is the Schmidt number, $Pe = u_\infty R/D$ is the Peclet number, u_∞ is the velocity far from the collecting element, and ν is the kinematic viscosity. For a collection surface area per unit cross-sectional area parallel to the flow, a, the deposition velocity is given by:

$$v_d = ka \tag{4}$$

For particle diameters <~0.1 μm, mass transfer at the interface is controlled by Brownian diffusion and $\psi(\mu) \sim \mu$:

$$\frac{(v_d - v_s)d_P}{aD} = A\left(\frac{d_P}{R}\right) Re^{1/2} Sc^{1/3} \tag{5}$$

where A is a constant and v_s is the gravitational settling velocity:

$$v_s = \frac{\rho_P d_P^2 g}{18\mu} \tag{6}$$

The terminal settling velocity is subtracted from the total deposition velocity to leave the contribution from diffusion and interception. For small particles, the settling contribution to deposition is negligible. Therefore,

$$v_d \sim D^{2/3} \tag{7}$$

For larger particles (d_P>1 μm), particle deposition is controlled by interception and $\psi(\mu) \sim \mu^3$:

$$\frac{(v_d - v_s)d_P}{aD} = B\left(\frac{d_P}{R}\right)^3 Re^{3/2} Sc \tag{8}$$

where B is a constant. Therefore,

$$v_d - v_s \sim d_P^2 \tag{9}$$

The terminal settling velocity is the lower limit for the dry deposition velocity for a given particle size.[47]

For particles in the transition region, between the diffusion- and interception-controlled regimes ($0.1 < d_P < 1.0$ μm), the dry deposition velocity reaches a characteristic minimum.

Meadow surfaces

A number of studies have been performed to quantify dry deposition fluxes to grass and meadow surfaces, either using direct measurements or micrometeorological techniques.

Results from the literature vary over several orders of magnitude and are difficult to compare because of insufficient information on experimental procedure and the difficulty of controlling experimental conditions.[46,36] Most of these field studies do not report particle size distribution information.

The most extensive field study that we found in the literature was reported by Nicholson and Davies.[37] This yearlong study used the profile technique to measure the dry deposition of fine sulfate particles ($0.1 < d_p < 1.0$ μm) to rural surfaces. Details on the profile technique are given by Garland[17] and Businger.[4]

Nicholson and Davies[37] measured concentration, temperature, and wind speeds for several heights up to 2.3 m in a rural site near Norwich, England. The site contained a wide range of surface types, including short (3 cm) and long (10 to 30 cm) grass, barley (maximum height 1 m), and bare soil — these surfaces correspond with the description of a meadow surface given for this project. Meteorological conditions ranged from stable ($Ri = 0.093$) to unstable ($Ri = -0.054$), with measurements taken both at night and during the day. Wind speeds ranged from 1.06 to 6.03 m/s at 1 m height, the zero-plane displacement from 8 to 31 cm, roughness lengths from 0.1 to 4.3 cm, and friction velocities from 6 to 41 cm/s.

The particle densities were unknown. We assumed the sulfate particles have densities of about 1.5 g/cm^3, which is close to the specified unit density.[13] The greatest proportion of the mass of the sulfate particles fell in the size range 0.1 to 1.0 μm. The mean sulfate concentration was 13.9 μg/m^3 at 1 m height. with values ranging from 1.2 to 47.4 μg/m^3. Deposition velocities ranged from -0.5 to 0.6 cm/s at 1 m height, with an overall mean value of 0.07 cm/s and standard deviation (σ) 0.20 cm/s. Negative values were attributed to experimental error or resuspension.

A similar yearlong study was performed by Allen et al.[1] on a grass surface at Essex University, also using the profile technique to measure v_d for sulfate particles. In this study, a prefilter was used to remove particles with diameters larger than 2.0 μm. Deposition velocities ranged from -0.33 to 0.57 cm/s at 1 m height, with an overall mean value of 0.10 cm/s, with $\sigma = 0.18$ cm/s.

The deposition velocities measured by Nicholson and Davies[37] and Allen et al.[1] are shown in Figure B-1 for the range of particle size assumed by the investigators. Also included in Figure 1 are field measurements made by Garland and Cox,[18] Little and Wiffen,[30] and Horbert et al.[24] These studies did not cover the wide range of experimental conditions that Nicholson and Davies[37] and Allen et al.[1] did, but their results offer a test of the predicted ranges of deposition velocities. The operating conditions for the data presented in Figure B-1 are summarized in Table B-1.

Even for fixed wind velocities, it is well known that for a given type of surface, that is, a surface composed of elements (grass blades, gravel, etc.) of more or less uniform size, the deposition velocity (collection efficiency) as a function of particle diameter goes through a rather deep minimum.[45,46] However, we assume here that the minimum is quite broad, occurring over perhaps an order of magnitude in particle size. The existence of a broad minimum is based on the assumption that there are several different types of collecting surfaces composing the meadow, each having its own typical "V" shaped deposition velocity curve. These curves operate roughly at the same order of magnitude and the various minima are not coinciding. The superposition of these different single element deposition curves, with sharp minima, form a composite curve with a broad minimum.

The spread in the minimum depends on the detailed structure of the surface; this information is generally not available and was not given to us for the purposes of this analysis. A meadow surface was defined to consist of bare soil, freshly cut grass, pasture, and crops such as harvestable corn. We therefore assume the deposition velocity to be constant across the transition region ($0.1 < d_p < 1.0$ μm).

To extrapolate the deposition velocities beyond the transition region values, Equations (7) and (9) can be used. For particle diameters less than 0.1 μm, where diffusion processes dominate, Equation (7) was used. For particle diameters greater than 1 μm, where interception and impaction effects are greater than diffusion, Equation (9) was used. These extrapolated values are shown in Figure B-1 (solid curve).

Over of the wide range of surface and meteorological conditions covered by the Nicholson and Davies[37] field study (78 data points), the distribution of the deposition velocities was approximately normal. To represent the subjective probability distribution, the standard deviations from the field data were used. The 95% level for $0.1 < d_p < 1.0$ μm was set at two standard deviations (2σ) above the mean; 4σ was used for the 100% level.

Table B-1. Summary of data for dry deposition to meadow surfaces

Study	surface	spec.	d_P µm	u m/s	u_* cm/s	d cm	z_0 cm	v_d cm/s
Allen et al.[1]	grass	$SO_4^=$	0.1–2.0	1.7–6.7	11–40	2–5	——	-0.33–0.57
Garland and Cox[18]	grass	$SO_4^=$	0.05–1.0	1.3–6.5	——	8	1.5	0.06±0.03
Horbert et al.[24]	grass	$CuSO_4$	3.0–6.5	0.6–3.1	8–43	——	10	0.022–0.18
Little and Wiffen[30]	grass	Pb	0.03–0.045	0.8–5.0	——	——	——	0.25–4.36
Nicholson and Davies[37]	grass barley	$SO_4^=$	0.1–1.0	1.1–6.0	6–41	8–31	0.1–4.3	-0.5–0.6

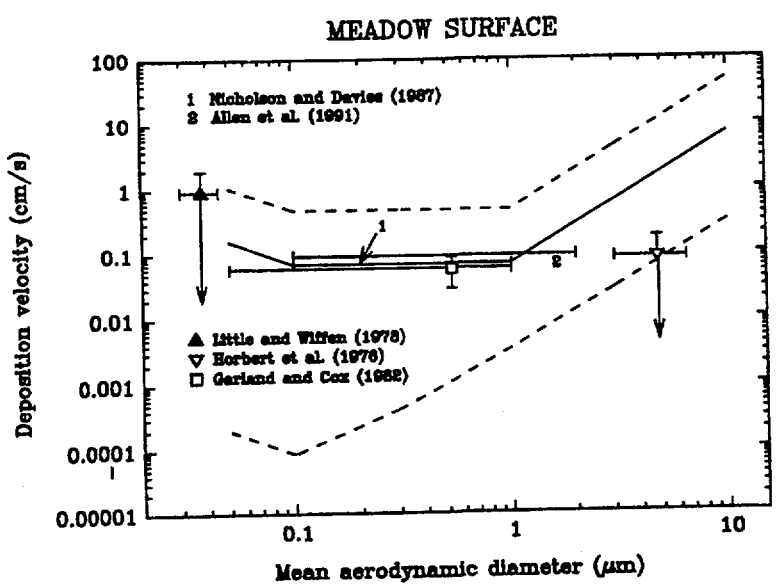

Figure B-1. Dry deposition velocities based on concentrations at 1 m height for meadow surfaces under various meteorological conditions. Solid curve corresponds to data of Nicholson and Davies[37] (full data set) and extrapolations based on Fernandez de la Mora and Friedlander.[12] Dashed curves indicate the 5% and 95% confidence levels. Error bars on deposition velocities represent one standard deviation; error bars on particle diameter represent range of size distribution. Arrows indicate negative value for lower limit of uncertainty. The reason for the broad minimum is probably that the field data represent the superposition of many different single element deposition curves, with sharp minima, to form a composite curve with a broad minimum.

Because the lower limit (0%) based on the standard deviation is negative, the terminal settling velocity for the nominal particle size was used for the lower level for $d_P > 0.1$ μm. By placing this lower limit on the dry deposition velocity based on physical constraints, we have altered the probability distribution function (PDF) for v_D. If we assume the upper half (>50%) to follow a normal distribution, but cut the lower half at a physical limit, the lower half of the PDF must be skewed to satisfy the constraint that the area under the curve is unity. We assumed the lower half of the PDF to follow a lognormal distribution. The geometric mean and standard deviation were determined from the arithmetic mean and standard deviation,[19] and the cumulative lognormal distribution was solved to determine the 5% level.

Equations (7) and (9) were again used to extrapolate 5% and 95% values beyond the transition region. The 5% and 95% levels are also shown in Figure B-1 (dashed curves).

To determine the estimated dry deposition velocities at wind speeds of 2 and 5 m/s (at 10 m height), the subset of the Nicholson and Davies[37] data for those wind speeds, the subsets consisting of 20 and 32 data points, respectively, were averaged. The wind speeds at 10 m height were calculated assuming a logarithmic wind profile,

$$\frac{u(z)}{u_*} = \kappa \ln\left(\frac{z-d}{z_0}\right) \qquad (10)$$

where κ is the von Kármán constant. The mean values for each subset were assumed to be valid for particle sizes between 0.1 and 1.0 μm. These were scaled using Equation (9) to yield estimates for the larger particle sizes requested. Again, the 95% level for $0.1 < d_P < 1.0$ μm was set at 2σ above the mean, and the 100% level at 4σ. The 5% level was calculated by assuming a lognormal distribution for the lower half of the PDF. The 0% level was set at the terminal settling velocity for the nominal particle size.

Forest surfaces

Vegetation is an important sink for airborne material. Because of their large surfaces of interaction, the foliage of vegetative canopies serve as very effective receptors for particles. Only a few studies have been reported using natural foliar surfaces as particle deposition collectors. This stems from the increased difficulty of obtaining representative measurements. The wide range of surfaces on which deposition occurs makes direct measurements difficult. Profile techniques are also more difficult because of anomalies in the flux-gradient relationship for forests.[44,23]

Several studies have been published where the deposition onto leaf surfaces is directly measured, either by sequential extraction of leaves[29] or by *in situ* removal of the deposited material.[11,48] These studies took place in rural and suburban areas near Detroit, MI,[11] Walker Branch Watershed in eastern Tennessee,[29] and Black Forest, FRG.[48]

The total surface area of leaves is considerably larger than the soil surface over which they are situated. Because results are reported as particle fluxes to individual surfaces in the forest canopy, it is necessary to adjust these deposition velocities for the full canopy effect. This requires knowledge of representative leaf areas per unit of ground area. This quantity, known as the leaf area index (LAI), has been measured for different tree species. Typical values range from 3 to 11, with an average of ~6, and are summarized in Table B-2.

Lindberg and Harriss[29] and Shanley[48] reported dry deposition velocities based on concentrations of the depositing species measured above the canopy height. In order to determine the dry deposition velocity in terms of the concentration at the 1 m reference height, we need to estimate this reference concentration based on the above-canopy measurements. Gravenhorst and Höfken[20] measured the concentrations of atmospheric aerosol particles above and beneath the canopies of a beech and a spruce forest to determine the filtering effect of a closed stand of trees. The two forests consisted of about 25 to 30 m high trees. The concentration beneath the canopy normalized by the concentration above ranged from 63 to 75% for beech and 59 to 77% for spruce. We therefore adopted a mean value of 68% to scale the concentration from its value above the forest canopy to its value at 1 m. Dasch[11] sampled ambient air below the trees, therefore his results were not scaled in this manner.

Figure B-2 shows the dry deposition velocities from the published field studies. These data are also summarized in Table B-3. The data for the particle sizes 0.1 to 1.0 μm were averaged to determine our estimate of the dry deposition velocity in the transition region, with the 95% level at 2σ and the 100% level at 4σ. The 5% level was calculated by assuming a lognormal distribution for the lower half of the PDF. The 0% level was taken to be the terminal settling velocity multiplied by the lowest LAI in Table B-2 (3.0). We used Equations (7) and (9) to determine dry deposition velocities in the diffusion- and interception-controlled size ranges. These values are represented in Figure B-2 by the solid curve.

Table B-2. Leaf area indices (LAI) for different tree species

Tree species	LAI	Reference
Common beech	6.5	Jonas and Heinemann[27]
Silver birch	5.3	Jonas and Heinemann[27]
Douglas fir	3.0	Fritschen et al.[16]
Hornbeam	8.0	Jonas and Heinemann[27]
Horse chestnut	5.0	Jonas and Heinemann[27]
European larch	3.0	Jonas and Heinemann[27]
Japanese larch	4.6	Jonas and Heinemann[27]
Norway maple	5.0	Jonas and Heinemann[27]
Red maple	5.0–11.6	Miller and Lin[35]
Common oak	3.7–9.0	Dasch[11] Hutchison et al.[26] Jonas and Heinemann[27]
Red oak	4.3	Jonas and Heinemann[27]
Austrian pine	6.0	Dasch[11]
Scots pine	3.9–6.6	Halldin[21] Jonas and Heinemann[27]
Spruce	11.0	Jonas and Heinemann[27]

The wind speed was not reported for these studies, so a typical value of 1 m/s at 10 m height was assumed.[44] To scale the values up for 2 and 5 m/s, Equations (5) and (8) were used. In the diffusion range,

$$v_d \sim u^{1/2} \qquad (11)$$

and in the interception range,

$$v_d - v_s \sim u^{3/2} \qquad (12)$$

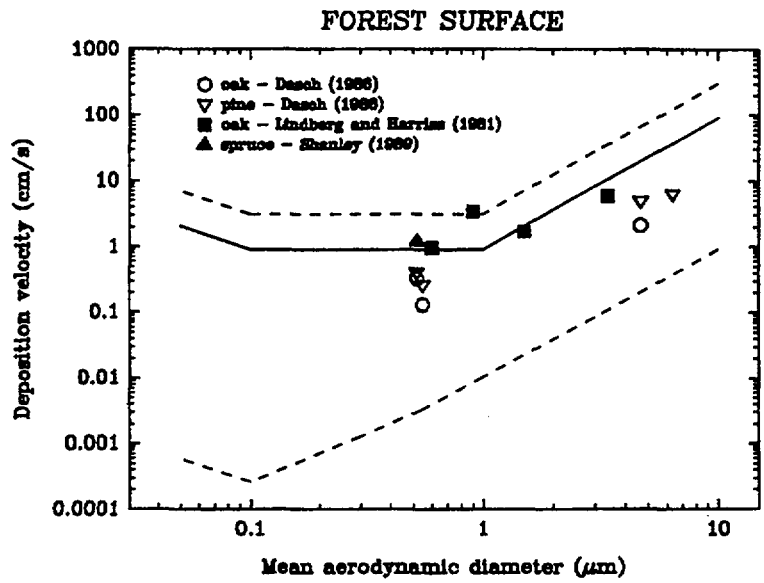

Figure B-2. Dry deposition velocities for forest surfaces under various meteorological conditions. Solid curve represents extrapolations based on Fernandez de la Mora and Friedlander.[12] Dashed curves indicate the 5% and 95% confidence levels. Wind speed assumed to be 0.5 m/s at 10 m height.[14]

Table B-3. Summary of data for dry deposition to forest surfaces

Study	forest type (LAI)	species	d_p μm	v_d (leaf) cm/s	v_d (canopy)[1] cm/s
Dasch[11]	oak (6.0)	Pb^{++}	0.55[†]	0.015	0.09
		Ca^{++}	4.64[†]	0.24	1.44
		$SO_4^{=}$	0.52[‡]	0.037	0.22
	pine (9.0)	Pb^{++}	0.55[†]	0.020	0.18
		Ca^{++}	4.64[†]	0.37	3.33
		$SO_4^{=}$	0.52[‡]	0.030	0.27
		Mg^{++}	6.34[†]	0.47	4.23
Lindberg and Harriss[29]	chestnut oak (5.0)	Cd	1.5	0.23	1.69
		Mn	3.4	0.8	5.88
		Zn	0.9	0.46	3.38
		$SO_4^{=}$	0.6	0.13	0.96
Shanley[48]	young spruce (2.5)	$SO_4^{=}$	0.52[‡]	0.33	1.21

[1]Deposition velocity adjusted for leaf area index (LAI) and 68% reduction in concentration between top of forest canopy and 1 m reference height (when necessary)
[†]Milford and Davidson[34]
[‡]Milford and Davidson[31]

Urban surfaces

Previous work in urban environments has largely made use of surrogate surfaces for deposition collection.[39,43] To avoid placing undue emphasis on any particular surrogate surface, we opted to focus on indirect means for measuring urban dry deposition. Gradient techniques are questionable because of the large spacing between buildings, the limited extent of areas of uniform housing, and the existence of local pollution sources.[36]

Main and Friedlander[31] used the dual tracer method during the Southern California Air Quality Study (SCAQS) to estimate dry deposition in urban areas. The deposition velocity can be estimated from measurements of the ratio of the concentration of a depositing tracer species (c_2), such as Pb or ZnS, to a nondepositing (conserved) tracer species (c_1), such as CO or SF_6, when both originate from the same source. Deposition of species 2 takes place continuously so the ratio c_2/c_1 in the atmosphere differs from the concentration in the source c_{20}/c_{10}. The difference depends on the average residence time of the air flowing through the region of interest and the deposition velocity. Further details on the dual tracer method are given by Friedlander et al.[15] and Main and Friedlander.[31]

This model makes a continuously stirred atmosphere approximation for an air basin and accounts for particle growth. Average wind speeds during the SCAQS study were ~2 m/s.[50] The dry deposition velocities at wind speeds of 5 m/s were determined using Equations (5) and (8). The results for Los Angeles are shown in Figure B-3. These dry deposition velocities were assumed to be representative of a typical urban environment. The 95% level corresponds to the upper bound on the experimental error determined by Main and Friedlander.[31] Assuming the 95% level represents 2σ, the 100% level was set at 4σ. The 5% level was calculated by assuming a lognormal distribution for the lower half of the probability distribution function. The 0% level is the terminal settling velocity for the nominal particle size.

Human skin

For estimating dry deposition to human skin, we assume the head to be the skin that is exposed to a passing plume, and we approximate the head as a spherical collecting element. Parnas and Friedlander[40] developed the following relationship for particle deposition to a sphere by diffusion and interception:

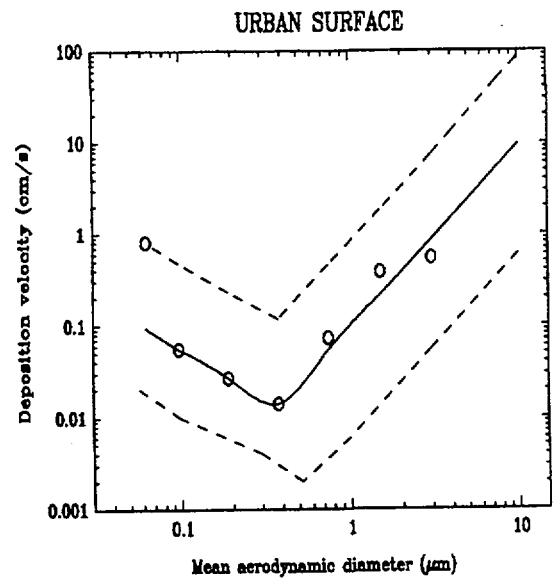

Figure B-3. Dry deposition velocities for urban surfaces. Data (open circles) taken from Main and Friedlander[31] for Los Angeles, 1987, using the dual tracer method. Solid curve represents extrapolations based on Fernandez de la Mora and Friedlander.[12]

$$\frac{kd_P}{D} = \frac{2.4\mu + 1.1\mu^3}{4} \qquad (13)$$

where μ is defined by Equation (3) and the diameter of the collecting element d_{col} (assumed to be 25 cm for a human head) is the characteristic length. These parameters are summarized in Table B-4.

To evaluate the role of impaction in particle deposition to the head, the Stokes number $Stk=\rho_P d_P^2 u_\infty/18\mu a$, is an important parameter. Impaction becomes significant when the $Stk>0.2$.[14] However, as shown in Table B-4, the Stokes number never exceeds 0.012. Therefore gravitational settling and diffusion are the only significant mechanisms for deposition to the head.

The 50% level was determined by using Equation (13) for the nominal particle size. The 95% level was also determined with Equation (13) for the maximum in the particle size range. This 95% level was assumed to represent 2σ, and the 100% level was set at 4σ. The 5% level is the terminal settling velocity for the nominal particle size, and the 0% level is the terminal settling velocity for the minimum in each size range.

These low values for v_d suggest that dry deposition is not a significant route of exposure to humans. However, these results do not account for deposition to the lungs due to inhalation, which is a major exposure pathway.

Elemental Iodine and Methyl Iodide

A number of studies have been published on the transport of elemental iodine and methyl iodide to the ground. These data are summarized in Table B-5. The studies cover a wide range of meteorological conditions and atmospheric stability; therefore the values reported from these studies will be the basis of our estimated deposition velocities. The most extensive data set was given by Heinemann et al.[22] for a grass/clover surface. We therefore selected the averages of their subsets of data with wind speeds of 2 m/s and 5 m/s at 10 m height to represent our 50% estimated values for v_d; the 95% value was two standard deviations above the mean, and the 5% value was the minimum value in the data subset. The corresponding values for a forest surface were adjusted for LAIs of 3, 6, and 11 for the 5%, 50%, and 95% levels. Deposition to urban surfaces were taken to be the same as the values for grass.

Atkins et al.[2] found methyl iodide to be poorly absorbed by vegetation. In a series of experiments, with a wind speed of 6.2 m/s at 2 m height, a roughness length of 2 cm, and a friction velocity of 52 cm/s, they measured dry deposition velocities to grass ranging from 1.4×10^{-4} to 2.4×10^{-3} cm/s, with an average of 1.0×10^{-3} cm/s. These lower, mean, and upper values were taken to be the 5%, 50%, and 95% level values of the dry deposition velocity to grass, scaling for the wind speed using Equation (11). For forest surfaces, the values for grass were multiplied by LAIs of 3, 6, and 11 for the 5%, 50%, and 95% levels, respectively.

For deposition of I_2 and CH_3I to human skin, Equation (13) was used. For gases, only the diffusion range needs to be considered. Therefore Equation (13) reduces to:

$$v_d = \frac{2.4}{4}\left(\frac{u_* R}{\nu}\right)^{1/2}\left(\frac{(\nu D^2)^{1/3}}{R}\right) \qquad (14)$$

The dry deposition velocities calculated by this equation were taken to represent the 50% level. The 5% and 0% levels were taken at 2 and 3 orders of magnitude below this value, and the 95% and 100% values at 1 and 2 orders of magnitude above. These were comparable to the levels of uncertainty for the other surface types.

Specific Surface I: Moorland/Peatland

The moorland/peatland surface has 40 cm high tussocks and a surface roughness of 5±1 cm. Assuming the zero-displacement height to be three fourths the height of the vegetation, as suggested by Hosker and Lindberg,[25] d≈30 cm. Therefore, assuming a logarithmic wind profile, the wind speed at 1 m height is 2.9±0.1 m/s. From the data of Nicholson and Davies,[37] the dry deposition velocity of sulfate for similar conditions (u=2.3 m/s, d=31 cm, z_0=0.4 cm) is 0.21 cm/s.

Table B-4. Parameters for determining deposition to human skin, based on spherical collecting element d_{col}=25 cm

d_P (μm)	D (cm²/s)	Re (u=2)	Re (u=5)	Sc	μ (u=2)	μ (u=5)	Stk
0.1	6.8E-06	1.7E+04	4.1E+04	2.2E+04	1.90	3.01	1.2E-06
0.3	1.2E-06	1.7E+04	4.1E+04	1.2E+05	0.377	0.597	1.1E-05
1.0	2.7E-07	1.7E+04	4.1E+04	5.5E+05	0.0844	0.133	1.2E-04
3.0	8.3E-08	1.7E+04	4.1E+04	1.8E+05	0.0153	0.0243	1.1E-03
10.0	2.4E-08	1.7E+04	4.1E+04	6.3E+06	0.00289	0.00458	1.2E-02
I_2	0.0930	1.7E+04	4.1E+04	1.62	——	——	——
CH_3I	0.0870	1.7E+04	4.1E+04	1.73	——	——	——

As was done for the general meadow surface, the standard deviation for the entire Nicholson and Davies[37] data set was used to determine the 95% and 100% levels, and the terminal settling velocities for the nominal particle size were used for the 0% level. The 5% level was calculated by assuming a lognormal distribution for the lower half of the PDF. These values were adjusted for the higher wind speed using Equation (12) and for larger particle sizes using Equation (9).

Specific Surface II: Heather and Green Grass

The heather and green grass has a surface roughness length of 4.5±1.5 cm. By comparison with Nicholson and Davies,[37] we assumed a zero-displacement height of 10 cm, which yields a wind speed at 1 m height of 3.2±0.1 m/s. From Nicholson and Davies,[37] the dry deposition velocity for similar conditions (u=1.5 m/s, d=9 cm, z_0=4.3 cm) is 0.08 cm/s. Again, the standard deviation for the entire Nicholson and Davies[37] data set was used to determine the 95% and 100% levels, and the terminal settling velocities for the nominal particle size were used for the 0% level. The 5% level was calculated by assuming a lognormal distribution for the lower half of the PDF. These values were then adjusted for wind speed and particle size.

Specific Surface III: Grassland

The dry deposition velocity on grassland with unknown meteorological parameters was taken to be the average from the entire Nicholson and Davies[37] field study. This is the range represented by Figure B-1.

Table B-5. Summary of elemental iodine and methyl iodide dry deposition data

Study	surface	u m/s	u_* cm/s	d cm	z_0 cm	v_d cm/s
IODINE						
Bunch[3]	grass	0.6–5.0	—	—	—	0.087–3.5
Chamberlain[5]	grass	1.4–4.4	24–57	—	1.0–5.0	1.1–3.7
Chamberlain and Chadwick[7]	grass clover	1.8–5.6	24–57	5–25	0.8–9.5	0.93–2.94
Clark and Smith[8]	grass	—	—	—	—	0.27–0.3
Heinemann et al.[22]	grass clover	0.52–4.8	6–60	—	—	0.31–6.3
Vögt et al.[51]	grass clover	1.1–5.1	14–53	—	1.1–9.1	0.12–6.9
Zimbrick and Voilleqúe[54]	grass	6.3–6.6	76–82	—	—	2.0–2.4
average						1.38
standard deviation						1.29
METHYL IODIDE						
Atkins et al.[2]	grass	6.2	52	—	2.0	1.4×10^{-4} – 2.4×10^{-3}
Bunch[3]	grass	3.7	—	—	—	1.0×10^{-4}
average						1.0×10^{-3}

Wet Deposition

Wet deposition is often represented as an exponential decay process:[9]

$$\frac{dc}{dt} = -\Lambda c \qquad (15)$$

where Λ is the scavenging coefficient, which is a function of particle size and rainfall intensity, among other factors.[49] This equation can be integrated to determine the fraction of a species in a plume remaining:

$$\frac{c}{c_0} = \exp(-\Lambda t) \qquad (16)$$

Aerosols

Wet removal processes by which aerosol particles may be scavenged include diffusion, interception, and inertial capture.[41] The scavenging coefficient can be approximated by Slinn:[49]

$$\Lambda(a) = \frac{p}{2R_m} E(a, R_m) \qquad (17)$$

where a is the particle radius, p is the rainfall rate (mm h^{-1}), R_m is the mass mean raindrop radius, and $E(a, R_m)$ is the collection efficiency. For R_m, Slinn[49] uses:

$$R_m = 0.35\,\mathrm{mm}\,(p/1\,\mathrm{mm\,h^{-1}})^{0.25} \qquad (18)$$

for steady frontal rain. The collection efficiency varies according to the nature of the controlling process:[10]

$$E(a,R_m) = (0.65\times10^{-12})\left[\frac{10^{-7}}{a^2R_m^2} + \frac{1}{a^{4/3}R_m}\right] + 3\frac{a}{r_m} + \left[\frac{S-1/12}{S+7/12}\right]^{3/2} \qquad (19)$$

where the three RHS terms represent collection by diffusion, interception, and impaction. The Stokes parameter S is approximated by:

$$S = 0.1\times10^8 a^2 \rho_P \qquad (20)$$

(a in cm, ρ_P in g cm^{-3}). Combining Equations (18) through (20) with (17), the scavenging coefficient is plotted in Figure B-4 as a function of particle diameter and rainfall rate.

Limited field data are available to evaluate these equations, especially in the submicron range. Comparison with literature data[32,42,38] suggests that theoretical values may underpredict Λ by as much as two orders of magnitude. For our calculations, we assume the following: the median value for the fraction removed is calculated by Equations (16) and (17); the 95% level is calculated using a value of Λ two orders of magnitude higher, the 100% level three orders of magnitude higher, the 5% level at one order of magnitude lower, and the 0% level at two orders of magnitude lower. Because Equation (18) approximates the mean raindrop radius under steady rain conditions, R_m was reduced by 20% for drizzle conditions and increased by 20% for showers.

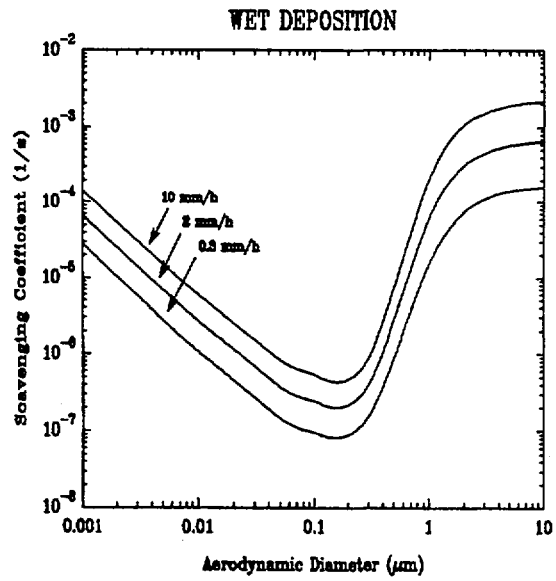

Figure B-4. Scavenging coefficient for particles as a function of particle diameter and rainfall rate, based on the semi-empirical equations of Slinn[49] and Dana and Hales.[10]

Elemental iodine and methyl iodide

Jylhä[28] investigated the precipitation scavenging of radioactive pollutants released from Chernobyl in Southern Finland. He found that for I^{131}, the scavenging coefficient

could be related to the precipitation rate by:

$$\Lambda = ap^{b} \tag{21}$$

where $a=(7\pm5)\times10^{-5}$ and $b=0.69\pm0.12$. It should be noted that these parameters were determined for particle-bound iodine; the removal of gaseous iodine by rain was ineffective.

Because of widespread concern over acid precipitation, the scavenging of SO_2 by rainfall has been studied extensively.[52,53] Scavenging coefficients have been reported[32] for SO_2 and are on the order of 10^{-5} s^{-1}. The rate of SO_2 uptake[32] is controlled by a coupled resistance to diffusion inside and outside the rain drops. Because the solubility of methyl iodide is about an order of magnitude lower than for SO_2, so we will assume that Λ for CH_3I is also an order of magnitude lower than for SO_2. Our estimates of the fraction of methyl iodide remaining are based on the following:

$$\Lambda = 17\times10^{-6}p^{0.6} . \tag{22}$$

Deposition Tables

Units of velocity are in cm/s; N/A = not provided by expert; unkn = unknown

DD-A: Dry deposition velocity of aerosols - Wind Speed at 2m/s					
PARTICLE SIZE	QUANTILE	URBAN	MEADOW	FOREST	HUMAN SKIN
0.10μ	0%	8.63E-05	8.63E-05	7.32E-04	3.75E-05
	5%	4.71E-02	4.47E-03	7.78E-01	8.63E-05
	50%	2.88E-01	4.85E-02	2.55E+00	1.27E-03
	95%	4.63E-01	3.37E-01	8.70E+00	2.75E-03
	100%	1.22E+00	6.17E-01	1.49E+01	4.23E-03
0.30μ	0%	4.21E-04	4.21E-04	3.58E-03	2.25E-04
	5%	1.54E-02	4.47E-03	7.78E-01	4.21E-04
	50%	9.22E-02	4.85E-02	2.55E+00	7.99E-04
	95%	1.48E-01	3.37E-01	8.70E+00	1.24E-03
	100%	3.89E-01	6.17E-01	1.49E+01	1.68E-03
1.00μ	0%	3.48E-03	3.48E-03	2.96E-02	9.96E-04
	5%	1.23E-02	4.47E-03	7.78E-01	3.48E-03
	50%	7.52E-02	4.85E-02	2.55E+00	3.62E-03
	95%	8.29E-01	3.37E-01	8.70E+00	1.30E-02
	100%	2.17E+00	6.17E-01	1.49E+01	2.24E-02
3.00μ	0%	2.84E-02	2.84E-02	2.41E-01	1.29E-02
	5%	1.14E-01	3.73E-02	6.99E+00	2.84E-02
	50%	6.74E-01	4.34E-01	2.29E+01	2.85E-02
	95%	7.46E+00	3.03E+00	7.83E+01	7.72E-02
	100%	1.96E+01	5.55E+00	1.34E+02	1.26E-01
10.00μ	0%	3.04E-01	3.04E-01	2.58E+00	7.72E-02
	5%	1.23E+00	4.02E-01	7.77E+01	3.04E-01
	50%	7.47E+00	4.81E+00	2.55E+02	3.05E-01
	95%	8.28E+01	3.37E+01	8.70E+02	6.80E-01
	100%	2.17E+02	6.16E+01	1.49E+03	1.06E+00

DD-B: Dry deposition velocity of aerosols - Wind Speed at 5m/s					
PARTICLE SIZE	QUANTILE	URBAN	MEADOW	FOREST	HUMAN SKIN
0.10μ	0%	8.63E-05	8.63E-05	2.90E-03	3.75E-05
	5%	7.60E-02	5.94E-03	3.07E+00	8.63E-05
	50%	4.56E-01	8.32E-02	1.01E+01	1.95E-03
	95%	7.33E-01	5.03E-01	3.44E+01	4.23E-03
	100%	1.92E+00	9.23E-01	5.87E+01	6.69E-03
0.30μ	0%	4.21E-04	4.21E-04	1.41E-02	2.25E-04
	5%	2.45E-02	5.94E-03	3.07E+00	4.21E-04
	50%	1.46E-01	8.32E-02	1.01E+01	1.02E-03
	95%	2.34E-01	5.03E-01	3.44E+01	1.11E-03
	100%	6.15E-01	9.23E-01	5.87E+01	1.20E-03
1.00μ	0%	3.48E-03	3.48E-03	1.17E-01	9.96E-04
	5%	4.75E-02	5.94E-03	3.07E+00	3.48E-03
	50%	2.87E-01	8.32E-02	1.01E+01	3.71E-03
	95%	3.27E+00	5.03E-01	3.44E+01	1.31E-02
	100%	8.58E+00	9.23E-01	5.87E+01	2.25E-02
3.00μ	0%	2.84E-02	2.84E-02	9.52E-01	1.29E-02
	5%	4.33E-01	5.05E-02	2.76E+01	2.84E-02
	50%	2.58E+00	7.46E-01	9.07E+01	2.85E-02
	95%	2.94E+01	4.52E+00	3.10E+02	7.73E-02
	100%	7.73E+01	8.30E+00	5.29E+02	1.26E-01
10.00μ	0%	3.04E-01	3.04E-01	1.02E+01	7.72E-02
	5%	4.77E+00	5.49E-01	3.07E+02	3.04E-01
	50%	2.86E+01	8.28E+00	1.01E+03	3.05E-01
	95%	3.27E+02	5.02E+01	3.44E+03	6.80E-01
	100%	8.58E+02	9.22E+01	5.87E+03	1.06E+00

DD-C: Dry deposition velocity of elemental iodine - Wind Speed at 2 and 5m/s					
WIND SPEED	QUANTILE	URBAN	MEADOW	FOREST	HUMAN SKIN
2.m/s	0%	1.50E-02	1.50E-02	4.50E-02	6.75E-06
	5%	1.50E-01	1.50E-01	4.50E-01	6.75E-05
	50%	1.40E+00	1.40E+00	8.40E+00	6.75E-03
	95%	4 02E+00	4.02E+00	4.42E+01	6.75E-02
	100%	6 64E+00	6.64E+00	7.30E+01	6.75E-01
5.m/s	0%	4.40E-02	4.40E-02	1.32E-01	1.07E-05
	5%	4.40E-01	4.40E-01	1.32E+00	1.07E-04
	50%	1.88E+00	1.88E+00	1.13E+01	1.07E-02
	95%	3.82E+00	3.82E+00	4.20E+01	1.07E-01
	100%	5.76E+00	5.76E+00	6.34E+01	1.07E+00

DD-D: Dry deposition velocity of methyl iodide - Wind Speed at 2 and 5m/s					
WIND SPEED	QUANTILE	URBAN	MEADOW	FOREST	HUMAN SKIN
2.m/s	0%	6.84E-06	6.84E-06	2.05E-05	6.46E-06
	5%	6.84E-05	6.84E-05	2.05E-04	6.46E-05
	50%	4.89E-04	4.89E-04	2.93E-03	6 46E-03
	95%	1.17E-03	1.17E-03	1.29E-02	6.46E-02
	100%	1.85E-03	1.85E-03	2.29E-02	6.46E-01
5.m/s	0%	1.08E-05	1.08E-05	3.24E-05	1.02E-05
	5%	1.08E-04	1.08E-04	3.24E-04	1.02E-04
	50%	7.73E-04	7.73E-04	4.64E-03	1.02E-02
	95%	1.85E-03	1.85E-03	2.04E-02	1.02E-01
	100%	2.93E-03	2.93E-03	3.62E-02	1.02E+00

DD-E-1: Dry deposition velocity of aerosols on Moorland/Peatland Surface		
PARTICLE SIZE	QUANTILE	
0.55μ	0%	1.18E-03
	5%	1.81E-01
	50%	2.97E-01
	95%	6.97E-01
	100%	1.10E+00
0.70μ	0%	1.81E-03
	5%	1.81E-01
	50%	2.97E-01
	95%	6.97E-01
	100%	1.10E+00
0.90μ	0%	2.87E-03
	5%	1.81E-01
	50%	2.97E-01
	95%	6.97E-01
	100%	1.10E+00
1.20μ	0%	4 90E-03
	5%	3.22E-01
	50%	5.28E-01
	95%	1.24E+00
	100%	1.95E+00
1.60μ	0%	8.44E-03
	5%	5.71E-01
	50%	9.38E-01
	95%	2.20E+00
	100%	3.47E+00

DD-E-2: Dry deposition velocity of aerosols on Heather/Green Grass Surface		
PARTICLE SIZE	**QUANTILE**	
0.55μ	**0%**	1.18E-03
	5%	1.27E-01
	50%	2.47E-01
	95%	6.47E-01
	100%	1.05E+00
0.70μ	**0%**	1.81E-03
	5%	1.27E-01
	50%	2.47E-01
	95%	6.47E-01
	100%	1.05E+00
0.90μ	**0%**	2.87E-03
	5%	1.27E-01
	50%	2.47E-01
	95%	6.47E-01
	100%	1.05E+00
1.20μ	**0%**	4.90E-03
	5%	2.26E-01
	50%	4.39E-01
	95%	1.15E+00
	100%	1.86E+00
1.60μ	**0%**	8.44E-03
	5%	4.01E-01
	50%	7.80E-01
	95%	2.04E+00
	100%	3.31E+00

DD-E-2: Dry deposition velocity of aerosols on Heather/Green Grass Surface (continued)		
PARTICLE SIZE	QUANTILE	
2.30μ	0%	1.69E-02
	5%	8.28E-01
	50%	1.61E+00
	95%	4.22E+00
	100%	6.83E+00
3.20μ	0%	3.22E-02
	5%	1.60E+00
	50%	3.12E+00
	95%	8.17E+00
	100%	1.32E+01
4.20μ	0%	5.48E-02
	5%	2.76E+00
	50%	5.37E+00
	95%	1.41E+01
	100%	2.28E+01

DD-F: Dry deposition velocity of aerosols on Grassland Surface		
PARTICLE SIZE	QUANTILE	
1.0μ	0%	3.48E-03
	5%	3.74E-03
	50%	7.00E-02
	95%	4.70E-01
	100%	8.70E-01

WD-A: Elemental iodine—fraction removed by rain ($1-f_w$)							
Rainfall/ Time	Wind Speed	Quantile	$1-f_w$	Rainfall/ Time	Wind Speed	Quantile	$1-f_w$
.3mm/hr	unkn	0%	5.70E-03	2.mm/hr	unkn	0%	8.29E-03
		5%	4.30E-02			5%	9.37E-02
		50%	1.11E-01			50%	3.34E-01
		95%	1.98E-01			95%	6.88E-01
		100%	2.36E-01			100%	8.88E-01
.075mm/10min	10 m/s	0%	1.01E-03	.05mm/ 10min	unkn	0%	9.31E-04
		5%	8.34E-03			5%	6.96E-03
		50%	2.39E-02			50%	1.81E-02
		95%	4.74E-02			95%	3.27E-02
		100%	6.17E-02			100%	3.88E-02
.17mm/10min	5 m/s	0%	1 20E-03	.17mm/ 10min	14 m/s	0%	1.20E-03
		5%	1.19E-02			5%	1.19E-02
		50%	4.11E-02			50%	4.11E-02
		95%	9.70E-02			95%	9.70E-02
		100%	1.50E-01			100%	1.50E-01
.23mm/10min	12 m/s	0%	1.28E-03	.5mm/10min	unkn	0%	1.51E-03
		5%	1.38E-02			5%	1.95E-02
		50%	5.11E-02			50%	8.57E-02
		95%	1.29E-01			95%	2.47E-01
		100%	2.10E-01			100%	4.43E-01
.33mm/10min	unkn	0%	1.39E-03	1.0mm/ 10min	14 m/s	0%	1.75E-03
		5%	1.63E-02			5%	2.65E-02
		50%	6.55E-02			50%	1.35E-01
		95%	1.77E-01			95%	4.17E-01
		100%	3.05E-01			100%	7.32E-01

WD-A: Elemental iodine—fraction removed by rain ($1\text{-}f_w$) (continued)			
Rainfall/Time	**Wind Speed**	**Quantile**	$1\text{-}f_w$
1.67mm/10min	**unkn**	0%	1.94E-03
		5%	3.33E-02
		50%	1.86E-01
		95%	5.80E-01
		100%	9.09E-01

WD-B: Methyl iodide—fraction removed by rain (Wind Speed=unknown)		
Rainfall/Time	**Quantile**	***1-f$_w$***
.3mm/hr	**0%**	1.22E-03
	5%	1.22E-02
	50%	2.93E-02
	95%	4.61E-02
	100%	6.26E-02
2.mm/hr	**0%**	3.81E-03
	5%	3.75E-02
	50%	8.86E-02
	95%	1.37E-01
	100%	1.83E-01
.05mm/10min	**0%**	2.04E-04
	5%	2.04E-03
	50%	4.94E-03
	95%	7.84E-03
	100%	1.07E-02
.33mm/10min	**0%**	6.35E-04
	5%	6.35E-03
	50%	1.53E-02
	95%	2.43E-02
	100%	3.31E-02
1.67mm/10min	**0%**	1.67E-03
	5%	1.66E-02
	50%	3.98E-02
	95%	6.25E-02
	100%	8.46E-02

WD-C: Fraction of aerosols removed by rain						
PARTICLE SIZE	QUANTILE	Rainfall: .3mm/hr	Rainfall: 2.mm/hr	Rainfall: .05mm/10 min	Rainfall: .33mm/10 min	Rainfall: 1.67mm/10 min
0.10μ	0%	3.40E-06	8.75E-06	8.87E-07	1.46E-06	2.26E-06
	5%	3.40E-05	8.75E-05	8.87E-06	1.46E-05	2.26E-05
	50%	3 40E-04	8.75E-04	8.87E-05	1.46E-04	2.26E-04
	95%	3.34E-02	8.38E-02	8.83E-03	1.45E-02	2.24E-02
	100%	2.88E-01	5.83E-01	8.48E-02	1.36E-01	2.02E-01
0.30μ	0%	5.43E-06	1.40E-05	1.41E-06	2.33E-06	3.62E-06
	5%	5.43E-05	1.40E-04	1.41E-05	2.33E-05	3.62E-05
	50%	5.42E-04	1.40E-03	1.41E-04	2.33E-04	3.62E-04
	95%	5.28E-02	1.31E-01	1.40E-02	2.31E-02	3.56E-02
	100%	4.19E-01	7.54E-01	1.32E-01	2.08E-01	3.04E-01
1.00μ	0%	5.35E-04	2.19E-03	1.12E-04	3.65E-04	1.01E-03
	5%	5.33E-03	2.17E-02	1.12E-03	3.65E-03	1.00E-02
	50%	5.21E-02	1.97E-01	1.12E-02	3.59E-02	9.60E-02
	95%	9.95E-01	9.97E-01	6.75E-01	9.74E-01	9.95E-01
	100%	9 99E-01	9.99E-01	9.99E-01	9.99E-01	9.99E-01
10.00μ	0%	5.72E-03	2.33E-02	1.20E-03	3.91E-03	1.08E-02
	5%	5.57E-02	2.10E-01	1.20E-02	3.85E-02	1.03E-01
	50%	4.36E-01	9.05E-01	1.13E-01	3.24E-01	6.62E-01
	95%	9.97E-01	9.98E-01	9.97E-01	9.97E-01	9.97E-01
	100%	9.99E-01	9.99E-01	9.99E-01	9.99E-01	9.99E-01

References

1. Allen, A.G., R.M. Harrison, and K.W. Nicholson, "Dry Deposition of Fine Aerosol to a Short Grass Surface," *Atmospheric Environment*, 25A:2671-2676, 1991.

2. Atkins, D.H.F., R.C. Chadwick, and A.C. Chamberlain, "Deposition of Radioactive Methyl Iodide to Vegetation," *Health Physics*, 13:91-92, 1967.

3. Bunch, D.F., "Controlled Environmental Radioiodine Tests, Progress Report No. 3," IDO-12063, Idaho Operations Office (AEC), available National Technical Information Service, U.S. Dept. of Commerce, Springfield, VA, January 1968.

4. Businger, J. A., "Evaluation of the Accuracy with Which Dry Deposition Can Be Measured with Current Micrometeorological Techniques," *Journal of Climate and Applied Meteorology*, 25:1100-1124, 1986.

5. Chamberlain, A.C., "Aspects of the Deposition of Radioactive and Other Gases and Particles," *International Journal of Air Pollution*, 3:63-88, 1960.

6. Chamberlain, A.C., and R.C. Chadwick, "Transport of Iodine from Atmosphere to Ground, *Tellus*, XVIII:226-237, 1966.

7. Chamberlain, A.C., and R.C. Chadwick, "Deposition of Air-Borne Radioiodine Vapor," *Nucleonics*, 8:22-25, 1953.

8. Clark, M.J., and F.B. Smith, "Wet and Dry Deposition of Chernobyl Releases," *Nature*, 332:245-249, 1988.

9. Dana, M.T., "Overview of Wet Deposition and Scavenging," (D.S. Shriner, C.R. Richmond, and S.E. Lindberg, eds.), *Atmospheric Sulfur Deposition: Environmental Impact and Health Effects, Proceedings of the Second Life Sciences Symposium, Potential Environmental and Health Consequences of Atmospheric Sulfur Deposition, 14-18 October 1979*, Ann Arbor Science, Ann Arbor, MI, pp. 263-274, 1980.

10. Dana, M.T., and J.M. Hales, "Statistical Aspects of the Washout of Polydisperse Aerosols," *Atmospheric Environment*, 10:45-50, 1976.

11. Dasch, J.M., "Measurement of Dry Deposition to Vegetative Surfaces," *Water, Air, & Soil Pollution*, 30:205-210, 1986.

12. Fernandez de la Mora, J., and S.K. Friedlander, "Aerosol and Gas Deposition to Fully Rough Surfaces: Filtration Model for Blade-Shaped Elements," *International Journal of Heat and Mass Transfer*, 25:1725-1735, 1982.

13. Friedlander, S.K., "A Review of the Dynamics of Sulfate Containing Aerosols," *Atmospheric Environment*, 12:187-195, 1978.

14. Friedlander, S.K., *Smoke, Dust, and Haze*, John Wiley & Sons, New York, 1977.

15. Friedlander, S.K., J.R. Turner, and S.V. Hering, "A New Method for Estimating Dry Deposition Velocity for Atmospheric Aerosols," *Journal of Aerosol Science*, 17:240-244, 1986.

16. Fritschen, L.J., J. Hsia, and P. Doraiswamy, "Evapotranspiration of a Douglas Fir Determined With a Weighing Lysimeter," *Water Resources Research*, 13:145-148, 1977.

17. Garland, J.A., "The Dry Deposition of Sulphur Dioxide to Land and Water Surfaces," *Proceedings of the Royal Society of London*, A354:245-268, 1977.

18. Garland, J.A., and L.C. Cox, "Deposition of Small Particles to Grass," *Atmospheric Environment*, 16:2699-2702, 1982.

19. Georgopoulos, P.G., and J.H. Seinfeld, "Statistical Distributions of Air Pollutant Concentrations," *Environmental Science and Technology*, 16:401A-416A, 1982.

20. Gravenhorst, G., and K.D. Höfken, "Concentration of Aerosol Constituents Above and Beneath a Beech and a Spruce Forest Canopy," (H.-W. Georgii and J. Pankrath, eds.), *Deposition of Atmospheric Pollutants, Proceedings of a Colloquium, 9-11 November 1981*, D. Reidel, Boston, MA, pp. 187-190, 1982.

21. Halldin, S., "Leaf and Bark Area Distribution in a Pine Forest," *The Forest-Atmosphere Interaction*, (B.A. Hutchison and B.B. Hicks, eds.), D. Reidel, Boston, MA, pp. 39-58, 1985.

22. Heinemann, K.M., et al., "Studies on the Deposition and Release of Iodine on Vegetation," ORNL-tr-4313, available National Technical Information Service, U.S. Dept. of Commerce, Springfield, VA, 1967.

23. Hicks, B.B., "Application of Forest Canopy-Atmosphere Turbulent Exchange Information," (B.A. Hutchison and B.B. Hicks, eds.), *The Forest-Atmosphere Interaction, Proceedings of the Forest Environmental Measurements Conference, 23-28 October 1983*, D. Reidel, Boston, MA, pp. 631-644, 1985.

24. Horbert, M., K.J. Vogt, and L. Angeletti, "Studies on the Deposition of Aerosols on Vegetation and Other Surfaces," ORNL-tr-4314, Oak Ridge National Laboratory, Oak Ridge, TN, April 1976.

25. Hosker, R.P., and S.E. Lindberg, "Review: Atmospheric Deposition and Plant Assimilation of Gases and Particles," *Atmospheric Environment*, 16:889-910, 1982.

26. Hutchison, B.A., et al., "The Architecture of a Deciduous Forest Canopy in Eastern Tennessee, U.S.A.," *Journal of Ecology*, 74:635-646, 1986.

27. Jonas, R., and K. Heinemann, "Studies on the Dry Deposition of Aerosol Particles on Vegetation and Plane Surfaces," *Journal of Aerosol Science*, 16:463-471, 1985.

28. Jylhä, K., "Precipitation Scavenging of Radioactive Substances Released from the Chernobyl Power Plant," Report 38, Dept. of Meteorology, University of Helsinki, Finland, 1990.

29. Lindberg, S.E., and R.C. Harriss, "The Role of Atmospheric Deposition in an Eastern U.S. Deciduous Forest," *Water, Air, & Soil Pollution*, 16:13-31, 1981.

30. Little, P., and R.D. Wiffen, "Emission and Deposition of Lead from Motor Exhausts — II. Airborne Concentration, Particle Size and Deposition of Lead Near Motorways," *Atmospheric Environment*, 12:1331-1341, 1978.

31. Main, H.H., and S.K. Friedlander, "Dry Deposition of Atmospheric Aerosols by Dual Tracer Method—I. Area Source," *Atmospheric Environment*, 24A:103-108, 1990.

32. McMahon, T.A., and P.J. Denison, "Empirical Atmospheric Deposition Parameters — A Survey," *Atmospheric Environment*, 13:571-585, 1979.

33. Milford, J.B., and C.I. Davidson, "The Sizes of Particulate Sulfate and Nitrate in the Atmosphere — A Review," *Journal of the Air Pollution Control Association*, 37:125-134, 1987.

34. Milford, J.B., and C.I. Davidson, "The Sizes of Particulate Trace Elements in the Atmosphere — A Review," *Journal of the Air Pollution Control Association*, 35:1249-1260, 1985.

35. Miller, D.R., and J.D. Lin, "Canopy Architecture of a Red Maple Edge Stand Measured by a Point Drop Method," (B.A. Hutchison and B.B. Hicks, eds.), *The Forest-Atmosphere Interaction, Proceedings of the Forest Environmental Measurements Conference, 23-28 October 1983*, D. Reidel, Boston, MA, pp. 59-70, 1985.

36. Nicholson, K.W., "The Dry Deposition of Small Particles: A Review of Experimental Measurements," *Atmospheric Environment*, 22:2653-2666, 1988.

37. Nicholson, K.W., and T.D. Davies, "Field Measurements of the Dry Deposition of Particulate Sulphate," *Atmospheric Environment*, 21:1561-1571, 1987.

38. Nicholson, K.W., J.R. Branson, and P. Giess, "Field Measurements of the Below-Cloud Scavenging of Particulate Material," *Atmospheric Environment*, 25A:771-777, 1991.

39. Noll, K.E., P.-F. Yuen, and K.Y.-P. Fang, "Atmospheric Coarse Particulate Concentrations and Dry Deposition Fluxes for Ten Metals in Two Urban Environments," *Atmospheric Environment*, 24A:903-908, 1990.

40. Parnas, R., and S.K. Friedlander, "Particle Deposition by Diffusion and Interception from Boundary Layer Flows," *Aerosol Science and Technology*, 3:3-8, 1984.

41. Pruppacher, H.R., and J.D. Klett, *Microphysics of Clouds and Precipitation*, D. Reidel, Boston, MA, 1978.

42. Radke, L.R., P.V. Hobbs, and M.W. Eltgroth, "Scavenging of Aerosol Particles by Precipitation," *Journal of Applied Meteorology*, 19:715-722, 1980.

43. Rao, P.S.P., et al., "Measurements of Wet and Dry Deposition at an Urban Location in India," *Atmospheric Environment*, 26B:73-78, 1992.

44. Raupach, M.R., "Anomalies in Flux-Gradient Relationships Over Forest," *Boundary-Layer Meteorology*, 16:467-486, 1979.

45. Schack, C.J., Jr., S.E. Pratsinis, and S.K. Friedlander, "A General Correlation for Deposition of Suspended Particles from Turbulent Gases to Completely Rough Surfaces," *Atmospheric Environment*, 19:953-960, 1985.

46. Sehmel, G.A., "Particle and Gas Dry Deposition: A Review," *Atmospheric Environment*, 14:983-1011, 1980.

47. Sehmel, G.A., and W.H. Hodgson, "A Model for Predicting Dry Deposition of Particles and Gases to Environmental Surfaces," (W. Licht, ed.), *Implications of the Clean Air Amendments of 1977 and of Energy Considerations for Air Pollution Control*, Symposium Series No. 196, American Institute of Chemical Engineers, New York, pp. 218-230, 1980.

48. Shanley, J.B., "Field Measurements of Dry Deposition to Spruce Foliage and Petri Dishes in the Black Forest, F.R.G.," *Atmospheric Environment*, 23:403-414, 1989.

49. Slinn, W.G.N., "Some Approximations for the Wet and Dry Removal of Particles and Gases from the Atmosphere," *Water, Air, & Soil Pollution*, 7:513-543, 1977.

50. Taylor, G.H., et al., "Comparisons of SCAQS Upper-Air Conditions with Long-Term Averages for the Los Angeles Basin," In *Proc. Southern California Air Quality Study Data Analysis*, Air & Waste Management Association, Pittsburgh, PA, pp. 237-242, 1993.

51. Vögt, K.J., et al., "Propagation of Pollutants in the Atmosphere and Stress on the Environment," *Investigations on Deposits of Elementary and Organically Bound Iodine on Grass. Result Report: July 1971-December 1972 (Part II)*, BNWL-tr-204, available National Technical Information Service, U.S. Dept. of Commerce, Springfield, VA, August 1976.

52. Walcek, C.J., and H.R. Pruppacher, "On the Scavenging of SO_2 by Cloud and Raindrops: I. A Theoretical Study of SO_2 Absorption and Desorption for Water Drops in Air," *Journal of Atmospheric Chemistry*, 1:269-289, 1984.

53. Walcek, C.J., et al., "On the Scavenging of SO_2 by Cloud and Raindrops: II. An Experimental Study of SO_2 Absorption and Desorption for Water Drops in Air," *Journal of Atmospheric Chemistry*, 1:291-306, 1984.

54. Zimbrick, J.D., and P.G. Voilleqúe, "Controlled Environmental Radioiodine Tests at the National Reactor Testing Station, 1967 Cert Progress Report," Progress Report No. 4, IDO-12065, AEC Operations Office, Idaho Falls, ID, January 1969.

Expert C

Dry Deposition

Information from deposition models and deposition measurements in the Norwegian Arctic has been used to estimate the uncertainty distributions in dry deposition velocity. Three models described by Davidson et al.,[1] Slinn,[2] and Sehmel[3] have been reviewed to calculate dry deposition velocities. Information on form, surface type, aerosol particle size, wind speed, and friction velocity was taken as suggested in the project description and used in the Sehmel model selected for dry deposition velocity calculations. Then the roughness parameters were selected on the basis of literature studies (e.g., a review of our knowledge on dry deposition of trace elements by Davidson and Wu).[4] The selected values are presented in Table C-1.

Table C-1. Roughness parameter values

urban	z_0 = 0.8 cm
meadow	z_0 = 0.03 cm
forest	z_0 = 1.0 cm
human skin	z_0 = 0.001 cm

It was then considered that the wind speed is a function of friction velocity as given in the following equation:

$$u(z) = \frac{u_*}{k} \ln\left(\frac{z}{z_0}\right) \qquad (1)$$

where k = 0.4 — von Kármán constant.

It was also assumed that the particle sizes are associated with spherical particles of unit density as suggested in the project description and that the particle size values given in Table C-2 represent various particle classes.

It was assumed that the values in Table C-2 can be regarded as median and that the distribution is equal in the proposed ranges.

Distributions of probability densities for the particle sizes defined in Table C-2 are quite simple as shown in Figure C-1 for the 0.05 to 0.2 size range.

Table C-2. Size values of various particle classes

particle size indicated	range assumed
0.1 μ	0.05 μ – 0.2 μ
0.3 μ	0.2 μ – 0.5 μ
1.0 μ	0.5 μ – 2.0 μ
3.0 μ	2.0 μ – 5.0 μ
10.0 μ	5.0 μ – 15.0 μ

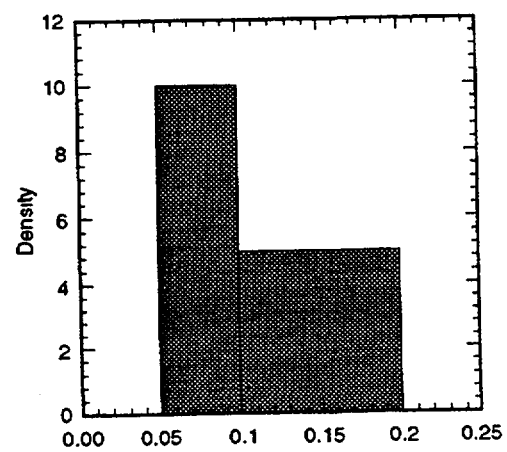

Figure C-1. Distributions of probability densities.

A flat distribution of particle sizes was applied for both sides of the median as no further information was given on this matter. An example is given in Figure C-2.

Taking into account the above input data, an approach was made to calculate minimum, 0.05 quantile, median, 0.95, and maximum values of dry deposition velocities of aerosols as requested in the project.

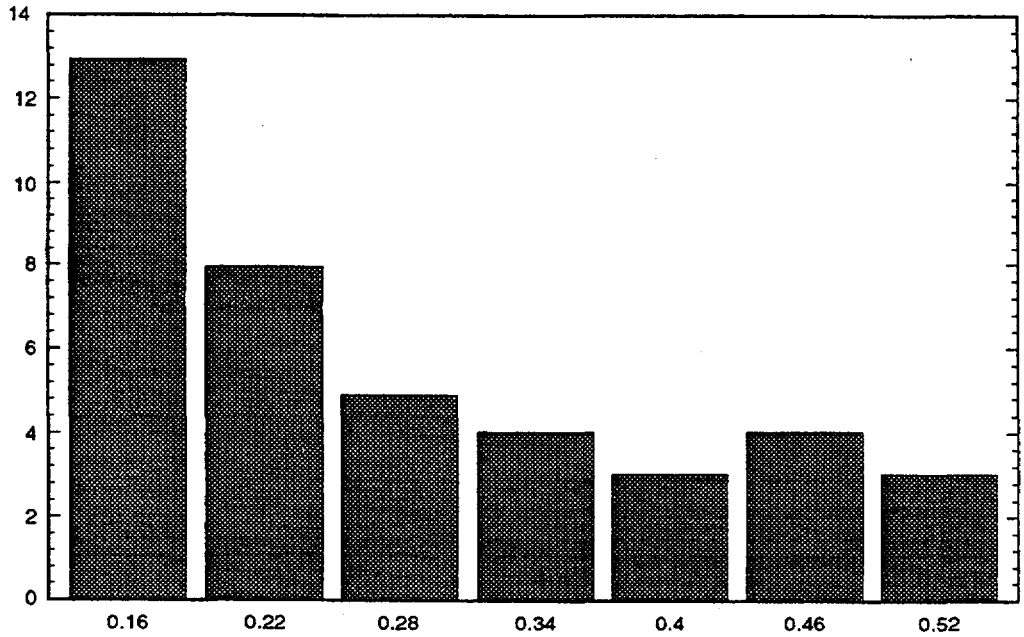

Figure C-2. Flat distribution of particle sizes.

Dry deposition velocities of elemental iodine were estimated in the next part of the project. It was mentioned in the project description that for the purposes of the elicitation, iodine is assumed not to deposit in aerosols. This assumption has been used in the estimates here; however, some reservations should be mentioned. The gaseous portion of elemental iodine in the air observed after the Chernobyl accident was between 70% and 80% (e.g., Cambray et al.).[5] It was further assumed that the dry deposition velocity of elemental iodine varies from 0.11 to 0.33 cm/s as estimated from measurement data for locations around Chilton, UK (Cambray et al.).[5] Taking into account the above assumptions, the estimates of minimum, 0.05 quantile, median, 0.95 quantile, and maximum values of dry deposition velocity of elemental iodine were carried out.

Similar information on the distribution of dry deposition velocities has been also estimated for methyl iodide. It has been suggested that this compound is a major atmospheric methyl group donor since it is photolytically cleaved into methyl radicals and iodine atoms. Photolysis of methyl iodide in the air is rapid and the lifetime of the compound is between 4 and 8 days (e.g., Zafiriou).[6] Taking into account the above information, it was assumed here that the mechanism of dry deposition of methyl iodide is similar to that of fine particles of Ca 1 μm in diameter. The estimates of minimum, 0.05 quantile, median, 0.95 quantile, and maximum values of dry deposition velocities of methyl iodide were carried out.

In the next part of the project, the extent to which humidity, ambient temperature, variations in surface type, and day/night differences affect the dry deposition velocities of aerosols was discussed. The discussion has been based on the results obtained during several measurement campaigns carried out in the Norwegian Arctic and Scandinavia since 1982 (e.g., Pacyna, et al.).[7,8] Both aircraft and ground measurements have been carried out in the winter and summer with the major goal of assessing the origin and behavior of aerosols in the Arctic. Several conclusions have been drawn from this research. Major conclusions from measurements carried out in summer that are related to the present project can be summarized as follows:

- lower temperatures result in higher stability of air masses lowering dry deposition velocities of aerosols, and

- higher humidity values indicate the possibility for particle growth and then increase of dry deposition velocities.

The results of measurements in the Arctic and Scandinavia seem to suggest that the narrow ranges of dry deposition velocities within the 0.05 and 0.95 quantiles obtained from model estimates can be widened. It is very difficult for the expert to precisely quantify to what extent these ranges can be widened. However, it was assumed that the 0.05 quantile value of dry deposition velocities estimated by the model can be lowered by one order of magnitude, while the 0.95 quantile value could be higher by at least a factor of 3. Taking this assumption into account, the modeled data were recalculated and the results are shown in the reporting tables in this volume.

It should be noted that the above assumption was made on the basis of measurements carried out in cold regions with grass being the only surface on which dry deposition had occurred. It was also difficult to assess the median value on the new probability distribution curve of dry deposition velocities due to an insufficient amount of dry deposition velocity values. However, it can be assumed that the median values should not differ substantially from the values obtained from model calculations. These values should be somewhat lower than those modeled due to larger differences in the 0.05 quantile values when compared with the differences in the 0.95 quantile values.

Wet Deposition

If the initial concentration of aerosols is c then the concentration after period t is defined by the equation:

$$\frac{\partial c}{\partial t} = -k_w c \qquad (2)$$

where:

$$k_w = \frac{WP}{h}$$

is the wet deposition coefficient, P = precipitation intensity, h = mixing height, and W = the scavenging ratio. The following can be obtained from Equation (2):

$$c(\Delta t) = c_0 e^{-k_w \Delta t} \qquad (3)$$

and the fraction of aerosol removed by rain can be calculated as:

$$\frac{\Delta_c}{c_0} = \frac{c_0 - c(\Delta t)}{c_0} = 1 - e^{k_w \Delta t} \qquad (4)$$

The values of $\Delta c/c_0$ belong to the (0,1) range. The scavenging ratio is a function of precipitation intensity and the particle size of the aerosol. It was difficult for the expert to find a general function describing the change in scavenging ratio as dependent on the precipitation intensity and its duration. However, it can be generalized that with increasing precipitation intensity and duration, removal of aerosols by rain becomes less efficient (for snow intensity the opposite is true). An example of the relationship between the scavenging ratio for radionuclides and precipitation intensity is presented in Figure C-4. The decrease in scavenging ratio with increased precipitation intensity is not necessarily true for convective storms (Figure C-5) and the variability of the scavenging ratio is very large (one order of magnitude or more) during such a storm. Therefore, due to the large uncertainty and the lack of detailed data, a relationship between the scavenging ratio and precipitation duration was assumed, rather than between the scavenging ratio and precipitation intensity.

The following relationship was obtained from data shown in Figure C-4:

$$W(\Delta t) = e^{\alpha\left(\frac{\Delta t}{24\ hours}\right)} \qquad (5)$$

where t is the period of rain and $\alpha = -0.7$.

The scavenging ratio depends also on the particle size and in general is higher for larger particle sizes. An example of the relationship between the washout ratio and dry particle radius is shown in Figure C-3.

Thus, the final expression of the scavenging ratio as a function of the rain period and particle size has the following form:

$$W(\Delta t, a) = W_0 e^{\alpha\left(\frac{\Delta t}{24\ hours}\right)} \left(\frac{a}{a_0}\right)^{\beta} \qquad (6)$$

where a is the particle diameter in μm, a_0 = 1 μm and β = 0.84.

The fraction of aerosols removed by rain can now be calculated using the following equation:

$$\frac{\Delta c}{c_0} = 1 - \exp\left(-\frac{W_0 e^{\alpha\left(\frac{\Delta t}{24\ hours}\right)} \left(\frac{a}{a_0}\right)^{\beta} P_{tot} \Delta t}{h}\right) \qquad (7)$$

The above equation was used to calculate the fraction of aerosols removed by rain as requested in the project.

In the next part of the project, Probability Density Functions (PDFs) have been presented using the input parameters to the above equation. The standard value of the scavenging

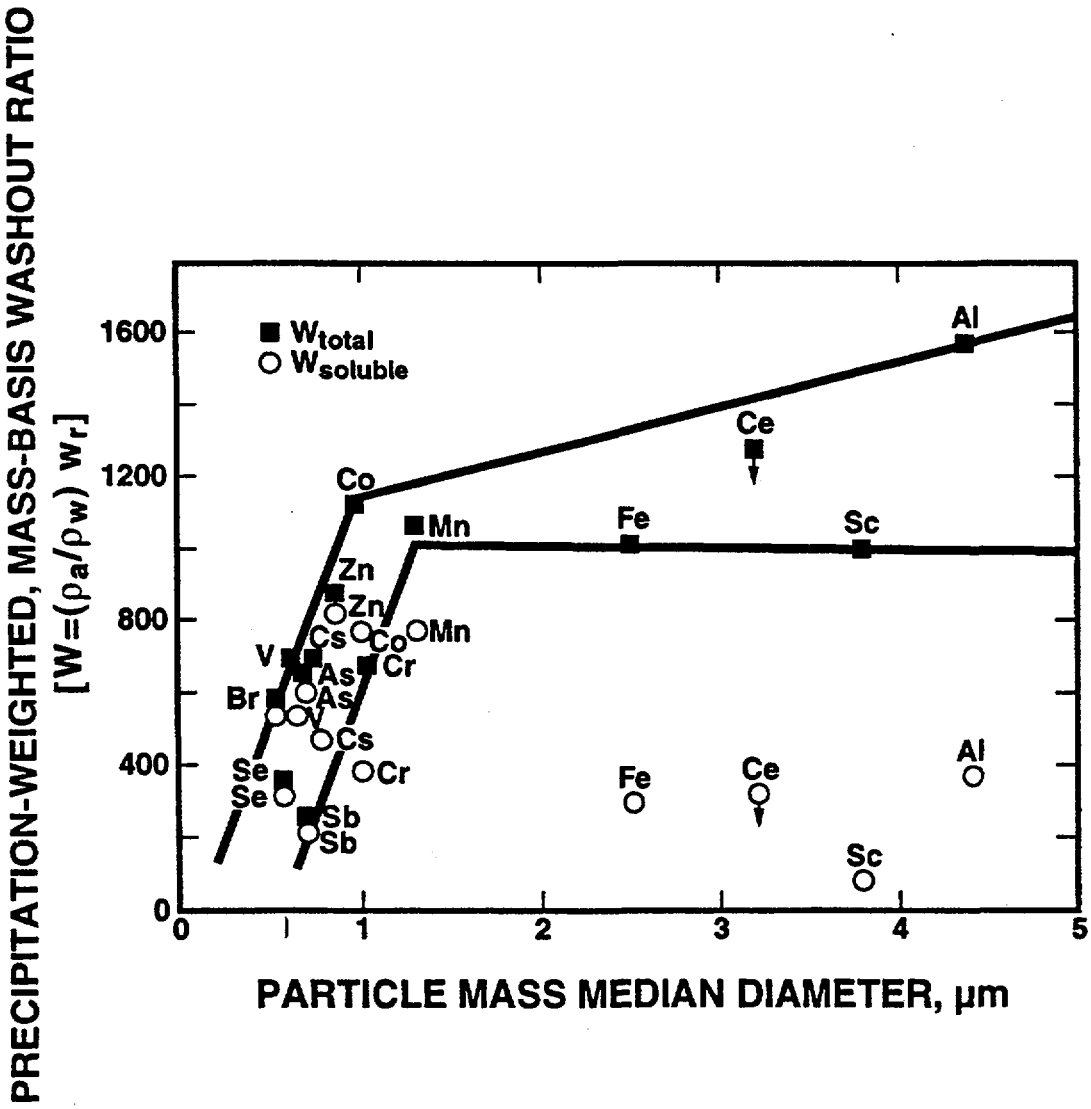

Figure C-3. Variations of precipitation washout or scavenging ratios with particle mass median diameter.

Data obtained by Cawse (1974)[10] at Chilton, U K , during July-December, 1973, much of the data is probably for frontal storms The solid squares represent washout ratios computed from total (soluble plus insoluble) concentrations in precipitation. Open circles represent w_r values calculated using only the soluble concentrations The precipitation samples included contributions from both dry and wet deposition Downward pointing arrows indicate upper limit values. Washout ratios on a mass basis are about 3 orders of magnitude smaller than those on a volume basis; $p = 1.23 \times 10^{-3} g/cm^3$. (Based on D.F. Gatz, "Wet Deposition Estimates Using Scavenging Ratios," in *First Specialty Symposium of the International Association for Great Lakes Research, 28 September 1975, Journal of Great Lakes Research*, 2:21-29, 1976.)[11]

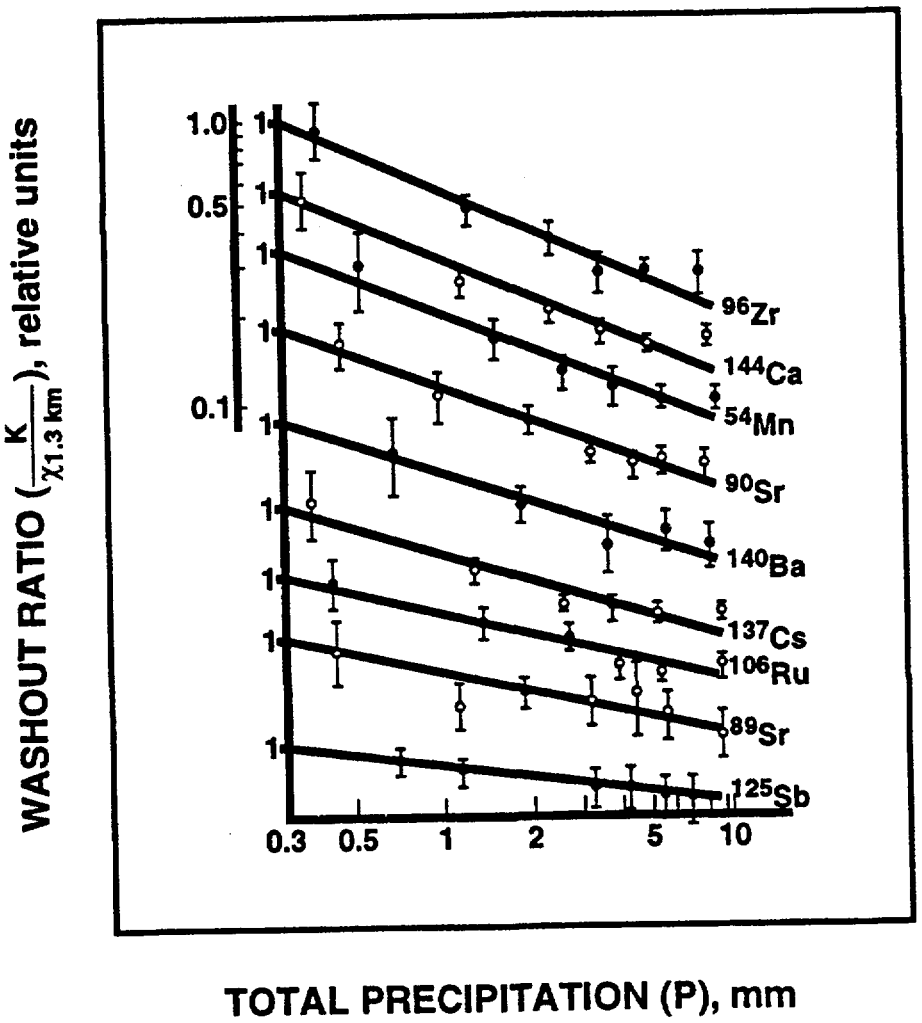

Figure C-4. Monthly average κ/χ values for a number of radionuclides as a function of total precipitation.

The air concentration, χ, was measured at the cloud-layer altitude (typically 1.3 km); the 24-hour precipitation totals, P, were calculated by dividing the monthly precipitation by the number of rain days in the month. The curves are displaced vertically to improve clarity; for all curves, the 0.1 to 1.0 ordinate is appropriate Original data were taken from a number of Harwell reports, graph redrawn from Makhonko, Avramenko, and Makhonko (1970)[12] where the original references can be found.

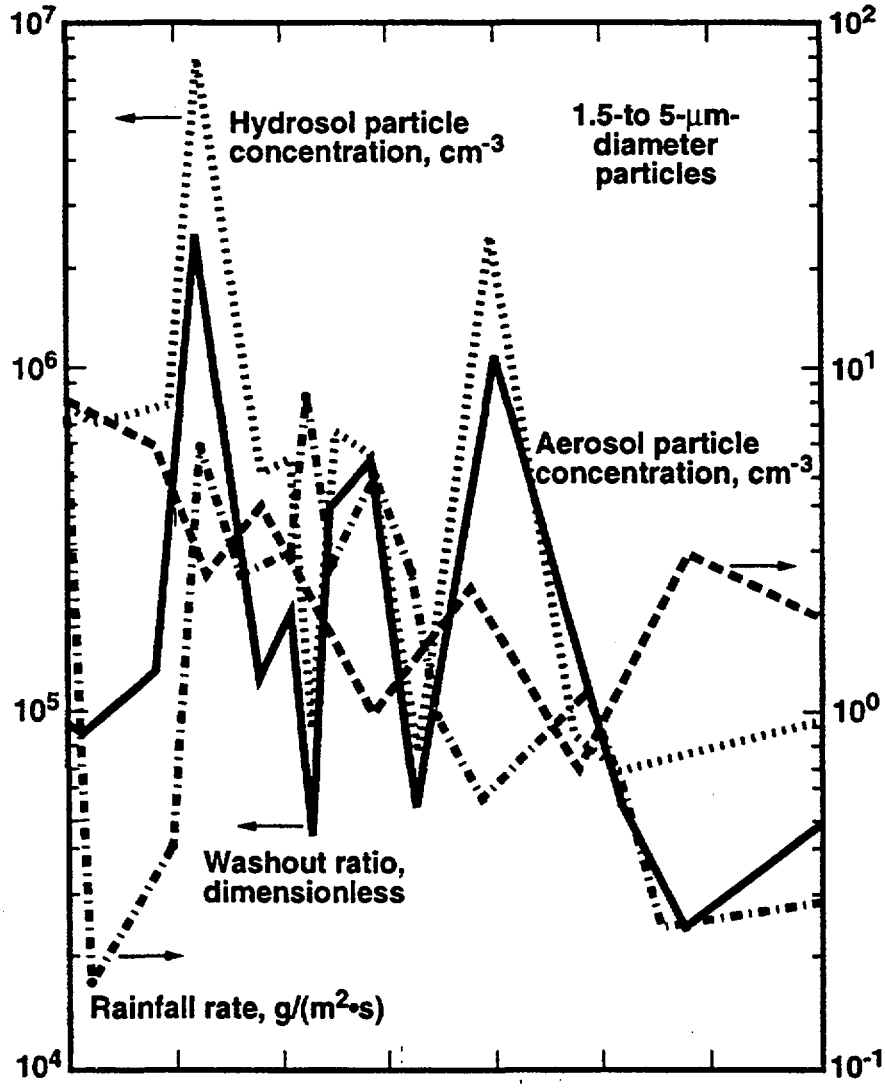

Figure C-5. Variation in κ, χ, w_m and p during a single convective storm on June 30, 1966.

Data were taken from Rosinski (1967) [13] From W G.N. Slinn, "Parameterizations for Resuspension and for Wet and Dry Deposition of Particles and Gases for Use in Radiation Dose Calculations," in *Nuclear Safety*, 19(2). 205-219 (1978).[14]

ratio coefficient (W_0) has a value within at least a one order of magnitude range. Therefore, a flat PDF function to this parameter has been assigned as shown in Figure C-6.

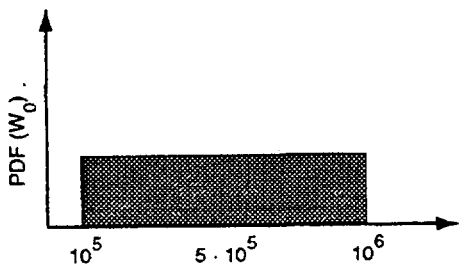

Figure C-6. PDF function of W_0

The mixing height h depends on meteorological conditions and varies significantly between day and night as well as between different seasons The PDF function for mixing height has been assumed and is shown in Figure C-7.

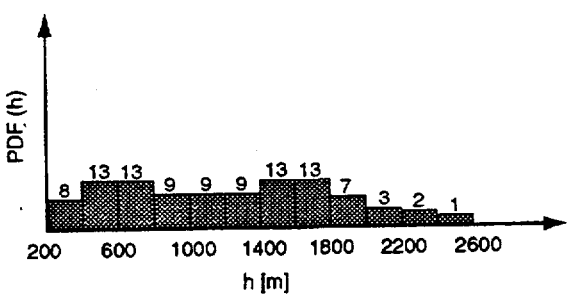

Figure C-7. PDF function for *h*

The α coefficient in Equation (7) has values within the range (-1.0, -0.1). The triangle PDF distribution defined in 9 classes has been assumed for the purpose of the project. The distribution is shown in Figure C-8.

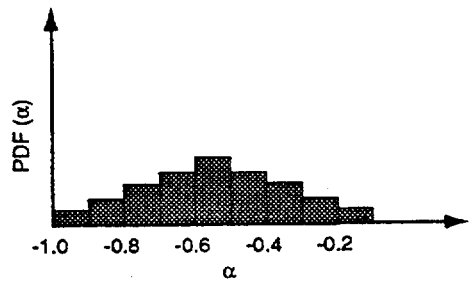

Figure C-8. PDF function for α coefficient

Finally, the PDF function for the coefficient in Equation (7) has been assumed in 7 classes and is presented in Figure C-9.

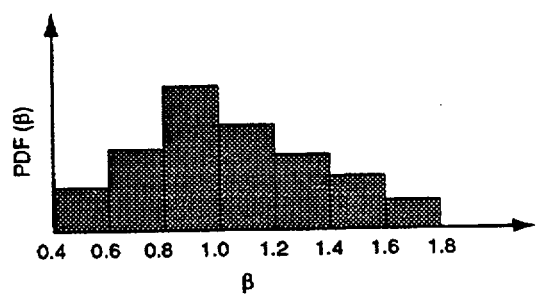

Figure C-9. PDF function for β coefficient

A Monte Carlo method was applied after defining the PDFs for all parameters in Equation (7). The input parameters were selected according to their probability function. The

number of runs in the experiment carried out for the project was 100,000. In this, a PDF of the fraction of aerosols removed by rain was computed. The results of these calculations are provided in this appendix.

It was then assumed that the washout of elemental iodine in a gas form is about 3 times lower than that of iodine particles (after ApSimon and Goddard)[9] and the portion of elemental iodine removed by rain was calculated accordingly.

Finally, it was assumed that the portion of methyl iodide removed by rain can be calculated in a fashion similar to that for the portion of aerosols with diameter of 1.0 μm.

Final Remarks

There are several parameters affecting the dry and wet deposition of aerosols, elemental iodine, and methyl iodide. Only some of them were discussed in this work, including those presented in the project description. Chemical reactions with a surface, electrostatic effects, and gas-to-particle conversions in the air are among the parameters important for removal processes, but the quantitative assessment of their impact was difficult to detemine due to a lack of representative data.

Chemical reactions with a surface will result in quicker removal of gaseous substances from the atmosphere and deposition on aerosol surfaces. This will cause particle growth and subsequently faster dry or wet deposition of aerosols. In the case of wet removal, the solubility of the reacting substances would be an important factor.

Gas-to-particle conversion processes are an important source of secondary aerosol formation. Methyl iodide is known as an important donor of methyl radicals and, as such, contributes to the formation of aerosols in the atmosphere. Aging of newly formed aerosols will be followed by their growth and thus quicker removal from the atmosphere.

It will be interesting to assess in a quantitative way to what extent the above presented parameters may affect the removal of studied compounds and aerosols from the atmosphere. More time is needed to perform such an assessment.

Deposition Tables

Units of velocity are in cm/s; unkn = unknown

DD-A: Dry deposition velocity of aerosols - Wind Speed at 2m/s					
PARTICLE SIZE	QUANTILE	URBAN	MEADOW	FOREST	HUMAN SKIN
0.10μ	0%	1.00E-02	5.00E-03	1.00E-02	5.00E-03
	5%	1.00E-02	5.00E-03	1.00E-02	5.00E-03
	50%	2.20E-01	5.00E-02	2.00E-01	1.00E-02
	95%	6.60E-01	1.50E-01	6.00E-01	3.00E-02
	100%	9.00E-01	2.00E-01	8.00E-01	4.00E-02
0.30μ	0%	1.00E-02	5.00E-03	1.00E-02	5.00E-03
	5%	1.00E-02	5.00E-03	1.00E-02	5.00E-03
	50%	1.10E-01	4.00E-02	1.00E-01	1.00E-02
	95%	3.30E-01	1.20E-01	3.00E-01	3.00E-02
	100%	5.00E-01	1.70E-01	4.00E-01	4.00E-02
1.00μ	0%	1.20E-02	8.00E-03	1.20E-02	7.00E-03
	5%	1.40E-02	1.00E-02	1.40E-02	9.00E-03
	50%	2.50E-01	7.00E-02	2.30E-01	3.00E-02
	95%	7.50E-01	2.10E-01	6.90E-01	9.00E-02
	100%	1.00E+00	2.50E-01	9.00E-01	1.20E-01
3.00μ	0%	4.00E-02	3.50E-02	4.00E-02	3.00E-02
	5%	5.80E-02	4.00E-02	5.70E-02	3.50E-02
	50%	7.70E-01	2.20E-01	7.50E-01	1.20E-01
	95%	2.31E+00	6.60E-01	2.25E+00	1.60E-01
	100%	3.00E+00	8.00E-01	2.80E+00	2.00E-01
10.00μ	0%	3.00E-01	3.50E-01	3.00E-01	3.00E-01
	5%	3.50E-01	4.00E-01	3.50E-01	3.50E-01
	50%	1.25E+00	5.70E-01	1.26E+00	4.20E-01
	95%	1.08E+01	6.00E+00	1.08E+01	6.00E+00
	100%	1.20E+01	6.50E+00	1.20E+01	6.50E+00

DD-B: Dry deposition velocity of aerosols - Wind Speed at 5m/s					
PARTICLE SIZE	QUANTILE	URBAN	MEADOW	FOREST	HUMAN SKIN
0.10μ	0%	1.00E-02	5.00E-03	1.00E-02	5.00E-03
	5%	2.00E-02	8.00E-03	2.00E-02	1.00E-02
	50%	3.90E-01	5.00E-02	3.90E-01	1.20E-02
	95%	1.00E+00	2.20E-01	1.00E+00	4.00E-02
	100%	1.00E+00	2.60E-01	1.00E+00	5.00E-02
0.30μ	0%	1.00E-02	5.00E-03	1.00E-02	5.00E-03
	5%	1.70E-02	8.00E-03	1.70E-02	1.00E-02
	50%	1.80E-01	4.00E-02	1.80E-01	1.20E-02
	95%	5.40E-01	1.30E-01	6.50E-01	3.00E-02
	100%	7.00E-01	2.00E-01	7.00E-01	5.00E-02
1.00μ	0%	1.40E-02	1.00E-02	1.40E-02	1.00E-02
	5%	2.40E-02	2.00E-02	2.50E-02	1.20E-02
	50%	5.00E-01	7.00E-02	4.90E-01	2.00E-02
	95%	1.00E+00	2.20E-01	1.00E+00	1.80E-01
	100%	1.00E+00	3.00E-01	1.00E+00	2.10E-01
3.00μ	0%	6.00E-02	5.00E-02	6.00E-02	5.00E-02
	5%	1.20E-01	8.00E-02	1.20E-01	5.00E-02
	50%	1.94E+00	5.40E-01	1.18E+00	1.30E-01
	95%	5.70E+00	1.80E+00	3.60E+00	5.50E-01
	100%	6.50E+00	2.50E+00	4.00E+00	8.00E-01
10.00μ	0%	3.00E-01	4.00E-01	3.00E-01	3.00E-01
	5%	5.00E-01	5.00E-01	5.00E-01	3.50E-01
	50%	3.25E+00	1.10E+00	3.10E+00	6.20E-01
	95%	1.10E+01	6.50E+00	1.10E+01	6.00E+00
	100%	1.20E+01	7.00E+00	1.20E+01	6.50E+00

DD-C: Dry deposition velocity of elemental iodine - Wind Speed at 2 and 5m/s					
WIND SPEED	QUANTILE	URBAN	MEADOW	FOREST	HUMAN SKIN
2.m/s	0%	1.00E-02	5.00E-03	1.00E-02	5.00E-03
	5%	1 00E-02	5.00E-03	1 00E-02	5.00E-03
	50%	2.20E-01	5.00E-02	2.00E-01	1.00E-02
	95%	6 60E-01	1.50E-01	6.00E-01	3.00E-02
	100%	8.00E-01	2.00E-01	8.00E-01	4.00E-02
5.m/s	0%	1.00E-02	5.00E-03	1.00E-02	5.00E-03
	5%	2.00E-02	8.00E-03	2.00E-02	1.00E-02
	50%	3.90E-01	7.00E-02	3 90E-01	1.20E-02
	95%	1.00E+00	2.20E-01	1.00E+00	4.00E-02
	100%	1.00E+00	2.60E-01	1.00E+00	5.00E-02

DD-D: Dry deposition velocity of methyl iodide - Wind Speed at 2 and 5m/s					
WIND SPEED	QUANTILE	URBAN	MEADOW	FOREST	HUMAN SKIN
2.m/s	0%	1 20E-02	8.00E-03	1.20E-02	7.00E-03
	5%	1.40E-02	1.00E-02	1.40E-02	9.00E-03
	50%	2.50E-01	7.00E-02	2 30E-01	2.50E-02
	95%	7.50E-01	2.20E-01	6.90E-01	1.60E-01
	100%	1.00E+00	2.60E-01	9.00E-01	2.50E-01
5.m/s	0%	1.40E-02	1.00E-02	1.40E-02	1.00E-02
	5%	2.40E-02	2.00E-02	2.50E-02	1.20E-02
	50%	5.00E-01	1.00E-01	5.00E-01	3.00E-02
	95%	1.00E+00	2.60E-01	1.00E+00	1.80E-01
	100%	1.00E+00	3.00E-01	1.00E+00	2.50E-01

DD-E-1: Dry deposition velocity of aerosols on Moorland/Peatland Surface		
PARTICLE SIZE	**QUANTILE**	
0.55μ	**0%**	4.00E-03
	5%	1.00E-02
	50%	5.10E-02
	95%	1.60E-01
	100%	2.10E-01
0.70μ	**0%**	4.00E-03
	5%	1.00E-02
	50%	6.50E-02
	95%	2.10E-01
	100%	2.60E-01
0.90μ	**0%**	4.00E-03
	5%	1.00E-02
	50%	8.80E-02
	95%	3.00E-01
	100%	3.60E-01
1.20μ	**0%**	8.00E-03
	5%	1.20E-02
	50%	1.34E-01
	95%	4.40E-01
	100%	5.00E-01
1.60μ	**0%**	1.20E-02
	5%	1.90E-02
	50%	2.10E-01
	95%	6.80E-01
	100%	8.00E-01

DD-E-2: Dry deposition velocity of aerosols on Heather/Green Grass Surface		
PARTICLE SIZE	QUANTILE	
0.55μ	0%	4.00E-03
	5%	8.00E-03
	50%	5.00E-02
	95%	1.60E-01
	100%	2.00E-01
0.70μ	0%	4.00E-03
	5%	8.00E-03
	50%	6.00E-02
	95%	2.20E-01
	100%	2.80E-01
0.90μ	0%	4.00E-03
	5%	8.00E-03
	50%	8.00E-02
	95%	2.80E-01
	100%	3.20E-01
1.20μ	0%	5.00E-03
	5%	1.00E-02
	50%	1.25E-01
	95%	4.40E-01
	100%	5.00E-01
1.60μ	0%	1.00E-02
	5%	1.60E-02
	50%	2.00E-01
	95%	6.90E-01
	100%	8.00E-01

DD-E-2: Dry deposition velocity of aerosols on Heather/Green Grass Surface (continued)		
PARTICLE SIZE	**QUANTILE**	
2.30μ	**0%**	1.50E-02
	5%	2.80E-02
	50%	3.50E-01
	95%	1.20E+00
	100%	1.60E+00
3.20μ	**0%**	2.50E-02
	5%	4.30E-02
	50%	5.30E-01
	95%	1.80E+00
	100%	2.50E+00
4.20μ	**0%**	3.50E-02
	5%	5.90E-02
	50%	7.30E-01
	95%	2 50E+00
	100%	3.20E+00

DD-F: Dry deposition velocity of aerosols on Grassland Surface		
PARTICLE SIZE	**QUANTILE**	
1.0μ	**0%**	8.00E-03
	5%	1.00E-02
	50%	1.60E-01
	95%	1.00E+00
	100%	1.20E+00

WD-A: Elemental iodine—fraction removed by rain ($1-f_w$)							
Rainfall/ Time	Wind Speed	Quantile	$1-f_w$	Rainfall/ Time	Wind Speed	Quantile	$1-f_w$
.3mm/hr	unkn	0%	3.00E-04	2.mm/hr	unkn	0%	2.80E-03
		5%	9.00E-04			5%	6.40E-03
		50%	3.80E-03			50%	2.48E-02
		95%	8.20E-03			95%	5.10E-02
		100%	1.55E-02			100%	8.44E-02
.075mm/ 10min	10 m/s	0%	1.00E-04	.05mm/ 10min	unkn	0%	1.00E-04
		5%	1.00E-04			5%	2.00E-04
		50%	4.00E-04			50%	7.00E-04
		95%	8.00E-04			95%	1.40E-03
		100%	1.40E-03			100%	2.60E-03
.17mm/ 10min	5 m/s	0%	2.00E-04	.17mm/ 10min	14 m/s	0%	2.00E-04
		5%	4.00E-04			5%	5.00E-04
		50%	1.60E-03			50%	2.10E-03
		95%	3.60E-03			95%	4.20E-03
		100%	7.00E-03			100%	8.50E-03
.23mm/10min	12 m/s	0%	3.00E-04	.5mm/ 10min	unkn	0%	1.00E-03
		5%	6.00E-04			5%	2.00E-03
		50%	2.80E-03			50%	7.00E-03
		95%	6.30E-03			95%	1.40E-02
		100%	1.10E-02			100%	2.60E-02
.33mm/10min	unkn	0%	4.00E-04	1.0mm/ 10min	14 m/s	0%	1.50E-03
		5%	1.00E-03			5%	2.80E-03
		50%	4.20E-03			50%	1.50E-02
		95%	9.20E-03			95%	3.50E-02
		100%	1.50E-02			100%	5.00E-02

WD-A: Elemental iodine—fraction removed by rain ($1-f_w$) (continued)			
Rainfall/Time	**Wind Speed**	**Quantile**	$1-f_w$
1.67mm/10min	**unkn**	**0%**	1.80E-03
		5%	3.30E-03
		50%	2.09E-02
		95%	4.41E-02
		100%	7.30E-02

WD-B: Methyl iodide—fraction removed by rain (Wind Speed=unknown)		
Rainfall/Time	**Quantile**	$1-f_w$
.3mm/hr	**0%**	1.00E-03
	5%	2.80E-03
	50%	1.15E-02
	95%	2.47E-02
	100%	4.66E-02
2.mm/hr	**0%**	8.50E-03
	5%	1.92E-02
	50%	7.44E-02
	95%	1.53E-01
	100%	2.53E-01
.05mm/10min	**0%**	2.00E-04
	5%	5.00E-04
	50%	2.00E-03
	95%	4.20E-03
	100%	7.80E-03
.33mm/10min	**0%**	1.30E-03
	5%	3.20E-03
	50%	1.28E-02
	95%	2.77E-02
	100%	4.45E-02

WD-B: Methyl iodide—fraction removed by rain (Wind Speed=unknown) (continued)		
Rainfall/Time	**Quantile**	$1\text{-}f_w$
1.67mm/min	**0%**	5.50E-03
	5%	1.59E-02
	50%	6.27E-02
	95%	1.32E-01
	100%	2.20E-01

WD-C: Fraction of aerosols removed by rain						
PARTICLE SIZE	**QUANTILE**	**Rainfall: .3mm/hr**	**Rainfall: 2.mm/hr**	**Rainfall: .05mm/10min**	**Rainfall: .33mm/10min**	**Rainfall: 1.67mm/10min**
0.1μ	**0%**	3.00E-04	2.20E-03	1.00E-04	3.00E-04	1.70E-03
	5%	9.00E-04	6.10E-03	2.00E-04	1.00E-03	5.20E-03
	50%	3.60E-03	2.39E-02	6.00E-04	4.00E-03	2.05E-02
	95%	7.80E-03	5.14E-02	1.30E-03	8.80E-03	4.39E-02
	100%	1.31E-02	9.46E-02	2.40E-03	1.55E-02	7.88E-02
0.3μ	**0%**	7.00E-04	4.70E-03	1.00E-04	7.00E-04	4.40E-03
	5%	1.60E-03	1.08E-02	3.00E-04	1.80E-03	9.00E-03
	50%	6.30E-03	4.15E-02	1.10E-03	7.20E-03	3.57E-02
	95%	1.29E-02	8.30E-02	2.20E-03	1.44E-02	7.14E-02
	100%	2.05E-02	1.30E-01	3.70E-03	2.45E-02	1.20E-01
1.0μ	**0%**	1.00E-03	8.50E-03	2.00E-04	1.30E-03	5.50E-03
	5%	2.80E-03	1.92E-02	5.00E-04	3.20E-03	1.59E-02
	50%	1.15E-02	7.44E-02	2.00E-03	1.28E-02	6.27E-02
	95%	2.47E-02	1.53E-01	4.20E-03	2.77E-02	1.32E-01
	100%	4.66E-02	2.53E-01	7.80E-03	4.40E-02	2.20E-01
10.0μ	**0%**	3.60E-03	2.48E-02	6.00E-04	4.10E-03	2.10E-02
	5%	8.60E-03	5.64E-02	1.50E-03	9.80E-03	4.80E-02
	50%	3.44E-02	2.09E-01	5.90E-03	3.86E-02	1.79E-01
	95%	7.05E-02	3.88E-01	1.22E-02	7.84E-02	3.35E-01
	100%	1.19E-01	5.21E-01	2.03E-02	1.21E-01	5.05E-01

References

1. Davidson, C.I., J.M. Miller, and M.A. Pleskow, "The Influence of Surface Structure on Predicted Particle Dry Deposition , to Natural Grass Canopies," *Water, Air, and Soil Pollution*, 18: 25-43, 1982.

2. Slinn, W.G.N., "Predictions for Particle Deposition to Vegetative Canopies," *Atmospheric Environment*, 16:1785-1794, 1982.

3. Sehmel, G.A., "Particle and Gas Dry Deposition: A Review," *Atmospheric Environment*, 14:983-1011, 1980.

4. Davidson, C.I., and Y.-L. Wu, "Dry Deposition of Trace Elements," (J.M. Pacyna and B. Ottar, eds.), *Control and Fate of Atmospheric Trace Metals, NATO Advanced Research Workshop on Fate and Control of Toxic Metals in the Atmosphere, 12-16 September 1988*, NATO ASI Series, Series C: Mathematical and Physical Sciences Volume 268, Kluwer Academic Publishers, Boston, MA, 1989.

5. Cambray, R.S , et al., "Observations on Radioactivity from the Chernobyl Accident," *Nuclear Energy*, 26:77-101, 1987.

6. Zafiriou, O.C., "Photochemistry of Halogens in the Marine Atmosphere," *Journal of Geophysical Research*, 79: 2730-2732, 1974.

7. Pacyna, J.M., et al., *Aircraft Measurement of Air Pollution in the Norwegian Arctic*, Appendices A, B, C, and D, Norwegian Institute for Air Research, NILU Rept. OR-67-85, Lillestrom, Norway, 1985.

8. Pacyna, J.M., et al., *Chemical Composition of Aerosols at BP Project Ground Stations*, Norwegian Institute for Air Research, NILU Rept. OR-64-85, Lillestrom, Norway, 1985.

9. ApSimon, H.M., and A.J.H. Goddard, *Atmospheric Transport of Radioisotopes and the Assessment of Population Doses on a European Scale, Application of the MESOS Code to the Meteorological Dispersion of Radioactive Discharges from National Nuclear Sites in the European Community with Particular Reference to the Mesoscale*. EUR-9128-EN, Commission of the European Communities, Luxembourg, 1983.

10. Cawse, P.A., "Survey of Atmospheric Trace Elements in the U.K. (1972-73)," AERE-R-7669, UKAEA Research Group, Atomic Energy Research Establishment, England, October 1974.

11. Gatz, D.F., "Wet Deposition Estimation Using Scavenging Ratios," *First Specialty Symposium of the International Association for Great Lakes Research, 28 September 1975, Journal of Great Lakes Research*, 2:21-29, 1976.

12. Makhonko, Avramenko, and Makhonko (1970) - unable to verify reference with these three authors and publication date of 1970.

13. Rosinski, J., "Insoluble Particles in Hail and Rain," *Journal of Applied Meteorology*, 6:1066-1074, 1967.

14. Slinn, W.G.N., "Parameterizations for Resuspension and for Wet and Dry Deposition of Particles and Gases for Use in Radiation Dose Calculations," *Nuclear Safety*, 19:205-219, 1978.

Expert D

General Remarks

Some points raised at the earlier meeting are so important that I wish to endorse them by stating them here:

1) For dry deposition (gases or particles) the formation of a nocturnal low-level temperature inversion will essentially decouple the atmosphere above from the ground and reduce deposition to a very low level. The meteorology driving the computer models will, of course, have included that in its friction component; its influence on particle retention would not, however, be included just by using that meteorology.

2) As Expert E pointed out at the earlier meeting, by excluding from consideration processes occurring in cloud and fog, what is probably the major scavenging factor is being excluded. Condensation, for example, provides an almost instantaneous conversion of particulate material from a size range that is difficult to remove to a size range that is removed very effectively. Even if a cloud evaporates, it has transformed a lot of particulate material up the size scale.

3) It is perhaps redundant to note that if the aerosol source term consists of particles around 1 μm, that happens to be where the scavenging process is acutely sensitive to size; dependences as high as fourth power of diameter have appeared in the literature. Given such a sensitive dependence, and the likelihood that the particle sizes produced in a release incident will be influenced by incident size, extent, and duration, as well as the rate of dilution after release, accurate predictions for a specified size would have little utility.

4) Water-soluble substances are likely to be included among the chemical mix that constitutes the particle source term. Under conditions of high humidity these will exist in equilibrium as solution droplets, the size of which will vary with relative humidity and can easily become two or three times the diameter when dry. Retaining the *dry* size under all conditions would lead to a serious underestimation of scavenging (dry or wet).

Dry Deposition

For particles in the inertial size range, particle trajectories can be computed as accurately as desired once the flow field has been specified. In the diffusion size range, deposition probabilities can be computed with equal confidence. The main source of uncertainty is a flow field about which little is known, other than a few statistical descriptors which relate to averaged quantities. In the literature, most treatments, whether theoretical or experimental (laboratory or field), have adopted friction velocity u_* and particle size as the variables that control deposition; the latter is not related to the flow, so the flow is entirely categorized by the single quantity u_*, i.e., $\langle u'v' \rangle$. The adequacy of simplification can only be judged on the basis of experimental measurements, especially the degree of agreement among sets of measurements.

Examining different experimental results, one is immediately struck (but not surprised) by the size-dependence of agreement among them; it is good at and above 10 μm—where inertia is large and particles fall at speeds ~ cm/s, and, to a lesser extent, below 0.1 μm—where Brownian motion is predominant. Unfortunately the questions posed to this panel relate to the particle size range *in between*, where deposition drops to a minimum and where disagreement between experimental results is greatest. The location of the minimum, around 0.3 μm, is reasonably well defined among investigations, and its dependence on u_* is not strong, but the depth of the minimum (i.e., the minimum value attained by v_d when graphed against particle size) is quite variable, from experiment to experiment. For the kind of conditions specified in most of the panel questions ($v \sim 5$ m/s at 5m; roughness length ~ 5 cm) experimental minima in v_d have often been reported in the range 0.01 to 0.03 cm/s; values down to .001 have been reported. Simpler theory predicts a minimum v_d also ~ 0.01. In contrast, a handout of "right answers" to the training exercise at the Rotterdam meeting gave values of v_d which *exceeded 1 cm/s* for submicron particles. (There was no explanation or elaboration of these values, so one is unsure how to regard them.) I am aware of indirect conclusions from field measurements that suggest appreciable deposition, with only slight dependence on size, in the sub-micron region, but probably would have discounted them were it not for the Rotterdam handout. Rather than ignoring the latter, or in some way averaging the "conventional wisdom" ($v_d \sim 0.01$ at its minimum) with values about two orders of magnitude larger, it seemed more sensible to set a high value ~ 1 cm/s for the high quantile. By so doing I may be offending the statistical processing that will be applied to the responses. The

implication of my response is an "either–or" proposition, not a very wide unimodal distribution.

My responses for dry deposition of aerosols were mainly obtained by going to the refereed literature for results from laboratory experiments and field measurements; theory was used mainly to try to compensate for differences in experimental conditions and make inter-comparison possible. Some personal experimental experiences have contributed to my bias in favor of filling in (partially) the Greenfield Gap, making the minimum value of v_d or fractional removal, as the case may be, appreciably larger than that predicted by most theories.

Washout

In Rotterdam it was stipulated that removal inside a cloud or fog was to be excluded from consideration. That apparent simplification causes difficulties if one is to look at experimental field results, since the *experimenter* cannot separate collected amounts of a substance into two categories: removed inside the cloud, and removed below the cloud by collection by raindrops or other precipitation. Many people believe that in-cloud processes are most effective for removal, so unless one can be confident that particles or gases never found their way into clouds, measured deposition in rain would require a sizeable downward adjustment to allow for in-cloud scavenging.

Many assessments of washout have used as a starting point results from cloud-physics work (experimental and/or theoretical) relating to water drop interactions. Two problems present themselves in that context: (a) Cloud physics involves interaction of objects in the size range above 1 μm. Extrapolation to sub-micron sizes involves additional assumptions. (b) Theoretical collection efficiencies and kernels, even though computed using detailed hydrodynamics, require an ad hoc definition of "contact," since true geometric contact (i.e., for spheres, separation of centers equal to the sum of the radii) is precluded by the infinite time that squeezing out *all* the intervening air would require. Contact is in fact stipulated as a separation $\geq r_1 + r_2 + \delta$, with δ being a fixed small distance or a fixed fraction of radius. Transcribing drop/drop results to drop/particle encounters, given that particles are more irregular in shape and that the surface free energy of water is high, will probably underestimate particle washout.

For washout of gases there is again an obvious cloud physics analog—the evaporation of falling drops, about which there is extensive literature and generally excellent agreement. The only catch seems to be the accommodation coefficients, but theory and experiment suggest that the accommodation coefficient has an imperceptible effect provided $D/\alpha\upsilon \ll$ radius. (D = diffusivity of the condensing gas, υ = kinetic coefficients, $6.4 \times 10^4\ M_w^{-1/2}$ at room temperature, M_w = molecular weight). Iodine, being chemically reactive, almost certainly has $\alpha \sim 1$, meaning that accommodation/slip correction would be needed only for $r < 0.1$ μm. I am not very familiar with the idiosyncrasies of methyl iodide, but guess that it is unlikely to have an accommodation coefficient so low (10^{-4}) that it must be taken into account for condensation on rain or drizzle drops. The only adjustment needed would then be for diffusivity, and a fairly secure prediction of removal rate would ensue.

Again, unfortunately, a complicating factor emerges. In this case it is the sequestration of mobile condensible gas molecules that have previously condensed on particles and become virtually immobilized. As an illustration, we consider the formation by condensation of a 5×10^{-8} cm layer on 1 μm particles such as those shown in Expert H's outline. With N such particles per cm^3 the condensation is $4\pi a^2 N \rho_c \delta$ (δ being layer thickness, taken here to be 5×10^{-8} cm). The condensed layer is found to form so quickly that it is virtually instantaneous (~ 1 ms); the molecules that, when free, had diffusivities ~ 0.05 cm^2s^{-1} now diffuse at ~ 10^{-7} cm^2s^{-1}. The sequestered molecules amount to about 0.01 μg m^{-3} on each 1 μm particle. Subsequent washout then depends not just on raindrop size and rainfall, but also on the number concentration of accompanying particles and the proportion of gas to particles. It is not then realistic to treat gas scavenging independently of particles. This interaction can only act in the direction of retarding removal, i.e., removal rates should be reduced because of it. For that reason I have shown a low 5-percentile, that is, a lot smaller than what one might otherwise estimate. However the effect, involving interaction of two pollutants, is concentration-dependent and requires a knowledge of sizes and numbers (and, for methyl iodide, absorption properties) before one could attempt to put it on a quantitative basis.

The estimates of gas and particle washout given in my response are computed by the straightforward cloud-physics analogies, utilizing data in Pruppacher and Klett's text and other similar sources. The complications mentioned above were not included other than widening the 5-percentile values because of the uncertainties introduced.

Bounds

More recently the panel was asked to supply estimates of upper and lower bounds for the various quantities.

Dry deposition: A fairly obvious upper bound suggests itself here—the friction velocity u_*. The system cannot in a steady state have a larger deposition flux than what is being brought down by turbulence.

For aerosols, a fairly obvious lower bound is provided by the sedimentation velocity. That, however, is not absolute, since turbulent eddies can move the falling particle back up. A not entirely secure lower bound estimate might be about half the sedimentation speed, i.e.:

Diameter	Lower Bound cm/s
0.55	5×10^{-4}
0.7	7×10^{-4}
0.9	1.2×10^{-3}
1.2	.002
1.6	.004
2.3	.008
3.2	.015
4.2	.026

For gases there is no similar bound. Given the possibility of very poor accommodation or filling of absorbed monolayers, a lower bound of zero is indicated.

An upper bound for washout would be set by the consideration that a particle or gas molecule that has never been close to a raindrop cannot be scavenged. The sum of the projected area becomes of interest here, and a realistic upper bound would be, say, twice the sum of areas of all drops fallen during a rain event (per unit surface area). For all the stipulated rain amounts, that sum is ≥ 1, except for the two lightest rainfalls, where it is about 0.4 and 0.7. These would then become the upper bounds (not applicable for gases).

Dry deposition of gases at $z_o = 5$ cm; $u_* = 44.4$

ThB	12 cm/s
H_2O	32 cm/s
I_2	17 cm/s
CH_3I	14 cm/s

Dry Deposition—Method

(a) Particles

My decision was to use experimental results, both field and laboratory, in the published refereed journals, for dry deposition data. I use theory only to bring the data to the same parameter values, then use the composite set of data (e.g., multiple graphs of v_d versus diameter) to estimate the required deposition velocities. The great spread in the results (even on log/log plots) made estimation of the mean (much less 95 or 5 percentiles) somewhat arbitrary.

None of the v_d values which I found in the literature were as high as those in the handout which we received in Rotterdam. They prompted me to yield to a sense that I have formed from various, somewhat indirect, measurement results that have confronted me, and place the high 95-percentile around 1 cm sec^{-1}.

(b) Gases

Again the preferred source was experimental data, especially that from Chamberlain and coworkers. Their investigations did not use Iodine and/or Methyl Iodide, and they showed differences between Thorium B and water vapor that were larger than could be attributed to differences in diffusivity. I feel fairly confident that Iodine will be well accommodated on most surfaces, wet or dry, but Methyl Iodide may be another story. For that reason I assigned a much lower 5-percentile to Methyl Iodide deposition, except for the "urban" category, where a wide variety of surface compositions would be encountered.

Removal by Rain (Washout)—Rationale

(a) Particles

Cloud-physics data (collection efficiencies, collection kernels as a function of collecting drop size) can be used to find the washout factor for one size of collecting drop, then integrated over the raindrop size distribution for the specified rain intensities. For particles > 1 μm that should be fairly good, but for sizes like 0.1 μm there is more uncertainty for the collection kernels, and factors like electric charge, electric field, thermophoresis, and diffusiophoresis become important and introduce more uncertainty.

(b) Gases

The same equations that apply to a gas (e.g., iodine) diffusing towards a falling drop also apply to the gas H_2O diffusing away from an evaporating drop. I therefore went to cloud physics measurements and calculations for such evaporation, adjusting for the different diffusivities of water vapor and iodine (or methyl iodide).

The principal source of error/uncertainty here is that drops will evaporate (how much depends on relative humidity, which is unspecified). A drop could reach the ground 0.1 mm in diameter having left the cloud base 2 mm or more in diameter; it will collect for much of its path as a millimeter-size drop and will carry what it collects to the surface. But if it evaporates *totally* everything it collected is returned to the atmosphere and no iodine or CH_3I is deposited.

Deposition Tables

Units of Velocity are in cm/s; N/A = not provided by expert; unkn = unknown

DD-A: Dry deposition velocity of aerosols - Wind Speed at 2m/s					
PARTICLE SIZE	**QUANTILE**	**URBAN**	**MEADOW**	**FOREST**	**HUMAN SKIN**
0.10μ	**0%**	3.00E-05	3.00E-05	3.00E-05	3.00E-05
	5%	1.00E-03	1.00E-03	3.00E-03	1.00E-03
	50%	5.00E-02	2.00E-02	3.00E-02	5.00E-01
	95%	1.00E+00	1.00E+00	1.00E+00	1.00E+01
	100%	N/A	N/A	N/A	N/A
0.30μ	**0%**	2.70E-04	2.70E-04	2.70E-04	2.70E-04
	5%	1.00E-03	1.00E-03	2.00E-03	1.00E-03
	50%	2.00E-02	1.00E-02	2.00E-02	5.00E-01
	95%	1.00E+00	1.00E+00	1.00E+00	1.00E+01
	100%	N/A	N/A	N/A	N/A
1.00μ	**0%**	3.00E-03	3.00E-03	3.00E-03	3.00E-03
	5%	2.00E-03	2.00E-03	3.00E-02	3.00E-03
	50%	8.00E-02	3.00E-02	6.00E-02	2.00E-01
	95%	1.00E+00	1.00E+00	1.50E+00	1.00E+01
	100%	N/A	N/A	N/A	N/A
3.00μ	**0%**	N/A	2.70E-02	2.70E-02	2.70E-02
	5%	8.00E-03	2.00E-02	5.00E-02	3.00E-02
	50%	2.00E-01	1.50E-01	2.50E-01	1.00E+00
	95%	1.50E+00	1.00E+00	3.00E+00	2.00E+01
	100%	N/A	N/A	N/A	N/A
10.00μ	**0%**	N/A	N/A	N/A	N/A
	5%	1.00E-01	1.00E-01	2.00E+00	3.00E-01
	50%	2.50E+00	4.00E-01	4.00E+00	8.00E+00
	95%	8.00E+00	5.00E+00	2.00E+01	2.50E+01
	100%	N/A	N/A	N/A	N/A

DD-B: Dry deposition velocity of aerosols - Wind Speed at 5m/s					
PARTICLE SIZE	QUANTILE	URBAN	MEADOW	FOREST	HUMAN SKIN
0.10μ	0%	3.00E-05	3.00E-05	3.00E-05	3.00E-05
	5%	2.00E-03	2.00E-03	5.00E-03	1.00E-03
	50%	1.00E-01	5.00E-02	1.20E-01	5.00E-01
	95%	1.00E+00	1.00E+00	2.50E-01	1.00E+01
	100%	N/A	N/A	N/A	N/A
0.30μ	0%	2.70E-04	2.70E-04	2.70E-04	2.70E-04
	5%	2.00E-03	2.00E-03	3.00E-03	1.00E-03
	50%	4.00E-02	3.00E-02	5.00E-02	5.00E-01
	95%	1.00E+00	1.00E+00	1.00E-01	1.00E+01
	100%	N/A	N/A	N/A	N/A
1.00μ	0%	3.00E-03	3.00E-03	3.00E-03	3.00E-03
	5%	5.00E-03	5.00E-03	8.00E-03	3.00E-03
	50%	1.50E-01	1.20E-01	4.00E-01	5.00E-01
	95%	1.00E+00	1.00E+00	8.00E-01	1.00E+01
	100%	N/A	N/A	N/A	N/A
3.00μ	0%	N/A	2.70E-02	2.70E-02	2.70E-02
	5%	2.00E-02	4.00E-02	8.00E-02	3.00E-02
	50%	7.50E-01	1.00E+00	1.50E+00	2.00E+00
	95%	2.00E+00	3.00E+00	4.00E+00	2.00E+01
	100%	N/A	N/A	N/A	N/A
10.00μ	0%	3.00E-01	3.00E-01	3.00E-01	3.00E-01
	5%	5.00E-01	1.00E+00	2.00E+00	3.00E-01
	50%	6.00E+00	1.20E+00	1.60E+01	1.00E+01
	95%	1.00E+01	1.00E+01	4.00E+01	4.00E+01
	100%	N/A	N/A	N/A	N/A

DD-C: Dry deposition velocity of elemental iodide - Wind Speed at 2 and 5m/s					
WIND SPEED	QUANTILE	URBAN	MEADOW	FOREST	HUMAN SKIN
2.m/s	0%	1.00E+00	2.00E+00	1.00E+01	1.00E-01
	5%	1.00E+00	2.00E+00	1.00E+01	1.00E-01
	50%	4.00E+00	6.00E+00	2.00E+01	3.00E+00
	95%	1.00E+01	1.50E+01	5.00E+01	3.00E+01
	100%	1.00E+01	1.50E+01	5.00E+01	3.00E+01
5.m/s	0%	2.50E+00	4.00E+00	2.00E+01	2.00E-01
	5%	2.50E+00	4.00E+00	2.00E+01	2.00E-01
	50%	1.00E+01	1.60E+01	5.00E+01	5.00E+00
	95%	3.00E+01	3.00E+01	1.00E+02	5.00E+01
	100%	3 00E+01	3.00E+01	1.00E+02	5.00E+01

DD-D: Dry deposition velocity of methyl iodide - Wind Speed at 2 and 5m/s					
WIND SPEED	QUANTILE	URBAN	MEADOW	FOREST	HUMAN SKIN
2.m/s	0%	0.00E+00	0.00E+00	0.00E+00	0.00E+00
	5%	2.00E-01	1.00E-01	1.00E+00	1.00E-01
	50%	1.00E+00	2.00E+00	8.00E+00	3.00E+00
	95%	1.00E+01	1.50E+01	5.00E+01	3.00E+01
	100%	N/A	N/A	N/A	N/A
5.m/s	0%	0.00E+00	0.00E+00	0.00E+00	0.00E+00
	5%	5.00E-01	2.00E-01	1.00E+00	2.00E-01
	50%	2.00E+00	5.00E+00	2.00E+01	5.00E+00
	95%	3.00E+01	3.00E+01	5.00E+01	5.00E+01
	100%	N/A	N/A	N/A	N/A

DD-E-1: Dry deposition velocity of aerosols on Moorland/Peatland Surface		
PARTICLE SIZE	QUANTILE	
0.55μ	0%	2.50E-03
	5%	5.00E-03
	50%	2.00E-02
	95%	1.00E+00
	100%	N/A
0.70μ	0%	3.50E-03
	5%	7.00E-03
	50%	2.50E-02
	95%	1 00E+00
	100%	N/A
0.90μ	0%	5.00E-03
	5%	1.00E-02
	50%	3.00E-02
	95%	1.00E+00
	100%	N/A
1.20μ	0%	1.00E-02
	5%	2.00E-02
	50%	5.00E-02
	95%	1.00E+00
	100%	N/A
1.60μ	0%	2 00E-02
	5%	4.00E-02
	50%	1.00E-01
	95%	1.00E+00
	100%	N/A

DD-E-2: Dry deposition velocity of aerosols on Heather/Green Grass Surface		
PARTICLE SIZE	QUANTILE	
0.55μ	0%	2.50E-03
	5%	5.00E-03
	50%	2.00E-02
	95%	1.00E+00
	100%	N/A
0.70μ	0%	3.50E-03
	5%	7.00E-03
	50%	2.50E-02
	95%	1.00E+00
	100%	N/A
0.90μ	0%	5.00E-03
	5%	1.00E-02
	50%	3.00E-02
	95%	1.00E+00
	100%	N/A
1.20μ	0%	1.00E-02
	5%	2.00E-02
	50%	5.00E-02
	95%	1.00E+00
	100%	N/A
1.60μ	0%	2.00E-02
	5%	4.00E-02
	50%	7.00E-02
	95%	1.00E+00
	100%	N/A

DD-E-2: Dry deposition velocity of aerosols on Heather/Green Grass Surface (continued)		
PARTICLE SIZE	QUANTILE	
2.30μ	0%	3.70E-02
	5%	7.50E-02
	50%	1.20E-01
	95%	1.20E+00
	100%	N/A
3.20μ	0%	7.50E-02
	5%	1.50E-01
	50%	2.00E-01
	95%	1.50E+00
	100%	N/A
4.20μ	0%	1.25E-01
	5%	2.50E-01
	50%	3.00E-01
	95%	2.00E+00
	100%	N/A

DD-F: Dry deposition velocity of aerosols on Grassland Surface		
PARTICLE SIZE	QUANTILE	
1.0μ	0%	2.00E-03
	5%	2.00E-02
	50%	2.00E-01
	95%	1.50E+00
	100%	N/A

WD-A: Elemental iodine—fraction removed by rain ($1-f_w$)							
Rainfall/ Time	Wind Speed	Quantile	$1-f_w$	Rainfall/ Time	Wind-Speed	Quantile	$1-f_w$
.3mm/hr	unkn	0%	5.00E-03	2.mm/hr	unkn	0%	4.00E-02
		5%	1.00E-02			5%	8.00E-02
		50%	3.00E-02			50%	2.20E-01
		95%	1.20E-01			95%	9.00E-01
		100%	1.00E+00			100%	1.00E+00
.075mm/ 10min	10 m/s	0%	1.50E-03	.05mm/ 10min	unkn	0%	1.00E-03
		5%	3.00E-03			5%	2.00E-03
		50%	1.00E-02			50%	5.00E-03
		95%	5.00E-02			95%	2.00E-02
		100%	2.20E-01			100%	1 70E-01
.17mm/ 10min	5 m/s	0%	3.50E-03	.17mm/ 10min	14 m/s	0%	3.50E-03
		5%	7.00E-03			5%	7 00E-03
		50%	2.00E-02			50%	2.00E-02
		95%	8.00E-02			95%	8 00E-02
		100%	4.20E-01			100%	4.20E-01
0.23mm/ 10min	12 m/s	0%	5.00E-03	.5mm/ 10min	unkn	0%	1.00E-02
		5%	1.00E-02			5%	2.00E-02
		50%	2.50E-02			50%	6 00E-02
		95%	1.00E-01			95%	2.00E-01
		100%	5.20E-01			100%	9.50E-01
.33mm/ 10min	unkn	0%	7.50E-03	1.0mm/ 10min	14 m/s	0%	1.50E-02
		5%	1.50E-02			5%	3.00E-02
		50%	4.00E-02			50%	1.20E-01
		95%	1.50E-01			95%	6.00E-01
		100%	7.00E-01			100%	1.00E+00

WD-A: Elemental iodine—fraction removed by rain ($1-f_w$) (continued)			
Rainfall/Time	**Wind Speed**	**Quantile**	$1-f_w$
1.67mm/10min	**unkn**	**0%**	2.50E-02
		5%	5.00E-02
		50%	2.00E-01
		95%	9.00E-01
		100%	1.00E+00

WD-B: Methyl iodide—fraction removed by rain (Wind Speed=unknown)		
Rainfall/Time	**Quantile**	$1-f_w$
.3mm/hr	0%	0.00E+00
	5%	1.00E-03
	50%	3.00E-02
	95%	1.50E-01
	100%	1.00E+00
2.mm/hr	0%	0.00E+00
	5%	7.00E-03
	50%	2.00E-01
	95%	8.00E-01
	100%	1.00E+00
.05mm/10min	0%	0.00E+00
	5%	3.00E-04
	50%	1.00E-02
	95%	5.00E-02
	100%	2.00E-01
.33mm/10min	0%	0.00E+00
	5%	1.00E-03
	50%	4.00E-02
	95%	2.00E-01
	100%	7.00E-01
1.67mm/10min	0%	0.00E+00
	5%	7.00E-03
	50%	2.00E-01
	95%	8.00E-01
	100%	1.00E+00

WD-C: Fraction of aerosols removed by rain						
PARTICLE SIZE	**QUANTILE**	**Rainfall: .3mm/hr**	**Rainfall: 2.mm/hr**	**Rainfall: .05mm/10 min**	**Rainfall: .33mm/10 min**	**Rainfall: 1.67mm/10 min**
0.1μ	**0%**	1 00E-04	4.00E-03	1.00E-05	5.00E-04	1.00E-03
	5%	2.00E-04	8.00E-03	2.00E-05	1.00E-03	2.00E-03
	50%	5 00E-03	2.00E-02	1.00E-03	1.00E-02	2.00E-02
	95%	2.00E-02	4.00E-02	5.00E-03	3.00E-02	6.00E-02
	100%	1.00E+00	1.00E+00	1.70E-01	7.00E-01	1.00E+00
0.3μ	**0%**	5.00E-05	5.00E-04	1.00E-05	1.00E-04	2 50E-04
	5%	1.00E-04	1.00E-03	2 00E-05	2.00E-04	5.00E-04
	50%	5.00E-04	2.00E-03	8.00E-05	2.00E-03	2.00E-03
	95%	2.00E-02	4.00E-02	4.00E-03	3.00E-02	6.00E-02
	100%	1.00E+00	1.00E+00	1.70E-01	7.00E-01	1.00E+00
1.00μ	**0%**	1.00E-03	2 00E-03	5.00E-05	1.00E-03	2.00E-03
	5%	2 00E-03	4.00E-03	1.00E-04	2 00E-03	4.00E-03
	50%	5.00E-03	1.60E-02	8.00E-04	8.00E-03	2.00E-02
	95%	2 00E-02	4.00E-02	5.00E-03	3.00E-02	9.00E-02
	100%	1.00E+00	1.00E+00	1 70E-01	7.00E-01	1.00E+00
10.00μ	**0%**	5.00E-02	3.00E-01	1.00E-02	1.00E-01	3.25E-01
	5%	1.00E-01	6.00E-01	2.00E-02	2.00E-01	6.50E-01
	50%	3.00E-01	9.00E-01	5.00E-02	3.50E-01	9.50E-01
	95%	4.50E-01	9 50E-01	1.20E-01	5.00E-01	9.80E-01
	100%	9.99E-01	9.99E-01	9.99E-01	9.99E-01	9.99E-01

Expert E

As a scientist I look for an improved understanding of nature; as a technologist I look for something useful as an outcome of any planned exercise.

This exercise has led me to rethink, in the sense of re-examine and re-substantiate, some old thoughts about the concepts we use to describe turbulence and physical properties of objects and materials. I had imagined that the intended outcome would be a more correct estimate of what would happen if there were a release of radioactive material at ground level.

As a meteorologist I have to face a reality in which each and every day has its own particular mix of wind, temperature, cloud, rain, etc. The wind fluctuates in response to temperature changes that themselves depend on sunshine and reflection and radiation from ground and clouds, and absorption by them. Even these objects on the ground are living organisms whose behavior varies diurnally and with the seasons.

These factors form an infinite variety that makes each time and place different. The words "dispersion" and "deposition" are the resulting consequences of the "emission" of pollutants described as if there were only these two mechanisms to be added to make behavior of pollution an order of magnitude more complex to describe than the weather.

Actually, the spreading of a cloud or plume of pollution is adequately described by drawing an angle or spread, a distribution within the cloud or plume, and a track; for then a footprint of the pollution can be drawn. Similarity at all stages of spread is assumed in the distribution. Can we do better than sketch the spread and the distribution on a bit of paper? Of course that will not do for the purposes of sophisticated computation and the perceived complexity of reality.

A wide variation in the dispersion and deposition is observed. Therefore, an accurate assembly of facts is desired so that the wide variations can be mapped. Although they are clearly understood to be unpredictable as to detail, the possibility and probabilities will be tied down and put in place.

However tidily those probabilities are mapped, the nature of the initiating incident remains largely unspecified, and the ranges of weather and other determining factors have been restricted to supposedly manageable proportions, so that the answers emerging from the exercise are likely to bear little relation to the well-known occurrences at Windscale, Three Mile Island, Chernobyl, and Tomsk.

So who will be impressed by the present parade of expertise? The numbers provided are honest attempts to delineate the magnitudes of the phenomena that have been carefully described. But actuality has been, and always will be, different because nature provides more choices than can possibly be taken into account.

In the meantime, real meteorologists, used to the problems of forecasting, compose models that can usefully employ the predictive charts they make a few times every day. Into the situations they describe, any source of pollution can be inserted, so as to warn the world's fire brigades what their jobs are likely to be in the actual event presently being unfurled.

For such a purpose (and what better purpose can be planned in advance to supersede this purpose?) the calculation might as well be done graphically on the back of an old envelope that can be trashed and replaced as necessary when reports of reality come in.

Theoretical Case Studies

The weather forecasting services engage in many exercises that are far more significant than the trivial testing for correctness of rain or no-rain forecasts.

To make numerical forecasts, the numerical models have to be far more sophisticated than is usually understood, in order to produce predictions of the weather for many hours ahead. From the weather charts almost every other aspect of the forecasts follow. The exercise includes providing a satisfactory starting situation, which in itself is consistent with the basic equations of mechanics and physics; this alone is no mean task.

It is known from long experience of testing forecasting models on documented past cases that predictions of wind can and must be made so that a good starting point for the prediction of the transport of pollution routinely exists.

The largest obstacle to success is not the difficulty of representing lateral or vertical dispersion but rather the problem of calculating, with enough accuracy to determine future horizontal transport, the vertical displacements of the air (and the pollution contained in it).

I see no reason why case histories should not be synthesized from recorded weather to provide stimulating suggestions, for which we should be prepared if an accident occurred at a nuclear power station. Would not such cases be of great interest to decision makers?

In such cases, the interesting factors "predicted" would include air concentrations, and from these it would be possible to calculate deposition or ingestion without hiding the assumptions about deposition velocities in computations where the numbers used half-way would not be obvious, but hidden in sophisticated uncertainty concepts.

Atmospheric Stability

This term refers to the static stability represented by the vertical potential temperature gradient. It has been customary in dispersion and other pollution studies to represent this gradient by stating the value of the potential temperature at two different heights above the ground. By limiting the information to these two values, it is impossible to represent the very relevant features of the potential temperature profile in relation to the vertical displacement of pollution particles.

Thus there is no differentiation between cases in which the air is being warmed and those in which it is being cooled (between morning and evening situations). It is obvious that a positive potential temperature gradient suppresses turbulence of a kind which would cause vertical transfer of pollution. It is therefore illogical to discuss, as steady states, stable turbulent situations. It is even nonsense to supply, as basic data, a condition that the air is turbulent and stable, and to request values of transfer coefficients or outcomes which it is to be supposed would be produced if that state continued.

If, for example, the potential temperature at 100 m was stated to be greater than at 10 m (or 1 m), implying that the air was stable, it could still be turbulent on account of mechanically or thermally produced eddies from the ground up to 50 m. On the other hand, it might be without turbulence if the potential temperatures at 10 and 100 m were the same, and the air below 10 m (or even, in another case, only below 1m) happened to be very stable, as it often is around sunset.

The assumption that the average gradient between two levels is adequate or suitable to represent the stability is hallowed by its use to compute the prestigious Monin-Obukhov length. But in a serious study of the present kind that is nonsense. The Monin-Obukhov length is not an adequate parameter to represent the effect of stability on diffusion pollution.

Deposition Velocity

The conditions under which the deposition velocity has been measured vary greatly, and the circumstances, such as the nature of the surface, are in many cases described only qualitatively. Furthermore, the time of day and conditions of sunshine are not always (or even usually) described, although they make a great deal of difference to the outcome.

Bearing all the circumstances in mind that might explain the great variations between occasions, I have tried to picture the limiting circumstances and the variations they may produce and which of these actually have been the result in the numbers recorded.

The result is not satisfactory because the methods of using the numbers provided are not in any way descriptive of the causes of the variations. The numbers are posed as physical coefficients representing a mechanism, whereas actually they represent the outcome of a great many mechanisms involving the behavior of different vegetable components and rates of different geometrical objects that act to generate the turbulence.

The fact that the quantities proposed as representing the complex capture process vary by two (decimal) orders of magnitude means that on any occasion the situations are not properly appreciated and described. This is scarcely a suitable starting point for numerical calculations that can lead to results on the basis of which action can be taken.

In the case of washout by rain, any measurements recorded do not really describe how the deposited material came to be within the raindrops. It makes very much difference whether the particles captured and deposited were included in a droplet by acting as a condensation nucleus, by capture from the air within a cloud of droplets, or, as seemingly presumed in this exercise, captured in the air below a cloud by a falling raindrop. This has been particularly important in the past when the captured particles may have come from several different origins according to the altitude at which they entered a droplet.

Estimation of Proportion of Washout

Large raindrops capture less of anything than the same amount of water in the form of smaller droplets because of the smaller cross section area. Heavy rainfall rates are assumed to be composed of larger drops, and so do not capture smaller particles and at a proportionately increased rate. Thus the same amount of rain falling on the same area in a longer time captures more than in the shorter time.

Chamberlain gives a diagram expressing this for the capture (washout) of SO_2 and I_2 (paragraph 76 of Chamberlain's chapter in "The Aerodynamic Capture of Particles," edited by E.G. Richardson, published by Pergamon). This diagram was used directly for Iodine and also for Methyliodide by comparison with the larger molecule of SO_2.

The formula used by Chamberlain to calculate the curves was originated by Ranz and Marshall, and is used for lack of better information and because it is found to be reasonable. Chamberlain's original report is an official publication of 1953 (reference given in Chamberlain's article).

The size spectrum (originated by Best) is considered fair for rain. It is more easily measured than cloud droplet size spectra and is less variable in time than in clouds, and is, on the whole, acceptable. The diagram in Figure E-1 is for SO_2 & I_2. Human skin is assumed not to include hairs. With hairs and fidgety movement or cycling (increased airflow), much higher values are expected.

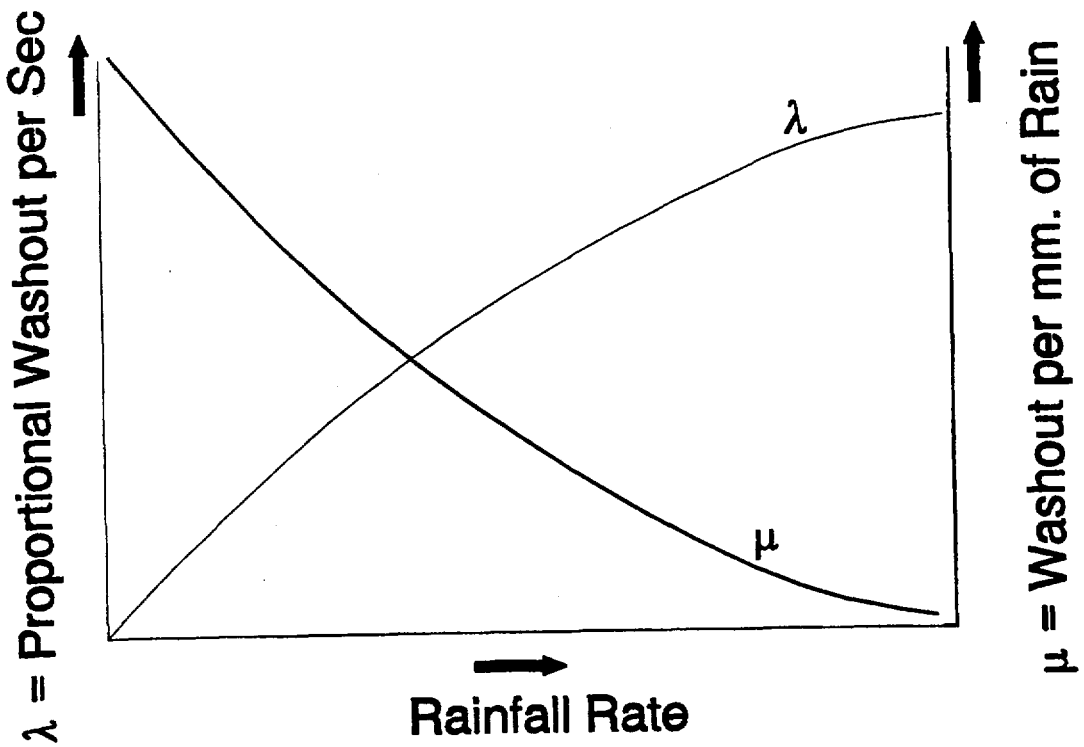

Figure E-1. Capture curves for SO_2 and I_2.

Deposition Tables

Units of velocity are in cm/s; N/A = not provided by expert; unkn = unknown

DD-A: Dry deposition velocity of aerosols - Wind Speed at 2m/s					
PARTICLE SIZE	**QUANTILE**	**URBAN**	**MEADOW**	**FOREST**	**HUMAN SKIN**
0.10μ	**0%**	5.00E-03	5.00E-03	2.00E-02	5.00E-03
	5%	1.00E-02	1.00E-02	3.00E-02	1.00E-02
	50%	1.00E-01	2.00E-01	5.00E-02	4.00E-02
	95%	5.00E-01	5.00E-01	2.00E+00	1.00E-01
	100%	N/A	N/A	N/A	N/A
0.30μ	**0%**	5.00E-03	5.00E-03	5.00E-03	2.00E-03
	5%	5.00E-03	1.00E-02	1.00E-02	5.00E-03
	50%	1.00E-01	1.00E-01	1.00E-01	4.00E-02
	95%	5.00E-01	5.00E-01	1.50E-01	1.00E-01
	100%	N/A	N/A	N/A	N/A
1.00μ	**0%**	5.00E-03	8.00E-03	5.00E-03	5.00E-03
	5%	2.00E-02	1.00E-02	1.00E-02	1.00E-02
	50%	5.00E-01	5.00E-01	2.00E-01	1.00E-01
	95%	5 10E-01	7.00E-01	5.00E-01	3.00E-01
	100%	N/A	N/A	N/A	N/A
3.00μ	**0%**	1.00E-02	1.00E-02	5.00E-02	1.00E-02
	5%	5.00E-02	3.00E-02	1.00E-01	3.00E-02
	50%	7.00E-01	9.00E-01	8.50E-01	3.00E-01
	95%	1.00E+00	2.50E+00	1.00E+00	1.00E+00
	100%	N/A	N/A	N/A	N/A
10.00μ	**0%**	8.00E-02	5.00E-02	5.00E-01	1.00E-01
	5%	1.00E-01	1.00E-01	1.00E+00	5.00E-01
	50%	9.00E-01	1.70E+00	1.80E+00	1.00E+00
	95%	2.00E+00	2.50E+00	2.00E+00	3.00E+00
	100%	N/A	N/A	N/A	N/A

DD-B: Dry deposition velocity of aerosols - Wind Speed at 5m/s					
PARTICLE SIZE	QUANTILE	URBAN	MEADOW	FOREST	HUMAN SKIN
0.10μ	0%	5.00E-03	5.00E-03	5.00E-02	5.00E-03
	5%	1.00E-02	1.00E-02	5.00E-02	1.00E-02
	50%	1.00E-01	1.00E-01	1.50E-01	5.00E-02
	95%	5.00E-01	1.00E+00	2.00E-01	1.00E-01
	100%	1.00E+00	2.00E+00	4.00E-01	1.50E-01
0.30μ	0%	5.00E-03	5.00E-03	5.00E-03	4.00E-03
	5%	5.00E-03	1.00E-02	8.00E-03	7.00E-03
	50%	1.00E-01	1.00E-01	1.00E-01	4.00E-02
	95%	5.00E-01	8.00E-01	1.50E-01	9.00E-02
	100%	1.00E+00	2.00E+00	4.00E-01	1.50E-01
1.00μ	0%	5.00E-03	8.00E-03	5.00E-03	5.00E-03
	5%	2.00E-02	2.00E-02	1.00E-02	1.00E-02
	50%	5.00E-01	5.00E-01	2.00E-01	1.00E-01
	95%	6.00E-01	8.00E-01	3.00E-01	3.00E-01
	100%	1.00E+00	2.00E+00	1.00E+00	4.00E-01
3.00μ	0%	1.00E-02	1.00E-02	5.00E-02	3.00E-02
	5%	5.00E-02	5.00E-02	7.00E-02	5.00E-02
	50%	1.00E+00	1.00E+00	8.00E-01	3.00E-01
	95%	1.20E+00	1.50E+00	2.00E+00	1.00E+00
	100%	1.50E+00	2.00E+00	3.00E+00	1.50E+00
10.00μ	0%	8.00E-02	5.00E-02	5.00E-01	1.00E-01
	5%	1.00E-01	1.00E-01	1.00E+00	2.00E-01
	50%	1.00E+00	2.00E+00	2.00E+00	1.00E+00
	95%	2.00E+00	3.00E+00	4.00E+00	3.00E+00
	100%	3.00E+00	3.50E+00	4.50E+00	4.00E+00

DD-C: Dry deposition velocity of elemental iodine - Wind Speed at 2 and 5m/s					
WIND SPEED	QUANTILE	URBAN	MEADOW	FOREST	HUMAN SKIN
2.m/s	0%	5.00E-02	5.00E-02	8.00E-02	1.00E-02
	5%	1.00E-01	1.00E-01	1.00E-01	5.00E-02
	50%	5.00E-01	1.00E+00	1.50E+00	3.00E-01
	95%	1.00E+00	1.50E+00	2.00E+00	1.00E+00
	100%	2.00E+00	2.50E+00	3.00E+00	1.50E+00
5.m/s	0%	5.00E-02	8.00E-02	9.00E-02	2.00E-02
	5%	1.00E-01	1.00E-01	1.00E-01	6.00E-02
	50%	7.00E-01	1.50E+00	2.50E+00	7.00E-01
	95%	1.50E+00	2.00E+00	3.00E+00	1.50E+00
	100%	4.00E+00	2.50E+00	4.00E+00	2.00E+00

DD-D: Dry deposition velocity of methyl iodide - Wind Speed at 2 and 5m/s					
WIND SPEED	QUANTILE	URBAN	MEADOW	FOREST	HUMAN SKIN
2.m/s	0%	3.00E-03	5.00E-03	2.00E-02	5.00E-03
	5%	5.00E-03	3.00E-02	3.00E-02	1.00E-02
	50%	5.00E-02	7.00E-01	1.00E+00	6.00E-01
	95%	5.00E-01	1.50E+00	2.00E+00	1.00E+00
	100%	7.00E-01	2.00E+00	2.50E+00	1.50E+00
5.m/s	0%	5.00E-03	3.00E-02	3.00E-02	1.00E-02
	5%	1.00E-02	5.00E-02	5.00E-02	2.00E-02
	50%	1.00E-01	1.00E+00	1.30E+00	1.00E+00
	95%	7.00E-01	2.50E+00	3.00E+00	1.50E+00
	100%	1.00E+00	3.00E+00	4.00E+00	2.00E+00

DD-E-1: Dry deposition velocity of aerosols on Moorland/Peatland Surface		
PARTICLE SIZE	QUANTILE	
0.55μ	0%	1.00E-03
	5%	1.00E-03
	50%	4.00E-02
	95%	2.00E-01
	100%	3.00E-01
0.70μ	0%	1.00E-03
	5%	1.00E-03
	50%	4.00E-02
	95%	2.00E-01
	100%	3.00E-01
0.90μ	0%	1.00E-03
	5%	1.00E-03
	50%	5.00E-02
	95%	3.00E-01
	100%	4.00E-01
1.20μ	0%	1.00E-03
	5%	2.00E-03
	50%	5.00E-02
	95%	3.00E-01
	100%	4.00E-01
1.60μ	0%	2.00E-03
	5%	2.00E-03
	50%	6.00E-02
	95%	4.00E-01
	100%	5.00E-01

DD-E-2: Dry deposition velocity of aerosols on Heather/Green Grass Surface		
PARTICLE SIZE	**QUANTILE**	
0.55μ	**0%**	1.00E-03
	5%	2.00E-03
	50%	1.00E-01
	95%	5.00E-01
	100%	7.00E-01
0.70μ	**0%**	3.00E-03
	5%	5.00E-03
	50%	1.00E-01
	95%	5.00E-01
	100%	7.00E-01
0.90μ	**0%**	3.00E-03
	5%	5.00E-03
	50%	2.00E-01
	95%	5.00E-01
	100%	8.00E-01
1.20μ	**0%**	5.00E-03
	5%	1.00E-02
	50%	2.00E-01
	95%	5.00E-01
	100%	8.00E-01
1.60μ	**0%**	5.00E-03
	5%	1.00E-02
	50%	2.00E-01
	95%	6.00E-01
	100%	9.00E-01

DD-E-2: Dry deposition velocity of aerosols on Heather/Green Grass Surface (continued)		
PARTICLE SIZE	**QUANTILE**	
2.30μ	**0%**	5.00E-03
	5%	1.00E-02
	50%	2.00E-01
	95%	8.00E-01
	100%	1.00E+00
3.20μ	**0%**	1.00E-02
	5%	2.00E-02
	50%	3.00E-01
	95%	9 00E-01
	100%	1.20E+00
4.20μ	**0%**	1.00E-02
	5%	2.00E-02
	50%	4.00E-01
	95%	1 00E+00
	100%	1.50E+00

DD-F: Dry deposition velocity of aerosols on Grassland Surface		
PARTICLE SIZE	**QUANTILE**	
1.0μ	**0%**	5.00E-03
	5%	1.00E-02
	50%	6.00E-01
	95%	1.50E+00
	100%	2.00E+00

WD-A: Elemental iodine—fraction removed by rain ($1-f_w$)							
Rainfall/ Time	Wind Speed	Quantile	$1-f_w$	Rainfall/ Time	Wind Speed	Quantile	$1-f_w$
.3mm/hr	unkn	0%	N/A	2.mm/hr	unkn	0%	N/A
		5%	5.00E-02			5%	2.00E-01
		50%	1.00E-01			50%	4.00E-01
		95%	1.50E-01			95%	6.00E-01
		100%	N/A			100%	N/A
.075mm/ 10min	10 m/s	0%	N/A	.05mm/ 10min	unkn	0%	N/A
		5%	2.00E-02			5%	1.50E-02
		50%	3.00E-02			50%	2.50E-02
		95%	5.00E-02			95%	4.00E-02
		100%	N/A			100%	N/A
.17mm/ 10min	5 m/s	0%	N/A	.17mm/ 10min	14 m/s	0%	N/A
		5%	2.00E-02			5%	3.00E-02
		50%	4.00E-02			50%	5.00E-02
		95%	5.50E-02			95%	7.00E-02
		100%	N/A			100%	N/A
.23mm/ 10min	12 m/s	0%	N/A	.5mm/ 10min	unkn	0%	N/A
		5%	4.00E-02			5%	5.00E-02
		50%	6.00E-02			50%	8.00E-02
		95%	7.00E-02			95%	1.00E-01
		100%	N/A			100%	N/A
.33mm/ 10min	unkn	0%	N/A	1.0mm/ 10min	14 m/s	0%	N/A
		5%	4.00E-02			5%	1.00E-01
		50%	7.00E-02			50%	1.30E-01
		95%	9.00E-02			95%	1.60E-01
		100%	N/A			100%	N/A

WD-A: Elemental iodine—fraction removed by rain ($1\text{-}f_w$) (continued)			
Rainfall/Time	**Wind Speed**	**Quantile**	$1\text{-}f_w$
1.67mm/10min	**unkn**	**0%**	N/A
		5%	1.20E-01
		50%	1.50E-01
		95%	1.90E-01
		100%	N/A

WD-B: Methyl iodide—fraction removed by rain (Wind Speed=unknown)		
Rainfall/Time	**Quantile**	$1-f_w$
.3mm/hr	**0%**	N/A
	5%	6.00E-02
	50%	1.00E-01
	95%	1.60E-01
	100%	N/A
2.mm/hr	**0%**	N/A
	5%	2.00E-01
	50%	5.00E-01
	95%	7.00E-01
	100%	N/A
.05mm/10min	**0%**	N/A
	5%	1.50E-02
	50%	3.00E-02
	95%	5.00E-02
	100%	N/A
.33mm/10min	**0%**	N/A
	5%	5.00E-02
	50%	8.00E-02
	95%	1.00E-01
	100%	N/A
1.67mm/10min	**0%**	N/A
	5%	1.20E-01
	50%	2.00E-01
	95%	2.50E-01
	100%	N/A

WD-C: Fraction of aerosols removed by rain						
PARTICLE SIZE	**QUANTILE**	**Rainfall: .3mm/hr**	**Rainfall: 2.mm/hr**	**Rainfall: .05mm/10 min**	**Rainfall: .33mm/10 min**	**Rainfall: 1.67mm/10 min**
0.10μ	**0%**	N/A	N/A	N/A	N/A	N/A
	5%	4.00E-02	2.00E-01	5.00E-03	1.00E-02	7.00E-02
	50%	2.00E-01	4.00E-01	2.00E-02	6.00E-02	2.00E-01
	95%	3.00E-01	6.00E-01	4.00E-02	8.00E-02	4.00E-01
	100%	N/A	N/A	N/A	N/A	N/A
0.30μ	**0%**	N/A	N/A	N/A	N/A	N/A
	5%	6.00E-02	3.00E-01	1.00E-02	2.00E-02	1.00E-01
	50%	2 00E-01	5.00E-01	5.00E-02	7.00E-02	2.50E-01
	95%	3 00E-01	7 00E-01	1.00E-01	1.00E-01	5.00E-01
	100%	N/A	N/A	N/A	N/A	N/A
1.00μ	**0%**	N/A	N/A	N/A	N/A	N/A
	5%	1.00E-01	3.00E-01	1.00E-02	2 00E-02	1.50E-01
	50%	3.00E-01	5.00E-01	7.00E-02	1.00E-01	2.50E-01
	95%	5.00E-01	7.00E-01	1.00E-01	1.50E-01	6 00E-01
	100%	N/A	N/A	N/A	N/A	N/A
10.00μ	**0%**	N/A	N/A	N/A	N/A	N/A
	5%	2.00E-01	3.00E-01	3.00E-02	5.00E-02	2.00E-01
	50%	4.00E-01	6.00E-01	1.00E-01	2.50E-01	5.00E-01
	95%	8 00E-01	9.00E-01	3.00E-01	5.00E-01	9.00E-01
	100%	N/A	N/A	N/A	N/A	N/A

Expert F

The Urban Area

In the case of an urban area, the v_d may vary not only as a function of pollutant characteristics, meteorological variables, and surface characteristics, but also as a function of such variables as the downwind distance from the rural-urban transition or other local transitions in the urban complex, such as that from a building cluster or a park.

It is suggested that one way of solving these problems might be to use 'local deposition velocities', v_{di}, defined as

$$v_{di} = F(i) / x(z),$$

where F(i) is the flux towards a local surface (e.g., a roof or a wall) and x(z) is the air concentration at the imaginary boundary surface well above the roughness elements of the city that are also above the city canopy. These 'local deposition velocities' can then be used for calculating the total flux to the area and then the deposition velocity over the urban surface. Such a simplified model was proposed by Roed.[1]

The surface types, i.e., the local surfaces, can be assigned their own individual deposition velocities, each obtained as the result of experiments or calculations. Thus the ratio of the deposition velocity of the urban canopy to the area as a whole is the weighted aggregate of the local deposition velocity, i.e.,

$$v_d \text{ (urban)} = \Sigma A_i \cdot v_{di}$$

where A_i is the total surface type 'i' in a horizontally projected area of the city.

The simplified model contrasts with the usual one which makes use of the overall aerodynamic roughness length of the urban complex (the macrosurface roughness). In the former case the spatial proximity of various microsurfaces plays no part, whereas in the latter case it is very important.

However, the total deposition in both cases is dependent on the density of bluff bodies such as buildings, the simplified model giving a higher deposition velocity because of the larger integrated area per projected horizontal area.

Measurements before Chernobyl

To find the local velocities on selected urban surfaces, Roed[2,3] measured the deposition of ^{137}Cs—mainly bomb fallout accumulated over many years—on the surface of a building; he then related it, after applying a correction for radioactive decay, to the known time-integrated air concentration of ^{137}Cs. Also he measured the deposition of naturally produced ^{7}Be on artificial plates placed against vertical walls.

This type of measurement has the advantage that the surfaces studied have been immersed in an actual turbulent environment generated by wind flow on an array of buildings and that the deposition velocity is averaged over enough time to include a wide variety of weather conditions.

The measurements also have a number of drawbacks such as:

1) The areas of plane surfaces chosen in the experiment may not be representative for a number of reasons: deposition could be highly non-uniform spatially, for example, with enhancement occurring near edges, discontinuities, projections, etc. This calls for measurements of large surface areas at different types of locations.

2) The ^{137}Cs deposited on walls had an unknown contribution from wet deposition for some of the samples, whereas others were well protected from the rain. Weathering can diminish the deposition. Roed[2] presented an argument to explain why weathering was not expected to have a dominant influence on the results, and the ^{7}Be results bear this out.

3) The characteristics of the aerosols associated with the deposition of ^{137}Cs are not known in detail, whereas those associated with ^{7}Be have a mean aerodynamic size of about 0.4 μm.

The values of local deposition velocities obtained were notably low. Values for ^{137}Cs onto vertical surfaces largely protected from the rain were below 10^{-4} m/s. The ^{7}Be results for vertical surfaces not exposed to rain were below 1.6×10^{-4} m/s and horizontal surfaces below 7×10^{-1}.

Measurements after Chernobyl

There is a paucity of experimental data on dry deposition on urban surfaces. Roed's[1,4,5] measurements, however, have provided some insight into how various isotopes are distributed on different surfaces. These deposition measurements were made during the passage of the first radioactive cloud from Chernobyl over the Roskilde area in Denmark. The measurements were carried out at noon on Sunday, 27 April 1986; the cloud cleared the area some time during the following week. When deposition took

place, the weather was not changeable: the wind speed was 3 m/s at 8 m above the ground and the Pasquil stability category was B-C.

The measurements were made in the city as well as in suburban and rural areas. The measured deposition velocities are listed in Tables F-1 and F-2. Table F-1 shows the deposition velocities for different isotopes originating from the Chernobyl accident and Table F-2 shows the deposition on different urban surfaces relative to deposition on roads.

There is no obvious indication that the deposition velocity changed from one area to another. It clearly differed for various isotopes, however. Particle-bound caesium had the smallest values, with a mean v_d of about 1×10^{-4} m/s for road surfaces. The next group, consisting of particulate ruthenium, lanthanum, and elementary iodine, had deposition velocities of around 5×10^{-4} m/s. The highest deposition velocity, 10×10^{-4} m/s, was found for particulate cerium and zirconium. The deposition velocity of iodine was similar to that on road surfaces. For caesium, however, it was one order of magnitude lower. The wall surface samples were identical, as they had been fabricated in the laboratory for deposition velocity measurement purposes. However, the walls of which they were part were situated at very different locations, varying from very open areas to very dense city areas. Nevertheless, the deposition velocities of caesium, lanthanum, and cerium were some 5 to 10 times higher than on roads. Only ruthenium had the same deposition velocity on both roads and walls.

Table F-1. Deposition velocity in 10^{-4} m/s

Isotope	I	Cs	Ru	Ba	Ce	Zr
Paved Areas	4.6	0.7	3.5	4.6	8.1	3.5
Walls	3.0	0.1	0.4	0.4	0.9	1.3
Windows	2.3	0.05	0.1	0.2		0.1
Grass (clipped)	22	4.3	4.1	5.8	7.7	7.1
Trees	8.0	7	25	26	39	45
Roofs	33	2.8	3.4	53	40	

Table F-2. Deposition on various urban surfaces relative to deposition on paved areas

Isotope	I	Cs	Ru	Ba	Ce	Zr
Paved areas	1	1	1	1	1	1
Walls	0.6	0.2	0.1	0.1	0.1	0.2
Windows	0.5	0.1	0.04	0.04		0.02
Grass (clipped)	5	6	1.1	1.2	1.0	1.0
Trees	17	10	7	6	13	6
Roofs	7	4	1	12	13	

The deposition velocities of the volatile group of elements (I, Te, Cs, Ru) are lower than those of the refractory group (La, Ba, Ce, Zr). As shown by Rulik et al.[6], these two groups have different particle sizes; the first group has an AMAD of about 0.4 μm.

Dry deposition velocities reported by Magua et al.[7] for ^{137}Cs and ^{131}I on grass are shown in Table F-3.

Nicholson[8] reported dry deposition velocities for vertical surfaces and roofs, and these values are shown in Table F-4.

Sehmel[9] showed the importance of gravitational particle settling as a deposition mechanism. He suggested that the settling velocity for 1 μm diameter particles is of the order of $10^{-4}m^{-1}$ while those for 3, 5, and 10 μm particles can be of the order of 10^{-3}, 3×10^{-3}, and 10^{-2} m/s.

Deposition on trees and grass

The first cloud from the Chernobyl release arrived under dry weather conditions at the Roskilde area, where the measurements were carried out at noon on 27 April 1986; the cloud cleared the area some time during the following day. The dry weather conditions persisted throughout the following week.

In the time interval during which deposition took place, the weather continued unchanged with a mean wind speed of 3 m/s at 8 meters height and a Pasquill stability category of B-C.

The airborne radioactivity was measured by sucking air through a Whatman glass-fibre paper and measuring the material collected using gamma-spectroscopy. Such filters provide an efficiency close to 100% for particulate pollution. Thus, for isotopes existing only in particulate form, representative deposition velocities can be calculated based on the airborne activity collected on the glass-fibre filters.

For iodine, however, a problem arises because this element can be present in the atmosphere in three forms: (i) attached to particles, (ii) as elemental iodine vapour, and (iii) as gaseous organic compounds of iodine. Organic iodine is deposited neither on glass-fibre filters, nor significantly on surfaces, so it can be excluded from further consideration. Of the remaining forms of iodine, only the particulatefraction is found in the filter, whereas the major fraction of the deposition may arise from the more rapidly deposited iodine vapour. Calculated deposition velocities are therefore unrepresentative of either form. However, some measurements made in Germany[10] indicate that the levels of elemental iodine in the initial Chernobyl cloud were about equal to those of the particulate fraction. Thus the deposition velocities given here provide an approximate value for the elemental iodine component (assuming the composition of the cloud reaching Roskilde to be similar

Table F-3. Deposition velocities for ^{137}Cs and ^{131}I, derived from measurements at the RWTH Aachen after the Chernobyl accident[7]

Nuclide	Remarks	v_d grass (cm/s)
^{137}Cs	all samples considered	0.03 - 0.15 mean: 0.07
	calculated with fitted curves	0.05 ± 0.01
^{131}I	total iodine:	
	mean for daytime minimum	0.15
	overall mean	0.2
	iodine species*:	
	elemental:	
	mean for daytime minimum	0.5
	overall mean	0.8
	particle bound:	0.1

*Calculated with 30% elemental, 30% particle bound, and 40% organic iodine.

Table F-4. Deposition Velocities (cm s^{-1})

Location	^{134}Cs	Deposition Velocities (cm s^{-1}) ^{137}Cs (Total)	^{137}Cs (Weapons fallout)
Building Bricks			
Norwich	$<5 \times 10^{-4}$	2×10^{-3}	$>4.4 \times 10^{-3}$
Harwell Lab.	$<4 \times 10^{-3}$	1×10^{-2}	$>1.2 \times 10^{-2}$
Clay Roof Tiles (Building 1)			
North Upper	6×10^{-2}	6×10^{-2}	6×10^{-2}
Lower	9×10^{-2}	11×10^{-2}	11×10^{-2}
Mean	8×10^{-2}	8×10^{-2}	8×10^{-2}
South: Upper	8×10^{-2}	12×10^{-2}	13×10^{-2}
Lower	7×10^{-2}	8×10^{-2}	9×10^{-2}
Mean	7×10^{-2}	10×10^{-2}	11×10^{-2}
Clay Roof Tiles (Building 2)			
East	4×10^{-2}	5×10^{-2}	5×10^{-2}
West	5×10^{-2}	6×10^{-2}	6×10^{-2}
South	3×10^{-2}	7×10^{-2}	8×10^{-2}
East: Upper	$<4 \times 10^{-2}$	7×10^{-2}	8×10^{-2}
Middle	9×10^{-2}	8×10^{-2}	6×10^{-2}
Lower	5×10^{-2}	6×10^{-2}	6×10^{-2}
Mean	6×10^{-2}	7×10^{-2}	7×10^{-2}
Concrete Roof Tiles (Building 3)			
			$^{137}Cs/^{134}Cs$ (Surface Activity)
East Upper	4.2×10^{-2}	5.5×10^{-2}	2.0
East Lower	4.5×10^{-2}	5.8×10^{-2}	2.0
West Upper	3.9×10^{-2}	5.0×10^{-2}	2.0
West Lower	3.2×10^{-2}	4.7×10^{-2}	2.2
Roofing Felt (Building 4)			
Flat Roof	8×10^{-2}	18×10^{-2}	3.4

* Deposition velocities could be up to 50% greater

to that observed in Germany). The measured deposition velocities can therefore be considered as those of elementary iodine.

The investigation was carried out in the Boserup forest 5 km southwest of Risø, consisting mainly of common spruce with an average height of about 6.4 m. Two trees chosen at random were felled and cut into sections, one into 8 and the other into 4. The branches and needles were then chopped into pieces and the deposition on each section was measured separately, as was the cortex of each section. To find the total deposition, the number of trees per m^2 of forest area was determined and samples of the forest soil were taken.

In the case of trees from the suburban area, only the local deposition velocity was of interest; a yew tree 2.5 m high was measured in two sections.

The material deposited on the two common spruces chosen from the Boserup forest was very evenly distributed per unit mass of bulk material (small branches, twigs, and needles). Besides the total deposition velocity, it is therefore interesting to know as well the amount of bulk mass per unit forest area, as the even distribution indicates that the total deposition velocity is proportional to the bulk mass per unit forest area within the limitations of the ability of the atmosphere turbulence to carry enough material to the boundary layer at the canopy of the forest.

Tables F-5 and F-7 show the distribution of the deposited material on branches, twigs, and needles with height above the ground. The bulk deposition with height is shown in Tables F-6 and F-8. In Tables F-9 and F-11 the distribution of the deposition on the cortex of each tree is shown, and Tables F-10 and F-12 show the deposition per unit area of the cortex. The total deposition velocity of the forest is given in Table F-13. It is calculated as the total deposited material on the trees and on the forest soil per unit area divided by the integrated air concentration. A yew and a juniper berry tree were cut in the urban environment. They were part of a tight hedge in a suburban front garden. Table F-14 shows the local deposition velocity, i.e., the deposited material per unit mass of small branches, twigs, and needles divided by the time-integrated air concentration for all the trees. The bulk deposition constant is shown in Table F-15. It is seen that the bulk deposition constant is about the same for both the trees in the suburban area and equal to that of the forest trees.

In Table F-16, the local deposition velocity is shown, and a bulk deposition constant B_d for grass is given as the deposited material per unit mass for grass, divided by the time-integrated air concentration. When modeling deposition on trees and grass, it seems that the important parameters to be used are the mass of the bulk material and the bulk deposition constant.

Table F-5. Deposited material on branches, twigs, and needles of common spruce at different heights, in Bq: tree no. 1

Height	cm	0-75	75-135	135-215	215-315	315-405	405-472	472-545	545-654	0-654
^{7}Be	Bq	6.3	8 1	11.6	11.2	19.3	11.2	26 5	7.9	102
^{95}Nb	"	19 4	72 2	57 0	28 0	95.2	52.2	69.7	63.1	456.7
^{95}Zr	"	10 4	37.4	36.0	16.6	59.5	30.4	40.2	36.2	266.8
^{103}Ru	"	4.7	14.0	10.6	17.9	16.8	17.3	26.8	19.5	127.5
^{106}Ru	"	0 71	4.6	3.1	4 0	3 8	5.1	8.7	7.8	37.7
^{131}I	"	226.7	226.2	282.2	294.7	-	182.6	585.5	116.5	1916.4
^{134}Cs	"	0 97	1 5	2 0	3.2	3 6	2.2	5.4	2.9	21.6
^{137}Cs	"	2.7	3.8	4.4	7.2	8.9	5.0	11.7	7.4	50.9
^{141}Ce	"	7 7	30.0	52.7	22.7	49.3	39.0	57.4	32 3	291.2
^{144}Ce	"	5.1	22.8	25.2	14 4	34 6	27.0	42.7	16 7	188.5
^{152}Eu	"	-	-	-	0.55	-	0.16	0 60	0.40	1.71
^{154}Eu	"	0.07	0.31	0.18	0.23	0.73	0.09	0.15	0.68	2.44

Table F-6. Deposited material on branches, twigs, and needles of common spruce in Bq per m² of cortex: tree no. 1

Height	cm	0-75	75-135	135-215	215-315	315-405	405-472	472-545	545-654	0-654
^{7}Be	Bq/kg	7.4	6.5	6 6	6.6	8.1	7 5	10.4	4.9	7.3
^{95}Nb	"	22 8	57 7	32 6	16.5	39 7	34.8	27.3	39.4	33 9
^{95}Zr	"	12 3	30.0	20.6	9 8	24 8	20.3	15.8	22.6	19 5
^{103}Ru	"	5.5	11.2	6 1	10.5	7 0	11 5	10 5	12 2	9 3
^{106}Ru	"	0 84	3 7	1 8	2 3	1 6	3 4	3 4	4.9	2.7
^{131}I	"	266 7	181 0	162 4	173 4	-	121 7	229 6	72 8	172.5
^{134}Cs	"	1 1	1.2	1.2	1.9	1.5	1.5	2.1	1 8	1.5
^{137}Cs	"	3 1	3 0	2 5	4.2	3.7	3.3	4.6	4 6	3.6
^{141}Ce1	"	9 1	24 0	30.1	13 3	20 5	26 0	22.5	20 2	20.7
^{144}Ce	"	6 0	18 2	14 4	8.5	14 4	18.0	16.8	10.4	13 3
^{152}Eu	"	-	-	-	0 32	-	0 11	0 24	0.25	0.23
^{154}Eu	"	0 052	0 25	0 10	0 14	0 30	0 06	0 059	0.43	0.17

Table F-7. Deposited material on branches, twigs, and needles of common spruce at different heights, in Bq: tree no. 2

Height of tree	cm	0 125	125-275	275-390	390-610	0-610
^{7}Be	Bq	14 2	19.5	15 9	56 1	105 6
^{95}Nb	"	67 5	150.7	44 6	243.7	506.5
^{95}Zr	"	51 3	56 3	27.0	153.6	288 2
^{103}Ru	"	-	22 2	9 1	78 5	109 7
^{106}Ru	"	4 5	7.5	-	17.2	29 2
^{131}I	"	148 2	197 0	339.9	792.3	1477 3
^{134}Cs	"	1 8	3.6	3 5	13.0	21.8
^{137}Cs	"	3.9	8.4	7.7	29.0	48 9
^{141}Ce	"	42.9	49.9	24 8	171.6	289 2
^{144}Ce	"	27.3	35.9	20 1	110 4	193 6
^{152}Eu	"	0 71	0.56	0 13	1.92	3 3
^{154}Eu	"	0.16	0.42	0 93	0.81	2 3

Table F-8. Deposited material on branches, twigs, and needles of common spruce at different heights, in Bq per Kg (branches, twigs, and needles): tree no. 2

Height of tree	cm	0-125	125-275	275-390	390-610	0-610
^{7}Be	Bq/kg	10.9	11.5	8 1	13.2	11.0
^{95}Nb	"	57.9	88.7	22.9	57.3	56.7
^{95}Zr	"	39.5	33.1	13.9	36 2	30 7
^{103}Ru	"	-	13 0	4 7	18 46	12.1
^{106}Ru	"	3.5	4.4	-	4.1	4.0
^{141}I	"	114.0	115.8	174 0	186.4	147.6
^{134}Cs	"	1.4	2.1	1 8	3.0	2.1
^{137}Cs	"	3.0	5.0	3.9	6.8	4 7
^{141}Ce	"	33 0	29.4	12.7	40 4	28.9
^{144}Ce	"	21 0	21 1	10.3	26.0	19.6
^{152}Eu	"	0.55	0 33	0 067	0 45	0.35
^{154}Eu	"	0.12	0 25	0 48	0.19	0 26

Table F-9. Deposited material on cortex of common spruce at different heights in Bq: tree no. 1

Height	cm	0-75	75-135	135-215	215-315	315-405	405-472	472-545	545-654	0-654
^{7}Be	Bq	1 6	1.7	2.1	1 7	1.9	1.2	0.93	2 5	13.6
^{95}Nb	"	8 3	0 27	0 19	0 19	-	0 51	0.31	2 2	12 0
^{95}Zr	"	6 0	0.37	0.16	0 16	-	0 25	0 49	1.4	8.8
^{103}Ru	"	2 5	0 13	0 18	0 24	1 5	0 22	0.22	0.49	5.5
^{106}Ru	"	1.1	0 003	0.38	0 15	-	0.069	-	0.14	1.8
^{131}I	"	15 6	10.1	14.2	13 8	-	-	248.8	117.7	420 2
^{134}Cs	"	0 19	0.052	0 017	0.11	0.053	-	(0.008)	0 056	0 49
^{137}Cs	"	0.45	0 22	0 27	0.27	0 18	0 06	0.03	0.16	1.6
^{141}Ce	"	4 8	0 09	-	-	0 44	-	-	0 75	6.1
^{144}Ce	"	3 4	0.20	0 13	-	-	0 26	-	0.75	4.7
^{152}Eu	"	0.04	-	-	0.015	-	-	-	-	0.055
^{154}Eu	"	0.12	0 089	0.17	0.13	-	0 098	0.064	0.03	0.7

Table F-10. Deposited material on cortex of common spruce at different heights, in Bq per m² of cortex: tree no. 1

Height	cm	0-75	75-135	135-215	215-315	315-405	405-472	472-545	545-654	0-654
^{7}Be	Bq/m²	5.5	8.3	8.4	6.1	8.9	9.4	8.5	23.1	9.8
^{95}Nb	"	29.4	1.4	0.78	0.68	-	3.9	2.9	20.9	8.6
^{95}Zr	"	21.2	1.9	0.66	0.61	-	1.9	4.5	13.1	6.3
^{103}Ru	"	8.8	0.67	0.71	0.88	7.2	1.7	2.0	4.6	3.3
^{106}Ru	"	3.8	0.016	1.5	0.53	-	0.52	-	1.3	1.3
^{131}I	"	55.3	50.7	56.9	50.0	-	-	2284.3	1675.0	695.4
^{134}Cs	"	0.68	0.26	0.069	0.22	0.25	-	(0.074)	0.53	0.3
^{137}Cs	"	1 9	1.1	1.1	1.0	0.83	0.47	0.25	1.5	1.0
^{141}Ce	"	17.0	0.47	-	-	2.1	-	-	7.1	6.7
^{144}Ce	"	12.1	1 0	0.54	-	-	2.0	-	7.0	4.5
^{152}Eu	"	0.2	-	-	0.05	-	-	-	-	0.13
^{154}Eu	"	0.42	0.44	0.66	0.47	-	0.74	0.59	0.28	0.51

Table F-11. Deposited material on cortex of common spruce at different heights, in Bq: tree no. 2

Height of tree	cm	0-125	125-275	275-390	390-610	0-610
^{7}Be	"	1.7	1 1	1.7	3.5	8.0
^{95}Nb	"	0.35	7.3	3.0	-	10.7
^{95}Zr	"	0.45	4 4	1.7	0.068	6.6
^{103}Ru	"	0.23	0.94	0.33	0.22	1.7
^{106}Ru	"	0.13	0.073	0.086	0.36	0.65
^{131}I	"	263.0	103.7	28.9	9.6	405.2
^{134}Cs	"	0.11	0.13		0.083	0.33
^{137}Cs	"	0.4	0.44	0.17	0.23	1.2
^{141}Ce	"	-	2.1	0.24	0.57	2.9
^{144}Ce	"	0.13	1.7	0.93	0.26	3.0
^{152}Eu	"	-	0.074	-	0.13	0.13
^{154}Eu	"	0.065	0.074	0.21	0.052	0.40

Table F-12. Deposited material on cortex of common spruce at different heights, in Bq per m² of cortex: tree no. 2

Height of tree	cm	0-125	125-275	275-390	390-610	0-610
^{7}Be	Bq/m²	4.4	3.1	8.3	20 0	9.0
^{95}Nb	"	0.91	20.7	14.4	-	12.0
^{95}Zr	"	1.2	12 5	8.3	0 39	5.6
^{103}Ru	"	0.59	2 7	1.6	1.2	1 5
^{106}Ru	"	0.32	0.21	0.42	2.1	0.76
^{131}I	"	678.1	293.4	139.9	54.6	291.5
^{134}Cs	"	0.28	0.37	0 046	0.47	0.29
^{137}Cs	"	1 0	1.2	0.82	1.3	1.1
^{141}Ce	"	-	5.9	1.2	3.3	3 5
^{144}Ce	"	0.32	4.7	4.5	1.5	2.8
^{152}Eu	"	-	-	-	0.72	0.72
^{154}Eu	"	0 17	0.21	1.0	0.29	0.42

Table F-13. Deposition velocity in a forest (units: 10^{-4} ms^{-1}): 40.5 trees per 100 m², average tree height = 6.4 m

Isotope	Common Spruce
^{134}Cs	7.3
^{131}I	89
^{103}Ru	28
^{106}Ru	53

Table F-14. Local deposition velocities (units: 10^{-4} ms^{-1})

Isotope	Yew trees height 2.5 m	Juniper berry height 2 m
^{134}Cs	9	3
^{131}I	105	32
^{141}Ce	46	23
^{144}Ce	46	28
^{140}La	32	14
^{103}Ru	32	13
^{106}Ru	47	28
^{95}Zr	55	26
^{95}Nb	58	26

Table F-15. Bulk deposition constant, B_d (in kg^{-1} m^3 s^{-1} × 10^{-4})

Isotope	Yew trees height 2.5 m	Juniper berry height 2.0m	Common Spruce height 6.5 m	Common Spruce height 6.1 m
^{137}Cs	2.8	3.2	1.8	2.3
^{134}Cs	2.2	2.7	1.4	1.9
^{131}I	24.5	26.5	19.4	16.6
^{141}Ce	12.2	21.9	13.9	19.4

Table F-16. Deposition velocity, v_d: 10^{-4} ms^{-1}; bulk deposition, B_d: 10^{-4} m^3 s^{-1} kg^{-1}, for grass

Sample no.		^{137}Cs	^{134}Cs	^{131}I
1384	V_d B_d	4.3 21	4.4 21	22 110
1387	V_d B_d	1.8 10	1.5 8.7	18 100
1388	V_d B_d	8.8 10	7.2 8.5	93 110
1391	V_d B_d	6.0 7.9	6.6 8.7	86 110
1392	V_d B_d	7.4 9.1	9.9 12	120 140

Dependence of V_d on Reference Height

Those portions of the deposition velocity that are due to eddy diffusion (adiabatic conditions) are dependent on the height above the surface that is chosen as reference height.

$$v_d = (K \cdot u_*) / (\ln((z-L)/z_0) + K \cdot X_0/X_*),$$

where K is the von Kármán constant (K≈0.4), u_* the fiction velocity, z the height above the ground, and L is about 0.6 · H, where H is the mean height of the roughness elements.

For very small particles where sedimentation is negligible, this equation represents the total deposition velocity.

Over a grass field with average windspeed, where z_0 = 1 cm and u_* = 30 cm/s and where the field is a perfect sink, that is X_0 = 0, we find that

v_d = 2.3 cm/s for z-L = 2m
v_d = 2.6 cm/s for z-L = 1m, and
v_d = 5.2 cm/s for z-L = 0.1 cm.

It can be seen that if the reference height is chosen to exceed 1m above L, then the deposition velocity becomes almost independent of the reference height.

Dependence of v_d on Atmospheric Stability

It was seen above that the maximum deposition velocity under adiabatic conditions was about 2.6 cm/s. Jensen[11] has shown that under moderately stable weather conditions, the deposition velocity will be less than a quarter of the maximum deposition velocity for adiabatic conditions due to the reduction in u_* in stable conditions.

Dependence of v_d on Windspeed

The portion of v_d that is due to eddy diffusion is close to proportional to the mean wind speed u.

Dependence of v_d on Particle Size

From laboratory measurements reported by Sehmel[12], McMahon and Deninson[13] constructed a curve that describes the deposition velocity on smooth surfaces as a function of particle size. McMahon and Deninson also constructed a curve that shows the relation between the deposition velocity on grass and particle size. The curve was constructed from literature values. The two curves are compared in Figure F-1. It can be seen that the deposition velocity is at a minimum when the particle diameter is about 0.5 μm, and that the deposition velocity increases for particles larger than 0.5 μm. This increase is due to the gravitational force.

Dependence of v_d on Surface Roughness

Figure F-2 shows that deposition velocities on grass for particles between 0.1 μm and 2 μm in diameter are about an order of magnitude greater than those on smooth surfaces. The figure also shows sedimentation to be relatively more important on smooth surfaces than on rough surfaces. The

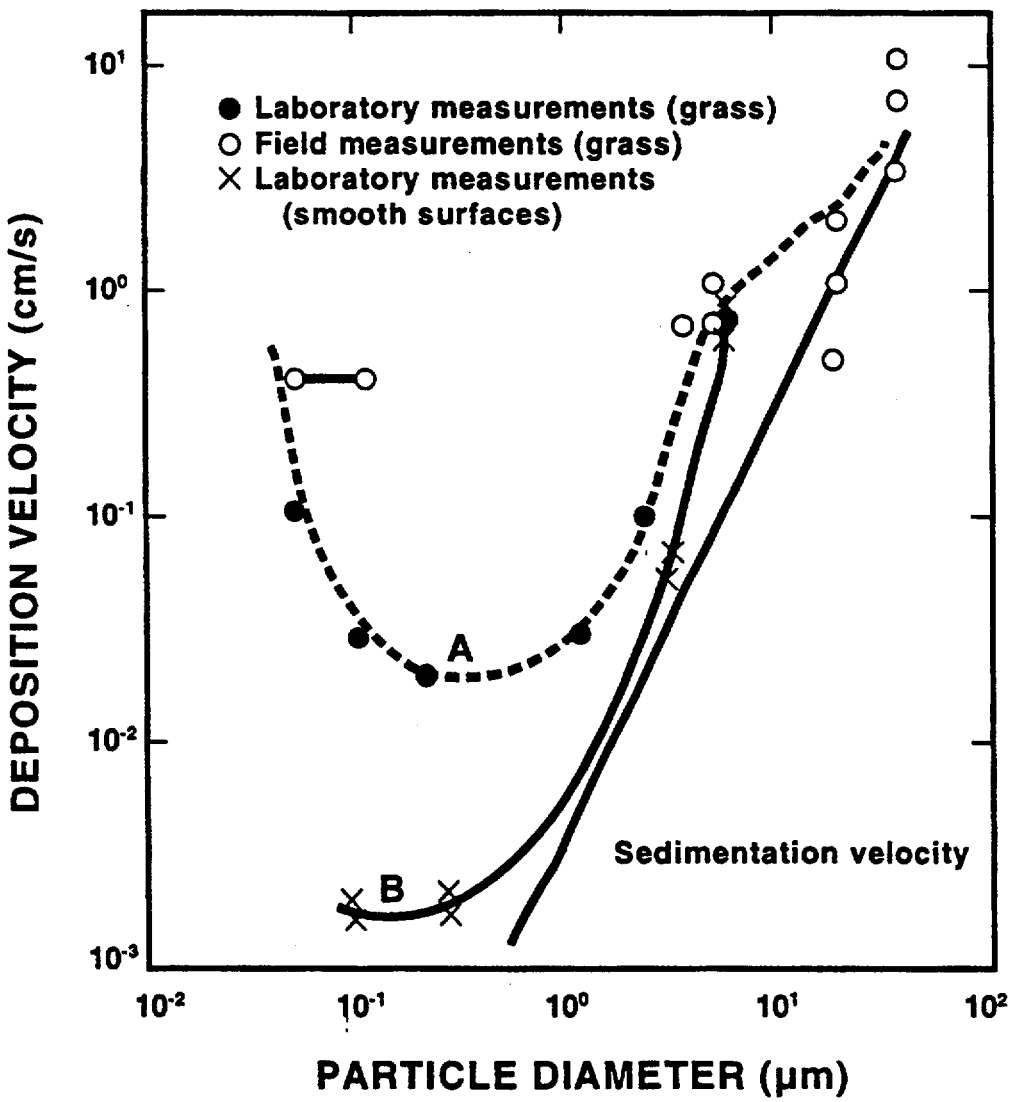

Figure F-1. Relationship between deposition velocity and particle diameter.

Curve A: Laboratory and field measurements of deposition velocity of particles onto grass.[13]
Curve B: Laboratory measurements of deposition velocity on smooth surfaces ($u_* = 73$ cm/s, $u = 13.4$ m/s).[13]

measured deposition velocities before 1962 were reviewed by Gifford and Pack[14]. They concluded that deposition velocities of particles of copper sulphate have a mean diameter of 4 μm and a frictional velocity of 27 cm^{-1}. They found deposition velocities on grass (0.1 cm/s) and clover (0.24 cm/s) that are 3 to 8 times higher than those measured on smooth surfaces (0.03 cm/s). Ahmed[15] produced curves for deposition velocities as a function of windspeed for both smooth and rough surfaces. He found the deposition velocities on rough surfaces to be an order of magnitude greater than on smooth surfaces.

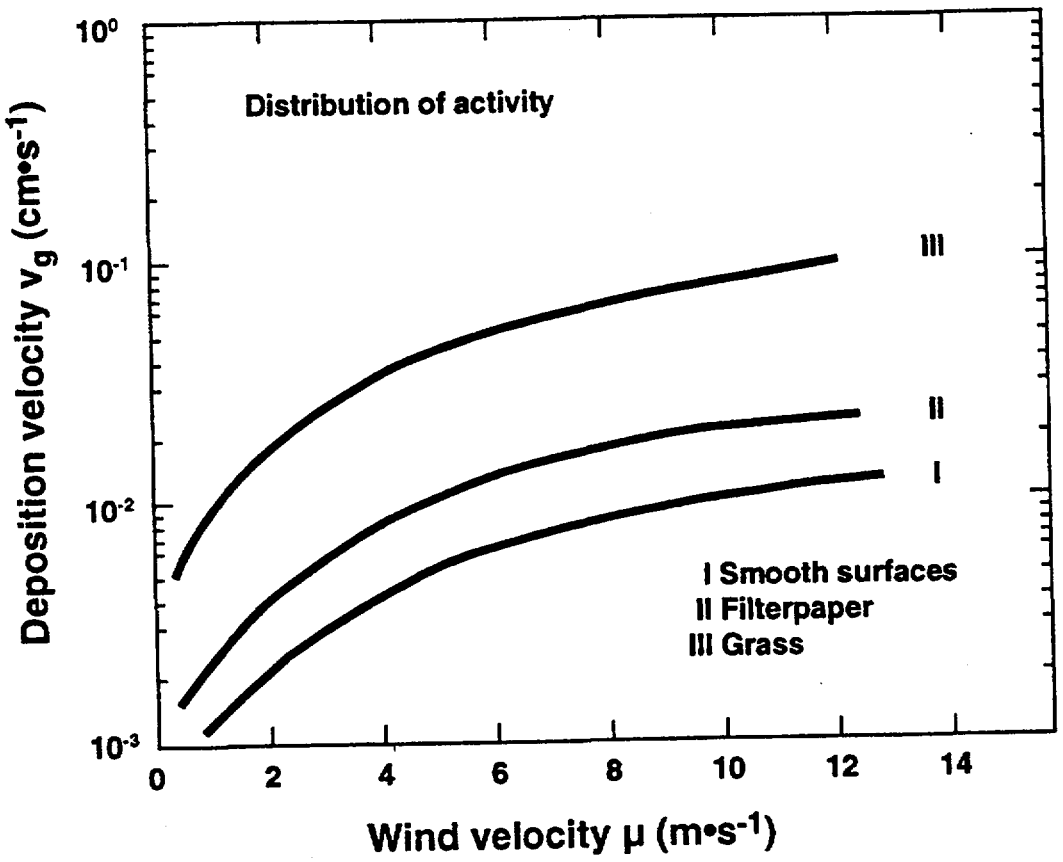

Figure F-2. Deposition velocity for natural radioactive aerosols as a function of wind velocity (from Ahmed).[15]

Iodine as Methyl Iodide

Investigations have shown that iodine in the form of methyl iodide CH_3I has a very low deposition velocity. In the laboratory, Vogt[16] has measured deposition velocities for CH_3I which are 100 times less than the deposition velocities for iodine vapour in the elementary iodine form, I_2. Bunch[17] found corresponding results from a field experiment. In agreement with this, Atkins[18] measured very low values of deposition velocity of CH_3I, both in wind tunnel experiments and in field experiments.

Iodine as Elementary Iodine

Gifford and Pack[14] pointed out in their review of the investigations carried out before 1962 that reactive matter such as iodine vapour in the form of elementary iodine has a higher deposition velocity than non-reactive matter such as caesium. Gifford and Pack found that v_d for I_2 was in the order of 1 to 3 cm/s for vegetation and one order of magnitude less for soil without vegetation and plane collectors. Further, they found that deposition velocities for non-reactive particles were generally one order of magnitude less than the deposition velocities which were measured for reactive matter.

In field experiments, Hawley et al.[19] and Adams et al.[20] measured deposition velocities on grass and soil under grass cover of 1.3 to 1.4 cm/s at unstable weather conditions and wind speeds of 7-9 m/s. In other experiments, Adams et al.[20] found deposition velocities on snow of 0.22 cm/s (snow has a smooth surface). The weather conditions here were neutral and the wind speed was 6 m/s. Further, the deposition velocity on grass was measured under stable weather conditions to 0.11 cm/s at a wind speed of 4 m/s. The deposition on soil under grass cover has not been included in this figure. It is, however, important to distinguish between deposition on the grass and deposition on a grass field, where the contribution from soil under the grass cover is included.

By far in most deposition experiments on overgrown soil only the deposition on the growth has been measured. This will therefore be noticed when the total deposition (soil and growth) is measured.

In field experiments, Cline et al.[21] measured deposition velocities with a mean value of 0.5 cm/s on plants, e.g., on grass. The deposition on soil under grass was found to be about 15 % of the deposition on grass.

Hull[22] found deposition velocities of 0.25 cm/s on grass from the fallout from Chinese bomb testing.

Field measurements carried out in Jülich by Vogt et al.[16] gave deposition velocities of 1.2 cm/s for average wind conditions on a typical grass cover.

Other Measurements of Deposition Velocities for Non-Reactive Particles

Jonas[23] and Horbert et al.[24] measured deposition velocities by field experiments in which $CuSO_4$ particles labeled with radiotracers were used.

On growth, they measured deposition velocities between 0.24 and 0.05 cm/s. On smooth collectors and on bare soil they found deposition velocities between 0.03 and 0.01 cm/s, that is, a factor of 5 less. The wind conditions during the measurements were normal for Germany.

Clough[25] found deposition velocities on moss, in wind tunnel experiments, that were 10 times higher than those found on grass.

Peirson et al.[26] carried out measurements on dust far from industry. He found that deposition velocities for large particles originating from physical impact on soil were considerably higher than deposition velocities of particles originating from industrial pollution, which he assumed would have a particle size of less than 2 μm.

Wilson et al.[27] found deposition velocities of 0.4 cm/s for lucerne and 0.8 cm/s for ^{137}Ca bomb fallout particles. These high values correspond well with those found by Horbert,[22] who measured deposition velocities on clover (0.24 cm/s).

Little and Wiffen[28] have measured deposition velocities for lead from car exhausts in wind tunnel experiments. The measurements were carried out on fresh lead particles with a mean diameter of about 0.05 μm and on aged lead particles with a mean diameter of about 0.2 μm.

The deposition velocities on grass were measured as 0.13 cm/s on grass, 0.015 cm/s on soil under grass, and 0.035 cm/s on bare soil for fresh lead particles. The corresponding figures for aged particles were 0.019 cm/s on grass, 0.007 cm/s on soil under grass, and 0.0081 cm/s on bare soil.

The relationships between the deposition velocity on a grass field (grass and soil under grass) and the deposition velocity on bare soil were thus found to be 3 and 4, respectively.

Deposition Velocities Measured After Other Reactor Accidents than that at Chernobyl

Some very important measurements have been made on fallout from reactor accidents.

Windscale

Following the Windscale accident, which occurred on 10 October 1957, measurements were made at Preston, Burnley, and Sheffield, which are 85, 100, and 180 km, respectively, from Windscale (Stewart and Crooks).[29] At these locations the deposition velocity for iodine on grass was measured as about 0.3 cm/s while corresponding measurements in the south of England showed deposition velocities on grass in the order of 0.11 cm/s.

The deposition velocity for caesium and ruthenium was found to be about 15% of that of iodine.

On the measurement sites, the weather conditions were stable in the deposition period.

SL–1 Accident

At the SL–1 accident, releases occurred in the period from the 6th to the 30th of January 1961.

The weather conditions were stable in the period where the release took place. A deposition velocity for iodine on growth was measured to be about 0.2 cm/s.

Recommended Deposition Velocities in Dose Calculations After Releases of Radioactive Matter

For reactive matter such as iodine, deposition velocities near the source of about 1 cm/s were measured on rough surfaces (growth). Farther away from the source, the deposition velocities were generally found to be lower.

In connection with the Windscale accident and the SL-1 accident, deposition velocities of 0.1 to 0.3 cm/s were measured on rough surfaces for reactive matter.

Deposition velocities for non-reactive matter, such as caesium, are generally considerably lower than those found for iodine. After the Windscale accident, deposition velocities for ^{137}Cs and ^{103}Ru on grass were measured to be about 15% of the deposition velocity for iodine. Gifford pointed out already in 1962 that the deposition velocities for reactive matter were considerably higher than those for non-reactive matter (by a factor of 10). For non-reactive matter, values of less than 0.2 cm/s have generally been reported for rough surfaces. There is, therefore, a clear difference between deposition velocities for reactive and for non-reactive substances. On average, this difference can be expressed as a factor of 5. Another important dividing line is between the deposition velocities measured on rough surfaces and the corresponding velocities found on smooth surfaces, such as house walls.

For plane surfaces, deposition velocities have been measured which are substantially lower than those found for rough surfaces, both for reactive and non-reactive matter. An exception is a series of measurements by Peirson et al.,[26] who found the deposition velocity for ^{137}Cs on filter paper (plane collector) to be 0.2 cm/s. However, other measurements have shown the deposition velocities for smooth surfaces to be 3 to 20 times less than those on rough surfaces.

Wet deposition

Various different processes are responsible for the uptake of aerosols by falling drops (Pruppacher and Klett; Slinn).[30,31] Small particles move very rapidly and irregularly due to bumps from molecules. These particles are transported to the drops by Brownian diffusion. The larger the particles, the less the movement after collision with the molecules. Therefore, Brownian diffusion is only important for particles with a radius of less than 0.01 μm. Raindrops move corresponding to the surrounding air. Small aerosols will follow the movement around the drop and therefore not come into contact with the drop. Larger particles have a mass, due to which they will not quite follow the air and thus be hit by the drop, even though the air stream will change when a drop falls through. It is assumed that nearly every collision leads to an uptake of the particle by the drop. The larger the particles, the higher the inertia, and thus the chance of a collision. This process, capture, is important only for particles with a radius larger than 1 μm.

For particles with radii between 0.01 μm and 1 μm, only very inefficient processes exist: phoretic processes. Due to temperature differences or differences in the air gas concentration, the particles move a little, which enhances the chance of capture by a drop. If a drop falls down from the cloud-base, it will 'sweep' a small vertical air column with a cross section of πr^2 (the cross section of the drop). If the air, and thereby the particles, did not move around the falling drop, all particles in the column would be captured in the drop. In reality, only a fraction, E (usually called the 'capture efficiency') of these aerosols will be captured. The fraction E has been measured in air where particles were produced and the captured fraction measured (Slinn[31]; Janssen et al.[32]). These experiments showed that E is much larger, particularly for particles with radii between 0.01 μm and 1 μm, than what was assumed for theoretical reasons. It was therefore recommended to use a constant capture efficiency of 0.02 for all particles without respect to the size. This efficiency has been found in Holland by Janssen et al.[32] in washout of smoke fans from a power station. The uncertainty associated with E is rather large, but it is unlikely that it is larger than 1, although it is theoretically possible. The washout of particles is not so efficient as removal of particles in clouds because they act as condensation kernels.

Drops can never be saturated with particles, as is the case for gases. But for some substances that have been taken up on particle form by the drops, it is possible to leave the drops again on a gaseous form.

Deposition Tables

Units of velocity are in 10^{-4} m/s; N/A = not provided by expert; unkn = unknown

DD-A: Dry deposition velocity of aerosols - Wind Speed at 2m/s					
PARTICLE SIZE	QUANTILE	URBAN	MEADOW	FOREST	HUMAN SKIN
0.10μ	0%	1.00E-03	2.00E-03	6.00E-03	5.00E-04
	5%	7.00E-03	1.50E-02	4.50E-02	1.50E-03
	50%	4.50E-02	9.00E-02	4.50E-01	7.00E-03
	95%	4.50E-01	9.00E-01	2.00E+00	7.00E-02
	100%	2.00E-00	2.00E-00	4.00E-00	2.00E-01
0.30μ	0%	1.00E-03	2.00E-03	6.00E-03	5.00E-04
	5%	5.00E-03	1.00E-02	3.00E-02	1.00E-03
	50%	3.00E-02	6.00E-02	3.00E-01	5.00E-03
	95%	3.00E-01	6.00E-01	2.00E+00	5.00E-02
	100%	2.00E-00	2.00E-00	4.00E-00	2.00E-01
1.00μ	0%	2.00E-03	3.00E-03	1.00E-02	5.00E-04
	5%	7.00E-03	1.50E-02	5.00E-02	1.50E-03
	50%	5.00E-02	1.00E-01	5.00E-01	8.00E-03
	95%	5.00E-01	1.00E+00	2.00E+00	8.00E-02
	100%	2.00E-00	2.00E-00	4.00E-00	2.00E-01
3.00μ	0%	1.00E-02	1.00E-02	1.50E-02	5.00E-04
	5%	2.00E-02	3.00E-02	7.00E-02	3.00E-03
	50%	1.50E-01	2.00E-01	7.00E-01	3.00E-02
	95%	7.50E-01	1.20E+00	2.20E+00	3.00E-01
	100%	3.00E-00	3.00E-00	6.00E-00	9.00E-01
10.00μ	0%	1.00E-01	1.00E-01	1.00E-01	5.00E-04
	5%	3.00E-01	3.00E-01	3.50E-01	5.00E-03
	50%	5.00E-01	6.00E-01	9.00E-01	5.00E-02
	95%	1.00E+00	1.40E+00	2.50E+00	5.00E-01
	100%	6.00E-00	6.00E-00	1.00E+01	1.50E-00

DD-B: Dry deposition velocity of aerosols - Wind Speed at 5m/s					
PARTICLE SIZE	QUANTILE	URBAN	MEADOW	FOREST	HUMAN SKIN
0.10μ	0%	2.00E-03	4.00E-03	1.00E-02	1.00E-03
	5%	1.50E-02	3.00E-02	9.00E-02	3.00E-03
	50%	9.00E-02	1.80E-01	9.00E-01	1.40E-02
	95%	6.00E-01	1.20E+00	3.50E+00	1.40E-01
	100%	3.00E+00	3.00E+00	5.00E+00	4.00E-02
0.30μ	0%	2.00E-03	4.00E-03	1.00E-02	1.00E-03
	5%	1.00E-02	2.00E-02	1.00E-01	2.00E-03
	50%	6.00E-02	1.20E-01	1.00E+00	1.00E-02
	95%	4.00E-01	8.00E-01	3.50E+00	1.00E-01
	100%	3.00E+00	3.00E+00	5.00E+00	4.00E-02
1.00μ	0%	4.00E-03	6.00E-03	2.00E-02	1.00E-03
	5%	1.50E-02	3.00E-02	1.00E-01	3.00E-03
	50%	1.00E-01	2.00E-01	1.00E+00	1.60E-02
	95%	6.50E-01	1.30E+00	3.50E+00	1.60E-01
	100%	3.00E+00	3.00E+00	5.00E+00	4.00E-01
3.00μ	0%	2.00E-02	2.00E-02	3.00E-02	1.00E-03
	5%	8.00E-02	1.00E-01	1.20E-01	6.00E-03
	50%	2.00E-01	3.00E-01	1.20E+00	6.00E-02
	95%	8.00E-01	1.50E+00	3.70E+00	5.00E-01
	100%	4.00E+00	4.00E+00	5.00E+00	2.00E+00
10.00μ	0%	1.50E-01	1.50E-01	1.50E-01	1.00E-03
	5%	3.50E-01	3.50E-01	4.00E-01	1.00E-02
	50%	5.50E-01	7.50E-01	1.50E+00	1.00E-01
	95%	1.10E+00	1.80E+00	4.00E+00	8.00E-01
	100%	6.00E+00	6.00E+00	7.00E+00	3.00E+00

DD-C: Dry deposition velocity of elemental iodine - Wind Speed at 2 and 5m/s					
WIND SPEED	QUANTILE	URBAN	MEADOW	FOREST	HUMAN SKIN
2.m/s	0%	1.00E-02	4.00E-02	1.00E-01	5.00E-03
	5%	2.50E-02	7.50E-02	5.00E-01	1.00E-02
	50%	2.50E-01	7.50E-01	2.00E+00	2.50E-02
	95%	2.00E+00	2.00E+00	4.00E+00	2.00E-01
	100%	4.00E+00	4.00E+00	6.00E+00	1.00E+00
5.m/s	0%	2.00E-02	5.00E-02	1.20E-01	5.00E-03
	5%	3.50E-02	1.00E-01	6.00E-01	1.00E-02
	50%	3.50E-01	1.00E+00	3.00E+00	3.50E-02
	95%	3.00E+00	3.00E+00	6.00E+00	3.00E-01
	100%	6.00E+00	6.00E+00	1.00E+01	1.50E+00

DD-D: Dry deposition velocity of methyl iodide - Wind Speed at 2 and 5m/s					
WIND SPEED	QUANTILE	URBAN	MEADOW	FOREST	HUMAN SKIN
2.m/s	0%	N/A	N/A	N/A	N/A
	5%	1.25E-05	3.75E-05	1.00E-04	1.50E-06
	50%	2.50E-03	7.50E-03	2.00E-02	2.50E-04
	95%	5.00E-02	1.50E-01	4.00E-01	5.00E-03
	100%	2.00E-01	7.00E-01	1.30E+00	2.00E-02
5.m/s	0%	N/A	N/A	N/A	N/A
	5%	1.75E-05	5.00E-05	1.50E-04	1.50E-06
	50%	3.50E-03	1.00E-02	3.00E-02	3.00E-04
	95%	7.00E-02	2.00E-01	5.00E-01	7.00E-03
	100%	3.00E-01	1.00E+00	2.00E+00	3.00E-02

DD-E-1: Dry deposition velocity of aerosols on Moorland/Peatland Surface		
PARTICLE SIZE	QUANTILE	
0.55μ	0%	4.00E-03
	5%	4.00E-02
	50%	1.20E-01
	95%	1.20E+00
	100%	3.00E+00
0.70μ	0%	5.00E-03
	5%	5.00E-02
	50%	1.60E-01
	95%	1.60E+00
	100%	3 50E+00
0.90μ	0%	6.00E-03
	5%	6 00E-02
	50%	1 80E-01
	95%	1.80E+00
	100%	4.00E+00
1.20μ	0%	7 00E-03
	5%	7.00E-02
	50%	2.00E-01
	95%	2.00E+00
	100%	4.00E+00
1.60μ	0%	8.00E-03
	5%	8.00E-02
	50%	2.30E-01
	95%	3.00E+00
	100%	5.00E+00

DD-E-2: Dry deposition velocity of aerosols on Heather/Green Grass Surface		
PARTICLE SIZE	QUANTILE	
0.55μ	0%	2.00E-03
	5%	2.00E-02
	50%	6.00E-02
	95%	6.00E-01
	100%	3.00E+00
0.70μ	0%	3.00E-03
	5%	3.00E-02
	50%	8.00E-02
	95%	8.00E-01
	100%	4.00E+00
0.90μ	0%	3.00E-03
	5%	3.00E-02
	50%	9.00E-02
	95%	9.00E-01
	100%	4.00E+00
1.20μ	0%	3.00E-03
	5%	3.00E-02
	50%	1.00E-01
	95%	1.00E+00
	100%	4.50E+00
1.60μ	0%	4.00E-03
	5%	4.00E-02
	50%	1.20E-01
	95%	1.20E+00
	100%	4.50E+00

DD-E-2: Dry deposition velocity of aerosols on Heather/Green Grass Surface (continued)		
PARTICLE SIZE	QUANTILE	
2.30μ	0%	5.00E-03
	5%	5.00E-02
	50%	1.40E-01
	95%	1.40E+00
	100%	5.00E+00
3.20μ	0%	5.00E-03
	5%	5.00E-02
	50%	1.60E-01
	95%	1.60E+00
	100%	5.00E+00
4.20μ	0%	7.00E-03
	5%	7.00E-02
	50%	2.00E-01
	95%	2.00E+00
	100%	5.00E+00

DD-F: Dry deposition velocity of aerosols on Grassland Surface		
PARTICLE SIZE	QUANTILE	
1.0μ	0%	3.00E-03
	5%	1.50E-02
	50%	1.50E-01
	95%	1.50E+00
	100%	6.00E+00

WD-A: Elemental iodine—fraction removed by rain ($1-f_w$)							
Rainfall/ Time	**Wind Speed**	**Quantile**	$1-f_w$	**Rainfall/ Time**	**Wind Speed**	**Quantile**	$1-f_w$
.3mm/hr	**unkn**	**0%**	0.00E+00	**2.mm/hr**	**unkn**	**0%**	0.00E+00
		5%	1.50E-02			**5%**	4.00E-02
		50%	1.40E-01			**50%**	3.00E-01
		95%	7.60E-01			**95%**	9.80E-01
		100%	1.00E+00			**100%**	1.00E+00
.075mm/ 10min	**10 m/s**	**0%**	0.00E+00	**.05mm/ 10min**	**unkn**	**0%**	0.00E+00
		5%	1.00E-04			**5%**	1.00E-04
		50%	2.00E-02			**50%**	2.00E-02
		95%	1.60E-01			**95%**	1.60E-01
		100%	8.00E-01			**100%**	8.00E-01
.17mm/ 10min	**5 m/s**	**0%**	0.00E+00	**.17mm/ 10min**	**14 m/s**	**0%**	0.00E+00
		5%	1.00E-04			**5%**	1.00E-04
		50%	3.00E-02			**50%**	3.00E-02
		95%	2.60E-01			**95%**	2.60E-01
		100%	9.50E-01			**100%**	9.50E-01
0.23mm/ 10min	**12 m/s**	**0%**	0.00E+00	**.5mm/ 10min**	**unkn**	**0%**	0.00E+00
		5%	1 00E-04			**5%**	1.00E-04
		50%	4.00E-02			**50%**	5.00E-02
		95%	3.00E-01			**95%**	3.80E-01
		100%	9.70E-01			**100%**	1.00E+00
.33mm/ 10min	**unkn**	**0%**	0.00E+00	**1.0mm/ 10min**	**14 m/s**	**0%**	0.00E+00
		5%	1.00E-04			**5%**	1.00E-02
		50%	4.00E-02			**50%**	7.00E-02
		95%	3.40E-01			**95%**	5.40E-01
		100%	1.00E+00			**100%**	1.00E+00

WD-A: Elemental iodine—fraction removed by rain ($1\text{-}f_w$) (continued)			
Rainfall/Time	**Wind Speed**	**Quantile**	$1\text{-}f_w$
1.67mm/10min	**unkn**	**0%**	0.00E+00
		5%	1.00E-02
		50%	9.00E-02
		95%	5.90E-01
		100%	1.00E+00

WD-B: Methyl iodide—fraction removed by rain (Wind Speed=unknown)		
Rainfall/Time	**Quantile**	***1-f$_w$***
.3mm/hr	**0%**	N/A
	5%	1.00E-04
	50%	2.00E-02
	95%	1.90E-01
	100%	8.80E-01
2.mm/hr	**0%**	N/A
	5%	1.00E-04
	50%	7.00E-02
	95%	5.10E-01
	100%	1.00E+00
.05mm/10min	**0%**	N/A
	5%	1.00E-04
	50%	1.00E-02
	95%	2.00E-02
	100%	1.60E-01
.33mm/10min	**0%**	N/A
	5%	1.00E-04
	50%	1.00E-02
	95%	6.00E-02
	100%	4.50E-01
1.67mm/10min	**0%**	N/A
	5%	1.00E-04
	50%	2.00E-02
	95%	1.60E-01
	100%	8.00E-01

WD-C: Fraction of aerosols removed by rain						
PARTICLE SIZE	QUANTILE	Rainfall: .3mm/hr	Rainfall: 2.mm/hr	Rainfall: .05mm/10 min	Rainfall: .33mm/10 min	Rainfall: 1.67mm /10 min
0.10μ	0%	0.00E+00	0.00E+00	0.00E+00	0.00E+00	0.00E+00
	5%	1.00E-04	1.00E-02	1.00E-04	1.00E-04	1.00E-04
	50%	4.00E-02	1.00E-01	1.00E-05	1.00E-02	3.00E-02
	95%	3.00E-01	6.60E-01	3.00E-02	9.00E-02	2.60E-01
	100%	1.00E+00	1.00E+00	7.00E-01	1.00E+00	1.00E+00
0.30μ	0%	0.00E+00	0.00E+00	0.00E+00	0.00E+00	0.00E+00
	5%	1.00E-04	2.00E-02	1.00E-04	1.00E-04	1.00E-02
	50%	7.00E-02	1.90E-01	1.00E-02	2.00E-02	6.00E-02
	95%	5.10E-01	8.80E-01	6.00E-02	1.60E-01	4.50E-01
	100%	1.00E+00	1.00E+00	7.00E-01	1.00E+00	1.00E+00
1.00μ	0%	0.00E+00	0.00E+00	0.00E+00	0.00E+00	0.00E+00
	5%	1.00E-02	4.00E-02	1.00E-04	1.00E-04	1.00E-02
	50%	1.00E-01	3.00E-01	1.00E-02	3.00E-02	9.00E-02
	95%	6.60E-01	9.80E-01	9.00E-02	2.60E-01	5.90E-01
	100%	1.00E+00	1.00E+00	7.00E-01	1.00E+00	1.00E+00
10.00μ	0%	0.00E+00	1.00E-02	0.00E+00	0.00E+00	0.00E+00
	5%	4.00E-02	1.00E-01	1.00E-04	1.00E-02	3.00E-02
	50%	3.00E-01	6.60E-01	3.00E-02	9.00E-02	2.60E-01
	95%	9.80E-01	1.00E+00	2.60E-01	5.90E-01	9.50E-01
	100%	1.00E+00	1.00E+00	7.00E-01	1.00E+00	1.00E+00

References

1. Roed, J., "Dry Deposition in Rural and in Urban Areas in Denmark," *Radiation Protection Dosimetry*, 21:33-36, 1987.

2. Roed, J., "Deposition Velocity of Caesium-137 on Vertical Building Surfaces," *Atmospheric Environment*, 17:663-664, 1983.

3. Roed, J., "Relationships in Indoor/Outdoor Air Pollution, Risø-M-2476, Riscoe National Laboratory, Roskilde, Denmark, January 1985.

4. Roed, J., "Dry Deposition on Smooth and Rough Urban Surfaces," *The Post-Chernobyl Workshop*, 3-5 February 1987, NKA-AKTU-245(87)1, available National Technical Information Service, U.S. Dept. of Commerce, Springfield, VA, January 1987.

5. Roed, J., "The Distribution on Trees of Dry Deposited Material from the Chernobyl Accident," (M. Olast and J. Sinnaeve, eds.), *Joint CEC/OECD(NEA) Workshop on Recent Advances in Reactor Accident Consequence Assessment, 25-29 January 1988*, EUR-11408-EN (CONF-8801124) Commission of the European Communities, Luxembourg, pp. 165-178, 1988.

6. Rulik, P., I. Bucina, and I. Malatova, "Aerosol Particle Size Distribution in Dependence on the Type of Radionuclide After the Chernobyl Accident and in the NPP Effluents," (W. Feldt, ed.), *The Radioecology of Natural and Artificial Radionuclides, Proceedings of the 15th Regional Congress of the International Radiation Protection Association (IRPA), 10-14 September 1989*, CONF-8909322, Köln Verlag TUEV, Rheinland, Germany, pp. 102-107, 1989.

7. Magua, M., et al., "Deposition Velocity and Washout Coefficient of Radionuclide Bound to Aerosol Particles and Elemental Radioiodine," presented at the *Workshop on Consequences of an Accidental Contamination of Urban Environment* in Roskilde, Denmark, June 9-12, 1987.

8. Nicholson, K.W., "Deposition of Caesium to Surfaces of Buildings," *Workshop on Accidental Urban Contamination, 9-12 June 1987, Radiation Protection Dosimetry*, 21:37-42, 1987.

9. Sehmel, G.A . "Particle and Gas Dry Deposition: A Review," *Atmospheric Environment*, 14:983-1011, 1980.

10. Schwibach, J., "Auswirkungen des Reaktorunfalls in Tschernobyl auf den Raum, München, ISH-103, Bundesgesundheitsamt, Neuherberg, FRG, November 1986.

11. Jensen, N.O., "A Micrometeorological Perspective on Deposition," *Health Physics*, 40:887-891, 1981.

12. Sehmel, G.A., "Particle Eddy Diffusitives and Deposition Velocities for Isothermal Flow and Smooth Surfaces," *Aerosol Science*, 4:125-138, 1973.

13. McMahon, T.A., and P.J. Denison, "Empirical Atmospheric Deposition Parameters - A Survey," *Atmospheric Environment*,13:571-585, 1979.

14. Gifford, F.A., and D.H. Pack, "Surface Deposition of Airborne Material," *Nuclear Safety*, 3(4):76-80.

15. Ahmed, A.-R., "Untersuchungen zur Aerosoldeposition an Oberflächen," Inaugural-Dissertation zur Erlangen des Doktorgrades der Naturwissenschaften der Justus-Liebig-Universität, Gissen, 1979.

16. Vogt, K.J., et al., "Untersuchungen zur Ablagerung von Jod und Aerosolen auf Vegetation und anderen Grenzflächen," Jül-1144-ST, Kernforschungsanlage Julich, Julich, Germany, 1974.

17. Bunch, D.F., "Controlled Environmental Iodine Tests, Progress Report No. 2," IDO-12053, Idaho Operations Office (AEC), Idaho Falls, ID, available National Technical Information Service, U.S. Dept. of Commerce, Springfield, VA, August 1966.

18. Atkins, D.H.F., "Deposition of Radioactive Methyl Iodide to Vegetation," *Health Physics*, 13:91-92, 1967.

19. Hawley, C.A., et al., "Controlled Environmental Radioiodine Tests at the National Reactor Testing Station," IDO-12035, USAEC Idaho Operations Office, Idaho Falls, ID, July 1964.

20. Adams, D.R., et al., "Controlled Environmental Radioiodine Tests at the National Reactor Testing Station, 1965 Progress Report," IDO-12047, Idaho Operations Office (AEC), Idaho Falls, ID, available National Technical Information Service, U.S. Dept. of Commerce, Springfield, VA, February 1966.

21. Cline, J.F., D.O. Wilson, and F.P. Hungate, "Effect of Physical and Biological Conditions on Deposition and Retention of ^{131}I on Plants," *Health Physics*, 11:713-717, 1965.

22. Hull, A.P., "Environmental Monitoring of ^{131}I in Small Concentrations and Some Comparisons with Meteorological Calculations," *Health Physics*, 12:1317-1325, 1966.

23. Jonas, R., *Statusbericht über die Feldversuche zur Bestimmung der Ablagerungsgeschwindligkeit won Aerosolen*, ZST-bericht Nr. 295, 1979.

24. Horbert, M., et al., *Untersuchungen zur Ablagerung von Aerosolen auf Vegetation und Anderen Grenzflächen*, Kernforschungsanlage Jülich Nr. 1288, Kernforschungsanlage Jülich, Jülich, Germany, 1976.

25. Clough, W.S., "The Deposition of Particles on Moss and Grass Surfaces," *Atmospheric Environment*, 9:1113-1119, 1975.

26. Peirson, D.H., et al., "Trace Elements in the Atmospheric Environment," *Nature*, 241:252-256, 1973.

27. Wilson, D.W., G.M. Ward, and J.E. Johnson, "Fallout ^{137}Cs: Direct Aerial Transfer as an Important Source of Foliar Deposition," *Radiation Botany*, 7:312-319, 1967.

28. Little, P., and R.D. Wiffen, "Emission and Deposition of Petrol Engine Exhaust Pb—I. Deposition of Exhaust Pb to Plant and Soil Surfaces," *Atmospheric Environment*, 11:437-447, 1977.

29. Stewart, N.G., and R.N. Crooks, "Long-Range Travel of the Radioactive Cloud From the Accident at Windscale," *Nature*, 182:627-628, 1958.

30. Pruppacher, H.R., and J.D. Klett, *Microphysics of Clouds and Precipitation*, D. Reidel, Boston, MA, 1978.

31. Slinn, W.G.N., "Air to Sea Transfer of Particles," (P.S. Liss and W.G.N. Slinn, eds.), *Air-Sea Exchange of Gases and Particles, Proceedings of the NATO Advanced Study Institute, 19-30 July 1982*, D. Reidel, Boston, MA, pp. 299-405, 1983.

32. Janssen, A.J., J. Slanina, and P.J. Voors, "A Simple Model of Below-Cloud Scavenging Processes," ECN-87-068, Netherlands Energy Research Foundation, Petten (N.H.), Holland, May 1987.

Expert G

Introduction

The reasoning to support the responses provided to the elicitation questions is given in the following sections.

The results of studies of deposition are very variable. Numerous methods have been attempted, and at least some part of the variability is attributable to the differences in methodology. Some methods have particular requirements of weather, geography, or freedom from interfering aerosol sources, which are difficult to fulfill. Many methods are likely to yield parameters with a particular bias if the conditions are not fulfilled. In selecting parameter values, some judgement regarding the reliability of varying results is essential. Otherwise the range of uncertainty is extremely wide, and the information content in the values provided is poor.

The author has therefore applied this judgement. As a result, the parameter values quoted do not reflect the entire population of field measurements or model results for deposition parameters, but rather the population of results that the author judges to be valuable because they provide valid estimates of the true population. Nevertheless, the estimates of the percentiles necessarily reflect lack of knowledge and experimental error as well as environmental variability.

Deposition of Particles

Urban Areas

Nicholson et al.[12] estimated deposition to various components of a built environment and aggregated the result to arrive at a bulk deposition velocity to such an area. Deposition per unit area to roofs, roads, and grass differed by no more than a factor of two, while individual trees could collect an order of magnitude more material than other surfaces. Vertical walls collected minor amounts. Thus the bulk deposition velocity is likely to be strongly dependent on the number of trees and bushes.

The wind velocity at which measurements were made varied widely from one experiment to another. There was a clear dependence on particle size, and an influence of wind speed was observed in some of the measurements. In tabulating the data, it has been assumed that the results of Nicholson et al. apply at a mean wind speed of 3 m s^{-1} and that the bulk deposition velocity is proportional to wind speed.

These are crude assumptions, but the precision of the description of an urban area does not justify a more detailed treatment. The range between the quantiles represents the variation likely in urban areas, largely influenced by the likely number of trees, but also allowing for other sources of uncertainty.

Grass and Other Short Vegetation: "Meadow"

A number of field and wind tunnel experiments have used monodisperse particle tracers for direct measurement of deposition to entire grass sward or crop surfaces. The results of these measurements are fairly consistent, and some allow interpolation to provide data at the particle sizes and wind speeds required in the elicitation. Such data are assumed to be representative of meadow. All such studies show a marked effect of particle size, but many of the field studies do not allow the effect of wind speed to be resolved. Table G-1 summarizes the interpolated results used.

Other workers have derived deposition velocities for such surfaces from models that represent the physical processes involved in deposition, from theoretical or empirical approaches. Table G-2 summarizes two papers giving such results.

In addition, papers exist in the literature that have applied micrometeorological techniques to investigate the deposition of tracers, generally of industrial origin. These differ from the results summarized in Table G-1, in that the size of the particles is not controlled, and in most cases the size is incompletely known or partly resolved. A few results of such measurements are summarized in Table G-3. Many of these determinations apply to tracers present principally in micron or sub-micron particles, but yield deposition velocities many times greater than expected from the results in Table G-1.

While there may be reasons related to the size distribution and measurement techniques for the differences between Table G-1 and Table G-3, it is not clear that the data in Table G-3 can be discounted as unreliable. It may appear improbable that they provide reliable information on the behavior of monodisperse aerosols released to the atmosphere, but they apparently indicate that deposition velocities may be an order of magnitude higher than indicated by other studies, and they have been kept in mind in setting the range in the elicitation table.

Forest

Direct measurement of deposition using monodisperse aerosols to entire forest canopies is difficult because of the height of the vegetation elements. Deposition has been measured to shoots or branches (Belot et al.),[1] and the deposition velocity to the entire forest has been estimated by modeling using the results. Other estimates can be made by application of general models for deposition to plant canopies.

Table G-4 summarizes the literature results used in evaluating deposition velocities for particulate material to forest. The values listed under Sehmel[16] necessitated some extrapolation to conditions considered in his paper, and this was carried out somewhat subjectively by eye; it is doubtful whether the extrapolation can be justified, but the numbers are included to give a feel for the difference between models.

Table G-1. Deposition velocities, v_d (m s^{-1}) for grass and short crops (meadow) for particles of diameter d (μm) and wind speed, u (m s^{-1})

Author and Details	u, m s^{-1}: d, μm:	0.1	0.3	~2 1	3	10	0.1	0.3	~5 1	3	10
Garland[7] (grass)							3.10^{-4}	$1.5.10^{-4}$	2.10^{-4}	2.10^{-3}	2.10^{-2}
Jonas and Vogt[9] (grass)*			2.10^{-4}	(1.2-2.5) $\times10^{-4}$	(0.15-2) $\times10^{-3}$	(3-6) $\times10^{-2}$					
Wedding and Montgomery[20] (maize and soybean)		-		(0.8-5) $\times10^{-4}$	(0.2-2) $\times10^{-4}$	(0.3-3) $\times10^{-2}$					
Pomeroy et al.[13] (wheat, lettuce)							-	-	-	(0.3-2) $\times10^{-3}$	(2.5-6) $\times10^{-3}$

*Wide range of wind speed included.

Table G-2. Deposition velocities (m s^{-1}) given by empirical or theoretical models

Author and Details	u, m s^{-1}: d, μm:	0.1	0.3	~2 1	3	10	0.1	0.3	~5 1	3	10
Davidson et al.[5] (Various grasses showing influence of species)		10^{-5} to 10^{-4}	2×10^{-5} to 2×10^{-4}	4×10^{-4} to 4×10^{-3}	10^{-3} to 3×10^{-2}	7×10^{-3} to 4×10^{-2}					
Sehmel and Hodgson[16]		4×10^{-4}	2×10^{-4}	6×10^{-4}	2×10^{-3}	9×10^{-3}	10^{-3}	6×10^{-4}	2×10^{-3}	7×10^{-3}	2×10^{-2}
Slinn[18]							3×10^{-4}	2×10^{-4}	3×10^{-4}	10^{-3}	10^{-2}

Table G-3. Deposition velocities (m s^{-1}) from field data using uncontrolled aerosols

Author	d, μm:	0.1	0.3	1
Sievering[17]	(0.5-5) $\times 10^{-3}$	(0.1-2) $\times 10^{-2}$		
Wesely et al.[21]			2.10^{-3}	~(0.1-1 μm)
Wesely et al.[22]	(5-9) $\times 10^{-3}$			

Table G-4. Summary of results used to evaluate deposition velocities

Author & Details	u, m s^{-1} d, μm:	0.1	0.3	~2 1	3	10	0.1	0.3	~5 1	3	10
Belot[1], pine				10^{-4}	10^{-3}	3.10^{-2}			10^{-4}	2.10^{-2}	3.10^{-1}
Sehmel and Hodgson*[16]		2.10^{-3}	10^{-3}	2.10^{-3}	7.10^{-3}	1.10^{-2}	6.10^{-3}	2.10^{-4}	5.10^{-3}	$3.1-^{-2}$	6.10^{-2}
Slinn,[18] eucalyptus		2.10^{-4}	10^{-4}	2.10^{-4}	10^{-3}	10^{-2}	4.10^{-4}	2.10^{-4}	4.10^{-4}	10^{-3}	2.10^{-2}
Wesely et al.,[22] pine+			7.6×10^{-3}								

*Extrapolation
+Particulate sulphur, mostly ~0.1 to 2 μm

Human Skin

It is expected that skin will be an aerodynamically smooth surface, but the deposition process will be influenced by the presence of local irregularities in the surface and impaction and interception on hairs.

The deposition mechanisms for particles may be identified: 'form' impaction, significant where the stopping distance of the particle is comparable with the dimensions of an obstacle, and 'eddy' impaction, where the transverse inertia acquired by particles in eddies a little distance from the surface is sufficient to carry the particles to the surface. Taking account of the movement of a human walking through the air, relative velocities of ~10 m s^{-1} may be significant to the deposition situations considered here.

At 5 and 10 m s^{-1} only the largest (10μm) particles are large enough for form impaction to be significant at the smallest obstacles (~1 cm: fingers, ears, etc.). Eddy impaction is likely to be significant for all sizes. Form impaction may contribute a significant fraction of the wind speed, relative to the body, to the deposition velocity upwind surfaces of small surface elements. This may cause substantial enhancement of deposition to a fraction of the skin surface. Although the area concerned is probably only a percent or less of the total body area, it may be a larger fraction of the skin area normally exposed when out of doors.

Eddy deposition is significant for all particle sizes. Deposition to smooth surfaces was studied by Chamberlain et al.[4] in 1984. Deposition to vertical filter paper surfaces was orders of magnitude greater than for polished metal surfaces; this difference is assumed to indicate the potential enhancement due to the small hairs that cover much of the body. Most of the exposed body surface is usually near vertical, but a contribution of 10 per cent of the sedimentation velocity has been included in the median estimate of deposition velocity. (This results in a minor increase.)

The upper percentile includes 50% of the sedimentation velocity, while the lower percentile allows only vertical smooth surface deposition. Thicker layers of hair (eyebrows, scalp hair, beards, etc.) are not allowed for.

Deposition of Elemental Iodine and Methyl Iodide

Iodine to Grass

MacMahon and Denison[10] and Sehmel[16] summarized available measurements. Sehmel's summary details more measurements and shows that the deposition velocity to fields of grass and other short vegetation generally range from about 0.02 to over 10 cm s^{-1}. Twenty-seven investigations are reported. It is likely that V_d is lower at night, and that nighttime measurements are under-represented. The values selected make allowance for this bias.

Few measurements are reported for methyl iodide by Sehmel. All show deposition velocity well below 0.1 cm s^{-1}. Windspeed is expected to have little effect, the deposition being controlled by the surface reaction (or lack of it). The observed deposition may actually be due to low levels of impurity (I_2 vapor or other reactive forms) in the CH_3I used in the experiment.

Iodine to Forest and Other Surfaces

The deposition of I_2 to forest differs from that to grass chiefly because the large roughness results in a reduced aerodynamic resistance. Correcting the median values for grass for the difference in aerodynamic resistance yields median V_d estimates. The extremes are based on the high surface resistance expected for dry leaf surfaces when stomata are closed (see Garland[8]) for the 5 percentile, and the scaling factor between the 95 percentile and the median for grass.

The deposition of methyl iodide is unlikely to be influenced at all by the increase in aerodynamic roughness. There is no reason to expect the deposition velocity to forest to be greater than that to grass.

Similar comments apply to urban areas. There is evidence of low surface resistance for building surfaces, (Chamberlain et al.[4]) and this reference allows the values of the aerodynamic and bluff body resistances to be estimated. For skin, iodine vapor may sorb with a low surface resistance at the surface. The three-component resistance model was used, assuming that the fraction velocity and additional laminar layer resistance for a smooth surface apply (see also Garland[6]).

There is little reason to expect methyl iodide to be more readily absorbed by skin than by leaf surfaces, since both have wax-like and lipid components. The uncertainty in this statement is reflected in the increased 95 percentile relative to the other surfaces.

Wet Deposition of Elemental Iodine Vapor

Caput et al.[3] observed the washout of iodine vapor released deliberately in a series of experiments. The results show substantial variation but were the same order as a

theoretical expression for irreversible capture of molecules by rain drops. The required fractions removed were calculated from median and extreme lines that describe the removal coefficient relationship with rainfall intensity. No use was made of wind speed in the calculation.

Particle Washout

Experimental studies of particle washout in field conditions include Nicholson et al.,[11] Radke et al.,[14] and Schumann.[15] Nicholson and Radke give values of the apparent collection efficiency E, related to the scavenging coefficient Λ by

$$\Lambda = \frac{cJE}{R_m}$$

where J is intensity of rainfall, R_m is the mass mean radius of raindrops, and c is a factor with a value of about 0.5(Slinn).[19] R_m increases with intensity of rainfall, and the correlation

$$R_m = 0.35\,mm\left\{\frac{J}{mm\,h^{-1}}\right\}^{0.25}$$

provides a convenient description. Schumann provides experimental values of Λ/J.

Having obtained an estimate of Λ, the fraction removed is simply

$$F = 1 - \exp(-\Lambda t)$$

Values used are shown in Table G-5.

Data based on Radke et al.[14] and Schumann[15] were used in calculations, and the results were used to judge the expected range of values of F for each of the conditions required in the elicitation.

Table G-5. Experimental data relating to the scavenging coefficient

Particle diameter μm	E (Nicholson and Branson[11])	E (Radke* et al.[14]) median and upper limit	$\Lambda/J, s^{-1}\ h\ mm^{-1}$ (Schumann[15]) lower, median and upper range
0.1		0.5, 1	
0.3		0.35, 0.7	0.02, 0.1, 0.3
1		0.15, 0.5	0.02, 0.2, 0.4
3	~0.5	0.85, 1.5	0.04, 0.2, 0.4
10	~0.9	1.9, 3	0.15, 0.7, 1.0

*see also Slinn[19]

Deposition Tables

Units of velocity are in cm/s; N/A = not provided by expert; unkn = unknown

DD-A: Dry deposition velocity of aerosols - Wind Speed at 2m/s					
PARTICLE SIZE	QUANTILE	URBAN	MEADOW	FOREST	HUMAN SKIN
0.10μ	0%	8.00E-04	8.00E-04	8.00E-04	N/A
	5%	1.00E-02	3.00E-03	1.00E-02	3.00E-04
	50%	5.00E-02	3.00E-02	3.00E-02	1.00E-03
	95%	2.00E-01	1.00E-01	2.00E-01	3.00E-03
	100%	5.00E-01	5.00E-01	5.00E-01	5.00E-01
0.30μ	0%	8.00E-04	8.00E-04	8.00E-04	N/A
	5%	1.00E-02	3.00E-03	1.00E-02	3.00E-04
	50%	5.00E-02	2.00E-02	2.00E-02	1.00E-03
	95%	2.00E-01	1.00E-01	2.00E-01	5.00E-03
	100%	5.00E-01	5.00E-01	5.00E-01	5.00E-01
1.00μ	0%	4.00E-03	4.00E-03	4.00E-03	N/A
	5%	1.00E-02	1.00E-02	1.00E-02	2.00E-04
	50%	5.00E-02	3.00E-02	3.00E-02	6.00E-03
	95%	2.00E-01	2.00E-01	3.00E-01	2.00E-02
	100%	5.00E-01	5.00E-01	5.00E-01	5.00E-01
3.00μ	0%	3.00E-02	3.00E-02	3.00E-02	N/A
	5%	5.00E-02	3.00E-02	1.00E-01	2.00E-04
	50%	7.00E-02	2.00E-01	3.00E-01	2.00E-02
	95%	4.00E-01	2.00E+00	2.00E+00	8.00E-02
	100%	5.00E-01	5.00E-01	5.00E-01	5.00E-01
10.00μ	0%	3.00E-01	3.00E-01	3.00E-01	N/A
	5%	3.00E-01	4.00E-01	5.00E-01	2.00E-04
	50%	5.00E-01	1.00E+00	2.00E+00	2.00E-01
	95%	1.00E+00	4.00E+00	5.00E+00	1.00E+00
	100%	5.00E-01	5.00E-01	5.00E-01	5.00E-01

DD-B: Dry deposition velocity of aerosols - Wind Speed at 5m/s					
PARTICLE SIZE	QUANTILE	URBAN	MEADOW	FOREST	HUMAN SKIN
0.10μ	0%	8.00E-04	8.00E-04	8.00E-04	N/A
	5%	2.00E-02	5.00E-03	2.00E-02	8.00E-04
	50%	1.30E-01	3.00E-02	4.00E-02	3.00E-03
	95%	6.00E-01	2.00E-01	5.00E-01	1.00E-02
	100%	5.00E-01	5.00E-01	5.00E-01	5.00E-01
0.30μ	0%	8.00E-04	8.00E-04	8.00E-04	N/A
	5%	2.00E-02	5.00E-03	2.00E-02	6.00E-04
	50%	1.30E-01	2.00E-02	4.00E-02	6.00E-03
	95%	6.00E-01	2.00E-01	3.00E-01	1.00E-01
	100%	5.00E-01	5.00E-01	5.00E-01	5.00E-01
1.00μ	0%	4.00E-03	4.00E-03	4.00E-03	4.00E-03
	5%	2.00E-02	1.00E-02	2.00E-02	4.00E-04
	50%	1.30E-01	3.00E-02	5.00E-02	5.00E-02
	95%	6.00E-01	3.00E-01	5.00E-01	3.00E-01
	100%	5 00E-01	5.00E-01	5.00E-01	5.00E-01
3.00μ	0%	3.00E-02	3.00E-02	3.00E-02	3.00E-02
	5%	5.00E-02	1.00E-01	1.00E-01	4.00E-04
	50%	2.00E-01	3.00E-01	1.00E+00	4.00E-01
	95%	8.00E-01	3.00E+00	3.00E+00	2.00E+00
	100%	5.00E-01	5.00E-01	5.00E-01	5.00E-01
10.00μ	0%	3.00E-01	3.00E-01	3.00E-01	3.00E-01
	5%	3.00E-01	5.00E-01	1.00E+00	6.00E-04
	50%	6.00E-01	3.00E+00	6.00E+00	5.00E+00
	95%	2.00E+00	6.00E+00	2.00E+01	2.00E+01
	100%	5.00E-01	5.00E-01	5.00E-01	5.00E-01

DD-C: Dry deposition velocity of elemental iodine - Wind Speed at 2 and 5m/s					
WIND SPEED	QUANTILE	URBAN	MEADOW	FOREST	HUMAN SKIN
2.m/s	0%	N/A	N/A	N/A	N/A
	5%	5.00E-02	3.00E-02	3.00E-02	2.00E-02
	50%	2.00E-01	6.00E-01	2.00E+00	3.00E-01
	95%	1.20E+00	4.00E+00	1.50E+01	1.00E+00
	100%	N/A	N/A	N/A	N/A
5.m/s	0%	N/A	N/A	N/A	N/A
	5%	5.00E-02	6.00E-02	6.00E-02	5.00E-02
	50%	5.00E-01	1.00E+00	6.00E+00	7.00E-01
	95%	2.00E+00	7.00E+00	3.00E+01	2.00E+00
	100%	N/A	N/A	N/A	N/A

DD-D: Dry deposition velocity of methyl iodide - Wind Speed at 2 and 5m/s					
WIND SPEED	QUANTILE	URBAN	MEADOW	FOREST	HUMAN SKIN
2.m/s	0%	N/A	N/A	N/A	N/A
	5%	2.00E-04	2.00E-04	2.00E-04	2.00E-04
	50%	1.00E-03	1.00E-03	1.00E-03	1.00E-03
	95%	5.00E-03	5.00E-03	5.00E-03	1.00E-01
	100%	N/A	N/A	N/A	N/A
5.m/s	0%	N/A	N/A	N/A	N/A
	5%	2.00E-04	2.00E-04	2.00E-04	2.00E-04
	50%	1.00E-03	1.00E-03	1.00E-03	1.00E-03
	95%	5.00E-03	5.00E-03	5.00E-03	2.00E-01
	100%	N/A	N/A	N/A	N/A

DD-E-1: Dry deposition velocity of aerosols on Moorland/Peatland Surface		
PARTICLE SIZE	QUANTILE	
0.55μ	0%	1.00E-03
	5%	6.00E-03
	50%	3.00E-02
	95%	2.00E-01
	100%	5.00E-01
0.70μ	0%	2.00E-03
	5%	6.00E-03
	50%	3.00E-02
	95%	2.00E-01
	100%	5.00E-01
0.90μ	0%	3.00E-03
	5%	1.00E-02
	50%	3.00E-02
	95%	3.00E-01
	100%	5.00E-01
1.20μ	0%	5.00E-03
	5%	1.00E-02
	50%	4.00E-02
	95%	3.00E-01
	100%	5.00E-01
1.60μ	0%	1.00E-02
	5%	2.00E-02
	50%	5.00E-02
	95%	1.50E-01
	100%	5.00E-01

DD-E-2: Dry deposition velocity of aerosols on Heather/Green Grass Surface		
PARTICLE SIZE	**QUANTILE**	
0.55μ	**0%**	1.00E-03
	5%	3.00E-03
	50%	3.00E-02
	95%	2.00E-01
	100%	N/A
0.70μ	**0%**	2.00E-03
	5%	6.00E-03
	50%	3 00E-02
	95%	2.00E-01
	100%	N/A
0.90μ	**0%**	3.00E-03
	5%	1.00E-02
	50%	3.00E-02
	95%	3.00E-01
	100%	N/A
1.20μ	**0%**	5.00E-03
	5%	1.00E-02
	50%	4 00E-02
	95%	3.00E-01
	100%	N/A
1.60μ	**0%**	1.00E-02
	5%	2.00E-02
	50%	5.00E-02
	95%	4.00E-01
	100%	N/A

DD-E-2: Dry deposition velocity of aerosols on Heather/Green Grass Surface (continued)		
PARTICLE SIZE	QUANTILE	
2.30μ	0%	1.50E-02
	5%	4.00E-02
	50%	1.00E-01
	95%	1.00E+00
	100%	N/A
3.20μ	0%	3.00E-02
	5%	1.00E-01
	50%	3.00E-01
	95%	3.00E+00
	100%	N/A
4.20μ	0%	5.00E-02
	5%	1.00E-01
	50%	5.00E-01
	95%	4.00E+00
	100%	N/A

DD-F: Dry deposition velocity of aerosols on Grassland Surface		
PARTICLE SIZE	QUANTILE	
1.0μ	0%	N/A
	5%	5.00E-03
	50%	4.00E-02
	95%	8.00E-01
	100%	N/A

WD-A: Elemental iodine—fraction removed by rain ($1-f_w$)							
Rainfall/ Time	Wind Speed	Quantile	$1-f_w$	Rainfall/ Time	Wind Speed	Quantile	$1-f_w$
.3mm/hr	unkn	0%	N/A	2.mm/hr	unkn	0%	N/A
		5%	3.50E-02			5%	7.00E-02
		50%	1.30E-01			50%	5.00E-01
		95%	5.00E-01			95%	9.00E-01
		100%	N/A			100%	N/A
.075mm/ 10min	10 m/s	0%	N/A	.05mm/ 10min	unkn	0%	N/A
		5%	7.00E-03			5%	6.00E-03
		50%	4.10E-02			50%	2.40E-02
		95%	2.10E-01			95%	1.10E-01
		100%	N/A			100%	N/A
.17mm/ 10min	5 m/s	0%	N/A	.17mm/ 10min	14 m/s	0%	N/A
		5%	1.20E-02			5%	1.20E-02
		50%	6.00E-02			50%	6.00E-02
		95%	3.00E-01			95%	3.00E-01
		100%	N/A			100%	N/A
.23mm/ 10mir	12 m/s	0%	N/A	.5mm/ 10min	unkn	0%	N/A
		5%	1.50E-02			5%	3.00E-02
		50%	9.00E-02			50%	1.60E-01
		95%	3.80E-01			95%	9.90E-01
		100%	N/A			100%	N/A
.33mm/ 10min	unkn	0%	N/A	1.0mm/ 10min	14 m/s	0%	N/A
		5%	1.80E-02			5%	5.00E-02
		50%	1.10E-01			50%	2.10E-01
		95%	2.60E-01			95%	4.50E-01
		100%	N/A			100%	N/A

WD-A: Elemental iodine—fraction removed by rain ($1-f_w$) (continued)			
Rainfall/Time	**Wind Speed**	**Quantile**	$1-f_w$
1.67mm/10min	**unkn**	**0%**	N/A
		5%	6.00E-02
		50%	3.00E-01
		95%	8.00E-01
		100%	N/A

WD-B: Methyl iodide—fraction removed by rain (Wind Speed=unknown)		
Rainfall/Time	**Quantile**	$1\text{-}f_w$
.3mm/hr	0%	N/A
	5%	N/A
	50%	N/A
	95%	N/A
	100%	N/A
2.mm/hr	0%	N/A
	5%	N/A
	50%	N/A
	95%	N/A
	100%	N/A
.05mm/10min	0%	N/A
	5%	N/A
	50%	N/A
	95%	N/A
	100%	N/A
.33mm/10min	0%	N/A
	5%	N/A
	50%	N/A
	95%	N/A
	100%	N/A
1.67mm/10min	0%	N/A
	5%	N/A
	50%	N/A
	95%	N/A
	100%	N/A

WD-C: Fraction of aerosols removed by rain						
PARTICLE SIZE	**QUANTILE**	**Rainfall: .3mm/hr**	**Rainfall: 2.mm/hr**	**Rainfall: .05mm/10 min**	**Rainfall: .33mm/10 min**	**Rainfall: 1.67mm / 10 min**
0.10μ	**0%**	N/A	N/A	N/A	N/A	N/A
	5%	6.00E-03	4.00E-02	2.00E-03	1.00E-02	4.00E-02
	50%	1.50E-01	4.00E-01	2.00E-02	1.00E-01	3.30E-01
	95%	4.40E-01	9.00E-01	9.00E-02	3.00E-01	7.00E-01
	100%	N/A	N/A	N/A	N/A	N/A
0.30μ	**0%**	N/A	N/A	N/A	N/A	N/A
	5%	6.00E-03	4.00E-02	1.00E-03	1.00E-02	3.00E-02
	50%	1.00E-01	3.00E-01	1.00E-02	8.00E-02	2.50E-01
	95%	3.30E-01	8.00E-01	6.00E-02	2.00E-01	6.00E-01
	100%	N/A	N/A	N/A	N/A	N0.3/A
1.00μ	**0%**	N/A	N/A	N/A	N/A	N/A
	5%	6.00E-03	8.00E-02	1.00E-03	1.00E-02	3.00E-02
	50%	7.00E-02	3.00E-01	1.00E-02	6.00E-02	2.00E-01
	95%	2.50E-01	7.00E-01	5.00E-02	2.00E-01	5.00E-01
	100%	N/A	N/A	N/A	N/A	N/A
10.00μ	**0%**	N/A	N/A	N/A	N/A	N/A
	5%	4.00E-02	2.60E-01	8.00E-03	5.00E-02	2.00E-01
	50%	4.00E-01	9.00E-01	1.00E-01	4.00E-01	8.00E-01
	95%	8.00E-01	9.90E-01	2.50E-01	7.00E-01	9.80E-01
	100%	N/A	N/A	N/A	N/A	N/A

References

1. Belot, Y., A. Baille, and J.-L. Delmas, "Modele Numerique de Dispersion des Pollutants Atmospheriques en Presence de Couverts Vegetaux," *Atmospheric Environment*, 10:89-98, 1976.

2. Bennett, M., *A Simple Physical Model of Dry Deposition to a Rough Surface: Application to Urban Deposition*, TPRD/L/3205/R87, GEGB Letherhead, 1987.

3. Caput, D., et al., "Lavage de L'Iode par les Precipitations," *Environmental Contamination Following a Major Nuclear Accident, Proceedings of an International Symposium, 16-20 October 1989*, IAEA-SM-306/65, International Atomic Energy Agency, Vienna, pp. 151-158, 1990.

4. Chamberlain, A.C., J.A. Garland, and A.C. Wells, "Transport of Gases and Particles to Surfaces with Widely Spaced Roughness Elements," *Boundary-Layer Meteorology*, 29:343-360, 1984.

5. Davidson, D.I., J.M. Miller, and M.A. Pleskow, "The Influence of Surface Structure on Predicted Particle Dry Deposition to Natural Grass Canopies," *Water, Air, and Soil Pollution*, 18:25-43, 1982.

6. Garland, J.A., "The Dry Deposition of Sulphur Dioxide to Land and Water Surfaces," *Proceedings of the Royal Society of London, Series A*, 354:245-268, 1977.

7. Garland, J.A., "Field Measurements of the Dry Deposition of Small Particles to Grass," (H.-W. Georgii and J. Pankrath, eds.), *Deposition of Atmospheric Pollutants, Proceedings of a Colloquium, 9-11 November 1981*, D. Reidel, Boston, MA, pp. 9-16, 1982.

8. Garland, J.A., "The Uptake of Elemental Iodine Vapour by Bean Leaves," *Atmospheric Environment*, 18:199-204, 1984.

9. Jonas, R., and K.J. Vogt, "Untersuchungen zur Ermitlung der Ablagerungsgeschwindigkeit von Aerosolen auf Vegetation und Anderen Probenahmeflachen," Jul-1780 KRA Julich, 1982.

10. McMahon, T.A., and P.J. Denison, "Empirical Atmospheric Deposition Parameters - A Survey," *Atmospheric Environment*, 13:571-585, 1979.

11. Nicholson, K.W., J.R. Branson, and P. Giess, "Field Measurements of the Below-Cloud Scavenging of Particulate Material," *Atmospheric Environment*, 25A:771-777, 1991.

12. Nicholson, K.W., et al., *The Dry Deposition of Particulate Materials in an Urban Environment*, AEA-EE-0424, 1993.

13. Pomeroy, I.R., et al., *Interception of Particulate Material by Food Crops*, AEA-EE-0452, 1993.

14. Radke, L.F., P.V. Hobbs, and M.W. Eltgroth, "Scavenging of Aerosol Particles by Precipitation," *Journal of Applied Meteorology*, 19:715-722, 1980.

15. Schumann, T., *Precipitation Scavenging of Aerosol Particles: A Wintertime Field Study*, Diss. ETH No. 8843, Swiss Federal Institute of Technology, 1989.

16. Sehmel, G.A., and W.H. Hodgson, "A Model for Predicting Dry Deposition of Particles and Gases to Environmental Surfaces," (W. Licht, ed.), *Implications of the Clean Air Amendments of 1977 and of Energy Considerations for Air Pollution Control*, Symposium Series No. 196, American Institute of Chemical Engineers, New York, pp. 218-230, 1980.

17. Sievering, H., "Profile Measurements of Particle Dry Deposition Velocity at an Air-Land Interface," *Atmospheric Environment*, 16:301-306, 1981.

18. Slinn, W.G.N., "Predictions for Particle Deposition to Vegetative Canopies," *Atmospheric Environment*, 16:1785-1794, 1982.

19. Slinn, W.G.N., "Precipitation Scavenging," (D. Randerson, ed.), *Atmospheric Science and Power Production*, DOE/TIC-27601, Technical Information Center, Office of Scientific and Technical Information, United States Department of Energy, Oak Ridge, TN, pp. 466-532, 1984.

20. Wedding, J.B., and M.E. Montgomery, "Deposition Velocities for Full-Scale Corn and Soybean Canopies: A Wind Tunnel Simulation," *Environmental International*, 3:91-96, 1980.

21. Wesely, M.L., et al., "Measurements and Parameterization of Particulate Sulfur Dry Deposition Over Grass," *Journal of Geophysical Research*, 90:2131-2143, 1985.

22. Wesely, M.L., et al., "Eddy-Correlation Measurements of the Dry Deposition of Particulate Sulfur and Submicron Particles," (H.R. Pruppacher, R.G. Semonin, and W.G.N. Slinn, eds.), *Precipitation Scavenging, Dry Deposition and Resuspension, Proceedings of the 4th International Conference, 29 November–3 December 1982*, Elsevier Science, New York, pp. 943-952, 1983.

Expert H

Dry Deposition

The dry deposition velocity is functionally dependent on a number of parameters and phenomena. It is the uncertainty in these parameters and phenomena that introduces uncertainty in deposition velocity measurements. In his review of dry deposition, Sehmel[1] shows the range of reported values to vary over several orders of magnitude for similar particle sizes. Not all the variation can be attributed to experimental causes. The differences in meteorological variables, surface properties, and the properties of the depositing materials plays a strong role in the variability of the deposition velocities. Sehmel lists a number of factors influencing dry deposition of material. The factors considered in this estimation of dry deposition are a subset of these and by no means exhaustive. Some of the variability has been eliminated in the case structure. The particle size, shape, and density have been specified. Particle chemical reaction, growth, and evaporation have been eliminated from consideration. Other factors still reflect a range of uncertainty. The wind speed is at 10 m. The deposition surfaces are classified into categories that still yield a range of uncertainty in canopy height and type. The collection efficiency of the canopy types is entirely unspecified, as are which collection mechanisms to consider. Atmospheric stability is unspecified.

The parameters that are treated in this estimate are friction velocity, velocity at the reference height, the canopy height, zero plane displacement, roughness height, and canopy collection efficiency.

Dry deposition velocities have been calculated using the model described by Slinn[2]. This model is based on approximate analytical solutions for momentum transfer in a vegetative canopy. It includes a model for the particle collection efficiency of the canopy that is based on the wind tunnel data. The model is expressed in the equation

$$v_d = v_s + \frac{C_D u_r}{1 + \frac{u_h}{u_r}\left[\frac{1-E}{E+\sqrt{E}\tanh(\gamma\sqrt{E})}\right]} \qquad (1)$$

where: v_d is the deposition velocity
v_s is the gravitational settling velocity
C_D is the overall drag coefficient of the canopy and is equal to $(u_*/u_r)^2$
u_* is the friction velocity
u_r is the velocity at the reference height
u_h is the velocity at the canopy height
E is the collection efficiency of the canopy for particles
γ is a parameter taken as $(hu_*)/(k(h-d_0)u_h)$
h is the canopy height
d_0 is the zero plane displacement taken as 0.76h
z_0 is the roughness height taken as 0.09h
k is von Kármán's constant taken as 0.4.

The efficiency of the canopy in removing particulates is given as

$$E = \frac{c_v}{c_d}Sc^{-2/3} + \frac{c_v}{c_d}\left[F_s\frac{d_p}{d_p+D_s} + (1-F_s)\frac{d_p}{d_p+D_L}\right] + \frac{St^2}{1+St^2} \qquad (2)$$

where: c_v/c_d is the ratio of viscous to total drag, taken as 1/4 to 1/3
Sc is the Schmidt number, ν/D
ν is the kinematic viscosity of the gas
D is the diffusivity of the particle
F_s is the fraction of collection by vegetative hairs
D_s is the diameter of the small vegetative structure
D_L is the diameter of the larger vegetative structure
d_p is the diameter of the particle
St is the Stokes number, $2u_*\tau/D_L$
τ is the particle relaxation time.

The velocity profile above the canopy is assumed to be described by

$$u(z) = \frac{u_*}{k}\ln\left(\frac{z-d_0}{z_o}\right) \qquad (3)$$

where u(z) is the velocity at height z above the ground.

In employing this model, I have taken some liberty in the definition of the reference height. It was decided that a reference height of 1 meter would be used and that in the case of a forest, the reference height referred to 1 meter above the canopy. Similar consideration is made for the 10 meter height at which the wind velocity is given. I have used a reference height of 1 meter above the canopy, i.e., z_r = h+1m, and a wind speed measured at 10 meters above the canopy for all canopy heights considered.

The wind speed at the reference and canopy heights and the friction velocity are taken from the above equation for two

cases. The first case uses the velocity given at 10 meters (h+10m) and z = (h+10m) to calculate u_*, u_r, and u_h. The second case assumes the velocity given at 10 meters is the same as the velocity at the reference height of 1 meter, and the equation above is used with z = h+1m) to calculate u_*, u_r, and u_h. The ratios of velocities are the same for both cases.

The canopy height ranges used for the deposition surfaces are given below:

Moorland/Peatland	35 cm to 65 cm
Heather	25 cm to 65 cm
Grassland	5 cm to 1m
Meadow	1 cm to 2 m
Forest	5 m to 30 m
Urban	0.1 mm to 10 m
Human Skin	0.1 mm to 2 m

Use of this model may not be appropriate for urban deposition surfaces and is almost certainly not applicable for human skin. However, given the time constraints, an attempt was made to apply it to these situations. The range of canopy heights covered the small to large structure present, and the selection of parameters for the efficiency model also attempt to accommodate the variation.

For the estimated deposition to human skin, higher friction velocities were taken to try to account for a person standing in the wind.

Three collection efficiency curves have been calculated using the above equation and parameters described in Slinn. These parameters have been varied to give high and low efficiencies.

The model has been exercised over the range of friction and reference velocities, the range of canopy heights, and the range of canopy collection efficiencies. From these results, the mean value was taken as the mean of the calculations for the first case friction velocity and intermediate collection efficiency. The 95 percentile was taken as the highest values calculated and the 5 percentile was taken as the lowest values calculated.

The 0 and 100 percentiles are considered to be 1 and 99 percentiles and are calculated in a somewhat arbitrary manner. The first case friction velocity for the 2 m/s wind is reduced by an order of magnitude, and the velocity ratios are adjusted accordingly. These values are used with the low collection efficiency curve to produce the 1 percentile values for both the 2 m/s and 5 m/s cases. These results give the settling velocity for larger particles, which is to be expected. The 99 percentile values are estimated by using the doubled friction velocity (velocity ratios appropriately adjusted) for the second case of the 5 m/s wind and the high collection efficiency curve.

The dry deposition velocity for elemental iodine (I_2 vapor) is calculated based on the assumption that iodine vapor will behave like a particle and be collected upon contact with a surface. The diffusion coefficient of 0.08 cm^2/s given by Chamberlain[3] was used in the calculation. A similar value was also calculated. The values reported by Sehmel[1] were compared to the calculations and seemed to compare well for the mean and 95 percentile but the calculated values for the 5 percentile seemed high. These 5 percentile values were decreased by an order of magnitude.

Methyl iodide was calculated to have a diffusion coefficient comparable to that of iodine vapor. The deposition velocity range reported by Sehmel indicated that the deposition velocity was from 0.001 to 0.005 that of iodine vapor. The estimated deposition velocities for iodine vapor have been multiplied by this factor to give the estimated deposition velocity for methyl iodide.

Wet Deposition

The problem for wet deposition is stated as one of washout in which rain falls through an aerosol or gas, removing material by interaction with the rain drops. This is clearly stated as raindrop scavenging. The principal uncertainties are in the drop size and distribution, and in the collection efficiency of the drops. Another area of uncertainty is in the effect of wind speed.

Removal of material by raindrop scavenging is described by

$$\frac{dC}{dt} = -\Lambda C \qquad (4)$$

where: C is the concentration of material
t is time
Λ is the removal coefficient defined as

$$\Lambda = \int_R \pi R^2 V(R) E(d_p, R) N(R) dR \qquad (5)$$

where: R is the drop radius
V(R) is the relative drop to particle velocity
$E(d_p, R)$ is the collection efficiency of a particle of diameter d_p by a drop of radius R
N(R) is the number distribution of the drops.

Generally, the particle settling velocity is negligible compared to the drop settling velocity so that in the absence of wind, V(R) is very nearly the terminal settling velocity of the drop. When there is wind, the particle velocity may be very near the wind velocity and the drop velocity may lag behind. These wind driven velocity differences may be superimposed over the settling velocities and, in the extreme, the velocity difference may be the wind velocity. However, this contribution is more likely to arise from fluctuations in the wind velocity. This has not been considered in the estimates of removal by drop scavenging. It has been assumed that the variation of the drop size and efficiency will account for the effect of wind.

The above equation for Λ is approximated by

$$\Lambda = \frac{3J}{4R_m} E(d_p, R_m) \qquad (6)$$

where: J is the rain intensity
R_m is the mean drop size given as a function of the rain intensity:

$$R_m = (350\mu m)\left[\frac{J}{mm/hr}\right]^{0.25} \qquad (7)$$

and is taken from Nicholson et al.[4]. The terminal velocity of the falling drop is taken from Clift et al.[5] and is

$$V(R) = \frac{\nu}{2R}\exp(-3.126 + 1.013\ \ln(N_D) - 0.01912\ \ln(N_D)^2) \qquad (8)$$

where: N_D is the Best number defined as

$$N_D = \frac{32\rho_{air}\rho_{water} g R^3}{3\mu_{air}^2} \qquad (9)$$

The drop collection efficiency is calculated from correlations recommended by Rimberg and Peng[6] for collection by diffusion, interception, and impaction. Other mechanisms, such as diffusiophoresis, thermophoresis, and electrostatics, can affect the collection efficiency of the drops, but these mechanisms are not explicitly treated in this exercise.

The case structure provided an accumulated amount of rain and a time over which the rain accumulated. The intensity and duration were uncertainties. In this estimation, the average intensity has been used. It has been assumed that the variation in drop size and efficiency will accommodate the uncertainty from other factors.

The mean value is taken from the model calculated drop size and efficiency. The 5 and 95 percentiles are taken from calculations using multipliers on the drop size and efficiency. The removal fraction is expressed as

$$FR = 1 - \exp\left(-\frac{3J}{4 f_R R_m} f_E E(d_p, f_R R_m)\ t\right) \qquad (10)$$

where: FR is the fraction removed
f_R is the drop size multiplier
f_E is the efficiency multiplier.

Note that the efficiency is calculated for the adjusted drop size and that efficiency is adjusted. The median is calculated for f_R and f_E both equal to 1. The 95 percentile is calculated for $f_R = 0.5$ and $f_E = 2$. The 5 percentile is calculated for $f_R = 2$ and $f_E = 0.5$. The 99 percentile is calculated for $f_R = 0.5$ and $f_E = 3$. The 1 percentile is calculated for $f_R = 2$ and $f_E = 0.3$. This is an admittedly arbitrary scheme, but it is felt that, short of a more detailed analysis, this covers the uncertainty.

Scavenging of iodine vapor has been treated as diffusive collection in the same way as the particles. Methyl iodide is treated similarly to the dry deposition treatment. The factors used in the dry deposition are applied to the collection efficiency for the iodine vapor and the removal fractions calculated.

Deposition Tables

Units of velocity are in cm/s; unkn = unknown

DD-A: Dry deposition velocity of aerosols - Wind Speed at 2m/s					
PARTICLE SIZE	**QUANTILE**	**URBAN**	**MEADOW**	**FOREST**	**HUMAN SKIN**
0.10μ	0%	3.00E-04	4.00E-04	1.00E-03	7.00E-04
	5%	2.80E-03	4.60E-03	1.00E-02	7.00E-03
	50%	1.20E-02	1.80E-02	5.20E-02	3.90E-02
	95%	1.10E-01	1.80E-01	4.40E-01	1.80E-01
	100%	1.10E+00	2.30E+00	4.50E+00	1.80E+00
0.30μ	0%	6.00E-04	6.00E-04	9.00E-04	1.20E-03
	5%	2.50E-03	2.80E-03	6.00E-03	8.70E-03
	50%	1.10E-02	2.20E-02	6.40E-02	5.20E-02
	95%	1.30E-01	3.90E-01	9.70E-01	2.70E-01
	100%	1.30E+00	5.00E+00	1.01E+01	2.70E+00
1.00μ	0%	4.00E-03	3.70E-03	4.00E-03	5.70E-03
	5%	8.20E-03	7.20E-03	1.20E-02	2.60E-02
	50%	3.00E-02	5.90E-02	1.69E-01	1.46E-01
	95%	3.40E-01	8.50E-01	2.30E+00	7.50E-01
	100%	4.10E+00	1.40E+01	1.30E+01	7.40E+00
3.00μ	0%	2.90E-02	2.90E-02	3.00E-02	3.40E-02
	5%	4.10E-02	3.70E-02	5.20E-02	9.10E-02
	50%	9.90E-02	1.60E-01	5.30E-01	4.10E-01
	95%	1.10E+00	1.59E+00	7.40E+00	1.90E+00
	100%	4.00E+01	5.30E+01	2.07E+02	1.90E+01
10.00μ	0%	3.00E-01	3.00E-01	3.00E-01	3.10E-01
	5%	3.30E-01	3.30E-01	5.20E-01	4.70E-01
	50%	4.90E-01	8.40E-01	4.50E+00	1.29E+00
	95%	8.70E+00	4.50E+00	2.60E+01	4.40E+00
	100%	1.75E+02	7.70E+01	2.75E+02	6.00E+01

DD-B: Velocity of aerosols - Wind Speed at 5m/s					
PARTICLE SIZE	QUANTILE	URBAN	MEADOW	FOREST	HUMAN SKIN
0.10μ	0%	3.00E-04	4.00E-04	1.00E-03	7.00E-04
	5%	6.90E-03	1.10E-02	2.70E-02	1.70E-02
	50%	3.00E-02	3.50E-02	1.30E-01	9.70E-02
	95%	2.70E-01	4.50E-01	1.10E+00	4.50E-01
	100%	1.10E+00	2.30E+00	4.50E+00	1.80E+00
0.30μ	0%	6.00E-04	6.00E-04	9.00E-04	1.20E-03
	5%	5.70E-03	6.20E-03	1.40E-02	2.10E-02
	50%	2.70E-02	4.20E-02	1.60E-01	1.30E-01
	95%	3.20E-01	9.70E-01	2.50E+00	6.70E-01
	100%	1.30E+00	5.00E+00	1.01E+01	2.70E+00
1.00μ	0%	4.00E-03	3.70E-03	4.00E-03	5.70E-03
	5%	1.50E-02	1.20E-02	2.60E-02	6.00E-02
	50%	7.00E-02	1.10E-01	4.40E-01	3.60E-01
	95%	8.90E-01	2.20E+00	7.10E+00	1.90E+00
	100%	4.10E+00	1.40E+01	1.30E+01	7.40E+00
3.00μ	0%	2.90E-02	2.90E-02	3.00E-02	3.40E-02
	5%	6.00E-02	5.30E-02	1.00E-01	1.80E-01
	50%	2.10E-01	3.00E-01	2.70E+00	9.90E-01
	95%	4.80E+00	5.80E+00	3.60E+01	4.70E+00
	100%	4.00E+01	5.30E+01	2.07E+02	1.90E+01
10.00μ	0%	3.00E-01	3.00E-01	3.00E-01	3.10E-01
	5%	3.90E-01	5.20E-01	2.10E+00	7.20E-01
	50%	8.40E-01	2.63E+00	9.50E+00	2.80E+00
	95%	3.60E+01	1.20E+01	6.90E+01	1.20E+01
	100%	1.75E+02	7.70E+01	2.75E+02	6.00E+01

DD-C: Dry deposition velocity of elemental iodine - Wind Speed at 2 and 5m/s					
WIND SPEED	QUANTILE	URBAN	MEADOW	FOREST	HUMAN SKIN
2.m/s	0%	2.00E-03	4.00E-03	3.00E-02	7.00E-03
	5%	1.70E-02	4.00E-02	3.00E-01	7.00E-02
	50%	8.00E-01	1.38E+00	7.40E+00	4.80E+00
	95%	1.00E+01	4.90E+00	1.30E+01	1.60E+01
	100%	1.00E+02	4.90E+01	1.30E+02	1.50E+02
5.m/s	0%	4.00E-03	1.00E-02	7.00E-02	1.80E-02
	5%	4.00E-02	1.00E-01	7.00E-01	1.80E-01
	50%	2.00E+00	3.40E+00	1.80E+01	1.20E+01
	95%	2.50E+01	1.20E+01	3.30E+01	4.00E+01
	100%	1.00E+02	4.90E+01	1.30E+02	1.50E+02

DD-D: Dry deposition velocity of methyl iodide - Wind Speed at 2 and 5m/s					
WIND SPEED	QUANTILE	URBAN	MEADOW	FOREST	HUMAN SKIN
2.m/s	0%	8.00E-06	2.00E-05	1.50E-04	3.00E-05
	5%	8.00E-05	2.00E-04	1.50E-03	3.00E-04
	50%	1.30E-03	2.20E-03	1.20E-02	7.70E-03
	95%	1.00E-02	4.90E-03	1.30E-02	1.60E-02
	100%	1.00E-01	1.00E-01	1.30E-01	1.50E-01
5.m/s	0%	2.00E-05	5.00E-05	3.50E-04	9.00E-05
	5%	2.00E-04	5.00E-04	3.50E-03	9.00E-04
	50%	3.20E-03	5.40E-03	2.90E-02	1.90E-02
	95%	2.50E-02	1.20E-02	3.30E-02	4.00E-02
	100%	1.00E-01	1.00E-01	1.30E-01	1.50E-01

DD-E-1: Dry deposition velocity of aerosols on Moorland/Peatland Surface		
PARTICLE SIZE	QUANTILE	
0.55μ	0%	1.00E-03
	5%	1.00E-02
	50%	1.20E-01
	95%	1.31E+00
	100%	8.00E+00
0.70μ	0%	2.00E-03
	5%	1.20E-02
	50%	1.40E-01
	95%	1.53E+00
	100%	9.00E+00
0.90μ	0%	5.00E-03
	5%	1.50E-02
	50%	1.70E-01
	95%	1.79E+00
	100%	1.10E+01
1.20μ	0%	7.00E-03
	5%	2.00E-02
	50%	2.10E-01
	95%	2.13E+00
	100%	1.30E+01
1.60μ	0%	9.00E-03
	5%	2.80E-02
	50%	2.70E-01
	95%	2.60E+00
	100%	1.60E+01

DD-E-2: Dry deposition velocity of aerosols on Heather/Green Grass Surface		
PARTICLE SIZE	QUANTILE	
0.55μ	0%	1.00E-03
	5%	1.00E-02
	50%	1.16E-01
	95%	1.34E+00
	100%	8.00E+00
0.70μ	0%	2.00E-03
	5%	1.20E-02
	50%	1 42E-01
	95%	1.53E+00
	100%	9.00E+00
0.90μ	0%	5.00E-03
	5%	1.40E-02
	50%	1.76E-01
	95%	1.79E+00
	100%	1.10E+01
1.20μ	0%	7.00E-03
	5%	1.90E-02
	50%	2.30E-01
	95%	2.13E+00
	100%	1.30E+01
1.60μ	0%	9.00E-03
	5%	2.70E-02
	50%	3.00E-01
	95%	2.59E+00
	100%	1.60E+01

DD-E-2: Dry deposition velocity of aerosols on Heather/Green Grass Surface (continued)		
PARTICLE SIZE	QUANTILE	
2.30μ	0%	2.80E-02
	5%	4.40E-02
	50%	4.40E-01
	95%	3.50E+00
	100%	2.10E+01
3.20μ	0%	2.90E-02
	5%	7.20E-02
	50%	6.90E-01
	95%	4.90E+00
	100%	5.30E+01
4.20μ	0%	4.40E-02
	5%	1.10E-01
	50%	1.11E+00
	95%	6.30E+00
	100%	6.50E+01

DD-F: Dry deposition velocity of aerosols on Grassland Surface		
PARTICLE SIZE	QUANTILE	
1.0μ	0%	3.00E-03
	5%	7.90E-03
	50%	1.00E-01
	95%	8.10E+00
	100%	5.00E+01

WD-A: Elemental iodine—fraction removed by rain ($1-f_w$)							
Rainfall/ Time	Wind Speed	Quantile	$1-f_w$	Rainfall/ Time	Wind Speed	Quantile	$1-f_w$
.3mm/hr	unkn	0%	1.77E-02	2.mm/hr	unkn	0%	4.82E-02
		5%	2.93E-02			5%	7.90E-02
		50%	2.04E-01			50%	4.25E-01
		95%	8.41E-01			95%	9.91E-01
		100%	9.37E-01			100%	9.99E-01
.075mm/ 10min	10 m/s	0%	3.64E-03	.05mm/ 10min	unkn	0%	2.97E-03
		5%	6.06E-03			5%	4.94E-03
		50%	4.40E-02			50%	3.70E-02
		95%	2.87E-01			95%	2.64E-01
		100%	3.98E-01			100%	3.69E-01
.17mm/ 10min	5 m/s	0%	5.63E-03	.17mm/ 10min	14 m/s	0%	5.54E-03
		5%	9.36E-03			5%	9.22E-03
		50%	6.80E-02			50%	6.50E-02
		95%	4.28E-01			95%	3.83E-01
		100%	5.60E-01			100%	5.16E-01
.23mm/ 10min	12 m/s	0%	6.68E-03	.5mm/ 10min	unkn	0%	1.02E-02
		5%	1.11E-02			5%	1.70E-02
		50%	7.80E-02			50%	1.16E-01
		95%	4.51E-01			95%	6.18E-01
		100%	5.94E-01			100%	7.64E-01
.33mm/ 10min	unkn	0%	8.19E-03	1.0mm/ 10min	14 m/s	0%	1.48E-02
		5%	1.36E-02			5%	2.46E-02
		50%	9.50E-02			50%	1.60E-01
		95%	5.45E-01			95%	5.20E-01
		100%	6.93E-01			100%	8.52E-01

WD-A: Elemental iodine—fraction removed by rain ($1\text{-}f_w$) (continued)			
Rainfall/Time	**Wind Speed**	**Quantile**	$1\text{-}f_w$
1.67mm/10min	**unkn**	**0%**	1.99E-02
		5%	3.30E-02
		50%	2.09E-01
		95%	8.29E-01
		100%	9.29E-01

WD-B: Methyl iodide—fraction removed by rain (Wind Speed=unknown)		
Rainfall/Time	**Quantile**	$1\text{-}f_w$
.3mm/hr	**0%**	8.00E-05
	5%	1.40E-04
	50%	3.80E-04
	95%	1.80E-03
	100%	3.00E-03
2.mm/hr	**0%**	2.00E-04
	5%	4.00E-04
	50%	9.20E-04
	95%	4.70E-03
	100%	7.00E-03
.05mm/10min	**0%**	1.40E-05
	5%	2.40E-05
	50%	6.30E-05
	95%	3.00E-04
	100%	4.60E-04
.33mm/10min	**0%**	4.00E-05
	5%	6.80E-05
	50%	1.70E-04
	95%	7.90E-04
	100%	1.20E-03
1.67mm/10min	**0%**	1.00E-04
	5%	1.60E-04
	50%	3.90E-04
	95%	1.80E-03
	100%	3.00E-03

WD-C: Fraction of aerosols removed by rain						
PARTICLE SIZE	**QUANTILE**	**Rainfall: .3mm/hr**	**Rainfall: 2.mm/hr**	**Rainfall: .05mm/10 min**	**Rainfall: .33mm/10 min**	**Rainfall: 1.67mm /10 min**
0.10μ	**0%**	7.00E-05	1.90E-04	1.20E-05	3.00E-05	7.00E-05
	5%	1.20E-04	3.20E-04	2.00E-05	5.40E-05	1.20E-04
	50%	9.60E-04	2.50E-03	1.60E-04	4.20E-04	9.50E-04
	95%	7.90E-03	1.20E-02	1.32E-03	3.30E-03	7.40E-03
	100%	1.20E-02	3 00E-02	2.00E-03	5.00E-03	1.11E-02
0.30μ	**0%**	1 30E-04	3.00E-04	2.00E-05	5.00E-05	1.20E-04
	5%	2.10E-04	5.70E-04	3.60E-05	9.40E-05	2.10E-04
	50%	1.67E-03	4.40E-03	2.80E-04	7.40E-04	1.70E-03
	95%	1.34E-02	3.40E-02	2.20E-03	5.80E-03	1.30E-02
	100%	2.00E-02	5.10E-02	3 40E-03	9.00E-03	2.00E-02
1.00μ	**0%**	7.00E-04	2.00E-03	1.20E-04	3.00E-04	8.00E-04
	5%	1.20E-03	3.50E-03	2 00E-04	5.90E-04	1.30E-03
	50%	7.70E-03	2.30E-02	1.30E-03	3.90E-03	9 90E-03
	95%	4 80E-02	1 37E-01	8.20E-03	2.40E-02	6.20E-02
	100%	7.10E-02	2 00E-01	1.23E-02	3 60E-02	9.10E-01
10.00μ	**0%**	8 00E-02	3 00E-01	1.50E-02	5.00E-02	1.60E-01
	5%	1 40E-01	4 40E-01	2.40E-02	9.40E-02	2.60E-01
	50%	4.60E-01	9.20E-01	9 90E-02	3.50E-01	7.50E-01
	95%	9.20E-01	1.00E+00	3 40E-01	8.20E-01	9.97E-01
	100%	9.80E-01	1 00E+00	4.60E-01	9.20E-01	1.00E+00

References

1. Sehmel, G.A., "Particle and Gas Dry Deposition: A Review," *Atmospheric Environment*, 14:983-1011, 1980.

2. Slinn, W.G.N., "Predictions for Particle Deposition to Vegetative Canopies," *Atmospheric Environment*, 16:1785-1794, 1983.

3. Chamberlain, A.C., *Radioactive Aerosols*, Cambridge University Press, New York, 1991.

4. Nicholson, K.W., J.R. Branson, and P. Giess, "Field Measurements of the Below-Cloud Scavenging of Particulate Material," *Atmospheric Environment*, 25A:771-777, 1991.

5. Clift, R., J.R. Grace, and M.E. Weber, *Bubbles, Drops, and Particles*, Academic Press, New York, 1978.

6. Rimberg, D., and Y.-M. Peng, "Aerosol Collection by Falling Droplets," (P.N. Cheremisinoff and R.A. Young, eds.), *Air Pollution Control and Design Handbook, Part 2*, Marcell Dekker, Inc., New York, pp. 729-745, 1977.

A.2 Expert Rationales, Unprocessed Dispersion Data

The Case Structures for the dispersion expert panel are presented in Volume III Appendix F of this document.

Expert I

Introduction

The twelve elicitation problems for dispersion were classified into five groups:

A) Dispersion in near-field under four meteorological conditions specified by wind speeds, σ_θ, and lapse rates (Problems 1 to 4). The uncertainties in plume centerline (y = 0 and z = H) concentrations (χ_c/Q), off-centerline (y >> 0 or z >> H) concentration ratios (χ/χ_c), and horizontal dispersion parameters (σ_y) are to be assessed at several downwind distances.

B) Dispersion in near-field under five different meteorological conditions specified by wind speeds, σ_θ, and lapse rates or Monin-Obukhov lengths (L) (Problems 5 to 9). The uncertainties in ground-level plume centerline (y = 0 and z = 0) concentrations (χ_g/Q) are to be estimated at two different downwind distances in Problems 5 to 8. In Problem 9, the elicited variables include concentration ratios (χ/χ_c) at off-centerline (y > 0 or z < H) locations, and the plume dispersion parameters (σ_y and σ_z). These assessments are for understanding the behavior of the plume close to the ground for short ranges over flat terrain.

C) Dispersion in near-field only under stable meteorological conditions specified by wind speeds and σ_θ (Problem 10). This assessment is for understanding the behavior of the plume near the ground for low wind speeds and varying time-integrated concentrations in case of a 1-hour release.

D) Dispersion very close to the source under stable meteorological conditions and very short sampling time (Problem 11). This assessment is for understanding the "snapshot" plume start.

E) Dispersion into far field at three distances: 80, 200, and 1000 km (Problem 12). This is for assessing the extent of the affected regions far downwind of a release.

The average wind speed was measured at 10 m height for all problems, and σ_θ was measured at the release height. Only flat or rolling terrain typical of rural or suburban sites was considered. Complex topography (valleys or coastal sites) and urban areas (with large roughness and heat island effects) were excluded from the assessments.

Approach and Rationale

Any concentration estimate from a dispersion model represents an ensemble average of numerous repetitions of the same event at a given site. The event is characterized by measured or known parameters that are input to the model, e.g., wind speed, dispersion parameters, source (release) conditions, etc. The dispersion parameters are functions of the atmospheric stability, which is usually specified by a lapse rate, standard deviation of horizontal wind direction fluctuation (σ_θ), or L. In addition to the known parameters, there are unmeasured or unknown variations in the conditions of this event, such as unresolved details of the atmospheric flow or the subgrid-scale atmospheric processes. Therefore, concentrations observed in individual repetitions of the event are likely to deviate from the ensemble-mean concentration predicted by even a "perfect" model.[1]

Uncertainties in estimated concentrations arise from (a) errors in model input data, (b) model inadequacy to account for all physical factors, and (c) uncertainty due to the stochastic (natural) variability of the atmosphere. In this assessment we modified PAL-2[2], a steady-state Gaussian plume dispersion model of the US EPA, to estimate the median concentrations and the concentration ratios and their uncertainty distributions (in terms of the .05 and .95 quantiles, and the 0. and 1.0 quantiles). The model we used was considered appropriate and adequate to provide this information for the assigned problems, and was consistent with the given input data; therefore, we did not consider uncertainty due to model physics errors (b) here.

The uncertainty introduced by input data errors is generally a major part of the total uncertainty in the model estimate.[1] These input data errors include uncertainties in wind speed (U) measurements and the specified σ_y and σ_z values, among others. Typical wind speed uncertainty quoted in the literature ranges from 0.1 m/s (for research-grade data) up to 1 m/s (for routine air quality data). These errors arise due to poor calibration and maintenance of anemometers, and use of wind data unrepresentative of the level of plume transport, especially at night, because of mesoscale or terrain variability and wind shear. We assumed the

uncertainty in U to be 0.5 m/s for all stability categories; this value has been suggested by my colleagues who have considerable experience in field measurements and familiarity with the NRC instrumentation. Values for σ_y and σ_z are usually derived from tracer experiments, and their uncertainties are difficult to estimate. Pasquill[3] assumed 20% uncertainties in these parameters for sensitivity studies related to long-term average concentrations. Jones[4] suggested a range of values midway between adjacent stability categories. Freeman et al.[5] used values ranging from 10% to 40%, and suggested that the base value of 10% is near the minimum that should be expected in actual practice. In this study, we took the uncertainties in the input values of σ_y and σ_z to be 30%, and assumed U, σ_y, and σ_z to be uncorrelated and normally distributed, with means given by the input values and standard deviations $(S_u, S_{\sigma_y}, S_{\sigma_z})$ by the magnitudes of their respective uncertainties.

Uncertainty analysis involves propagation through the model of the joint distribution of the uncertain input parameters to produce a distribution of model predictions. This process transforms the joint parameter PDF into the subjective PDF of the model prediction, which would permit quantitative uncertainty statements such as the degree of belief, in percentage, for the actual value to be below or above given limits.[6] There are two main classes of uncertainty propagation methods: analytical and numerical. The latter include simple random (Monte Carlo) sampling[5,7,8] or Latin hypercube sampling[9,10] methods. The choice of a specific propagation method will depend on the complexity of the model, the amount of information desired from the uncertainty analysis, and the effort, time, and costs required to obtain this information. Based on these considerations, we used an analytical method, suggested by Freeman et al.,[5] which uses an expansion of the concentration χ in a Taylor series and retains only terms of second order or less. This can be written as follows:

$$\chi = f(x_1, x_2, \ldots, x_n) \tag{1}$$

$$S_\chi^2 = \sum_{i=1}^{n} \left(\frac{\partial f}{\partial x_i}\right)^2 S_{x_i}^2 + \frac{1}{2}\sum_{i=1}^{n}\left(\frac{\partial^2 f}{\partial x_i^2}\right)^2 S_{x_i}^4 + \sum_{i=1}^{n}\sum_{j=1}^{n}\left(\frac{\partial^2 f}{\partial x_i \partial x_j}\right)^2 S_{x_i}^2 S_{x_j}^2 \tag{2}$$

This equation expresses S_χ, the uncertainty in the predicted value of χ, as a function of the uncertainties in the input variables. For a steady Gaussian model, Freeman et al.[5] showed that S_χ calculated from this approach will be generally within 25% of the true uncertainty (approximated by the standard deviation of model predicted χ values, which were calculated from Monte Carlo simulation of a randomly perturbed input data set) for all stability cases and most distances of interest here. The cross-derivative (last) term in Equation (2) is zero in this study. The contributions to the total variance from third and higher-order terms in the Taylor's series expansion are generally small, and are neglected.

For the Gaussian plume dispersion model used in this study, we can write

$$\chi/Q = (1/U)\, p(y,\sigma_y)\, q(z,\sigma_z; H) \tag{3}$$

where p and q are the horizontal and vertical probability densities given by:

$$p(y,\sigma_y) = \frac{1}{\sqrt{2\pi}\,\sigma_y} \exp\left\{\frac{-y^2}{2\sigma_y^2}\right\} \tag{4}$$

$$q(z,\sigma_z;H) = \frac{1}{\sqrt{2\pi}\,\sigma_z} \cdot \left[\exp\left\{-\frac{(z-H)^2}{2\sigma_z^2}\right\} + \exp\left\{-\frac{(z+H)^2}{2\sigma_z^2}\right\}\right] \tag{5}$$

Using a logarithmic transformation, we can write Equation (3) as

$$W = \ln(\chi/Q) = \ln(1/U) + \ln(p) + \ln(q) \tag{6}$$

From Equations (2) and (6), we can express the variance of W as

$$S_w^2 = \left[\frac{\partial}{\partial U}\left\{\ln\left(\frac{1}{U}\right)\right\}\right]^2 S_u^2 + \left[\frac{\partial}{\partial \sigma_y}\{\ln p\}\right]^2 S_{\sigma_y}^2 + \left[\frac{\partial}{\partial \sigma_z}\{\ln q\}\right]^2 S_{\sigma_z}^2 + \frac{1}{2}\left\{\left[\frac{\partial^2}{\partial U^2}\left\{\ln\left(\frac{1}{U}\right)\right\}\right]^2 S_u^4 + \left[\frac{\partial^2}{\partial \sigma_y^2}\{\ln p\}\right]^2 S_{\sigma_y}^4 + \left[\frac{\partial^2}{\partial \sigma_z^2}\{\ln q\}\right]^2 S_{\sigma_z}^4\right\} \tag{7}$$

where the partial derivatives can be analytically derived from Equations (4) and (5). The resulting expression was used in the model to compute the standard deviation S_w in each elicitation case.

The .05 and .95 quantiles of χ/Q were obtained[6,11] as:

$$\exp(\bar{W} - 1.645\,S_w), \quad \exp(\bar{W} + 1.645\,S_w) \qquad (8)$$

Here $\bar{W} = \ln(\overline{\chi/Q})$ and $\overline{\chi/Q}$ was the model-calculated ensemble-average value of the relative concentration (taken to be the median or .50 quantile value) in each elicitation case. The 0. and 1.0 quantiles of χ/Q were obtained as

$$\exp(\bar{W} - 3.5\,S_w), \quad \exp(\bar{W} + 3.5\,S_w) \qquad (9)$$

According to Equations (8) and (9), the subjective PDF of the model-estimated χ/Q has a lognormal distribution, which is consistent with the logarithmic transformation used in Equation (6).

Observed hourly concentrations are turbulent (random) variables. For a given set of mean wind speed and direction, stability, and emission rate, observed concentration can be expected to vary from hour to hour. This natural variability in observed hourly pollutant concentrations, studied by Hanna[12], is typically a factor of two. This means that a perfect Gaussian diffusion model under these conditions cannot predict hourly concentrations any better than a factor of two. To approximately account for this stochastic variability, we assumed that the calculated $\bar{W}$ can have any value between $\bar{W}_1 = 0.5\bar{W}$ and $\bar{W}_2 = 1.5\bar{W}$. For estimating the .05 and 0. quantiles, we used $\bar{W}_1$, in place of $\bar{W}$ in Equations (8) and (9); for the .95 and 1.0 quantiles, we used $\bar{W}_2$. For estimating the 0. and .05 quantiles of χ/Q, we limited the value of S_w such that $S_w \le \bar{W}_1/3.5$; similarly, for estimating the .95 and 1.0 quantiles, we limited S_w so that $S_w \le \bar{W}_2/3.5$. For values of $(y/\sigma_y) \le 1$ and $(z/\sigma_z) \le 1$ (i.e., within the plume core), the quantiles are reasonably close (as to be expected); for example, the ratio of .95 and .05 quantiles of χ_c/Q varies from a factor of 16 at $x = 0.5$ km to a factor of 11 at $x =$ 30 km in Problem 1. However, for values of $(y/\sigma_y) \gg 1$ or $(z/\sigma_z) \gg 1$, this ratio gets very large (several orders of magnitude), thus reflecting the inherent limitations in deriving the subjective uncertainty limits in the tails of the probability distributions for very small (near-zero) concentrations.

An approach similar to that described above was used to estimate the uncertainty distributions of the concentration ratio χ/χ_c, which was elicited in Problems 1 to 4, and 9. In this case, an analytical expression for χ/Q was derived from Equations (3) to (5) by setting y = 0 and z = H, and this expression was used to divide Equation (3). Uncertainty analysis, as described above, was performed on the resulting analytical equation for χ/χ_c. Again, we limited the value of S_w so that $S_w \le \bar{W}/3.5$, which is equivalent to limiting the 1.0 quantile value of χ/χ_c to unity. For the horizontal dispersion parameter (which was among the elicitation variables in many of the assigned problems), we arbitrarily limited the 0. and 1.0 quantiles to $0.25\sigma_y$ and $1.75\sigma_y$, respectively, in order to roughly approximate the σ_y values of adjacent stability classes.

Input Data, Assumptions, and Discussion

The stability classification for the elicitation problems is based on the lapse rate and/or σ_θ or $1/L$ values given. Generally these agreed well in all the problems (except Problem 5). Pasquill[3] recommended the direct use of wind direction fluctuation data (if available) in estimating σ_y, and using the Pasquill-Gifford (P-G) curves only in the absence of such data. Tangirala et al.[13] showed that Gaussian puff or plume models using "on-site" dispersion schemes based on turbulence data perform better than models that use the "handbook" P-G dispersion scheme. In this study, σ_θ measured over 10 min at release height were provided for the first 10 problems. These data are expected to include the effects of the local roughness and terrain,[14] so no additional correction for roughness effects was considered necessary. σ_y was computed from the widely used equation:

$$\sigma_y = \sigma_\theta x/[1 + 0.9(t/1000)^{1/2}] \qquad (10)$$

where $t = x/U$ is the travel time in seconds. σ_z was taken from the Pasquill-Gifford (P-G) curves for the given stability class. The original P-G curves were based on 10 min average tracer concentration data from prairie grass experiments (surface roughness = 3 cm). USEPA considers these curves to be appropriate for rural areas with flat or gently rolling terrain. The assumed 30% uncertainty in the dispersion parameters was large enough to account for the effects of possible variations in surface roughness.

The 10 min σ_y values were adjusted to calculate the 1-hour average values using the relation:

$$r_y = (\sigma_y)_A/(\sigma_y)_B = (T_A/T_B)^s \qquad (11)$$

where T_A = 60 min is the sampling time of interest, T_B = 10 min, and $(\sigma_y)_A$ and $(\sigma_y)_B$ are the corresponding σ_y values. Gifford[15] recommends a value of $s = 0.2$ for 3 min $< T_A <$ 1hr, which gives a value of $r_y = 1.43$, i.e., the 1-hour σ_y is expected to be 1.43 times larger than the σ_y sampled for 10 min. This sampling time correction was applied only to σ_y and not to σ_z. For sampling times

exceeding a few minutes (typically 3 to 5 min) for near surface sources, σ_z values are expected to be steady and time independent of sampling time.[3] Following the USNRC practice for unstable and neutral cases, for $\sigma_z > 1.6h$ where h is the mixing depth, the concentration was assumed to be well-mixed and uniform in the vertical. For $\sigma_z > 1.6h$, the inversion height at $z = h$ could affect the estimated concentrations. This plume trapping was taken into account through multiple eddy reflections.

In the first nine problems, the release duration and sampling time were 1 hour each; in Problem 11, the release duration was 1 hr and the sampling time was 1 min. In each of these problems, the sampling time was assumed to start at $t = t_0$ (where t_0 is the time at which the tracer material was first located at the sampler), and the average concentration over the sampling time and its uncertainty (in terms of various quantiles) were elicited. In Problem 10, the release duration was one hour starting from time $t = 0$ onwards; there were 3 sampling times (60, 120, and 240 min), each starting from $t = 0$, for which the time-integrated ground concentrations at 3 near-field samplers and their uncertainties were elicited.

The input data and assumptions made for each problem are given and briefly discussed below:

Problem-1

P-G stability class is A. Assumed mixing depth is 1600 m.

Problem-2

P-G stability class is C. Assumed mixing depth is 1200 m.

Problem-3

P-G stability class is D. Assumed mixing depth is 1000 m.

Problem-4

P-G stability class is F.

Problem-5

P-G stability class is taken to be D, as indicated by the given $1/L$ value, though the given σ_θ value indicates P-G class E. Assumed mixing depth is 1000 m. Power law was applied to estimate U at 22 m height.

Problem-6

P-G stability class is D. Assumed mixing depth is 1000 m. Power law was applied to estimate U at 22 m.

Problem-7

P-G stability class is C. Assumed mixing depth is 1200 m. Power law was applied to estimate U at 22 m.

Problem-8

P-G stability class is D. Assumed mixing depth is 1000 m. Power law was applied to estimate U at 22 m.

Problem-9

P-G stability class is F. Power law was applied to estimate U at 22 m.

Problem-10

Assumed P-G stability class is E. Power law was applied to estimate U = 3.22 m/s at 45 m. This problem was different from the previous 9 problems. Here, the release duration was one hour starting from time t=0 onwards; there were 3 sampling times (T_s = 3600, 7200, and 14400 sec), each starting from t=0, for which the time-integrated concentrations and their uncertainties were elicited. The plume front arrives at the 3 samplers at $t_1=x_1/U$, $t_2=x_2/U$, and $t_3=x_3/U$, respectively, where x_1 = 360 m, x_2 = 970 m, and x_3 = 1970 m are the downwind distances of the 3 samplers from the source. This implies that, for the T_s = 1-hr case, the plume was sampled only during the time periods $T_A=1-(t_1/3600)$, $1-(t_2/3600)$ and $1-(t_3/3600)$ hr, respectively, at the 3 samplers. The ground-level concentrations χ_g/Q for sampling times $0<T_A<T_B=1$ hr were computed from the relation:

$$R = \frac{(\chi/Q)_A}{(\chi/Q)_B} = (T_A/T_B)^{-s} \qquad (12)$$

where s was taken to be 0.2.[15] The RHS of Equation (12) also gives the ratio $1/r_y = (\sigma_y)_B/(\sigma_y)_A$, see Equation (11). Since T_A was larger than a few minutes, the sampling time correction was applied only to σ_y and not to σ_z, as discussed earlier. The average concentrations $(\chi/Q)_A$ calculated from Equation (12) were multiplied by T_A (in hrs) to obtain the time-integrated concentrations in units of (s/m^3) hr.

For sampling times of T_s = 7200 and 14400 sec, the plume of material (formed due to the release over a time period T_r = 3600 sec) completely passes over the 3 samplers. Following the plume passage, these samplers measure zero concentrations during the remainder of the sampling period, because $t_i \ll T_r \ll T_s$ for i = 1,2,3. Therefore, the effective

measurement period (T_A) was the same as the release duration, and the hourly average concentrations calculated by the model at the 3 samplers were multiplied by T_A = 1 hr to obtain the time-integrated concentrations. The latter were the same for the two larger sampling times in this problem.

Problem-11

Assumed P-G stability class is F, and assumed $\sigma_\theta = 2.5°$. These conditions are similar to those given for Problem 9. The release and travel times are larger than the sampling time of 1 min, so continuous plume diffusion equation is applicable.[1] The concentration generally increases as the sampling time is decreased. To estimate the concentration, Equation (11) is applied with T_A = 1 min and T_B = 60 min; the resulting value of r_y is 0.441. A similar equation, applied to adjust σ_z to the 1 min sampling time, gives r_z = 0.441. Following Equation (12), $R = 1/(r_y r_z) = 5.14$, i.e., the 1-min concentration is about 5 times larger than the 1-hr sampled concentration. For shorter sampling times, intermittency (caused by plume meander under stable conditions) becomes important; the concentration at a fixed sampler essentially varies between "in-plume" peaks and a zero value in the environment. We assumed that the sampler in this problem was within the plume.

Problem-12

We do not know much about the dispersion of plume at long distances from the source. This is a topic of current research. From Taylor's statistical diffusion theory, it was generally assumed that $\sigma_y^2 \propto t$ at large travel time t. However, Gifford[16] compiled large-scale atmospheric diffusion data that showed an accelerated diffusion regime in which $\sigma_y^2 \propto t^3$. Carras and Williams[17] summarized measurements in Australia of the relative dispersion, σ_y, of long plumes (up to travel times of 67 hrs) from a single source. These data provide evidence for the existence of an accelerated diffusion regime in which $\sigma_y^2 \propto t^3$ for $t > 3$ hrs, as predicted by Gifford.

Assuming a constant wind speed of 1.5 m/s, we estimated the plume age (travel time) and obtained the σ_y values from an expression fitted by Carras and Williams[17] to their diffusion data. At x = 80 km (or t = 14.8 hr), we estimated σ_y = 15.9 km. At x = 200 km (or t = 62.9 hr), we obtained σ_y = 62.9 km. From Draxler's[18] results of the ANATEX experiment in the U.S., we estimated σ_y = 410 km at x = 100 km (or t = 185.2 hr). This value of σ_y is between the $\sigma_y^2 \propto t^{3/2}$ and $\sigma_y^2 \propto t^{1/2}$ regimes. The errors in the estimates at the three distances were arbitrarily assumed to be 30, 35, and 40 percent, respectively. Assuming a Gaussian distribution in the horizontal, the width B of the plume consisting of 90% of the material is given by $3.29\sigma_y$.[11] The 0. and 1.0 quantiles were limited to $0.25\sigma_y$ and $1.75\sigma_y$, as before.

Dispersion Tables

N/A = not provided by expert

A-1: -2.0 K/100m Temp Lapse Rate Urban & Rural Surface Roughness					
Downwind distance	**Quantile**	**chiC/Q**	**chi(y)/chiC**	**chi(z)/chiC**	**sig-y**
0.5km	**0%**	6.10E-07	5.36E-01	7.29E-01	5.40E+01
	5%	1.54E-06	6.32E-01	7.92E-01	1.10E+02
	50%	7.00E-06	7.32E-01	8.54E-01	2.15E+02
	95%	2.39E-05	8.48E-01	9.20E-01	3.20E+02
	100%	6.02E-05	1.00E+00	1.00E+00	3.76E+02
1.0km	**0%**	7.92E-08	5.39E-01	8.84E-01	9.50E+01
	5%	2.01E-07	6.35E-01	9.13E-01	1.94E+02
	50%	9.19E-07	7.34E-01	9.40E-01	3.81E+02
	95%	3.15E-06	8.49E-01	9.68E-01	5.68E+02
	100%	8.00E-06	1.00E+00	1.00E+00	6 67E+02
3.0km	**0%**	1.74E-08	4.02E-01	1.00E+00	2.23E+02
	5%	3.63E-08	5.12E-01	1.00E+00	4.54E+02
	50%	1.40E-07	6.34E-01	1.00E+00	8.90E+02
	95%	4.04E-07	7.86E-01	1.00E+00	1.33E+03
	100%	8.46E-07	1.00E+00	1.00E+00	1.56E+03
10.0km	**0%**	7.47E-09	2.33E-01	N/A	5.18E+02
	5%	1.56E-08	3.43E-01	N/A	1.06E+03
	50%	6.02E-08	4.83E-01	N/A	2.07E+03
	95%	1.74E-07	6.80E-01	N/A	3.09E+03
	100%	3.63E-07	1.00E+00	N/A	3.62E+03
30.0km	**0%**	3.71E-09	7.60E-02	N/A	1.04E+03
	5%	7.55E-09	1.51E-01	N/A	2.13E+03
	50%	2.99E-08	2.76E-01	N/A	4.17E+03
	95%	8.62E-08	5.05E-01	N/A	6.22E+03
	100%	1.80E-07	1.00E+00	N/A	7.30E+03

A-2: -1.6 K/100m Temp Lapse Rate Urban & Rural Surface Roughness					
Downwind distance	Quantile	chiC/Q	chi(y)/chiC	chi(z)/chiC	sig-y
0.5km	0%	1.84E-06	6.09E-01	4.90E-02	3.60E+01
	5%	3.98E-06	6.95E-01	1.08E-01	7.20E+01
	50%	1.58E-05	7.81E-01	2.20E-01	1.42E+02
	95%	4.69E-05	8.77E-01	4.48E-01	2.12E+02
	100%	1.01E-04	1.00E+00	1.00E+00	2.49E+02
1.0km	0%	5.26E-07	5.49E-01	4.40E-02	6.50E+01
	5%	1.19E-06	6.44E-01	1.01E-01	1.32E+02
	50%	4.91E-06	7.41E-01	2.10E-01	2.58E+02
	95%	1.52E-05	8.53E-01	4.37E-01	3.84E+02
	100%	3.43E-05	1.00E+00	1.00E+00	4.52E+02
3.0km	0%	7.78E-08	5.34E-01	9.00E-02	1.58E+02
	5%	1.79E-07	6.31E-01	1.70E-01	3.22E+02
	50%	7.52E-07	7.31E-01	2.99E-01	6.32E+02
	95%	2.36E-06	8.47E-01	5.28E-01	9 42E+02
	100%	5 45E-06	1.00E+00	1.00E+00	1.11E+03
10.0km	0%	1.06E-08	3.90E-01	N/A	3.87E+02
	5%	2 44E-08	5.01E-01	N/A	7.89E+02
	50%	1.02E-07	6.25E-01	N/A	1.55E+03
	95%	3.23E-07	7.79E-01	N/A	2.30E+03
	100%	,7.46E-07	1.00E+00	N/A	2.71E+03
30.0km	0%	2.65E-09	2.19E-01	N/A	8.11E+02
	5%	6.12E-09	3.27E-01	N/A	1.65E+03
	50%	2.57E-08	4.68E-01	N/A	3.24E+03
	95%	8.10E-08	6.68E-01	N/A	4.83E+03
	100%	1.87E-07	1.00E+00	N/A	5.68E+03

A-3: -1.0K/100m Temp Lapse Rate Urban & Rural Surface Roughness					
Downwind distance	Quantile	chiC/Q	chi(y)/chiC	chi(z)/chiC	sig-y
0.5km	0%	3.20E-06	2.92E-01	2.51E-04	2.50E+01
	5%	6.25E-06	4.04E-01	2.26E-03	5.10E+01
	50%	2.27E-05	5.40E-01	1.58E-02	9.90E+01
	95%	6.17E-05	7.22E-01	1.11E-01	1.48E+02
	100%	1.21E-04	1.00E+00	1.00E+00	1.73E+02
1.0km	0%	1.00E-06	5.09E-01	2.28E-05	4.60E+01
	5%	2.12E-06	6.09E-01	3.88E-04	9.30E+01
	50%	8.25E-06	7.14E-01	4.78E-03	1.83E+02
	95%	2.41E-05	8.36E-01	5.89E-02	2.73E+02
	100%	5.10E-05	1.00E+00	1.00E+00	3.20E+02
3.0km	0%	1.92E-07	5.57E-01	1.74E-07	1.15E+02
	5%	4.27E-07	6.51E-01	1.08E-05	2.34E+02
	50%	1.74E-06	7.47E-01	4.17E-04	4.58E+02
	95%	5.30E-06	8.57E-01	1.62E-02	6.82E+02
	100%	1.18E-05	1.00E+00	1.00E+00	8.02E+02
10.0km	0%	3.64E-08	4.73E-01	N/A	2.89E+02
	5%	8.22E-08	5.77E-01	N/A	5.89E+02
	50%	3.39E-07	6.88E-01	N/A	1.16E+03
	95%	1.05E-06	8.20E-01	N/A	1.72E+03
	100%	2.36E-06	1.00E+00	N/A	2.02E+03
30.0km	0%	9.06E-09	3.64E-01	N/A	6.22E+02
	5%	2.05E-08	4.76E-01	N/A	1.27E+03
	50%	8.48E-08	6.03E-01	N/A	2.49E+03
	95%	2.63E-07	7.65E-01	N/A	3.71E+03
	100%	5.95E-07	1.00E+00	N/A	4.35E+03

A-4: 2.5K/100m Temp Lapse Rate Urban & Rural Surface Roughness					
Downwind distance	Quantile	chiC/Q	chi(y)/chiC	chi(z)/chiC	sig-y
0.5km	0%	3.53E-05	1.78E-01	2.17E-01	6.00E+00
	5%	7.51E-05	2.81E-01	3.26E-01	1.20E+01
	50%	2.93E-04	4.22E-01	4.66E-01	2.30E+01
	95%	8.57E-04	6.33E-01	6.67E-01	3.40E+01
	100%	1.82E-03	1.00E+00	1.00E+00	4.00E+01
1.0km	0%	1.69E-05	1.19E-01	6.00E-03	1.00E+01
	5%	3.39E-05	2.09E-01	2.20E-02	2.10E+01
	50%	1.26E-04	3.44E-01	7.40E-02	4.10E+01
	95%	3.50E-04	5.68E-01	2.52E-01	6.10E+01
	100%	7.03E-04	1.00E+00	1.00E+00	7.20E+01
3.0km	0%	4.05E-06	9.90E-02	3.82E-07	2.50E+01
	5%	8.81E-06	1.82E-01	1.92E-05	5.10E+01
	50%	3.51E-05	3.14E-01	6.20E-04	9.90E+01
	95%	1.05E-04	5.41E-01	2.00E-02	1.48E+02
	100%	2.28E-04	1.00E+00	1.00E+00	1.73E+02
10.0km	0%	9.69E-07	1.10E-02	7.86E-14	5.90E+01
	5%	2.22E-06	3.70E-02	2.33E-10	1.20E+02
	50%	9.25E-06	1.06E-01	2.80E-07	2.36E+02
	95%	2.89E-05	3.05E-01	3.37E-04	3.52E+02
	100%	6.63E-05	1.00E+00	1.00E+00	4.13E+02
30.0km	0%	3.14E-07	8.05E-04	3.96E-24	1.22E+02
	5%	7.32E-07	5.32E-03	6.30E-18	2.48E+02
	50%	3.10E-06	2.80E-02	2.00E-12	4.87E+02
	95%	9.85E-06	1.51E-01	6.29E-07	7.26E+02
	100%	2.30E-05	1.00E+00	1.00E+00	8.52E+02

B-1: Unknown Lapse Rate 6.0 m/s Aver. Wind Speed		
Downwind distance	**Quantile**	**chiC/Q(ground level)**
220. m	**0%**	1.32E-08
	5%	3.48E-07
	50%	1.26E-05
	95%	3.45E-04
	100%	9.07E-03
315. m	**0%**	5.94E-07
	5%	2.96E-06
	50%	2.47E-05
	95%	1.54E-04
	100%	7.68E-04

B-2: Unknown Lapse Rate 5.0 m/s Aver. Wind Speed		
Downwind distance	**Quantile**	**chiC/Q(ground level)**
220. m	**0%**	8.01E-09
	5%	2.11E-07
	50%	7.69E-06
	95%	2.10E-04
	100%	5.53E-03
315. m	**0%**	3.60E-07
	5%	1.80E-06
	50%	1.50E-05
	95%	9.40E-05
	100%	4.70E-04

B-3: Unknown Lapse Rate 8.0 m/s Aver. Wind Speed		
Downwind distance	Quantile	chiC/Q(ground level)
300. m	0%	1.51E-06
	5%	2.92E-06
	50%	1.05E-05
	95%	2.81E-05
	100%	5.43E-05
600. m	0%	6.11E-07
	5%	1.22E-06
	50%	4.48E-06
	95%	1.24E-05
	100%	2.46E-05

B-4: -1.0 K/100m Temp Lapse Rate Flat Surface Roughness		
Downwind distance	Quantile	chiC/Q(ground level)
300. m	0%	4.40E-07
	5%	2.60E-06
	50%	2.52E-05
	95%	1.83E-04
	100%	1.08E-03
600. m	0%	3.27E-06
	5%	6.50E-06
	50%	2.39E-05
	95%	6.59E-05
	100%	1.31E-04

B-5: 3.0 K/100m Temp Lapse Rate Flat Surface Roughness					
Downwind distance	Quantile	chi(y)/chiC	chi(z)/chiC	sig-y	sig-z
600. m	0%	4.40E-02	3.47E-01	7.00E+00	3.00E+00
	5%	1.01E-01	4.59E-01	1.40E+01	5.00E+00
	50%	2.10E-01	5.89E-01	2.80E+01	1.00E+01
	95%	4.37E-01	7.55E-01	4.20E+01	1.50E+01
	100%	1.00E+00	1.00E+00	4.90E+01	1.80E+01

C: Stable Conditions Urban & Rural Surface Roughness				
Downwind distance	Quantile	60 min	120 min	240 min
360. m	0%	2.09E-17	2.16E-17	2.16E-17
	5%	5.48E-13	5.66E-13	5.66E-13
	50%	9.05E-09	9.34E-09	9.34E-09
	95%	6.69E-05	6.90E-05	6.90E-05
	100%	9.70E-01	1.00E+00	1.00E+00
970. m	0%	1.91E-08	2.08E-08	2.08E-08
	5%	2.44E-07	2.66E-07	2.66E-07
	50%	4.66E-06	5.08E-06	5.08E-06
	95%	6.68E-05	7.29E-05	7.29E-05
	100%	8.52E-04	9.30E-04	9.30E-04
1970. m	0%	4.89E-07	5.89E-07	5.89E-07
	5%	1.28E-06	1.54E-06	1.54E-06
	50%	5.91E-06	7.12E-06	7.12E-06
	95%	2.07E-05	2.49E-05	2.49E-05
	100%	5.38E-05	6.48E-05	6.48E-05

D: Stable Conditions Flat Surface Roughness				
Downwind distance	Quantile	chiC/Q	sig-y	sig-z
60. m	0%	4.82E-03	4.00E-01	1.70E-01
	5%	1.13E-02	7.00E-01	3.40E-01
	50%	4.82E-02	1.50E+00	7.00E-01
	95%	1.54E-01	2.20E+00	1.00E+00
	100%	3.61E-01	2.50E+00	1.20E+00

E: Length of Arc Crossed By 90% of the Material		
Downwind distance	Quantile	90% arc
80.km	0%	1.30E+04
	5%	2.70E+04
	50%	5.20E+04
	95%	7.80E+04
	100%	9.20E+04
200.km	0%	5.20E+04
	5%	8.70E+04
	50%	2.07E+05
	95%	3.27E+05
	100%	3.62E+05
1000.km	0%	3.37E+05
	5%	4.59E+05
	50%	1.35E+06
	95%	2.24E+06
	100%	2.36E+06

References

1. Rao, K.S., and R.P. Hosker, "Uncertainty in the Assessment of Atmospheric Concentrations of Toxic Contaminants from an Accidental Release" *Radiation Protection Dosimetry*, at press, 1993.

2. Petersen, W.B., and E.D. Rumsey, "User's Guide for PAL 2.0: A Gaussian-Plume Algorithm for Point, Area, and Line Sources," EPA/600/8-87/009, U.S. EPA, Research Triangle Park, NC, Available as PB87-168 787/AS, NTIS, Springfield, VA, March 1987.

3. Pasquill, F., "Atmospheric Dispersion Parameters in Gaussian Plume Modeling, Part II. Possible Requirements for Change in the Turner Workbook Values," EPA/600/4-76-030b, U.S. EPA, Research Triangle Park, NC, June 1976.

4. Jones, J.A., "The Uncertainty in Dispersion Estimates Obtained from the Working Group Models," NPRB-R-199, National Radiological Protection Board, Chilton, UK, August 1986.

5. Freeman, D.L., et al., "A Method for Propagating Measurement Uncertainties through Dispersion Models," *Journal of the Air Pollution Control Association*, 36:246-253, 1986.

6. IAEA, "Evaluating the Reliability of Predictions Made Using Environmental Transfer Models," Safety Series No. 100, International Atomic Energy Agency, Vienna, 1989.

7. Irwin, J.S., et al., "Relating Error Bounds for Maximum Concentration Estimates to Diffusion Meteorology Uncertainty," *Atmospheric Environment*, 21:1927-1937, 1987.

8. Kocher, D.C., et al., "Sensitivity and Uncertainty Studies of the CRAC2 Computer Code," *Risk Analysis*, 7:497-507, 1987.

9. Iman, R.L., and J.C. Helton, "An Investigation of Uncertainty and Sensitivity Analysis Techniques for Computer Models," *Risk Analysis*, 8:71-90, 1988.

10. Fischer, F., J. Ehrhardt, and J. Raicevic, "Analysis of Uncertainties Caused by the Atmospheric Dispersion Model in Accident Consequence Assessments with UFOMOD," KFK-4262, Kernforschungszentrum Karlsruhe GmbH, Karlsruhe, Germany, June 1988.

11. Gilbert, R.O., *Statistical Methods for Environmental Pollution Monitoring*, Van Nostrand Co., New York, 1987.

12. Hanna, S.R., "Natural Variability of Observed Hourly SO_2 and CO Concentrations in St. Louis," *Atmospheric Environment*, 16:1435-1440, 1982.

13. Tangirala, R.S., K.S. Rao, and R.P. Hosker, Jr., "A Puff Model Simulation of Tracer Concentrations in the Nocturnal Drainage Flow in a Deep Valley," *Atmospheric Environment*, 26A:299-309, 1992.

14. Panofsky, H.A., C.A. Egolf, and R. Lipschutz, "On Characteristics of Wind Direction Fluctuations in the Surface Layer," *Boundary-Layer Meteorology*, 15:439-446, 1978.

15. Gifford, F.A., "Atmospheric Dispersion Models for Environmental Pollution Application," (D.A. Haugen, ed.), *Lectures on Air Pollution and Environmental Impact Analyses, Proceedings American Meteorological Society Workshop on Meteorology and Environmental Assessment, 29 September–3 October 1975*, American Meteorological Society, Boston, MA, pp. 35-38, 1975.

16. Gifford, F.A., "The Random Force Theory: Application to Meso- and Large-Scale Atmospheric Diffusion," *Boundary-Layer Meteorology*, 30:159-175, 1984.

17. Carras, J.N., and D.J. Williams, "Measurements of Relative σ_y up to 1800 km from a Single Source," *Atmospheric Environment*, 6:1061-1069, 1988.

18. Draxler, R.R., "Overview and Preliminary Results from the Across North America Tracer Experiment (ANATEX)," *Preprints, 6th Joint Conference on Applications of Air Pollution Meteorology*, 30 January–3 February 1989, American Meteorological Society, Boston, MA, p. 82, 1989.

Expert J

Introduction

The meteorological data for the cases are not comprehensive enough to apply complex models. It was assumed that these data are typical data for a certain stability condition in the atmospheric boundary layer. Therefore the Pasquill stability classes have been used to characterize the meteorological condition. Only in one case our Lagrangian particle model TRAVELING was applied additionally to answer the questions.

Determination of the Stability Classes

Wind Speed and Temperature Lapse Rate are Given

From the measurements at our 200 m high meteorological tower, a scheme was developed to determine the stability classes, if wind speed and temperature lapse rate are available (see Table J-1). The lapse rate is calculated from the temperatures between 100m and 30m. The given lapse rate belongs to a height difference of 100m and 2m. Therefore it was necessary to transform the data before the scheme could be used. From the temperature measurements at our tower the following relations have been derived:

$$\gamma_t = \alpha(\gamma_g + 1) - 1$$

with

γ_g = given temperature lapse rate
γ_t = transformed temperature lapse rate
$\alpha = 0.56$ for the unstable conditions, and
$\alpha = 1.59$ for the stable conditions.

Table J-1. Stability classes

$\bar{u}_{40}$ (m/s)	TG (K/100 m)
0.0 - 0.9	$A \le -1.13 < B \le -1.03 < C \le -0.91 < D \le -0.37 < E \le +0.78 < F$
1.0 - 1.9	$A \le -1.18 < B \le -1.05 < C \le -0.91 < D \le -0.22 < E \le +1.12 < F$
2.0 - 2.9	$A \le -1.39 < B \le -1.18 < C \le -0.97 < D \le -0.16 < E \le +1.25 < F$
3.0 - 3.9	$A \le -1.61 < B \le -1.33 < C \le -1.00 < D \le -0.10 < E \le +1.32 < F$
4.0 - 4.9	$A \le -1.82 < B \le -1.48 < C \le -1.04 < D \le -0.04 < E \le +1.39 < F$
5.0 - 5.9	$B \le -1.62 < C \le -1.08 < D \le +0.02 < E \le +1.46 < F$
6.0 - 6.9	$B \le -1.77 < C \le -1.16 < D \le +0.08$ E
7.0 - 7.9	$< C \le -1.25 < D$
8.0 - 9.9	$C \le -1.40 < D$
$\ge$ 10.0	D

The wind speed in our scheme belongs to an effective height of 30 m. Therefore the given speeds are related to the wind speed class having this speed as lower value. If standard deviations of the horizontal wind direction σ_θ are given, they are used only as an additional check. For this check, Table J-2 derived from Gifford was taken. The scheme, based on temperature lapse rate and wind speed, is less dependent on surface roughness than the σ_θ scheme. The variation of the surface roughness is considered additionally, corresponding to the given information.

Table J-2. Standard deviations

stability class	σ_θ (degrees)
A	25
B	20
C	15
D	10
E	5
F	2.5

Monin-Obukhov Length is Given

In this case, the Golder diagram was used to define the stability class. The roughness length for flat terrain was assumed to be several cm.

Only σ_θ Is Given

In this case, the relations in the presented table were used to define the stability class. The derived stability classes for all cases are summarized in Table J-3.

Table J-3. Derived stability classes

elicit. case	stability class
A1	A
A2	C
A3	D
A4	F
B1	D
B2	D/C
B3	C
B4	D/C
B5	F
C1	E
D1	D,EorF
E1	-

Determination of the Frequency Distributions

Based on the diffusion experiments carried out at the Karlsruhe Research Center, normalized frequency distributions of the horizontal and vertical standard deviations of the wind direction and the centerline concentrations were calculated. This was done only for the 27 experiments related to class D, because for the other classes not enough experimental data are available. The frequency distributions are normalized to their 50% quantile. The distributions are valid for a distance between 400 m and 2700 m. In this range, data from at least 13 experiments are available. The statistics for a range between 300 m and 5000 m differs not very much from that for the shorter range. But in this range we have only data from 9 experiments in the additional part of the distance range.

In the cases where the surface roughness is characterized as urban and rural, the σ parameters evaluated by Briggs are combined with the corresponding parameters derived from the Karlsruhe diffusion experiments. In the cases with unstable conditions (classes A and B), the Briggs σ_y parameters are multiplied by a factor of 1.43, taking into account an increase of the sampling time from 10 min to 1 hr. This factor is based on the relation:

$$\frac{\sigma_{60}}{\sigma_{10}} = \left(\frac{T_{60}}{T_{10}}\right)^{0.2} = 1.43$$

The parameters for the other classes are not modified, because in the other classes there are also a lot of cases where low frequencies hardly contribute to the power spectrum. To combine both sets of parameters it was assumed that the σ_y, the σ_z, and the centerline concentrations calculated with both sets are average values for the corresponding frequency distributions. The frequency distributions from both sets are combined (added) to get the final distribution. This distribution allows us to determine the desired quantiles.

In the case of flat terrain, the calculations are only based on the Briggs parameters. To take into account the effect of an increased sampling time, a second set of parameters is established by multiplying the σ_y parameters from Briggs with the factor 1.43. These two sets are then used in the same way as in the case with the other surface roughness characterization.

The ratio of the concentration away from the centerline to the centerline concentration was derived using the following assumptions.

Assumption I

$$\frac{C}{C_o} = \left(\frac{C}{C_o}\right)_{50} \cdot f(C) = \left(\frac{C}{C_o}\right)_{50} \cdot f(C_o)$$

f = frequency distribution normalized to the 50% quantile

C_o = centerline concentration

c = concentration away from centerline concentration

$$\left(\frac{C}{C_o}\right)_{50} = 50\%\ quantile\ of\ \frac{C}{C_o}$$

This assumption means that the concentration away from the centerline varies and the centerline concentration is held constant. This distribution overestimates the real variation, especially close to the centerline. As can be seen from the following diagram, this assumption becomes more reasonable further away from the centerline.

Assumption II

The concentration away from the centerline is always correlated with the centerline concentration by the well known Gaussian distribution. The meaning of this assumption leads to the following distribution of the ratio considered.

$$\frac{C}{C_0} = \exp - \frac{0.5\,y^2}{\left[(\sigma_y)_{50} \cdot f(\sigma_y)\right]^2}$$

or

$$\frac{C}{C_0} = \left\{ \exp - \frac{0.5\,(z-h)^2}{\left[(\sigma_z)_{50} \cdot f(\sigma_z)\right]^2} + \exp - \frac{0.5\,(z+h)^2}{\left[(\sigma_z)_{50} \cdot f(\sigma_z)\right]^2} \right\} \Big/ \left\{ 1 + \exp - \frac{2.0\,z^2}{\left[(\sigma_z)_{50} \cdot f(\sigma_z)\right]^2} \right\}$$

This distribution underestimates the real variation, especially further away from the centerline, because the measured concentrations deviate from the calculated ones. The real distribution of the concentration should be somewhere in between. In the cases considered here, the 50% quantile of the ratio is not very close to 1. Therefore both distributions have been combined (added) to determine the quantiles.

In the case of convective conditions (classes A and B) the plume axis rises from near ground to the middle of the mixed layer. The centerline defined in the cases here is along the release height close to the ground. Because of the rise of the plume, the measured concentration above this centerline will be higher than at the centerline, in contrast to the usually used Gaussian distribution. Therefore the described procedure to determine the ratio will fail under these conditions. Because the z-value is not too far away from the centerline, it can be assumed that the 50% quantile value is not much different from 1.0. To get the quantiles in this case, the second distribution is replaced by a narrow distribution around 1.0. This means that the extreme quantiles are only determined by the first distribution.

Mixing Height

Table J-4 shows the estimated average mixing height H for the stability classes A to D. During stable conditions, no mixing height has been considered. In the model, the σ_z value is restricted to 0.8H.

Table J-4. Estimated average mixing height

stability class	mixing height
A	1500m
B	1250m
C	1000m
D	750m
E	-
F	-

Case C

For case C with varying sampling time, the stability class E was determined from the σ_θ value of 6 degrees (see corresponding table). To estimate the retardation effect, our Lagrangian particle model TRAVELING was applied. Two model runs have been done. Both with the following assumptions:

$$U = \frac{U*}{k}\, h\left(\frac{z}{z_o}\right) + 4.7\,\frac{z}{L} \qquad z \le 10m$$

$U*$ = 0.1 m/s
$1/L$ = 0.02 m^{-1}
z_o = 0.25 m

In case 1, the wind profile above 10 m is approximated by a power law function:

$$U = U_{10}\left(\frac{z}{10}\right)^{0.35} \qquad z > 10\,m$$

and in case 2 by:

$$U = U_{10} \qquad z > 10m$$

Table J-5 summarizes the results of the simulations. Given are the percentages of the centerline concentration after 4 hours. For the second case, a simulation with a continuous release was carried out. The calculated centerline concentration, with a sampling time of 1 hr after 1 hr release, provided the same concentration as after 4 hrs sampling in the previous run. The results show that the variation of the concentration with sampling time is lower than the uncertainty defined by the extreme quantiles.

If there is, for example, a forest between the source and the receptors, the retardation effect may be much higher. The tracer penetrates into the forest and it lasts a longer time until the tracer is released again from the forest to the atmosphere. This effect has to be taken into account like a deposition and a following reemission. Because these effects have been excluded, they are not considered. The

Table J-5. Sampling Time

Distance	60 min		120 min		240 min	
	case 1	case 2	case 1	case 2	case 1	case 2
360 m	100%	95%	100%	100%	100%	100%
970 m	90%	80%	100%	100%	100%	100%
1970 m	75%	55%	100%	100%	100%	100%

numbers in the elicitation table are determined by assuming a continuous release as in the cases before. The results are multiplied by the mean of the percentages from the table before

Case D

In this case, the stability classes D, E or F are assumed. The Briggs σ parameters have been used to determine the quantiles. To take into account the reduced sampling time of 1 min, the σ_y curve for class D is replaced by that for class E. The same reduction is applied for the σ_y values of class F. The σ_z values are not altered.

The quantiles are determined as in the previous cases using the two modified sets of σ parameters for the stability classes D and F.

Case E

To estimate the quantiles in this case, the following approximations have been made:

- vertically integrated Gaussian distribution
- average transport speed of this plume corresponds to the wind speed 200 m above ground
- sampling time << travel time (puff diffusion).

Under these assumptions 90% of the material crosses through an angle ϕ, described by the relation:

$$\phi = 2\,arctg\left(\frac{1.645\sigma_y}{x}\right)$$

The radian of this arc times the distance x gives the length of the arc. The elicitation table contains both values. The σ_y value is calculated with the formula proposed by Hefter:

$$\sigma_y = 0.5t$$

The travel time t is defined by:

$$t = \frac{x}{\bar{u} \cdot P}$$

The value P is the persistence of the wind, which describes the ratio of the wind vector average to the wind speed average. Such a persistence distribution as a function of averaging time from 1 hr to 240 hrs has been determined based on the wind measurements at our meteorological tower. Table J-6 summarizes the data used to estimate the quantiles for this case.

The travel time up to 80 km is so short that stable conditions, characterized by stability class F, may persist during the whole time. In this case a lower spread of the plume is possible as compared to the cases considered, especially if elevated releases are taken into account. If 1/3 of these conditions are persistent and combined with σ_θ values less than 1.5 degrees, which is a rough estimate, the 5% quantile angle becomes about 5 degrees. This value is taken for the elicitation table.

Table J-6. Data summary for quantile estimates

Quantile	Distance					
	1000 km		200 km		80 km	
	Speed	P	Speed	P	Speed	P
5%	9 m/s	0.98	11 m/s	1.0	12 m/s	1.00%
50%	6 m/s	0.76	6 m/s	0.95	6 m/s	1.00%
95%	4 m/s	0.30	3 m/s	0.50	2.5 m/s	0.60%

Dispersion Tables

N/A = not provided by expert

A-1: -2.0 K/100m Temp Lapse Rate Urban & Rural Surface Roughness					
Downwind distance	**Quantile**	**chiC/Q**	**chi(y)/chiC**	**chi(z)/chiC**	**sig-y**
0.5km	**0%**	N/A	N/A	N/A	N/A
	5%	4.00E-07	2.00E-01	5.00E-01	9.50E+01
	50%	3.00E-06	7.00E-01	1.00E+00	2.80E+02
	95%	2.00E-05	1.50E+00	2.30E+00	9.10E+02
	100%	N/A	N/A	N/A	N/A
1.0km	**0%**	N/A	N/A	N/A	N/A
	5%	7.50E-08	2.00E-01	5.00E-01	1.80E+02
	50%	6.00E-07	7.50E-01	1.00E+00	5.50E+02
	95%	5.00E-06	1.50E+00	2.30E+00	1.78E+03
	100%	N/A	N/A	N/A	N/A
3.0km	**0%**	N/A	N/A	N/A	N/A
	5%	2.00E-08	2.00E-01	5.00E-01	5.00E+02
	50%	1.00E-07	7.50E-01	1.00E+00	1.54E+03
	95%	6.00E-07	1.50E+00	2.30E+00	5.15E+03
	100%	N/A	N/A	N/A	N/A
10.0km	**0%**	N/A	N/A	N/A	N/A
	5%	6.00E-09	1.00E-01	N/A	1.35E+03
	50%	2.50E-08	7.00E-01	N/A	4.56E+03
	95%	1.00E-07	1.50E+00	N/A	1.60E+04
	100%	N/A	N/A	N/A	N/A
30.0km	**0%**	N/A	N/A	N/A	N/A
	5%	2.00E-09	5.00E-02	N/A	2.85E+03
	50%	9.50E-09	6.00E-01	N/A	1.15E+04
	95%	5.00E-08	1.30E+00	N/A	4.80E+04
	100%	N/A	N/A	N/A	N/A

A-2: -1.6 K/100m Temp Lapse Rate Urban & Rural Surface Roughness					
Downwind distance	Quantile	chiC/Q	chi(y)/chiC	chi(z)/chiC	sig-y
0.5km	0%	N/A	N/A	N/A	N/A
	5%	5.50E-06	2.00E-02	5.00E-02	3.00E+01
	50%	2.00E-05	3.00E-01	3.50E-01	6.50E+01
	95%	6.50E-05	9.00E-01	9.00E-01	1.70E+02
	100%	N/A	N/A	N/A	N/A
1.0km	0%	N/A	N/A	N/A	N/A
	5%	1.50E-06	2.00E-02	4.00E-02	6.00E+01
	50%	5.00E-06	3.00E-01	4.00E-01	1.30E+02
	95%	2.00E-05	8.50E-01	9.50E-01	3.30E+02
	100%	N/A	N/A	N/A	N/A
3.0km	0%	N/A	N/A	N/A	N/A
	5%	1.50E-07	4.00E-02	5.00E-02	1.70E+02
	50%	7.00E-07	3.50E-01	5.00E-01	3.70E+02
	95%	2.50E-06	9.50E-01	1.10E+00	9.50E+02
	100%	N/A	N/A	N/A	N/A
10.0km	0%	N/A	N/A	N/A	N/A
	5%	2.50E-08	2.00E-02	N/A	4.70E+02
	50%	1.00E-07	3.50E-01	N/A	1.15E+03
	95%	4.00E-07	9.50E-01	N/A	2.96E+03
	100%	N/A	N/A	N/A	N/A
30.0km	0%	N/A	N/A	N/A	N/A
	5%	8.00E-09	1.00E-12	N/A	1.00E+03
	50%	3.00E-08	3.00E-01	N/A	2.90E+03
	95%	1.00E-07	1.00E+00	N/A	8.60E+03
	100%	N/A	N/A	N/A	N/A

A-3: -1.0 K/100m Temp Lapse Rate Urban & Rural Surface Roughness					
Downwind distance	**Quantile**	**chiC/Q**	**chi(y)/chiC**	**chi(z)/chiC**	**sig-y**
0.5km	**0%**	N/A	N/A	N/A	N/A
	5%	7.50E-06	1.00E-12	1.00E-12	2.30E+01
	50%	2.50E-05	1.50E-01	1.00E-01	5.30E+01
	95%	8.00E-05	8.00E-01	5.00E-01	1.37E+02
	100%	N/A	N/A	N/A	N/A
1.0km	**0%**	N/A	N/A	N/A	N/A
	5%	2.50E-06	1.00E-02	1.00E-12	4.50E+01
	50%	8.50E-06	3.00E-01	5.00E-02	1.05E+02
	95%	3.00E-05	9.00E-01	5.00E-01	2.70E+02
	100%	N/A	N/A	N/A	N/A
3.0km	**0%**	N/A	N/A	N/A	N/A
	5%	3.50E-07	4.00E-02	1.00E-12	1.25E+02
	50%	1.50E-06	4.00E-01	2.00E-02	3.00E+02
	95%	6.00E-06	1.00E+00	5.00E-01	7.60E+02
	100%	N/A	N/A	N/A	N/A
10.0km	**0%**	N/A	N/A	N/A	N/A
	5%	4.00E-08	4.00E-02	N/A	3.40E+02
	50%	2.00E-07	4.00E-01	N/A	9.20E+02
	95%	1.00E-06	1.00E+00	N/A	2.45E+03
	100%	N/A	N/A	N/A	N/A
30.0km	**0%**	N/A	N/A	N/A	N/A
	5%	9.00E-09	1.00E-02	N/A	7.30E+02
	50%	5.50E-08	4.00E-01	N/A	2.20E+03
	95%	3.00E-07	1.10E+00	N/A	7.00E+03
	100%	N/A	N/A	N/A	N/A

A-4: 2.5 K/100m Temp Lapse Rate Urban & Rural Surface Roughness					
Downwind distance	Quantile	chiC/Q	chi(y)/chiC	chi(z)/chiC	sig-y
0.5km	0%	N/A	N/A	N/A	N/A
	5%	2.50E-05	7.00E-02	4.00E-02	1.20E+01
	50%	1.50E-04	5.50E-01	4.50E-01	4.00E+01
	95%	7.50E-04	1.20E+00	9.50E-01	1.45E+02
	100%	N/A	N/A	N/A	N/A
1.0km	0%	N/A	N/A	N/A	N/A
	5%	1.00E-05	6.00E-02	2.00E-02	2.30E+01
	50%	5.00E-05	5.00E-01	2.50E-01	8.00E+01
	95%	2.60E-04	1.20E+00	7.50E-01	2.85E+02
	100%	N/A	N/A	N/A	N/A
3.0km	0%	N/A	N/A	N/A	N/A
	5%	2.30E-06	1.00E-01	1.00E-12	6.40E+01
	50%	1 20E-05	6.00E-01	1.00E-03	2.25E+02
	95%	6.30E-05	1.30E+00	1.50E-01	8.20E+02
	100%	N/A	N/A	N/A	N/A
10.0km	0%	N/A	N/A	N/A	N/A
	5%	4.00E-07	3.00E-02	1.00E-12	1.70E+02
	50%	3.00E-06	5.00E-01	1.00E-11	6.60E+02
	95%	1.50E-05	1.30E+00	5.00E-02	2.60E+03
	100%	N/A	N/A	N/A	N/A
30.0km	0%	N/A	N/A	N/A	N/A
	5%	8.00E-08	1.00E-02	1.00E-12	3.60E+02
	50%	7.00E-07	4.00E-01	1.00E-11	1.74E+03
	95%	6.50E-06	1.30E+00	1.00E-02	7.60E+03
	100%	N/A	N/A	N/A	N/A

B-1: Unknown Lapse Rate 6.0 m/s Aver. Wind Speed		
Downwind distance	**Quantile**	**chiC/Q(ground level**
220. m	**0%**	N/A
	5%	1.00E-05
	50%	3.00E-05
	95%	8.00E-05
	100%	N/A
315. m	**0%**	N/A
	5%	1.30E-05
	50%	3.50E-05
	95%	1.00E-04
	100%	N/A

B-2: Unknown Lapse Rate 5.0 m/s Aver. Wind Speed		
Downwind distance	**Quantile**	**chiC/Q(ground level)**
220. m	**0%**	N/A
	5%	1.50E-05
	50%	4.00E-05
	95%	1.10E-04
	100%	N/A
315. m	**0%**	N/A
	5%	1.40E-05
	50%	3.80E-05
	95%	1.10E-04
	100%	N/A

B-3: Unknown Lapse Rate 8.0 m/s Aver. Wind Speed		
Downwind distance	**Quantile**	**chiC/Q(ground level)**
300. m	0%	N/A
	5%	8.50E-06
	50%	2.50E-05
	95%	6.50E-05
	100%	N/A
600. m	0%	N/A
	5%	3.00E-06
	50%	8.50E-06
	95%	2.50E-05
	100%	N/A

B-4: -1.0 K/100m Temp Lapse Rate Flat Surface Roughness		
Downwind distance	**Quantile**	**chiC/Q(ground level)**
300. m	0%	N/A
	5%	2.50E-05
	50%	6.50E-05
	95%	2.00E-04
	100%	N/A
600. m	0%	N/A
	5%	1.00E-05
	50%	3.00E-05
	95%	9.00E-05
	100%	N/A

B-5: 3.0 K/100m Temp Lapse Rate Flat Surface Roughness					
Downwind distance	Quantile	chi(y)/chiC	chi(z)/chiC	sig-y	sig-z
600. m	0%	N/A	N/A	N/A	N/A
	5%	5.00E-03	5.00E-02	1.30E+01	3.00E+00
	50%	1.50E-01	3.80E-01	2.50E+01	7.00E+00
	95%	6.50E-01	9.00E-01	6.00E+01	1.50E+01
	100%	N/A	N/A	N/A	N/A

C: Stable Conditions Urban & Rural Surface Roughness				
Downwind distance	Quantile	60 min	120 min	240 min
360. m	0%	N/A	N/A	N/A
	5%	8.00E-09	8.00E-09	8.00E-09
	50%	7.00E-08	7.00E-08	7.00E-08
	95%	8.00E-06	8.00E-06	8.00E-06
	100%	N/A	N/A	N/A
970. m	0%	N/A	N/A	N/A
	5%	4.00E-06	4.50E-06	4.50E-06
	50%	1.00E-05	1.20E-05	1.20E-05
	95%	3.00E-05	3.50E-05	3.50E-05
	100%	N/A	N/A	N/A
1970. m	0%	N/A	N/A	N/A
	5%	2.00E-06	3.00E-06	3.00E-06
	50%	6.50E-06	1.00E-05	1.00E-05
	95%	2.50E-05	3.50E-05	3.50E-05
	100%	N/A	N/A	N/A

D: Stable Conditions Flat Surface Roughness				
Downwind distance	Quantile	chiC/Q	sig-y	sig-z
60. m	0%	N/A	N/A	N/A
	5%	1.80E-03	1.10E+00	5.00E-01
	50%	1.50E-02	2.30E+00	2.00E+00
	95%	6.00E-02	6.00E+00	4.80E+00
	100%	N/A	N/A	N/A

E: Length of Arc Crossed By 90% of the Material		
Downwind distance	Quantile	90% arc
80.km	0%	N/A
	5%	7.00E+03
	50%	2.20E+04
	95%	8.00E+04
	100%	N/A
200.km	0%	N/A
	5%	2.80E+04
	50%	5.60E+04
	95%	2.00E+05
	100%	N/A
1000.km	0%	N/A
	5%	1.75E+05
	50%	3.50E+05
	95%	1.20E+06
	100%	N/A

Expert K

1. In Europe as well as in the United States, the majority of the impact and consequence studies and assessments are based on the simple bi-Gaussian transport and dispersion formula given by:

$$C(x,y,z)=\frac{Q}{2\pi\cdot\sigma_y(x)\cdot\sigma_z(x)\cdot\bar{u}(H)}\cdot\exp\left(\frac{-y^2}{2\sigma_y^2}\right)$$
$$\cdot\left[\exp\left(\frac{-(z-H)^2}{2\sigma_z^2}\right)+\exp\left(\frac{-(z+H)^2}{2\sigma_z^2}\right)\right]$$

or by its multiple reflection extension for a limited mixing layer of height h_m.[11]

2. When applying this basic formula for a given, neutrally buoyant point source release (Q) at height H during a more or less completely specified and persistent meteorological condition, the calculated downwind (integrated) concentration values—generated by different operational models—are first of all influenced by:

   a) the choice of the specific turbulence typing scheme;
   b) the procedure to derive the proper stability category within the chosen turbulence typing scheme for a given, but quite often incompletely or not properly specified, meteorological condition;
   c) the corresponding [$\sigma_y(x)$, $\sigma_z(x)$] combination and their analytical formulas or expressions;
   d) the wind speed profile or m-factor determining the average transport wind speed $\bar{u}(H)$ at the height of the plume axis.

   When applicable and taken into account in the specific code, further differences in C(x,y,z) are generated by:

   e) the choice of the mixing layer height h_m as a function of the stability class, the season, the time of day, etc.;
   f) the surface roughness z_o and the corresponding corrections on $\sigma_z(x)$ and the exponent m of the vertical wind profile;
   g) the averaging time (t_{av}) and its influence on $\sigma_y(x)$.

3. The uncertainty analysis for a given model at a specific site and for a given range of release heights and ground-level receptors (e.g., $x \leq 30$ km) is normally done by:

   a) a sensitivity analysis of the model as a function of its input parameters (and their uncertainties);
   b) some type of verification or validation, e.g., by tracer releases or observations at already available monitoring stations. Quite often the local model is somewhat trimmed or calibrated, and the final comparisons between sets of observed and calculated values look quite convincing (e.g., overall means within ±20%, at least 50% of the calculated values within a factor two or less of the observed ones, and the extreme values within a factor 10 or better).

4. What is requested in the present elicitation process is nevertheless a broader uncertainty analysis, as only the release conditions and some meteorological parameters are specified—the latter without much detail—making difficult the abstraction of the specific characteristics of the site (meteorology, topography, orography, urbanization), of the locally used procedures and models, of the level of validation of the latter, etc.

5. To tackle this problem in a EC/US context, it seemed therefore appropriate to apply first of all some (routinely used) national approaches on the specified test cases and to evaluate the differences seen in the end results.

6. To keep it manageable the following alternatives were combined with the basic formula given under 1 above:

   6.1. The IFDM model (Belgium) with a site specific turbulence typing scheme, corresponding $\sigma_y(x)$ and $\sigma_z(x)$ sets, and m factors for the wind profile.[2]
   6.2. The TA Luft 86 procedure (Germany) with a country specific turbulence typing scheme and corresponding $\sigma_y(x)$ and $\sigma_z(x)$ values.[8, 10]
   6.3. The ISC model or Industrial Source Complex Model (EPA, US) with Pasquill's turbulence typing scheme and Briggs' $\sigma_y(x)$ and $\sigma_z(x)$ formulas for urban areas.[13]
   6.4. The same ISC model with Pasquill-Gifford's $\sigma_y(x)$ and $\sigma_z(x)$ formulas for rural areas.[13]
   6.5. The MACCS code for flat terrain with z_o = 3 cm and a $\sigma_y(x)$ correction for t_{av}.[11]
   6.6. The MACCS version for rural areas with z_o = 10 cm, m exponents for rural areas and $\sigma_y(x)$ correction for t_{av}.[11]
   6.7. The MACCS urban version for z_o = 1 m, m exponents for urban areas, and $\sigma_y(x)$ correction for t_{av}.[11]

Annexe 1 gives the details for each of the seven options.

Table K-1. Stability classes

Case Models	A1	A2	A3	A4	C	B1	B2	B3	B4	B5	D
IFDM TALuft ISC/MACCS PG	E6 V A	E4 III2 C	E3 III1 D	E1 II(I) F	E2 II E	E3 III1 D	E3-E4 III1-III2 D-C	E7 III2-III1 C	E3 III1 D	E1 I F	E1-E2 I-II F-E
z_o (cm)	50 cm				50 cm	3 to 10 cm					3-10 cm
H(m)	10 m				45 m	22 m					12 m
t_{av}(min)	60 min				60 min 120 min 240 min	60 min					1 min
PG-based models	MACCS + ISC rural + urban					MACCS + ISC rural					MACCS flat

7. The next step is deriving the appropriate stability class for each test case using the given meteorological information and the appropriate diffusion typing scheme. As different procedures exist to do this, even for the PG stability categories, some (reasonable) compromise was required, based on what is given in Annexe 1, complemented with the NRC's Proposed Revision 1 to Regulatory Guide 1.23 (1980), as well the $\Delta T/\Delta Z$ procedure as the $\Delta T/\Delta Z + \bar{u}(10)$ procedure (all given in Annexe 2), and using Golder's ($1/L$, z_o) curves as reproduced in Zanetti.[12] The final results are given in Table K-1.

8. The numerical results obtained for a given case with the combinations of models given in the previous table cannot be more than a starting point for a broader uncertainty analysis, taking into account that:

   8.1. Only a very limited and not even randomly selected number of versions of the linear Gaussian plume model, operationally used in a limited number of different countries, has been included in this (sensitivity) analysis generating a (possibly too) small foundation to build on;

   8.2 Especially for the A cases, with uncertainty ranges to be specified at downwind distances up to 30 km, the influence of the following phenomena has to be taken into account, too: inaccuracies in wind direction measured at release point; directional wind shear during transport; "width" of stability definition; leaky inversion layer, vertically changing turbulence and mixing height; time of the day and season;[8,9] terrain variability; roughness length variability; and others.

   8.3. Finally some more general information from previous studies, reviews, benchmark exercises, and uncertainty analyses have to be taken into account, such as:

      8.3.1. The CNSI Benchmark Exercise[4] with 25 models from 15 countries giving for: (1) stability D, $u_{10} = 5$ m/s, $h_m = 1000$ m, $z_o =$ 10 cm a (consistent) factor 6 to 7 in the range 1 km to 30 km between min and max values; (2) stability F, $u_{10} = 2$ m/s, $h_m =$ 250 m, $z_o = 10$ cm a (consistent) factor 8 to 10 in the range 1 to 30 km when two outliers are eliminated.

      8.3.2. The project 10C within CEC's indirect action research program on the safety of thermal water reactors showing that, for the same meteorological data set (3 years) at the same site in a flat region (Mol, Belgium) currently used combinations of "a turbulence typing scheme" and "a set of dispersion parameters" gave higher percentiles (P95, P98...) and maximum hourly concentration values within a range of a factor 10 to 100.[3,5,7]

      8.3.3. That findings from many field measurements—over flat terrain and in many stability conditions—lead to the conclusion that for $t_{av} = 1$ h, 90% of the observed data 30 km downwind the source lie within something like "one tenth of" and "ten times" the data predicted by Gaussian models.[6]

Dispersion Tables

N/A = not provided by expert

A-1: -2.0 K/100m Temp Lapse Rate Urban & Rural Surface Roughness					
Downwind distance	**Quantile**	**chiC/Q**	**chi(y)/chiC**	**chi(z)/chiC**	**sig-y**
0.5km	**0%**	N/A	N/A	N/A	N/A
	5%	2.00E-06	4.00E-01	8.00E-01	1.20E+02
	50%	5.00E-06	6.00E-01	9.00E-01	1.70E+02
	95%	1.00E-05	8.00E-01	1.00E+00	2.50E+02
	100%	N/A	N/A	N/A	N/A
1.0km	**0%**	N/A	N/A	N/A	N/A
	5%	5.00E-07	5.00E-01	6.00E-01	2.50E+02
	50%	1.00E-06	7.00E-01	8.00E-01	3.50E+02
	95%	4.00E-06	8.00E-01	1.00E+00	5.00E+02
	100%	N/A	N/A	N/A	N/A
3.0km	**0%**	N/A	N/A	N/A	N/A
	5%	8.00E-08	2.00E-01	4.00E-01	5.00E+02
	50%	2.00E-07	5.00E-01	8.00E-01	7.00E+02
	95%	8.00E-07	7.00E-01	1.00E+00	1.00E+03
	100%	N/A	N/A	N/A	N/A
10.0km	**0%**	N/A	N/A	N/A	N/A
	5%	7.00E-09	2.00E-01	N/A	1.40E+03
	50%	6.00E-08	5.00E-01	N/A	2.20E+03
	95%	1.40E-07	7.00E-01	N/A	3.00E+03
	100%	N/A	N/A	N/A	N/A
30.0km	**0%**	N/A	N/A	N/A	N/A
	5%	1.00E-09	1.00E-01	N/A	3.00E+03
	50%	1.00E-08	5.00E-01	N/A	5.50E+03
	95%	5.00E-08	7.00E-01	N/A	8.00E+03
	100%	N/A	N/A	N/A	N/A

A-2: -1.6 K/100m Temp Lapse Rate Urban & Rural Surface Roughness					
Downwind distance	**Quantile**	**chiC/Q**	**chi(y)/chiC**	**chi(z)/chiC**	**sig-y**
0.5km	**0%**	N/A	N/A	N/A	N/A
	5%	8.00E-06	1.50E-01	2.00E-01	5.00E+01
	50%	2.00E-05	4.50E-01	6.00E-01	8.00E+01
	95%	4.00E-05	6.00E-01	8.00E-01	1.00E+02
	100%	N/A	N/A	N/A	N/A
1.0km	**0%**	N/A	N/A	N/A	N/A
	5%	2.00E-06	1.50E-01	3.00E-01	1.00E+02
	50%	5.00E-06	4.50E-01	6.00E-01	1.60E+02
	95%	1.00E-05	6.00E-01	9.00E-01	1.90E+02
	100%	N/A	N/A	N/A	N/A
3.0km	**0%**	N/A	N/A	N/A	N/A
	5%	2.00E-07	1.50E-01	3.00E-01	2.50E+02
	50%	7.00E-07	4.00E-01	6.00E-01	3.50E+02
	95%	2.00E-06	5.50E-01	9.00E-01	4.50E+02
	100%	N/A	N/A	N/A	N/A
10.0km	**0%**	N/A	N/A	N/A	N/A
	5%	4.00E-08	1.00E-01	N/A	7.00E+02
	50%	2.00E-07	2.50E-01	N/A	9.00E+02
	95%	6.00E-07	6.00E-01	N/A	1.50E+03
	100%	N/A	N/A	N/A	N/A
30.0km	**0%**	N/A	N/A	N/A	N/A
	5%	2.00E-09	5.00E-02	N/A	1.40E+03
	50%	5.00E-08	1.50E-01	N/A	2.00E+03
	95%	8.00E-08	5.00E-01	N/A	3.50E+03
	100%	N/A	N/A	N/A	N/A

A-3: -1.0 K/100m Temp Lapse Rate Urban & Rural Surface Roughness					
Downwind distance	Quantile	chiC/Q	chi(y)/chiC	chi(z)/chiC	sig-y
0.5km	0%	N/A	N/A	N/A	N/A
	5%	1.00E-05	5.00E-02	1.00E-01	4.00E+01
	50%	3.00E-05	2.50E-01	4.00E-01	6.00E+01
	95%	6.00E-05	4.50E-01	7.00E-01	8.00E+01
	100%	N/A	N/A	N/A	N/A
1.0km	0%	N/A	N/A	N/A	N/A
	5%	3.00E-06	1.50E-01	1.00E-01	7.50E+01
	50%	7.00E-06	3.00E-01	4.00E-01	1.00E+02
	95%	2.00E-05	6.00E-01	7.00E-01	1.40E+02
	100%	N/A	N/A	N/A	N/A
3.0km	0%	N/A	N/A	N/A	N/A
	5%	5.00E-07	1.50E-01	1.00E-01	1.80E+02
	50%	2.00E-06	4.00E-01	4.00E-01	2.50E+02
	95%	5.00E-06	6.00E-01	7.00E-01	3.40E+02
	100%	N/A	N/A	N/A	N/A
10.0km	0%	N/A	N/A	N/A	N/A
	5%	4.00E-08	2.50E-01	N/A	6.00E+02
	50%	3.00E-07	5.50E-01	N/A	9.00E+02
	95%	7.00E-07	8.00E-01	N/A	1.40E+03
	100%	N/A	N/A	N/A	N/A
30.0km	0%	N/A	N/A	N/A	N/A
	5%	3.00E-09	1.50E-01	N/A	1.30E+03
	50%	5.00E-08	4.50E-01	N/A	2.00E+03
	95%	1.00E-07	7.50E-01	N/A	3.20E+03
	100%	N/A	N/A	N/A	N/A

A-4: 2.5 K/100m Temp Lapse Rate Urban & Rural Surface Roughness					
Downwind distance	**Quantile**	**chiC/Q**	**chi(y)/chiC**	**chi(z)/chiC**	**sig-y**
0.5km	**0%**	N/A	N/A	N/A	N/A
	5%	3.00E-05	3.00E-01	5.00E-01	2.00E+01
	50%	1.00E-04	7.50E-01	7.00E-01	4.00E+01
	95%	6.00E-04	9.50E-01	9.00E-01	9.00E+01
	100%	N/A	N/A	N/A	N/A
1.0km	**0%**	N/A	N/A	N/A	N/A
	5%	1.00E-05	2.50E-01	1.00E-01	3.50E+01
	50%	6.00E-05	7.00E-01	5.00E-01	7.00E+01
	95%	2.00E-04	9.00E-01	8.00E-01	1.40E+02
	100%	N/A	N/A	N/A	N/A
3.0km	**0%**	N/A	N/A	N/A	N/A
	5%	1.00E-06	2.50E-01	1.00E-12	9.00E+01
	50%	1.00E-05	7.00E-01	2.00E-01	1.80E+02
	95%	4.00E-05	9.00E-01	7.00E-01	3.50E+02
	100%	N/A	N/A	N/A	N/A
10.0km	**0%**	N/A	N/A	N/A	N/A
	5%	1.00E-07	1.50E-01	1.00E-12	2.50E+02
	50%	2.00E-06	4.50E-01	5.00E-01	4.00E+02
	95%	8.00E-06	8.00E-01	1.00E+00	8.00E+02
	100%	N/A	N/A	N/A	N/A
30.0km	**0%**	N/A	N/A	N/A	N/A
	5%	1.00E-08	2.00E-01	3.00E-01	7.00E+02
	50%	2.00E-07	7.00E-01	7.00E-01	1.50E+03
	95%	2.00E-06	9.00E-01	1.00E+00	3.00E+03
	100%	N/A	N/A	N/A	N/A

B-1: Unknown Lapse Rate 6.0 m/s Aver. Wind Speed		
Downwind distance	**Quantile**	**chiC/Q(ground level)**
220. m	**0%**	N/A
	5%	1.00E-06
	50%	2.00E-05
	95%	6.00E-05
	100%	N/A
315. m	**0%**	N/A
	5%	5.00E-06
	50%	2.00E-05
	95%	6.00E-05
	100%	N/A

B-2: Unknown Lapse Rate 5.0 m/s Aver. Wind Speed		
Downwind distance	**Quantile**	**chiC/Q(ground level)**
220. m	**0%**	N/A
	5%	1.00E-06
	50%	2.00E-05
	95%	6.00E-05
	100%	N/A
315. m	**0%**	N/A
	5%	5.00E-06
	50%	2.00E-05
	95%	6.00E-05
	100%	N/A

B-3: Unknown Lapse Rate 8.0 m/s Aver. Wind Speed		
Downwind distance	**Quantile**	**chiC/Q(ground level)**
300. m	**0%**	N/A
	5%	2.00E-06
	50%	1.00E-05
	95%	4.00E-05
	100%	N/A
600. m	**0%**	N/A
	5%	1.00E-06
	50%	5.00E-06
	95%	2.00E-05
	100%	N/A

B-4: -1.0 K/100m Temp Lapse Rate Flat Surface Roughness		
Downwind distance	**Quantile**	**chiC/Q(ground level)**
300. m	**0%**	N/A
	5%	8.00E-06
	50%	3.00E-05
	95%	1.00E-04
	100%	N/A
600. m	**0%**	N/A
	5%	6.00E-06
	50%	2.00E-05
	95%	8.00E-05
	100%	N/A

B-5: 3.0 K/100m Temp Lapse Rate Flat Surface Roughness					
Downwind distance	Quantile	chi(y)/chiC	chi(z)/chiC	sig-y	sig-z
600. m	0%	N/A	N/A	N/A	N/A
	5%	1.00E-01	5.00E-01	2.00E+01	5.00E+00
	50%	3.00E-01	6.00E-01	4.00E+01	1.50E+01
	95%	8.00E-01	1.10E+00	1.00E+02	3.00E+01
	100%	N/A	N/A	N/A	N/A

C: Stable Conditions Urban & Rural Surface Roughness				
Downwind distance	Quantile	60 min	120 min	240 min
360. m	0%	N/A	N/A	N/A
	5%	3.00E-08	1.50E-08	0.75E-08
	50%	7.00E-06	3.50E-06	1.75E-06
	95%	3.00E-05	1.50E-05	0.75E-05
	100%	N/A	N/A	N/A
970. m	0%	N/A	N/A	N/A
	5%	5.00E-07	2.50E-07	1.25E-07
	50%	2.00E-05	1.00E-05	0.50E-05
	95%	5.00E-05	3.00E-05	1.50E-05
	100%	N/A	N/A	N/A
1970. m	0%	N/A	N/A	N/A
	5%	1.00E-06	0.50E-06	0.25E-06
	50%	5.00E-06	2.50E-06	1.25E-06
	95%	2.00E-05	1.40E-05	0.70E-05
	100%	N/A	N/A	N/A

D: Stable Conditions Flat Surface Roughness				
Downwind distance	Quantile	chiC/Q	sig-y	sig-z
60. m	0%	N/A	N/A	N/A
	5%	1.00E-03	2.00E+00	2.00E+00
	50%	5.00E-03	4.00E+00	3.00E+00
	95%	2.00E-02	8.00E+00	5.00E+00
	100%	N/A	N/A	N/A

E: Length of Arc Crossed By 90% of the Material		
Downwind distance	Quantile	90% arc
80.km	0%	N/A
	5%	N/A
	50%	N/A
	95%	N/A
	100%	N/A
200.km	0%	N/A
	5%	N/A
	50%	N/A
	95%	N/A
	100%	N/A
1000.km	0%	N/A
	5%	N/A
	50%	N/A
	95%	N/A
	100%	N/A

References

1. Turner, D.B., *Workbook of Atmospheric Dispersion Estimates*, Environmental Health Series: Air Pollution, Public Health Service Publication No. 999-AP-26, U.S. Department of Health, Education, and Welfare, National Center for Air Pollution Control, Cincinnati, OH, 1970.

2. Bultynck, H., and L.M. Malet, "Evaluation of Atmospheric Dilution Factors for Effluents Diffused from an Elevated Continuous Point Source," *Tellus*, 24:455-472, 1972.

3. Kretzschmar, J.G., et al., "Influence of the Turbulence Typing Scheme Upon the Cumulative Frequency Distributions of the Calculated Relative Concentrations for Different Averaging Times," EUR-8478-EN, Commission of the European Communities, Luxembourg, 1983.

4. NEA/OECD (Nuclear Energy Agency/Organisation for Economic Co-Operation and Development), *International Comparison Study on Reactor Accident Consequence Modeling: Summary Report to CSNI by an NEA Group of Experts, September 1983*, Organisation for Economic Co-Operation and Development, Paris, France, 1984.

5. Kretzschmar, J.G., and I. Mertens, "Influence of the Turbulence Typing Scheme Upon the Cumulative Frequency Distributions of the Calculated Relative Concentrations for Different Averaging Times," *Atmospheric Environment*, 18:2377-2393, 1984.

6. Smith, F.B., et al., "Estimates of Uncertainty in Dispersion Modelling," (E. Skupinski, B. Tolley, and J. Vilain, eds.), *Safety of Thermal Water Reactors, Proceedings of a Seminar on the Results of the European Communities' Indirect Action Research Programme, 1 October 1984*, Graham and Trotman, Gaithersburg, MD, pp. 513-523, 1985.

7. Vanderborght, B., et al., "Sensitivity, Applicability and Validation of Bi-Gaussian Off- and On-line Models for the Evaluation of the Consequences of Accidental Releases in Nuclear Facilities," (E. Skupinski, B. Tolley, and J. Vilain, eds.), *Safety of Thermal Water Reactors, Proceedings of a Seminar on the Results of the European Communities' Indirect Action Research Programme, 1 October 1984*, Graham and Trotman, Gaithersburg, MD, pp. 497-504, 1985.

8. Feldhaus, G., et al., Die TA-Luft 1986, Deutsches Verwaltungsblatt (DVBI) 101, pp. 641-652, 1986.

9. USEPA, "Guideline on Air Quality Models (Revised)," EPA-450/2-78-027R, Environmental Protection Agency, Office of Air Quality Planning and Standards, Research Triangle Park, NC, July 1987.

10. Pankrath, J., "Dispersion Calculations in Accordance with TALuft '86 (Clean Air Technical Guide with the Uniform Federal Programme System AUSTAL 86," Staub–Reinhalt. Luft, 47:239-244, 1987.

11. Jow, H.-N., et al., "MELCOR Accident Consequence Code System (MACCS): Model Description," NUREG/CR-4691-V2 (SAND86-1562, Vol. 2), Sandia National Laboratories, Albuquerque, NM, February 1990.

12. Zannetti, P., *Air Pollution Modeling: Theories, Computational Methods and Available Software*, Computational Mechanics Publications, Boston, MA, available from Van Nostrand Reinhold, New York, 1990.

13. USEPA, "User's Guide for the Industrial Source Complex (ISC2) Dispersion Models. Vol. 2: Description of Model Algorithms," EPA-540/4-92-008B, Environmental Protection Agency, Research Triangle Park, NC, March 1992.

14. Pasquill, F., "The Estimation of the Dispersion of Windborne Material," *Met. Magazine*, 90:33-49, 1961.

15. U.S. Atomic Energy Commission, "On-Site Meteorological Programs," *Safety Guide 23 - 1972*, U.S. Atomic Energy Commission, 1972.

16. USNRC, "Nuclear Programs in Support of Nuclear Power Plants," Proposed Revision 1 to *Regulatory Guide 1.23*, 1980.

Annexe 1

6.1. IFDM or Immission Frequency Distribution Model (Belgium)

1. Bultynck-Malet stability classification scheme[1]

Atmospheric stability category	Differentiation criteria		
	S > O	S < 0	
E_1 : very stable	$\lambda \geq 2.75$		
E_2 : stable	$1.75 < \lambda < 2.75$		
E_3 : neutral	$\lambda \leq 1.75$	$\lambda \leq 2$	$\bar{u} \leq 11$ m.s^{-1}
E_4 : unstable		$2 < \lambda < 2.75$	
E_5 : very unstable		$2.75 \leq \lambda < 3.3$	
E_6 : extr. unstable		$\lambda \geq 3.3$	
E_7 : neutral	$\bar{u} > 11$ m.s^{-1}		

with $S = (\partial\theta/\partial z) / \bar{u}^2(69\ m)$
$\lambda = 6 + \log_{10} |S|$

2. Corresponding dispersion parameters and m factor[1]

$\sigma_y(x) = Ax^a$ and $\sigma_z(x) = Bx^b$
$u(z) = u(z_o)\ (z/z_o)^m$

Stability category	A	a	B	b	m*
E_1	0.235	0.796	0.311	0.711	0.53
E_2	0.297	0.796	0.382	0.711	0.40
E_3	0.418	0.796	0.520	0.711	0.33
E_4	0.586	0.796	0.700	0.711	0.23
E_5	0.826	0.796	0.950	0.711	0.16
E_6	0.946	0.796	1.321	0.711	0.10
E_7	1.043	0.698	0.819	0.669	0.33

* as implemented in IFDM

6.2. TA Luft 86 procedure[8]

1. Diffusion typing scheme

Based on wind speed at 10 m height, cloud cover, cloud type, month of the year and time of the day with stability classes from I : very stable to V : very unstable through III/1 and III/2 : neutral.

2. Dispersion parameters

$\sigma_y(x) = Fx^f$ and $\sigma_z(x) = Gx^g$ with F, f, G, g functions of stability class and (effective) release height H.
For $H \leq 50$ m the following numerical values are used :

stability class	F	f	G	g	m
V : very unstable	1.503	0.833	0.151	1.219	0.09
IV : unstable	0.876	0.823	0.127	1.108	0.20
III/2 : neutral	0.659	0.807	0.165	0.996	0.22
III/1 : neutral	0.640	0.784	0.215	0.885	0.28
II : stable	0.801	0.754	0.264	0.774	0.37
I : very stable	1.294	0.718	0.241	0.662	0.42

with $u(z) = u(z_0)\ (z/z_0)^m$ voor $z \leq 200$ m

6.3. ISC for urban areas[13]

1. Stability categories

Surface wind speed (m/s)	Pasquill Stability Categories				
	Insolation			Night	
	Strong	Moderate	Slight	Thinly overcast or ≥ 4/8 low cloud	≤ 3/8 cloud
< 2	A	A-B	B	-	-
2-3	A-B	B	C	E	F
3-5	B	B-C	C	D	E
5-6	C	C-D	D	D	D
> 6	C	D	D	D	D
(for A-B, take the average of values for A and B, etc.)					

Notes :
1. Strong insolation corresponds to sunny midday in midsummer in England; slight insolation to similar conditions in midwinter.
2. Night refers to the period from 1 hr before sunset to 1 hr after sunrise.
3. The neutral category D should also be used, regardless of wind speed, for overcast conditions during day or night and for any sky conditions during the hour preceding or following night as defined above.

2. Dispersion parameters and wind profile

BRIGGS FORMULAS USED TO CALCULATE McELROY-POOLER $\sigma_y(x)$ and $\sigma_z(x)$

Stability	σ_y(meters)	σ_z(meters)	m
A	$0.32 \times (1 + 0.0004\ x)^{-1/2}$	$0.24 \times (1 + 0.001\ x)^{1/2}$	0.15
B	$0.32 \times (1 + 0.0004\ x)^{-1/2}$	$0.24 \times (1 + 0.001\ x)^{1/2}$	0.15
C	$0.22 \times (1 + 0.0004\ x)^{-1/2}$	$0.20\ x$	0.20
D	$0.16 \times (1 + 0.0004\ x)^{-1/2}$	$0.14 \times (1 + 0.0003\ x)^{-1/2}$	0.25
E	$0.11 \times (1 + 0.0004\ x)^{-1/2}$	$0.08 \times (1 + 0.0015\ x)^{-1/2}$	0.30
F	$0.11 \times (1 + 0.0004\ x)^{-1/2}$	$0.08 \times (1 + 0.0015\ x)^{-1/2}$	0.30

6.4. ISC for rural areas[13]

1. Stability categories

as in ISC for urban areas

2. Dispersion parameters and wind profile

PARAMETERS USED TO CALCULATE PASQUILL-GIFFORD $\sigma_y(x)=465.12\ (x)\ tg(TH)$

Stability category	c	d	m
A	24.1670	2.5334	0.07
B	18.3330	1.8096	0.07
C	12.5000	1.0857	0.10
D	8.3330	0.72382	0.15
E	6 2500	0.54287	0.35
F	4.1667	0.36191	0.55

where σ_y is in meters, x in kilometers and TH = 0.01745 [c-d ln(x)]

PARAMETERS USED TO CALCULATE PASQUILL-GIFFORD $\sigma_z(x) = ax^b$

Stability category	x (km)	a	b
A*	<.10	122.800	0.94470
	0.10 - 0.15	158.080	1.05420
	0.16 - 0.20	170.220	1.09320
	0.21 - 0.25	179.520	1.12620
	0.26 - 0.30	217.410	1.26440
	0.31 - 0.40	258.890	1.40940
	0.41 - 0.50	346.750	1.72830
	0.51 - 3.11	453.850	2.11660
	> 3.11	**	**
B*	<.20	90.673	0.93198
	0.21 - 0.40	98.483	0.98332
	> 0.40	109.300	1.09710
C*	11	61.141	0.91465

PARAMETERS USED TO CALCULATE PASQUILL-GIFFORD $\sigma_z(x) = ax^b$ (continued)			
Stability category	x (km)	a	b
D	<.30	34.459	0.86974
	0.31 - 1.00	32.093	0.81066
	1.01 - 3.00	32.093	0.64403
	3.01 - 10.00	33.504	0.60486
	10.01 - 30.00	36.650	0.56589
	> 30.00	44.053	0.51179
E	<.10	24.260	0.83660
	0.10 - 0.30	23.331	0.81956
	0.31 - 1.00	21.628	0.75660
	1.01 - 2.00	21.628	0.63077
	2.01 - 4.00	22.534	0.57154
	4.01 - 10.00	24.703	0.50527
	10.01 - 20.00	26.970	0.46713
	20.01 - 40.00	35.420	0.37615
	> 40.00	47.618	0.29592
F	<.20	15.209	0.81558
	0.21 - 0.70	14.457	0.78407
	0.71 - 1.00	13.953	0.68465
	1.01 - 2.00	13.953	0.63227
	2.01 - 3.00	14.823	0.54503
	3.01 - 7.00	16.187	0.46490
	7.01 - 15.00	17.836	0.41507
	15.01 - 30.00	22.651	0.32681
	30.01 - 60.00	27.074	0.27436
	> 60.00	34.219	0.21716

with σ_z in meters and x in kilometers
* if the calculated value of σ_z exceeds 5000 m, σ_z is set to 5000 m.
** σ_z is equal to 5000 m

6.5. to 6.7. MACCS[11]

1. Stability categories

2. Dispersion parameters and wind profile for z_o = 3 cm

Pasquill

Stability class	$\sigma_y(x) = ax^b$		$\sigma_z(x) = cx^d$		m	
	a	b	c	d	urban	rural
A	0.3658	0.9031	0.00025	2.125	0.15	0.07
B	0.2751	0.9031	0.0019	1.6021	0.15	0.07
C	0.2089	0.9031	0.2	0.8543	0.20	0.10
D	0.1474	0.9031	0.3	0.6532	0.25	0.15
E	0.1046	0.9031	0.4	0.6021	0.40	0.35
F	0.0722	0.9031	0.2	0.6020	0.60	0.55

3. Corrections

3.1. Surface roughness correction:

$$\sigma_z(x) = (c.x^d)\ (z_o/3)^{0.2}$$

with z_o in cm

3.2. Lateral plume meandering increases, or $\sigma_y(x)$ increases wirelease duration for continuous sampling:

$$\sigma_y(x) = (ax^b)\ (\Delta t_{release}/10\ \text{min})^{0.2}$$

or $\sigma_y(x)$ increases with sampling time t_{av} for continuous releases:

$$\sigma_y(x) = (ax^b)\ (t_{av}/10\ \text{min})^{0.2}$$

Annexe 2

1. Different procedures to determine the appropriate stability class in Pasquill's diffusion typing scheme[3]

PASQUILL SYN[14]

	Day (insolation strength)			Night (cloud cover)	
ū(10) m/s	strong	moderate	slight	N ≥ 4/8	N ≤ 3/8
< 2	A	A-B	B	-	-
2-3	A-B	B	C	E	F
3-5	B	B-C	C	D	E
5-6	C	C-D	D	D	D
> 6	C	D	D	D	D

PASQUILL NRC Diffusion Typing Scheme[15,16]

Stability	Pasquill Category	ΔT/Δz (°C/100 m)
extremely unstable	A	ΔT/Δz ≤ -1.9
moderately unstable	B	-1.9 < ΔT/Δz ≤ -1.7
slightly unstable	C	-1.7 < ΔT/Δz ≤ -1.5
neutral	D	-1.5 < ΔT/Δz ≤ -0.5
slightly stable	E	-0.5 < ΔT/Δz ≤ 1.5
moderately stable	F	1.5 < ΔT/Δz ≤ 4.0
extremely stable	G	4.0 < ΔT/Δz

PASQUILL PRA Diffusion Typing Scheme[16]

ū(10) m/s	ΔT/Δz (°C/100 m)					
	< -1.9	-1.9 to -1.7	-1.7 to -1.5	-1.5 to -0.5	-0.5 to 1.5	1.5 to 4.0
< 2	A	B	B	B	E	F
2-3	A	B	C	C	E	F
3-5	B	B	C	D	E	F
5-6	C	C	C	D	D	D
> 6	C	C	C	D	D	D

2. Wind fluctuation criteria for estimating Pasquill stability categories*[9]

Stability Category	Standard deviation of the horizontal wind **
A	$\sigma_A \geq 22.5°$
B	$17.5° \leq \sigma_A < 22.5°$
C	$12.5° \leq \sigma_A < 17.5°$
D	$7.5° \leq \sigma_A < 12.5°$
E	$3.8° \leq \sigma_A < 7.5°$
F	$\sigma_A < 3.8°$

* These criteria are appropriate for steady-state conditions, a measurement height of 10 m, for level terrain, and an aerodynamic surface roughness length of 15 cm. Care should be taken that the wind sensor is responsive enough for use in measuring wind direction fluctuations.

** A surface roughness factor of $(z_o/15\ cm)^{0.2}$, where z_o is the average surface roughness in centimeters within a radius of 1-3 km of the source, may be applied to the table values It should be noted that this factor, while theoretically sound, has not been subjected to rigorous testing and may not improve the estimates in all circumstances. A table of z_o values that may be used as a guide to estimating surface roughness is given in Smedman-Hogstrom and Hogstrom.

*** These criteria are from an NRC proposal. It would seem reasonable to restrict the possible categories to A through D during daytime hours with a restriction that for 10 m wind speeds above 6 m/s, conditions are neutral. Likewise, during the nighttime hours, some restrictions, as in the table, are needed to preclude occurrences of categories A through C.

Nighttime* Corrections for the Previous Table[9]

If the σ_A stability category is	And $\bar{u}(10)$ is	Then change into
A	< 2.9 m/s	F
	2.9 to 3.6 m/s	E
	≥ 3.6 m/s	D
B	< 2.4 m/s	F
	2.4 to 3.0 m/s	E
	≥ 3.0 m/s	D
C	< 2.4 m/s	E
	≥ 2.4 m/s	D
D	wind speed not considered	D
E	wind speed not considered **	E
F	wind speed not considered ***	F

* Nighttime is considered to be from 1 hour prior to sunset to 1 hour after sunrise

** The original Mitchell and Timbre table had no wind speed restrictions; however, the original Pasquill criteria suggest that for wind speeds greater than 5 m/s, neutral conditions should be used.

*** The original Mitchell and Timbre table had no wind speed restrictions; however, the original Pasquill criteria suggest that for wind speeds greater than or equal to 5 m/s, the D category would be appropriate, and for wind speeds between 3 m/s and 5 m/s, the E category should be used

Expert L

Basic Philosophy of Approach

My approach to the elicitation questions is to use straightforward analytical formulas that can be solved by hand calculations. Most of the formulas are taken from the *Handbook on Atmospheric Diffusion* by Hanna et al.[1] These same formulas are used as the foundation for advanced computerized models such as OCD (Hanna et al.)[2] and HPDM (Hanna and Chang).[3] The estimates of uncertainty are based on more recent work that I have done in two areas: (1) the development of methods for estimating the probability distribution function (PDF) of concentration fluctuations,[4,5,6,7] and (2) the evaluation of many types of atmospheric dispersion models with observations from field experiments.[1-3,8-21] The reference list at the end of this report provides information on the publications used in this analysis.

Dispersion Model

The so-called straight-line Gaussian dispersion model is used:

$$\chi/Q = \left(2\pi u \sigma_y \sigma_z\right)^{-1} \exp\left(-(y - y_o)^2/2\sigma_y^2\right) \cdot \left(\exp\left((z - h_e)^2/2\sigma_z^2\right) + \exp\left((z + h_e)^2/2\sigma_z^2\right)\right) \quad (1)$$

where the plume centerline is located at lateral position y_o and release height h_e. The wind speed, u, should be representative of the release height. The dispersion parameters, σ_y and σ_z, are assumed to be given by the Briggs rural and urban formulas, as listed in Table 4.5 of Hanna et al.[1] In general, the rural curves are used in this exercise. The σ_y and σ_z parameters are given as functions of stability class, which can be estimated using the Pasquill method (based on wind speed and insolation - see Table 4.1 of Hanna et al.),[1] the dT/dz method, the σ_θ method (see Table 4.3 of Hanna et al.),[1] or as a function of 1/L and z_o (the Golder method, shown in Figure 4.3 of Hanna et al.).[1] These tables and figures are reproduced at the end of this brief discussion. The Briggs σ_y and σ_z curves are valid for averaging times in the range from about 10 minutes to one hour. For smaller averaging times, T_a, a one-fifth power law correction is applied to σ_y:

$$\sigma_y(T_a) = \sigma_y(Briggs)\ (T_a/10\ \text{min})^{1/5} \quad (2)$$

where T_a should not be allowed to drop below 1/3 minutes. This lower limit prevents σ_y from decreasing below the known σ_y for instantaneous puffs.

The Briggs σ_y curves are assumed to be valid to downwind distances of 10 km. At distances in the range from 10 km to 100 km, σ_y grows linearly with x, at a rate equal to the leading constant in the Briggs formulas. However, at very large distances (e.g., x = 80 km, 200 km, and 1000 km in Question E), it is assumed that $\sigma_y = 0.1$ x for all stabilities, in agreement with extensive regional scale field data.[1]

The mixing height, h, will act as a barrier to upward dispersion as σ_z approaches h. We do not allow σ_z to exceed 0.8 h, in agreement with recommendations in the EPA's Turner Workbook.[22]

Assumptions for Uncertainty Estimates

Recent comparisons[1] of the predictions of short-range air quality models with observations (Hanna, 1993)[3] demonstrate that, even in the best of circumstances, the root-mean-square-error (rmse) is about 30 or 40% of the mean. In routine applications, the rmse is in the range from 50% to a factor of two of the mean, similar to estimates made 15 years ago by a panel of experts.[20] In the current study, we assume a factor of four uncertainty for concentrations at locations not too far from the plume centerline (i.e., $(z - h_e)/\sigma_z \leq 1.5$ and $(y - y_o)/\sigma_y \leq 1.5$). This range of uncertainties covers the 5th to 95th percentile of the distributions. At greater distances from the centerline, this uncertainty is assumed to increase to a factor of eight.

The uncertainty in normalized concentration predictions, χ/Q, is assumed to be due solely and equally to uncertainties in σ_y and σ_z. It follows that the individual dispersion parameters each have an uncertainty of a factor of 2. Because the stability class is not well-defined in a few of the elicitation questions, in those cases the predictions are made over the range of possible stability classes, adding to the total uncertainty.

We were also asked to provide minimum and maximum bounds on the elicitation variables. These bounds are assumed to be about a factor of four on σ_y and σ_z. Near the plume centerline, the minimum χ/Q is assumed to be a factor of 20 below the median, and the maximum χ/Q is assumed to be a factor of 8 above the median. In most cases, the minimum χ/Q at distances of one σ_y or one σ_z or more from the plume centerline is assumed to be 0.0, on the grounds that the plume could completely miss the monitor. At these off-centerline distances the maximum χ/Q is assumed to be four times the calculated centerline concentration.

Dispersion Tables

N/A = not provided by expert

A-1: -2.0 K/100m Temp Lapse Rate Urban & Rural Surface Roughness					
Downwind distance	**Quantile**	**chiC/Q**	**chi(y)/chiC**	**chi(z)/chiC**	**sig-y**
0.5km	**0%**	N/A	N/A	N/A	N/A
	5%	8.50E-06	1.20E-02	1.77E-01	3.90E+01
	50%	3.40E-05	9.30E-02	7.10E-01	7.80E+01
	95%	1.36E-04	7.40E-01	2.84E+00	1.56E+02
	100%	N/A	N/A	N/A	N/A
1.0km	**0%**	N/A	N/A	N/A	N/A
	5%	2.17E-06	1.83E-02	1.15E-01	7.60E+01
	50%	8.66E-06	1.46E-01	4.60E-01	1.53E+02
	95%	3.46E-05	8.00E-01	1.84E+00	3.06E+02
	100%	N/A	N/A	N/A	N/A
3.0km	**0%**	N/A	N/A	N/A	N/A
	5%	2.63E-07	1.60E-02	9.50E-02	2.11E+02
	50%	1.05E-06	1.30E-01	3.80E-01	4.21E+02
	95%	4.20E-06	8.00E-01	1.52E+00	8.42E+02
	100%	N/A	N/A	N/A	N/A
10.0km	**0%**	N/A	N/A	N/A	N/A
	5%	4.40E-08	1.10E-02	N/A	5.65E+02
	50%	1.76E-07	8.70E-02	N/A	1.13E+03
	95%	7.04E-07	7.00E-01	N/A	2.26E+03
	100%	N/A	N/A	N/A	N/A
30.0km	**0%**	N/A	N/A	N/A	N/A
	5%	1.15E-08	3.80E-02	N/A	2.17E+03
	50%	4.59E-08	3.01E-01	N/A	4.33E+03
	95%	1.84E-07	9.00E-01	N/A	8.66E+03
	100%	N/A	N/A	N/A	N/A

A-2: -1.6 K/100m Temp Lapse Rate Urban & Rural Surface Roughness					
Downwind distance	Quantile	chiC/Q	chi(y)/chiC	chi(z)/chiC	sig-y
0.5km	0%	N/A	N/A	N/A	N/A
	5%	9.75E-06	2.26E-02	1.05E-01	2.70E+01
	50%	3.90E-05	1.81E-01	4.18E-01	5.40E+01
	95%	1.56E-04	9.00E-01	9.50E-01	1.08E+02
	100%	N/A	N/A	N/A	N/A
1.0km	0%	N/A	N/A	N/A	N/A
	5%	2.60E-06	2.00E-02	9.80E-02	5.30E+01
	50%	1.04E-05	1.64E-01	3.91E-01	1.05E+02
	95%	4.16E-05	9.00E-01	9.50E-01	2.10E+02
	100%	N/A	N/A	N/A	N/A
3.0km	0%	N/A	N/A	N/A	N/A
	5%	3.65E-07	2.80E-02	1.05E-01	1.45E+02
	50%	1.46E-06	2.24E-01	4.18E-01	2.89E+02
	95%	5.84E-06	9.50E-01	9.50E-01	5.78E+02
	100%	N/A	N/A	N/A	N/A
10.0km	0%	N/A	N/A	N/A	N/A
	5%	5.58E-08	1.94E-02	N/A	3.89E+02
	50%	2.23E-07	1.55E-01	N/A	7.78E+02
	95%	8 92E-07	9.00E-01	N/A	1.56E+03
	100%	N/A	N/A	N/A	N/A
30.0km	0%	N/A	N/A	N/A	N/A
	5%	8.40E-09	1.01E-01	N/A	1.49E+03
	50%	3.36E-08	4.07E-01	N/A	2.98E+03
	95%	1.34E-07	9.50E-01	N/A	5.96E+03
	100%	N/A	N/A	N/A	N/A

A-3: -1.0 K/100m Temp Lapse Rate Urban & Rural Surface Roughness					
Downwind distance	**Quantile**	**chiC/Q**	**chi(y)/chiC**	**chi(z)/chiC**	**sig-y**
0.5km	**0%**	N/A	N/A	N/A	N/A
	5%	1.50E-05	4.70E-03	1.10E-02	2.00E+01
	50%	6.01E-05	3.80E-02	8.70E-02	3.90E+01
	95%	2.40E-04	3.04E-01	6.90E-01	7.80E+01
	100%	N/A	N/A	N/A	N/A
1.0km	**0%**	N/A	N/A	N/A	N/A
	5%	4.60E-06	1.80E-02	3.90E-03	3.80E+01
	50%	1.84E-05	1.44E-01	3.10E-02	7.60E+01
	95%	7.36E-05	7.50E-01	2.48E-01	1.52E+02
	100%	N/A	N/A	N/A	N/A
3.0km	**0%**	N/A	N/A	N/A	N/A
	5%	8 23E-07	3.10E-02	6.10E-04	1.05E+02
	50%	3.29E-06	2.50E-01	4.90E-03	2.10E+02
	95%	1.32E-05	9.50E-01	3.92E-02	4.20E+02
	100%	N/A	N/A	N/A	N/A
10.0km	**0%**	N/A	N/A	N/A	N/A
	5%	1.56E-07	2.60E-02	N/A	1.42E+02
	50%	6.24E-07	2.10E-01	N/A	5.66E+02
	95%	2.50E-06	9.00E-01	N/A	2.26E+03
	100%	N/A	N/A	N/A	N/A
30.0km	**0%**	N/A	N/A	N/A	N/A
	5%	2.31E-08	6.50E-02	N/A	1.08E+03
	50%	9.23E-08	5.20E-01	N/A	2.17E+03
	95%	3.69E-07	9.50E-01	N/A	4.33E+03
	100%	N/A	N/A	N/A	N/A

A-4: 2.5 K/100m Temp Lapse Rate Urban & Rural Surface Roughness					
Downwind distance	Quantile	chiC/Q	chi(y)/chiC	chi(z)/chiC	sig-y
0.5km	0%	N/A	N/A	N/A	N/A
	5%	7.58E-05	2.10E-01	9.00E-02	2.50E+01
	50%	3.03E-04	8.40E-01	3.60E-01	5.00E+01
	95%	1.21E-03	9.90E-01	9.00E-01	1.00E+02
	100%	N/A	N/A	N/A	N/A
1.0km	0%	N/A	N/A	N/A	N/A
	5%	2.28E-05	1.02E-01	6.40E-03	4.75E+01
	50%	9.10E-05	8.20E-01	5.10E-02	9.50E+01
	95%	3.64E-04	1.00E+00	4.10E-01	1.90E+02
	100%	N/A	N/A	N/A	N/A
3.0km	0%	N/A	N/A	N/A	N/A
	5%	4.00E-06	2.13E-01	5.10E-05	1.30E+02
	50%	1.60E-05	8.50E-01	4.10E-04	2.60E+02
	95%	6.40E-05	9.90E-01	3.28E-03	5.20E+02
	100%	N/A	N/A	N/A	N/A
10.0km	0%	N/A	N/A	N/A	N/A
	5%	9.35E-07	1.00E-01	4.10E-10	3.55E+02
	50%	3.74E-06	7 80E-01	3.30E-09	7.10E+02
	95%	1.50E-05	1.00E+00	2.64E-08	1.42E+03
	100%	N/A	N/A	N/A	N/A
30.0km	0%	N/A	N/A	N/A	N/A
	5%	2.05E-07	2.23E-01	1.00E-12	1.36E+03
	50%	8.20E-07	8.90E-01	1.00E-11	2.71E+03
	95%	3.28E-06	1.00E+00	1.00E-10	5.42E+03
	100%	N/A	N/A	N/A	N/A

B-1: Unknown Lapse Rate 6.0 m/s Aver. Wind Speed		
Downwind distance	**Quantile**	**chiC/Q(ground level)**
220. m	**0%**	N/A
	5%	5.20E-06
	50%	4.14E-05
	95%	3.32E-04
	100%	N/A
315. m	**0%**	N/A
	5%	1.27E-05
	50%	5.07E-05
	95%	2.03E-04
	100%	N/A

B-2: Unknown Lapse Rate 5.0 m/s Aver. Wind Speed		
Downwind distance	**Quantile**	**chiC/Q(ground level)**
220. m	**0%**	N/A
	5%	1.72E-05
	50%	6.88E-05
	95%	2.75E-04
	100%	N/A
315. m	**0%**	N/A
	5%	1.33E-05
	50%	5.13E-05
	95%	2.05E-04
	100%	N/A

B-3: Unknown Lapse Rate 8.0 m/s Aver. Wind Speed		
Downwind distance	**Quantile**	**chiC/Q(ground level)**
300. m	**0%**	N/A
	5%	9.53E-06
	50%	3.81E-05
	95%	1.52E-04
	100%	N/A
600. m	**0%**	N/A
	5%	5.75E-06
	50%	2.30E-05
	95%	9.20E-05
	100%	N/A

B-4: -1.0 K/100m Temp Lapse Rate Flat Surface Roughness		
Downwind distance	**Quantile**	**chiC/Q(ground level)**
300. m	**0%**	N/A
	5%	2.53E-05
	50%	1.01E-04
	95%	4.04E-04
	100%	N/A
600. m	**0%**	N/A
	5%	1.52E-05
	50%	6.10E-05
	95%	2.44E-04
	100%	N/A

B-5: 3.0 K/100m Temp Lapse Rate Flat Surface Roughness					
Downwind distance	**Quantile**	**chi(y)/chiC**	**chi(z)/chiC**	**sig-y**	**sig-z**
600. m	**0%**	N/A	N/A	N/A	N/A
	5%	8.40E-02	5.90E-02	2.80E+01	4.00E+00
	50%	6.70E-01	4.70E-01	5.60E+01	8.10E+00
	95%	5.36E+00	9.70E-01	1.12E+02	1.62E+01
	100%	N/A	N/A	N/A	N/A

C: Stable Conditions Urban & Rural Surface Roughness				
Downwind distance	**Quantile**	**60 min**	**120 min**	**240 min**
360. m	**0%**	N/A	N/A	N/A
	5%	7.50E-10	8.00E-10	8.00E-10
	50%	6.10E-09	6.40E-09	6.40E-09
	95%	4.90E-08	5.20E-08	5.10E-08
	100%	N/A	N/A	N/A
970. m	**0%**	N/A	N/A	N/A
	5%	7.00E-07	8.00E-07	8.00E-07
	50%	5.40E-06	6.20E-06	6.00E-06
	95%	4.40E-05	4.80E-05	4.80E-05
	100%	N/A	N/A	N/A
1970. m	**0%**	N/A	N/A	N/A
	5%	1.35E-06	1.90E-06	2.00E-06
	50%	5.40E-06	7.60E-06	7.60E-06
	95%	2.00E-05	3.00E-05	3.00E-05
	100%	N/A	N/A	N/A

D: Stable Conditions Flat Surface Roughness				
Downwind distance	Quantile	chiC/Q	sig-y	sig-z
60. m	0%	N/A	N/A	N/A
	5%	6.60E-03	1.14E+00	8.90E-01
	50%	2.64E-02	2.27E+00	1.77E+00
	95%	1.06E-01	4.54E+00	3.54E+00
	100%	N/A	N/A	N/A

E: Length of Arc Crossed By 90% of the Material		
Downwind distance	Quantile	90% arc
80.km	0%	N/A
	5%	8.00E+03
	50%	3.20E+04
	95%	1.30E+05
	100%	N/A
200.km	0%	N/A
	5%	2.00E+04
	50%	8.00E+04
	95%	3.20E+05
	100%	N/A
1000.km	0%	N/A
	5%	1.00E+05
	50%	4.00E+05
	95%	1.60E+06
	100%	N/A

References

1. Hanna, S.R., G.A. Briggs, and R.P. Hosker, Jr., "Handbook on Atmospheric Diffusion," DOE/TIC-11223, Technical Information Center, U.S. Department of Energy, Oak Ridge, TN, p. 102, 1982.

2. Hanna, S.R., et al., "Development and Evaluation of the Offshore and Coastal Diffusion Model," *Journal of the Air Pollution Control Association*, 35:1039-1047, 1985.

3. Hanna, S.R., and J.C. Chang, "Hybrid Plume Dispersion Model (HPDM) Improvements and Testing at Three Field Sites," *Atmospheric Environment*, 27A:1491-1508, 1993.

4. Hanna, S.R., "Plume Dispersion and Concentration Fluctuations in the Atmosphere," (P.N. Cheremisinoff, ed.), *Encyclopedia of Environmental Control Technology, Volume 2: Air Pollution Control*, Gulf Publishing Co., Houston, TX, pp. 547-582, 1989.

5. Hanna, S.R., "The Effect of Line Averaging on Concentration Fluctuations," *Boundary-Layer Meteorology*, 40:329-338, 1987.

6. Hanna, S.R., "Spectra of Concentration Fluctuations: The Two Time Scales of a Meandering Plume," *Atmospheric Environment*, 20:1131-1137, 1986.

7. Hanna, S.R., "The Exponential Probability Density Function and Concentration Fluctuations in Smoke Plumes," *Boundary-Layer Meteorology*, 29:361-376, 1984.

8. Hanna, S.R., "Uncertainties in Air Quality Model Predictions," *Boundary-Layer Meteorology*, 62:3-20, 1993.

9. Hanna, S.R., J.C. Chang, and D.G. Strimaitis, "Hazardous Gas Model Evaluation with Field Observations," *Atmospheric Environment*, 27A:2265-2285, 1993.

10. Hanna, S.R., and J.C. Chang, "Representativeness of Wind Measurements on a Mesoscale Grid with Station Separations of 312 m to 10000 km," *Boundary-Layer Meteorology*, 60:309-324, 1992.

11. Hanna, S.R., and J.C. Chang, "Boundary-Layer Parameterizations for Applied Dispersion Modeling Over Urban Areas, *Boundary-Layer Meteorology*, 58:229-259, 1992.

12. Hanna, S.R., et al., "Results from the Model Evaluation Panel," *Plant Operations Progress*, 11:2-5, 1992.

13. Hanna, S.R., et al., "Evaluation of 14 Hazardous Gas Models with Ammonia and Hydrogen Fluoride Field Data, *Journal of Hazardous Materials*, 26:127-158, 1991.

14. Hanna, S.R., J.C. Chang, and D.G. Strimaitis, "Uncertainties in Source Emission Rate Estimates Using Dispersion Models," *Atmospheric Environment*, 24A:2971-2980, 1990.

15. Hanna, S.R., "Lateral Dispersion in Light-Wind Stable Conditions," *Il Nuovo Cimento*, 13C:889-894, 1990.

16. Hanna, S.R., "Confidence Limits for Air Quality Models, as Estimated by Bootstrap and Jackknife Resampling Methods," *Atmospheric Environment*, 23:1385-1398, 1989.

17. Hanna, S.R. "Air Quality Model Evaluation and Uncertainty," *Journal of the Air Pollution Control Association*, 38:406-412, 1988.

18. Hanna, S.R., "Lateral Dispersion From Tall Stacks," *Journal of Climate and Applied Meteorology*, 25:1426-1433, 1986.

19. Hanna, S.R., "Lateral Turbulence Intensity and Plume Meandering During Stable Conditions," *Journal of Climate and Applied Meteorology*, 25:1424-1430, 1983.

20. Hanna, S.R., "Accuracy of Dispersion Models, A Position Paper of the AMS 1977 Committee on Atmospheric Turbulence and Diffusion," *Bulletin American Meteorological Society*, 59:1025-1026, 1978.

21. Hanna, S.R., et al., "AMS Workshop on Stability Classification Schemes and Sigma Curves—Summary of Recommendations," *Bulletin American Meteorological Society*, 58:1305-1309, 1977.

22. Turner, D., "Workbook of Atmospheric Dispersion Estimates," Environmental Health Series: Air Pollution, Public Health Service Publication No. 999-AP-26, U.S. Dept. of Health, Education, and Welfare, National Center for Air Pollution Control, Cincinnati, OH, 1967.

Expert M

Introduction

The objective of this work is to assess the uncertainties associated with estimations of the concentrations expected at selected sites situated downwind from a hypothetical release point during a variety of meteorological conditions. The uncertainties are expressed as expected concentration distributions listing the median, the .05, and .95 quantiles. The approach used for deriving these distributions is based on (1) the variability of experimental data acquired from tracer studies, (2) uncertainties associated with estimating stability classification, (3) uncertainties due to non-representative meteorological measurements acquired at a single location, and (4) our model development and evaluation experience. Two different types of models were used for this work: a three-dimensional diagnostic wind field model coupled with a Lagrangian dispersion model and a standard sequential puff model. For the problems concerning dispersion over rural and urban areas the diagnostic wind field/Lagrangian dispersion models were used to derive the best estimates of the median concentrations (except for Problem 10) while the fast running sequential puff code was used to define the concentration distribution around the median values. However, only the sequential puff model was used for the flat terrain problems.

Model Description

The diagnostic wind field model interpolates wind observations over a three-dimensional numerical grid to calculate a mass-consistent wind field over flat and spatially varying terrain surfaces. All calculations performed in this work were over flat terrain surfaces. The Lagrangian particle model advects the marker particles downwind by using these wind fields while at the same time it diffuses the material due to atmospheric turbulence. The rate of diffusion was calculated by a statistical method based on the Langevin equation. The model input requires estimates of σ_v and σ_w, which may be derived from values of σ_θ and 1/L. The lapse rate was not used directly except as another indicator of atmospheric stability.

The sequential puff model simulated the dispersion of a series of individual puffs within a spatially homogeneous wind field over flat terrain. The downwind concentrations were acquired by integrating the individual puffs over the specified sampling times and locations. The meteorological input data required for this model consist of an average wind speed and the horizontal and vertical diffusion coefficients (σ_y and σ_z, respectively). Typically, 500 puffs were released over the sampling times of interest. The code was run 100 times for each sampling location using input data statistically chosen within a prescribed range of uncertainty associated with each model input parameter.

Source of Uncertainty

The primary sources of uncertainty considered in this work were (1) natural variations of boundary layer dispersion characteristics for supposedly similar meteorological and terrain situations, (2) the variability associated with estimating the stability classification, and (3) the uncertainty of measurements due to instrument error or non-representivity. An assessment of the first source of uncertainty can be achieved by a review of the data acquired from some of the field experiments conducted over the past four decades in both the U.S. and Europe. These include tracer releases coordinated with extensive sampling arrays extending out to several tens of kilometers over terrain surfaces that range from flat to complex and over rural and urban areas. Reviews by Gifford[1] and Draxler[2] are most useful. The data consistently show considerable scatter in the estimates of σ_y and σ_z values as a function of distance for a particular stability category. Typically, one observes scatter of the individual data within a factor of 2 - 3 or more of the best least squares fit to the data.

The uncertainties inherent in determining the dispersion characteristics of a particular meteorological situation (as usually defined by discrete stability categories) are due to a whole array of factors that are mainly associated with our lack of understanding of boundary layer behavior and our inability to measure the critical parameters accurately over the entire spatial and temporal domains of interest. Typically, we only have a single point of measurement such as an instrumented tower, where winds and temperature observations are made. Measurement uncertainties certainly include instrument error but often more importantly are due to the non-representativeness of the measurement location. For instance, the use of lapse rate measurements, acquired from a meteorological tower, has been found to be a generally poor indicator of atmospheric stability since it is not spatially representative of the vertical stability within the boundary layer. It is interesting to note that individual investigators may derive quite different stability frequency distributions for the same meteorological data sets as a result of our ignorance of boundary layer behavior. These distributions may differ by as much as a factor of two for the number of cases within a particular stability category.[3]

Model Results

Problems 1–4.

These problems are very similar in nature with the main difference being varying stability categories, starting with very unstable (Problem 1) and proceeding to very stable (Problem 4). The Lagrangian dispersion model was used to calculate a best estimate of the median concentration for each sampling location. These values are given in the attached tables for each problem. The .05 and the .95 quantiles associated with the median concentrations were derived from multiple runs of the sequential puff model using wind speed, σ_y, and σ_z values stochastically chosen within their respective range of uncertainty. The resulting concentration distributions were normalized to the Lagrangian model-generated median concentrations.

The input to the diagnostic wind field/Lagrangian dispersion models included the reported σ_θ values for estimating horizontal diffusion, a 1/L value derived from the surface roughness and the stability category (as determined by the reported lapse rate) and the Golder[4] curves for estimating vertical diffusion, and the wind speed. The sequential puff model requires values of wind speed, σ_y, and σ_z as a function of distance. Since the terrain and surface roughness involve a mixture of both rural and urban areas, it seemed appropriate to use a combination of σ_y and σ_z values acquired from experiments conducted over both types of areas. Thus, values intermediate between those relevant to flat terrain (Pasquill-Gifford curves) and those related to urban dispersion were derived (Briggs[5] urban values). The uncertainty associated with stability category estimation was assumed to be ± 1 stability category on either side (for example, a C category has an uncertainty range that includes B and D categories). The reported wind speeds were assumed to have an uncertainty of ± 1 m/s due to both instrument error and non-representivity over distances of tens of kilometers. Using these uncertainty bands, the sequential puff model was run 100 times to derive the .05 and the .95 quantiles associated with the median concentrations listed in the tables, as well as the medians and the quantiles associated with the ratios of off-center concentrations to plume centerline concentrations. The σ_y values given in the tables were derived from the distributions used by the model. The estimated stability category for each is: Problem 1 (greatly unstable), Problem 2 (unstable), Problem 3 (neutral), and Problem 4 (stable).

Problems 5–9

Since these problems involve flat terrain surfaces with short grass over very short distances, the concentration estimates were derived directly from the sequential puff model. This set of problems involve varying the stability categories for the same source configuration and in some cases even using different stability categories in the horizontal and vertical directions. The model calculations are based on using standard Pasquill-Gifford diffusion curves for flat terrain, an uncertainty of ± 1 stability category of the best estimate for both the vertical and horizontal directions, and a wind speed uncertainty of ±0.5 m/s (for flat terrain and short distance). Sampling the model input values within this range of uncertainty in a statistical fashion for 100 model calculations, the concentration distributions or the ratios are given in the attached tables for each sampling location. The stability classifications for each problem are: Problem 5 (horizontal - neutral to slightly stable; vertical - slightly unstable); Problem 6 (horizontal - neutral; vertical - neutral to slightly unstable); Problem 7 (horizontal - unstable; vertical - unstable); Problem 8 (horizontal - neutral; vertical-neutral); Problem 9 (horizontal - stable; vertical - stable). Since the Pasquill-Gifford curves were derived from 10 minute concentrations and Problems 5-9 specify 60 min sampling, the σ_y and σ_z values were adjusted by the factor $(60/10)^{0.2}$ to account for plume meander.

Problem 10

The sequential puff model was used in a manner similar to that for Problems 5-9 with σ_y and σ_z values derived from the Pasquill-Gifford and the Briggs curves as in Problems 1-4. The stability uncertainty was assumed to be ± 1 stability category. The wind speed uncertainty was assumed to be ± 0.5 m/s.

Problem 11

This problem represents a stable meteorological situation based on very little information. A Pasquill-Gifford E stability category was assumed. However, since one minute sample averaging is required the stability was increased to the F category to minimize plume meander.

Problem 12

No calculations were performed for this problem. Instead we utilized the data from the Australian experiments at Mt. Isa and Kalgoorlie[6] as well as the ANATEX[7] experiments carried out across the U.S. to estimate the arc lengths at various downwind distances.

Consistency Checks

After all the calculations were completed, a review was undertaken of all the results to ensure that the estimated

concentrations and their uncertainties agreed with our modeling experience and were consistent within the respective problem sets. This review led to a number of adjustments; mainly to tighten or broaden the range of uncertainties associated with specific problems. To assist in this process a number of model calculations were performed to evaluate the sensitivity of various model input parameter assumptions on the concentration frequency distributions.

Dispersion Tables

N/A = not provided by expert

A-1: -2.0 K/100m Temp Lapse Rate Urban & Rural Surface Roughness					
Downwind distance	**Quantile**	**chiC/Q**	**chi(y)/chiC**	**chi(z)/chiC**	**sig-y**
0.5km	**0%**	N/A	N/A	N/A	N/A
	5%	2.40E-06	1.00E-01	2.50E-01	7.00E+01
	50%	8.30E-06	5.40E-01	7.70E-01	1.10E+02
	95%	2.50E-05	9.00E-01	8.50E-01	1.50E+02
	100%	N/A	N/A	N/A	N/A
1.0km	**0%**	N/A	N/A	N/A	N/A
	5%	1.20E-06	1.00E-01	1.50E-01	1.30E+02
	50%	4.00E-06	3.50E-01	6.00E-01	2.00E+02
	95%	1.10E-05	4.80E-01	8.20E-01	2.70E+02
	100%	N/A	N/A	N/A	N/A
3.0km	**0%**	N/A	N/A	N/A	N/A
	5%	3.10E-07	5.00E-02	1.50E-01	3.60E+02
	50%	8.00E-07	2.50E-01	4.50E-01	5.10E+02
	95%	2.50E-06	4.00E-01	9.00E-01	6.50E+02
	100%	N/A	N/A	N/A	N/A
10.0km	**0%**	N/A	N/A	N/A	N/A
	5%	2.50E-08	5.00E-02	N/A	1.00E+03
	50%	1.50E-07	1.40E-01	N/A	1.30E+03
	95%	3.10E-07	2.60E-01	N/A	1.60E+03
	100%	N/A	N/A	N/A	N/A
30.0km	**0%**	N/A	N/A	N/A	N/A
	5%	9.10E-10	8.00E-03	N/A	2.00E+03
	50%	1.90E-08	4.00E-02	N/A	2.70E+03
	95%	6.00E-08	2.50E-01	N/A	4.20E+03
	100%	N/A	N/A	N/A	N/A

A-2: -1.6 K/100m Temp Lapse Rate Urban & Rural Surface Roughness					
Downwind distance	Quantile	chiC/Q	chi(y)/chiC	chi(z)/chiC	sig-y
0.5km	0%	N/A	N/A	N/A	N/A
	5%	5.80E-06	1.00E-01	3.00E-02	5.00E+01
	50%	1.50E-05	3.80E-01	6.70E-01	1.00E+02
	95%	6.20E-05	7.30E-01	8.30E-01	1.50E+02
	100%	N/A	N/A	N/A	N/A
1.0km	0%	N/A	N/A	N/A	N/A
	5%	2.10E-06	8.00E-02	2.00E-02	8.00E+01
	50%	5.60E-06	3.60E-01	3.80E-01	1.50E+02
	95%	2.30E-05	7.00E-01	8.40E-01	2.60E+02
	100%	N/A	N/A	N/A	N/A
3.0km	0%	N/A	N/A	N/A	N/A
	5%	2.80E-07	7.00E-02	2.00E-02	2.10E+02
	50%	1.20E-06	3.80E-01	7.50E-01	3.70E+02
	95%	4.40E-06	6.90E-01	9.00E-01	6.00E+02
	100%	N/A	N/A	N/A	N/A
10.0km	0%	N/A	N/A	N/A	N/A
	5%	5.00E-08	1.10E-01	N/A	6.50E+02
	50%	1.50E-07	4.70E-01	N/A	9.50E+02
	95%	6.70E-07	8.80E-01	N/A	1.40E+03
	100%	N/A	N/A	N/A	N/A
30.0km	0%	N/A	N/A	N/A	N/A
	5%	5.00E-09	3.00E-02	N/A	1.50E+03
	50%	2.80E-08	1.40E-01	N/A	2.00E+03
	95%	1.20E-07	3.70E-01	N/A	3.00E+03
	100%	N/A	N/A	N/A	N/A

A-3: -1.0 K/100m Temp Lapse Rate Urban & Rural Surface Roughness					
Downwind distance	**Quantile**	**chiC/Q**	**chi(y)/chiC**	**chi(z)/chiC**	**sig-y**
0.5km	**0%**	N/A	N/A	N/A	N/A
	5%	7.30E-06	8.00E-02	4.00E-02	3.00E+01
	50%	3.80E-05	2.40E-01	2.60E-01	6.00E+01
	95%	6.50E-05	5.80E-01	7.80E-01	1.00E+02
	100%	N/A	N/A	N/A	N/A
1.0km	**0%**	N/A	N/A	N/A	N/A
	5%	4.00E-06	8.00E-02	1.00E-02	5.00E+01
	50%	1.90E-05	3.20E-01	2.50E-01	1.00E+02
	95%	6.30E-05	6.70E-01	9.00E-01	1.70E+02
	100%	N/A	N/A	N/A	N/A
3.0km	**0%**	N/A	N/A	N/A	N/A
	5%	1.70E-06	5 00E-02	7.00E-03	1.50E+02
	50%	4.50E-06	2.70E-01	1.20E-01	2.50E+02
	95%	1 80E-05	6.30E-01	8.50E-01	4.10E+02
	100%	N/A	N/A	N/A	N/A
10.0km	**0%**	N/A	N/A	N/A	N/A
	5%	1.70E-07	7.00E-02	N/A	4.30E+02
	50%	6.10E-07	3.10E-01	N/A	6.50E+02
	95%	2.10E-06	5 40E-01	N/A	9.00E+02
	100%	N/A	N/A	N/A	N/A
30.0km	**0%**	N/A	N/A	N/A	N/A
	5%	2.50E-08	6.00E-02	N/A	1.00E+03
	50%	1 80E-07	2.80E-01	N/A	1.50E+03
	95%	5.50E-07	5.30E-01	N/A	2.20E+03
	100%	N/A	N/A	N/A	N/A

A-4: 2.5 K/100m Temp Lapse Rate Urban & Rural Surface Roughness					
Downwind distance	**Quantile**	**chiC/Q**	**chi(y)/chiC**	**chi(z)/chiC**	**sig-y**
0.5km	0%	N/A	N/A	N/A	N/A
	5%	2.10E-05	2.60E-01	5.30E-01	2.00E+01
	50%	7.80E-05	6.40E-01	7.00E-01	4.00E+01
	95%	3.00E-04	9.10E-01	9.60E-01	7.00E+01
	100%	N/A	N/A	N/A	N/A
1.0km	0%	N/A	N/A	N/A	N/A
	5%	1.80E-05	1.70E-01	8.00E-02	4.00E+01
	50%	4.80E-05	5.40E-01	5.20E-01	8.00E+01
	95%	2.60E-04	7.80E-01	9.40E-01	1.30E+02
	100%	N/A	N/A	N/A	N/A
3.0km	0%	N/A	N/A	N/A	N/A
	5%	4.30E-06	1 30E-01	2.00E-02	1.00E+02
	50%	1.50E-05	4.00E-01	2.80E-01	2.00E+02
	95%	8.00E-05	6.50E-01	9.20E-01	3.10E+02
	100%	N/A	N/A	N/A	N/A
10.0km	0%	N/A	N/A	N/A	N/A
	5%	5.20E-07	1.00E-01	3.00E-03	2.70E+02
	50%	2.20E-06	4.50E-01	2.90E-01	5.20E+02
	95%	9.10E-06	6.20E-01	9.00E-01	7.00E+02
	100%	N/A	N/A	N/A	N/A
30.0km	0%	N/A	N/A	N/A	N/A
	5%	1.50E-07	1.10E-01	1.00E-04	7.50E+02
	50%	5.20E-07	2.70E-01	1.00E-02	1.10E+03
	95%	3.90E-06	4.50E-01	1.00E-01	1.50E+03
	100%	N/A	N/A	N/A	N/A

B-1: Unknown Lapse Rate 6.0 m/s Aver. Wind Speed		
Downwind distance	**Quantile**	**chiC/Q(ground level)**
220. m	**0%**	N/A
	5%	8.00E-06
	50%	2.00E-05
	95%	6.00E-05
	100%	N/A
315. m	**0%**	N/A
	5%	1.00E-05
	50%	2.50E-05
	95%	6.50E-05
	100%	N/A

B-2: Unknown Lapse Rate 5.0 m/s Aver. Wind Speed		
Downwind distance	**Quantile**	**chiC/Q(ground level)**
220. m	**0%**	N/A
	5%	1.20E-05
	50%	3.10E-05
	95%	6.00E-05
	100%	N/A
315. m	**0%**	N/A
	5%	1.00E-05
	50%	2.60E-05
	95%	4.30E-05
	100%	N/A

B-3: Unknown Lapse Rate 8.0 m/s Aver. Wind Speed		
Downwind distance	**Quantile**	**chiC/Q(ground level)**
300. m	**0%**	N/A
	5%	6.10E-06
	50%	1.20E-05
	95%	3.00E-05
	100%	N/A
600. m	**0%**	N/A
	5%	2.10E-06
	50%	5.50E-06
	95%	1.30E-05
	100%	N/A

B-4: -1.0 K/100m Temp Lapse Rate Flat Surface Roughness		
Downwind distance	**Quantile**	**chiC/Q(ground level)**
300. m	**0%**	N/A
	5%	1.20E-05
	50%	3.70E-05
	95%	7.50E-05
	100%	N/A
600. m	**0%**	N/A
	5%	1.20E-05
	50%	2.70E-05
	95%	6.50E-05
	100%	N/A

B-5: 3.0 K/100m Temp Lapse Rate Flat Surface Roughness					
Downwind distance	Quantile	chi(y)/chiC	chi(z)/chiC	sig-y	sig-z
600. m	0%	N/A	N/A	N/A	N/A
	5%	1.00E-01	1.50E-01	2.00E+01	8.00E+00
	50%	3.50E-01	7.00E-01	3.50E+01	1.50E+01
	95%	7.60E-01	8.00E-01	5.00E+01	2.30E+01
	100%	N/A	N/A	N/A	N/A

C: Stable Conditions Urban & Rural Surface Roughness				
Downwind distance	Quantile	60 min	120 min	240 min
360. m	0%	N/A	N/A	N/A
	5%	1.00E-07	1.10E-07	1.10E-07
	50%	1.60E-05	1.70E-05	1.70E-05
	95%	6.60E-05	7.40E-05	7.20E-05
	100%	N/A	N/A	N/A
970. m	0%	N/A	N/A	N/A
	5%	1.20E-06	1.50E-06	1.40E-06
	50%	1.40E-05	1.70E-05	1.70E-05
	95%	3 40E-05	4.20E-05	4.40E-05
	100%	N/A	N/A	N/A
1970. m	0%	N/A	N/A	N/A
	5%	2.70E-06	3.40E-06	3.60E-06
	50%	5.40E-06	9.00E-06	8.80E-06
	95%	1.90E-05	3.60E-05	3.60E-05
	100%	N/A	N/A	N/A

D: Stable Conditions Flat Surface Roughness				
Downwind distance	Quantile	chiC/Q	sig-y	sig-z
60. m	0%	N/A	N/A	N/A
	5%	8.00E-05	3.00E+00	2.00E+00
	50%	3.00E-03	4.00E+00	4.00E+00
	95%	8.00E-03	1.00E+01	1.00E+01
	100%	N/A	N/A	N/A

E: Length of Arc Crossed By 90% of the Material		
Downwind distance	Quantile	90% arc
80.km	0%	N/A
	5%	1.20E+04
	50%	2.00E+04
	95%	5.00E+04
	100%	N/A
200.km	0%	N/A
	5%	3 00E+04
	50%	6.00E+04
	95%	1.60E+05
	100%	N/A
1000.km	0%	N/A
	5%	2.00E+05
	50%	4.50E+05
	95%	1.00E+06
	100%	N/A

References

1. Gifford, F.A., "Turbulent Diffusion-Typing Schemes: A Review," *Nuclear Safety*, 17:68-86, 1976.

2. Draxler, R.R., "Diffusion and Transport Experiments," (D. Randerson, ed.), *Atmospheric Science and Power Production*, DOE/TIC-27601, Technical Information Center, Office of Scientific and Technical Information, United States Department of Energy, Oak Ridge, TN, pp. 367-422, 1984.

3. Kretzschmar, J.G., and I. Mertens, "Influence of the Turbulence Typing Scheme Upon the Cumulative Frequency Distributions of the Calculated Relative Concentrations for Different Averaging Times," *Atmospheric Environment*, 18:2377-2393, 1984.

4. Golder D., "Relations Among Stability Parameters in the Surface Layer," *Boundary-Layer Meteorology*, 3:47-58, 1972.

5. Briggs, G.A., "Diffusion Estimation for Small Emissions," USAEC Report ATDL-106 (TID-28289), National Oceanic and Atmospheric Administration, Atmospheric Turbulence and Diffusion Laboratory, Oak Ridge, TN, May 1973.

6. Carras, J.N., and D.J. Williams, "Measurements of Relative σ_y up to 1800 Km From a Single Source," *Atmospheric Environment*, 22:1061-1069, 1988.

7. Clark, T.L., and R.D. Cohn, "The Across North America Tracer Experiment (ANATEX): Model Evaluation Study," EPA/600/3-90/051, Atmospheric Research and Exposure Assessment Laboratory, Office of Research and Development, U.S. Environmental Protection Agency, Research Triangle Park, NC, 1990.

Expert N

Introduction

The problem is to determine, for 11 given sets of meteorological conditions (called Case Structures), the downwind, centerline concentration and various other plume attributes, and to specify 5 and 95%, as well as 0 and 100%, quantiles of the uncertainty distributions of these quantities. The Case Structures refer to a non-depositing plume with negligible initial buoyancy and momentum, emitted from point sources at elevations of 10 to 45 m. Time-of-day of the releases is not specified as such. For the purpose of calculating diffusion, the surface roughness is essentially of the rural type. The surface is flat to gently rolling, and the given meteorological conditions are steady during the sampling time period. Sampling is assumed to begin at the time material is first observed at the sampling point, except in Case Structure #10, in which sampling starts at the time of release of material.

Diffusion Model

The diffusion model used, called GAUS1, is of the so-called "simple, straight-line, Gaussian" type. It evaluates over 70 of the most widely used Gaussian plume and puff equations and provides programs for evaluating indoor-outdoor concentration, explosion-cloud size, long-range diffusion, urban pollution, effective dosage and risk, buoyant rise, wet and dry deposition, and resuspension calculations GAUS1 is implemented on a Hewlett-Packard 48SX pocket calculator, making it ideal for the present study.

Some Properties of GAUS1

The general technical background of GAUS1 is that of Hanna et al.,[1] and most of the formulas it evaluates are found in that document. The following GAUS1 properties are relevant to the present application.

Atmospheric stability is defined in terms of the widely-used A,B,...F turbulence types as presented, for instance, in Table 4.5 of Hanna et al.,[1] the formulas recommended by Briggs.[2] When, as in the Case Structures, the stability is provided as vertical temperature lapse-rate and/or the horizontal wind standard deviation, sigma-theta, Tables V, VI, and VII of Briggs[2] provide the necessary conversions to the A...F types. (See also Hanna et al.,[1] p. 28, and Gifford[4] for useful conversions). Table 4.3 of Hanna et al.[1] enables the Monin-Obukhov stability length, L, to be converted to the corresponding letter-stability type. In some of the given case structures, enough data are provided to determine stability type in several alternate ways. In borderline cases this might produce two different stability classes. The procedure adopted here is to calculate the concentration and other end points using each stability class and then, in case there is a difference of a stability class, to average the resulting values. Mixing depth is handled as an input variable by GAUS1. The given Case Structures do not specify mixing depth, but we are asked to indicate the height of its possible influence. The default mixing depths of the model described during the Capelle meeting provide some guidance on this point, and have been used here. Wind Profile Adjustment: GAUS1 uses a power law to adjust the observed wind speed to that at the effective release height. Powers are those of Table 4.6, Hanna et al.,[1] which account for stability and surface roughness effects. Sampling Time: A power-law exponent equal to 0.2 is used to adjust the standard, 10-minute averaging period of diffusion lengths to times from 3 to 60 minutes, as recommended in Hanna et al.[1]

Estimates of Median Values of Concentrations and Standard Deviations

Case Structures 1-4:

These are evaluated on the BIVARIATE program of GAUS1, the standard bivariate Gaussian plume equation. For each of these cases we are asked to indicate the height at which the mixing depth is expected to be present. Lacking other guidance, I have used the default mixing depths discussed during the Capelle meeting, which ranged from 1500m for type A conditions to 400m for type F. In any cases for which the sum of the release height and σ_z exceeded these mixing depth defaults, GAUS1's program LIMITD MXG has been employed to calculate the uniform mixing concentration through the default depth. This occurs only at the 10km and 30km distances for Case Structure #1 and at 30km for #2. The difference at 10km is small, but at 30km for Case #1 the limited mixing concentration is 7 times higher than the ordinary (unlimited) result. Since we are given no information that might indicate the actual mixing depth (it could be several times 1500m), the uncertainty estimate will have to reflect this.

Case Structure #4 has been treated as a borderline case between F and E conditions, following the guideline discussed above. It is an F-case under both the lapse-rate and σ_θ criteria, but the 3 m/s wind makes it a borderline E-condition based on Pasquill's original scheme.

Case Structure #5:

This is a D-type bordering on E, judging by the small σ_θ value. Thus the results were calculated by each type and averaged.

Case Structure #6:

Similar to 5, with averaging between types C and D.

Case Structures #7 and 8:

Case Structure #7 is borderline between C and D; it was assigned to C on the basis of the considerable degree of instability indicated by the values of 1/L and σ_θ. Case Structure #8 is the classical "near-neutral" type D.

Case Structure #9:

Under the same ground-rule as for case #4, this case is treated as a borderline F-E type, and the results are averaged.

Case Structure #10:

This is an E-type according to the given σ_θ value. By the release duration and the averaged wind speed, the resulting cloud is almost 7 km long and will take about (slightly more than) an hour to pass overhead. By making the commonly used assumption that $\sigma_x = \sigma_y$, equating the cloud's border to $2 \times \sigma$ at each downwind distance, it is found that the elongation of the cloud along the axis of the wind adds about .5, 1.5, and 2.5 minutes to the passage time at the three downwind distances, respectively. Consequently the cloud elongation along the x-axis for the 60, 120, and 240 minutes' sampling time is accounted for by assuming that the sampler "sees" the cloud for the appropriate number of minutes, and the ground-level concentrations are calculated on that basis. That is, the cloud was assumed to be present at the sampler for those times, and absent for the remainder of the sampling interval.

Case Structure #11 (first part):

The turbulence type can only be approximately determined by Pasquill's rules as either D or E, depending on the cloud cover. Both were calculated and the average taken. It should be noted here that the 1-minute sampling time is quite an awkward one. It was found by Ekman, from plume observations made at Riso, that a low-level plume tends to behave like a Taylor time-averaged plume for as little as a 1-minute averaging. The same effect can be noticed in a 1-minute time-exposure photograph of a plume. There is, however, little data to support the time-averaging adjustment of concentrations and sigmas below about 3 minutes. It is interesting to compare the median values of the above calculation with those produced by a similar calculation on GAUS1's instantaneous source program, INST POINT. The results (averages of types D and E) are: χ/Q = .14; σ_y = 1.32m, σ_z = .83m. The relative concentration agrees quite well, but the instantaneous sigmas are appropriately somewhat smaller than the 1-minute values.

Case Structure #11 (second part):

At the distances in question, 80km, 200km, and 1000 km, the simple Gaussian plume model doesn't, in my opinion, apply. This was shown in the analysis of the Kinkaid[5] data to be true even at 50 km. At 80 km the cloud "age", assuming the given transport wind speed, is 7.4 hours. The cloud has passed well into the transition region between fully 3-D, planetary boundary layer turbulence and the essentially 2-D turbulent motions of the larger scales of motion, above several hundred km, as discussed in Gifford.[6] The time-scale defining the outer limit of the cloud-diffusing (3-D) range of atmospheric turbulence, the Lagrangian integral time-scale, is shown in the references to equal about 104 seconds (about 2.7 hours). Therefore the approach to calculating the cloud width (arc length) at these great distances uses the GAUS1 program LONG RANG, which implements the long-range cloud-spreading theory presented in Gifford.[6] The parameters required as inputs to this model are latitude, initial cloud width, transport wind speed, and a measure of the large-scale atmospheric mixing motions such as K, m^2/s, the tropospheric eddy diffusivity. The latitude has been assumed to equal 45 degrees, and the value of K to be 5×10^4, guided by the results described in Barr and Gifford,[7] which shows many applications to long-range cloud-spreading data. Further comparisons of this theory with more recent data, up to the Kuwait cloud, appear in Figure N-1. The given transport-wind speed of 3m/s is extremely unlikely to have applied during these long-range transports. A more reasonable value was calculated by using GAUS1's wind-profile program to extrapolate the given wind speed to 100 m. This should give a more appropriate value of the long-range transport wind. The required arc-length crossed by 90% of the cloud material was found by multiplying the calculated value of σ_y at a given distance by 1.3, to approximate the width corresponding to 90% of the plume material (90% of the area under a Gaussian distribution curve).

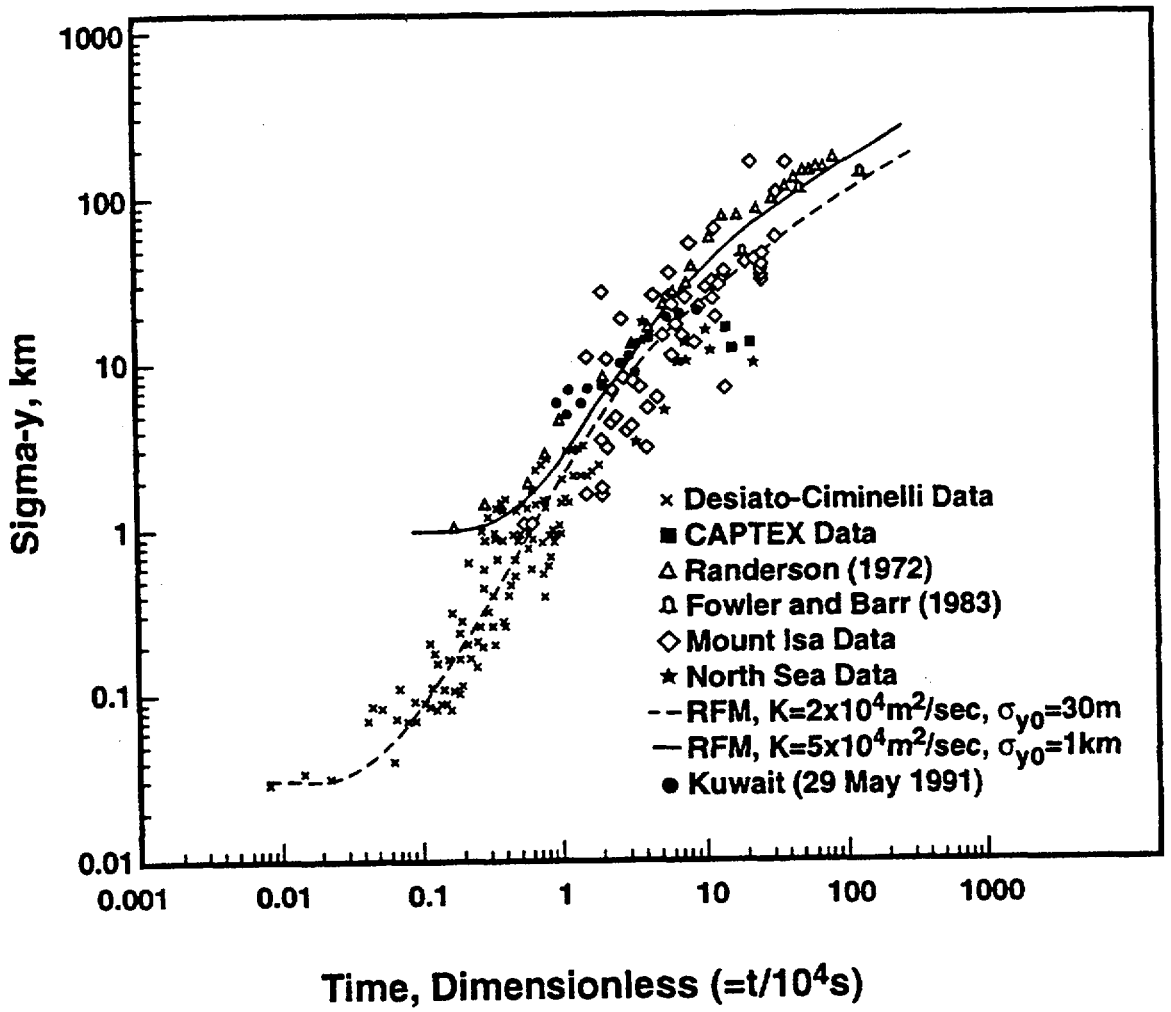

Figure N-1. Comparisons of transport data.

Percentile Estimates

In keeping with the approach of calculating the median values using the Gaussian equation, whose parameters are based on large amounts of experimental data, the determination of the 5th and 95th percentile points also relies heavily on the available data on plume model variability. Relevant data on the uncertainty of concentration estimates are contained in the summaries by Crawford[8] and Little and Miller.[9] (More recent data compilations, such as the EPRI Plume Model Validation data, are concerned with strongly buoyant plumes and hence do not apply here). The large body of experimentally-determined values of plume standard deviations has been summarized by Draxler,[10] for the near field of diffusion. Long-range diffusion studies were summarized by Barr and Gifford.[7] This body of information has been used to estimate approximate 5th and 95th percentile values. Generally speaking, the near-field concentrations have been judged to have a 5 to 95% variation of factors of .2 to 5 for B through F stability conditions, and 0.1 to 10 for type A, from the observed data. In the same distance range, sigma values are observed to vary between 0.5 and 2 times the median values. Little distinction between σ_y and σ_z variation can be made based on current knowledge, since σ_z is generally based on measurements of cross-wind concentration distributions. Thus the range of variation of σ_z is usually taken to be over the same factors as σ_y. At larger downwind distances, 30km and beyond, Figure N-1 shows that the 5 to 95% range of σ_y is about a factor of 0.33 to 3. Where a mixing layer, if present, could be a factor (only for A-C conditions and distances of 10 and 30 km), slight adjustments to the above ranges of sigma-values have been made. Sigma-values at 10 and 30km were usually assigned a range intermediate between the near- and far-field values.

The concentration-ratios corresponding to the 5 and 95% distribution points of sigma-values determined as above have been evaluated from the following equation,

$$\frac{C_{y,z}}{C_o} = e^{-1/2\,(y,z/\sigma_y,\sigma_z)^2}$$

using 5 and 95% sigma-values obtained by applying the range factors discussed above to the previously-calculated, median sigma values. This result is exact for σ_y and a close approximation for σ_z. The 0% and 100% points were evaluated as follows. For concentrations, the 5 and 95% values were multiplied by .1 and 10 for B-F and by .05 and 20 for A-type stability conditions. The sigma-values were similarly multiplied by .5 and 2 (except by .25 and 4 for A conditions. These values were selected arbitrarily as being reasonable. They should probably be reconsidered as time permits.

Dispersion Tables

N/A = not provided by expert

A-1: -2.0 K/100m Temp Lapse Rate Urban & Rural Surface Roughness					
Downwind distance	**Quantile**	**chiC/Q**	**chi(y)/chiC**	**chi(z)/chiC**	**sig-y**
0.5km	**0%**	3.00E-08	5.00E-03	4.00E-02	2.00E+01
	5%	7.20E-07	9.00E-02	7.90E-01	7.70E+01
	50%	7.20E-06	5.40E-01	9.40E-01	1.55E+02
	95%	7.20E-05	8.60E-01	9.80E-01	3.10E+02
	100%	3.00E-04	9.90E-01	9.90E-01	1.20E+03
1.0km	**0%**	1.00E-08	7.00E-03	5.00E-03	3.50E+01
	5%	1.90E-07	1.40E-01	1.10E-01	1.50E+02
	50%	1.90E-06	6.10E-01	5.80E-01	3.00E+02
	95%	1.90E-05	8.80E-01	8.70E-01	6.00E+02
	100%	1.00E-04	9.90E-01	9.90E-01	2.40E+03
3.0km	**0%**	1.00E-09	6.00E-03	1.20E-01	1.04E+02
	5%	2.20E-08	1.20E-01	5.10E-01	4.15E+02
	50%	2.20E-07	5.90E-01	8.40E-01	8.30E+02
	95%	2.20E-06	8.80E-01	9.60E-01	1.66E+03
	100%	1.00E-05	9.90E-01	9.90E-01	6.65E+03
10.0km	**0%**	1.00E-10	1.00E-08	N/A	1.10E+02
	5%	1.60E-09	1.50E-07	N/A	4.46E+02
	50%	3.20E-08	5.30E-01	N/A	2.23E+03
	95%	6.40E-07	9.60E-01	N/A	8.92E+03
	100%	1.00E-06	9.90E-01	N/A	3.50E+04
30.0km	**0%**	7.00E-11	3.00E-06	N/A	4 00E+02
	5%	1.40E-09	1.20E-04	N/A	1.58E+03
	50%	2.80E-08	3.70E-01	N/A	4.72E+03
	95%	5.60E-07	9.40E-01	N/A	1.90E+04
	100%	2.30E-06	9.90E-01	N/A	4.00E+04

A-2: -1.6 K/100m Temp Lapse Rate Urban & Rural Surface Roughness					
Downwind distance	**Quantile**	**chiC/Q**	**chi(y)/chiC**	**chi(z)/chiC**	**sig-y**
0.5km	**0%**	4.00E-07	1.00E-03	2.00E-02	1.00E+01
	5%	3.80E-06	2.10E-02	2.00E-01	3.60E+01
	50%	1.90E-05	4.30E-01	6.60E-01	7.70E+01
	95%	9.50E-05	8.10E-01	9.00E-01	1.54E+02
	100%	9.00E-04	9.90E-01	9.90E-01	3.10E+02
1.0km	**0%**	1.00E-05	1.00E-02	3.00E-04	3.80E+01
	5%	1.00E-06	3.00E-02	6.10E-04	7.50E+01
	50%	5.00E-06	4.10E-01	6.40E-01	1.50E+02
	95%	2.50E-05	8.00E-01	9.70E-01	3.00E+02
	100%	2.50E-04	9.90E-01	9.90E-01	6.00E+02
3.0km	**0%**	7.00E-09	1.00E-03	7.00E-03	8.30E+01
	5%	7.10E-08	1.10E-02	7.00E-02	1.70E+02
	50%	7.10E-07	4.80E-01	6.60E-01	4.15E+02
	95%	7.10E-06	9.20E-01	9.40E-01	1.24E+03
	100%	7.00E-05	9.90E-01	9.90E-01	2.50E+03
10.0km	**0%**	1.00E-09	3.00E-05	N/A	1.80E+02
	5%	1.10E-08	2.70E-04	N/A	3.70E+02
	50%	1.10E-07	4.00E-01	N/A	1.10E+03
	95%	1.10E-06	9.50E-01	N/A	4.45E+03
	100%	1.00E-05	9.90E-01	N/A	9.00E+03
30.0km	**0%**	4.00E-10	3.00E-07	N/A	3.90E+02
	5%	3.80E-09	2.50E-06	N/A	7.90E+02
	50%	3.80E-08	2.40E-01	N/A	2.40E+03
	95%	3.80E-07	9.10E-01	N/A	9.45E+03
	100%	4.00E-06	9.90E-01	N/A	1.90E+04

A-3: -1.0 K/100m Temp Lapse Rate Urban & Rural Surface Roughness					
Downwind distance	Quantile	chiC/Q	chi(y)/chiC	chi(z)/chiC	sig-y
0.5km	0%	5.00E-07	2.00E-04	8.00E-04	1.40E+01
	5%	5.40E-06	2.00E-03	8.00E-03	2.80E+01
	50%	2.70E-05	2.00E-01	3.00E-01	5.60E+01
	95%	1.30E-04	6.70E-01	7.40E-01	1.12E+02
	100%	1.30E-03	9.90E-01	9.90E-01	2.30E+02
1.0km	0%	9.00E-08	2.00E-03	1.00E-04	2.70E+01
	5%	9.00E-07	2.00E-02	1.10E-03	5.50E+01
	50%	8.70E-06	3.90E-01	1.80E-01	1.10E+02
	95%	9.00E-05	7.90E-01	6.50E-01	2.20E+02
	100%	9.00E-04	9.90E-01	9.90E-01	4.40E+02
3.0km	0%	1.60E-08	1.00E-03	1.30E-09	6.00E+01
	5%	1.60E-07	1.40E-01	1.30E-08	1.20E+02
	50%	1.60E-06	5.10E-01	7.60E-02	3.00E+02
	95%	1.60E-05	9.30E-01	7.50E-01	9.00E+02
	100%	1.60E-04	9.90E-01	9.90E-01	1.80E+03
10.0km	0%	3.00E-09	1.00E-04	N/A	1.40E+02
	5%	3.00E-08	1.00E-03	N/A	2.70E+02
	50%	3.00E-07	4.70E-01	N/A	8.10E+02
	95%	3.00E-06	9.50E-01	N/A	3.24E+03
	100%	3.00E-05	9.90E-01	N/A	6.50E+03
30.0km	0%	8.00E-10	7.00E-06	N/A	2.80E+02
	5%	8.10E-09	7.40E-05	N/A	5.73E+02
	50%	8.10E-08	3.50E-01	N/A	1.72E+03
	95%	8.10E-07	9 40E-01	N/A	6.88E+03
	100%	8.00E-06	9.90E-01	N/A	1.20E+04

A-4: 2.5 K/100m Temp Lapse Rate Urban & Rural Surface Roughness					
Downwind distance	**Quantile**	**chiC/Q**	**chi(y)/chiC**	**chi(z)/chiC**	**sig-y**
0.5km	**0%**	3.20E-06	2.50E-02	4.00E-02	1.00E+01
	5%	3.20E-05	2.50E-01	3.60E-01	1.80E+01
	50%	1.60E-04	6.90E-01	7.70E-01	3.50E+01
	95%	8.00E-04	9.10E-01	9.40E-01	7.00E+01
	100%	8.00E-03	9.90E-01	9.90E-01	1.40E+02
1.0km	**0%**	1.00E-07	2.00E-02	7.00E-03	1.70E+01
	5%	1.20E-06	2.10E-01	7.00E-02	3.40E+01
	50%	6.00E-05	6.80E-01	4.90E-01	6.80E+01
	95%	3.00E-04	9.10E-01	8.40E-01	1.36E+02
	100%	3.00E-03	9.90E-01	9.90E-01	2.80E+02
3.0km	**0%**	1.20E-05	4.00E-03	1.20E-06	3.80E+01
	5%	1.20E-06	4.40E-02	1.20E-05	7.60E+01
	50%	1.20E-05	7.30E-01	1.60E-01	1.90E+02
	95%	1.20E-04	9.70E-01	8.10E-01	5.70E+02
	100%	1.20E-03	9.90E-01	9.90E-01	1.15E+03
10.0km	**0%**	3.00E-08	1.40E-04	5.00E-19	8.50E+01
	5%	3.00E-07	1.40E-02	1.00E-12	1.70E+02
	50%	3.00E-06	6.20E-01	1.00E-02	5.10E+02
	95%	3.00E-05	9.70E-01	7.50E-01	2.04E+03
	100%	3.00E-04	9.90E-01	9.90E-01	4.10E+03
30.0km	**0%**	1.20E-08	1.40E-04	0.00E+00	1.80E+02
	5%	1.20E-07	1.40E-03	1.00E-12	3.60E+02
	50%	1.20E-06	4.80E-01	3.10E-06	1.08E+03
	95%	1.20E-05	9.60E-01	4.50E-01	4.30E+03
	100%	1.20E-04	9.90E-01	9.00E-01	8.60E+03

B-1: Unknown Lapse Rate 6.0 m/s Aver. Wind Speed		
Downwind distance	**Quantile**	**chiC/Q(ground level)**
220. m	**0%**	6.80E-07
	5%	6.80E-06
	50%	3.40E-05
	95%	1.70E-04
	100%	1.70E-03
315. m	**0%**	7.40E-07
	5%	7.40E-06
	50%	3.70E-05
	95%	1.90E-04
	100%	1.90E-03

B-2: Unknown Lapse Rate 5.0 m/s Aver. Wind Speed		
Downwind distance	**Quantile**	**chiC/Q(ground level)**
220. m	**0%**	1.10E-06
	5%	1.10E-05
	50%	5.70E-05
	95%	2.90E-04
	100%	2.90E-03
315. m	**0%**	8.00E-07
	5%	8.00E-06
	50%	4.00E-05
	95%	2.00E-04
	100%	2.00E-03

B-3: Unknown Lapse Rate 8.0 m/s Aver. Wind Speed		
Downwind distance	**Quantile**	**chiC/Q(ground level)**
300. m	0%	4.20E-07
	5%	4.20E-06
	50%	2.10E-05
	95%	1.00E-04
	100%	1.00E-03
600. m	0%	1.30E-07
	5%	1.30E-06
	50%	6.30E-06
	95%	3.20E-05
	100%	3.00E-04

B-4: -1.0 K/100m Temp Lapse Rate Flat Surface Roughness		
Downwind distance	**Quantile**	**chiC/Q(ground level)**
300. m	0%	1.30E-06
	5%	1.30E-05
	50%	8 60E-05
	95%	6.90E-04
	100%	7.00E-03
600. m	0%	5.40E-07
	5%	5.40E-06
	50%	3.60E-05
	95%	2.90E-04
	100%	3.00E-03

B-5: 3.0 K/100m Temp Lapse Rate Flat Surface Roughness					
Downwind distance	Quantile	chi(y)/chiC	chi(z)/chiC	sig-y	sig-z
600. m	0%	6.00E-03	5 00E-02	1.00E+01	4.00E+00
	5%	6.00E-02	4.60E-01	2.10E+01	8.00E+00
	50%	4.90E-01	8.40E-01	4.20E+01	1.70E+01
	95%	8.40E-01	9.60E-01	8.40E+01	3.40E+01
	100%	9.90E-01	9.90E-01	1.80E+02	7.00E+01

C: Stable Conditions Urban & Rural Surface Roughness				
Downwind distance	Quantile	60 min	120 min	240 min
360. m	0%	2.80E-08	1.00E-08	5.40E-09
	5%	2.10E-07	2 20E-07	2.20E-07
	50%	2.10E-06	2.20E-06	2.20E-06
	95%	2.10E-05	2.20E-05	2.20E-05
	100%	2.10E-04	1.00E-04	5.40E-05
970. m	0%	2.00E-07	1.30E-07	6.40E-08
	5%	2.10E-06	2.60E-06	2.60E-06
	50%	2.10E-05	2.60E-05	2.60E-05
	95%	2.10E-04	2.60E-04	2.60E-04
	100%	2.00E-03	1.00E-03	6.40E-04
1970. m	0%	1.00E-07	7.40E-08	3.70E-08
	5%	1.00E-06	1.50E-06	1.50E-06
	50%	1.00E-05	1.50E-05	1.50E-05
	95%	1.00E-04	1.50E-04	1.50E-04
	100%	1.00E-03	7.40E-04	3.70E-04

D: Stable Conditions Flat Surface Roughness				
Downwind distance	**Quantile**	**chiC/Q**	**sig-y**	**sig-z**
60. m	**0%**	1.50E-05	2.00E-01	5.00E-01
	5%	1.50E-04	1.30E+00	5.00E-01
	50%	1.50E-02	2.60E+00	1.70E+00
	95%	5.00E-02	1.50E+01	3.00E+00
	100%	5.00E-01	1.00E+01	3.00E+01

E: Length of Arc Crossed By 90% of the Material		
Downwind distance	**Quantile**	**90% arc**
80.km	**0%**	8.00E+03
	5%	1.60E+04
	50%	4.70E+04
	95%	1.41E+05
	100%	2.80E+05
200.km	**0%**	2.00E+04
	5%	3.90E+04
	50%	1.17E+05
	95%	3.51E+05
	100%	7.00E+05
1000.km	**0%**	6.00E+04
	5%	1.14E+05
	50%	3.42E+05
	95%	1.03E+06
	100%	2.05E+06

References

1. Hanna, S.R., G.A. Briggs, and R.P. Hosker, Jr., "Handbook on Atmospheric Diffusion," DOE/TIC-11223, Technical Information Center, U.S. Department of Energy, Oak Ridge, TN, 1982.

2. Briggs, G.A., "Diffusion Estimation for Small Emissions," *Contribution No. 106*, U.S. Atmospheric Turbulence and Diffusion Laboratory, Oak Ridge, TN, pp. 83-145, December 1974.

3. International Atomic Energy Agency, "Atmospheric Dispersion in Nuclear Power Plant Siting: A Safety Guide," Safety Series, IAEA Safety Guides, No. 50-SG-S3, IAEA, Vienna, sold by Unipub, New York, 1980.

4. Gifford, F.A., "Turbulent Diffusion-Typing Schemes: A Review," *Nuclear Safety*, 17:68-86, 1976.

5. Gifford, F.A., "The Time-Scale of Atmospheric Diffusion Considered in Relation to the Universal Diffusion Function, f_1," *Atmospheric Environment*, 21:1315-1320, 1987.

6. Gifford, F.A., "The Random-Force Theory: Application to Meso- and Large-Scale Atmospheric Diffusion," *Boundary-Layer Meteorology*, 30:159-175, 1984.

7. Barr, S., and F.A. Gifford, "The Random Force Theory Applied to Regional Scale Atmospheric Diffusion," *Atmospheric Environment*, 21:1737-1742, 1987.

8. Crawford, T.V., "Atmospheric Transport of Radionuclides, Report of the Working Group on Atmospheric Dispersion, Deposition, and Resuspension," (T.V. Crawford, Chairman), *Proceedings of a Workshop on the Evaluation of Models Used for the Environmental Assessment of Radionuclide Releases, 6-9 September 1977*, CONF-776901, Oak Ridge National Laboratory, Oak Ridge, TN, April 1978.

9. Little, C.A., and C.W. Miller, "The Uncertainty Associated with Selected Environmental Transport Models," ORNL-5528, Oak Ridge National Laboratory, Oak Ridge, TN, November 1979

10. Draxler, R.R., "Diffusion and Transport Experiments," (D. Randerson, ed.), *Atmospheric Science and Power Production*, DOE/TIC-27601, Technical Information Center, Office of Scientific and Technical Information, U.S. Department of Energy, pp. 367-422, 1984.

Expert O

Introduction

The elicitation requires the simulation of a very large number of "realizations" of dispersion episodes to provide the 5th, 50th and 95th quantiles of the probability distribution for each exercise. For this reason, it has been decided to use a simple model, i.e., a Gaussian plume model, which is fast and is controlled by a limited number of input variables. The effects not specified in the initial conditions listed in the exercise have been considered assuming an uncertainty distribution of the horizontal and vertical plume standard deviation σ_y and σ_z, and of the mixing layer height h. In order to generate a distribution of σ_y, σ_z and h values (v(i), i=1,3) representative of the "realizations" under the conditions specified in each exercise, the following procedure has been adopted. Firstly, the extreme values v_{min} and v_{max} (minimum and maximum) have been defined, based on literature values and on physical considerations, as described in some detail below. Then, 40 values of each variable have been randomly generated, assuming a normal probability distribution centered at $v_O(i) = [v_{max}(i) + v_{min}(i)]/2$, and a standard deviation $\sigma(i) = [v_{max}(i) - v_{min}(i)]/2$. The generated values $v(i)<v_{min}(i)$ or $v(i)>v_{max}(i)$ have been discarded. Finally, the plume model has been executed 40x40x40 = 64000 times by combining independently the input values. The 5th, 50th, and 95th quantiles of the computed concentration values were found.

In this process, two "strong" and, in some way, arbitrary, assumptions have been made. The first concerns the shape of the probability distribution of the varying input variables. The chosen shape gives preference to the central values of the distribution, which should represent typical or average empirical values under the stated initial conditions, but is still flat enough to enable the presence of a significant number of cases with values close to the extremes. A test with different shapes has been made (for example, with $\sigma(i) = [v_{max}(i) - v_{min}(i)]/4$, which resulted in a more peaked distribution of the concentration values), which has been considered less realistic. Secondly, the input variables have been assumed to vary independently. This was done mainly due to the difficulty of defining any criteria for coupling the values of different variables. However, it is worth it to outline that several studies show that, for example, the horizontal and vertical components of the turbulence can be very well decoupled (see, for example, Desiato and Lange[1]), and the same can happen between the turbulence and the mixing height, which can be influenced by geographical and synoptic features other than those influencing the turbulence (think, for example, of the IBL at coastal sites).

In the following paragraphs the assumptions made for each exercise are commented on, and the results obtained with this simple method are compared, where possible, with experimental results.

Exercise 1

The meteorological conditions fixed in this exercise are characteristic of an extremely unstable situation (temperature lapse rate= -2.0 K/100m, and standard deviation of wind direction at 10 m measured over 10 minutes = 25).

The first question regards the **sampling time** (60 minutes). As the common values of σ_y are related to sampling times of about 10 minutes, we must find a way to extrapolate such values to 1 hour. If the wind during this time is steady and constant in the mean direction, it is well known that the dependence on the sampling time will follow a law like $(T/T)^{\alpha}$, where α is very close to the unity if the time $T \approx 1$ hour, due to the fact that the turbulence spectrum presents a minimum in that interval of time. However different authors[2,3] suggest $\alpha = 0.5$.

In our case we have supposed that the minimum value ($v_{min}(i)$, see § 1) for σ_y will be that corresponding to a Pasquill category B: in fact, at the presence of breeze effect the wind lateral dispersion is very narrow.[4] A mean value (the $v_O(i)$ of the §1 = $[v_{max}(i) + v_{min}(i)]/2$) for σ_y has been then fixed as a category A value multiplied by the factor $(T/T)^{\cdot 05} = (60/10)^{05} = 2.5$. After the choice of $v_O(i)$ and $v_{min}(i)$, $v_{max}(i)$ is automatically defined, due to the symmetry of the distribution assumed in §1.

The second question is about the evaluation of the vertical standard deviation σ_z of the plume at a given distance from the source: it is a function of the atmospheric stability, the downwind distance from the source and the average roughness of the ground over the distance of travel. Adopting a scheme proposed by Smith,[5] a working group in the U.K.[6] suggested that the values of σ_z in the required category can be modified for other ground roughness lengths using the ratios of σ_z at a range of roughness lengths to that at 0.1 m shown in Figure O-1.

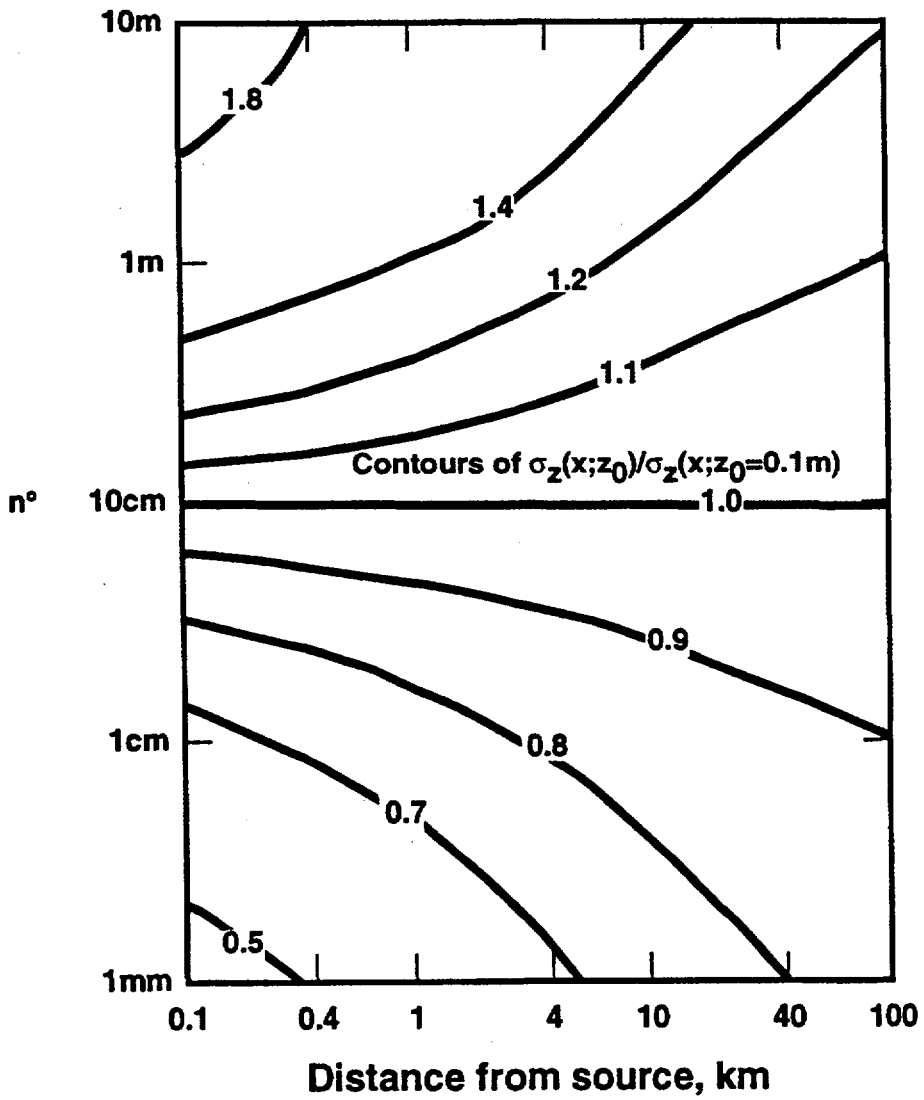

Figure O-1. Ratio of vertical dispersion standard deviation σ_z at any ground roughness length to that at 0.1 m. The ratio is virtually independent of the atmospheric stability parameter.[6]

Supposing that the experimental data of σ_z refers to a roughness length of ≈ 10 cm, the data of Figure O-1 can be directly used to find out some range of values for the vertical dispersion σ_z.

A maximum value (the $v_{max}(i)$ of § 1) for σ_z has been fixed as a category A with a roughness length of 1 m, while the minimum value was chosen as for a category B with a roughness length of 1 cm. After the choice of $v_{min}(i)$ and $v_{max}(i)$, $v_O(i)$ is automatically defined, due to the symmetry of the distribution assumed in §1. For the numerical values of σ_y and σ_z versus downwind distance from the source, we utilized the Pasquill estimates for his turbulence types: the use of different values from other authors will not significantly affect the final results.

A last assumption, which is important mainly for this particular exercise 1, is the variability of the boundary layer depth H_{mix}. Taking into account that in the first part of the trajectory it is possible to have a stable layer aloft due to the last effects of the morning stability, we have chosen 200 m at x=0.5 km from the source up to 500 m to 30 km from the source for the minimum value of H_{mix}. The maximum has been fixed to 2000 m, independently of the distance, because when a situation of high pressure is present there is also the presence of an inversion aloft due to the subsidence of air masses.

Our assumptions are also in agreement with the work of Smith,[7] who produced nomograms for the estimation of this depth based on values of the time, date, cloud cover and windspeed, suggesting for category A a mean value of 1300 m. For the evaluation of the air concentrations, the value of the boundary layer H_{mix} is utilized up to about two reflections in a fumigation model, considering a homogeneous vertical distribution of the air concentration after a distance for which $\sigma_z = H_{mix}$. On the basis of the criteria fixed above, the data in Table O-1 were chosen for the run of the program based on the specifications of § 1, (three values, v_{min}, v_O and v_{max} are shown for σ_y and σ_z, and two for H_{mix}, i.e., v_{min} and v_{max}):

Table O-1. Input data for Exercise 1

Distance X (km)	σ_y (m)	σ_z (m)	H_{mix} (m)
0.5	80, 275, 480	40, 105, 170	200-2000
1.0	140, 500, 860	100, 360, 620	250-2000
3.0	400, 1400, 2400	560, 1550, 2540	350-2000
10.0	1200, 4300, 7400	—	500-2000
30.0	3300, 10000, 16700	—	500-2000

As can be seen from the results shown in the tables for the expert-elicitor communication, there is generally an order of magnitude difference between the maximum and the minimum centerline air concentration values: it is obvious that this is the result of the methodology followed in the present exercise.

In general, if actual field experiments were carried out, lower values could be experienced. However, if the results of these exercises must be utilized for risk analysis in accident consequence codes, it will be important to adopt an approach which, in a realistic way, must take into account the upper levels of every situation, for safety's sake. What must be said as a comment, if we take into account the experience coming from field tests, is that the distribution will be skewed and not symmetrical, depending on the local situation, and the minimum values will be lower than those chosen here, but the maximum values will not be higher than the maximum found here.

Exercise 2

The meteorological conditions fixed in this exercise are characteristic of a slightly unstable situation (temperature lapse rate= -1.6 K/100m, and standard deviation of wind direction at 10 m measured over 10 minutes = 15).

Concerning **lateral dispersion** in this case we supposed that the minimum value $v_{min}(i)$ for σ_y will be that corresponding to a Pasquill category D: in fact the wind

speed of 4 m/s is elevated enough to allow a well defined plume direction, so that a category D might be representative of the minimum lateral dispersion. The mean value for σ_y has been fixed as one characteristic of a category C, multiplied by the factor $(T/T)^{-05} = (60/10)^{05} =$ 2.5. After the choice of $v_O(i)$ and $v_{min}(i)$, $v_{max}(i)$ is automatically defined, due to the symmetry of the distribution assumed in §1.

For the **vertical dispersion** a maximum value (the $v_{max}(i)$ of § 1) for σ_z has been fixed as a category C with a roughness length of 1 m (for the methodology see § 2), while the minimum value was chosen as for a category D with a roughness length of 1 cm. After the choice of $v_{min}(i)$ and $v_{max}(i)$, $v_O(i)$ is automatically defined, due to the symmetry of the distribution assumed in §1.

As concerns the variability of the boundary layer depth H_{mix}, taking into account that in the first part of the trajectory it will be possible to have a stable layer aloft to the last effects of the morning stability (even more pronounced than in exercise 1), we have chosen 100 m at x=0.5 km from the source up to 500 m to 30 km from the source for the minimum value of H_{mix}. The maximum has been fixed to 2000 m, independently of the distance, for the same reasons described in the previous paragraph. The mean evaluation suggested by Smith for the depth H_{mix} at the presence of category C is 850 m.

As can be seen, the boundary layer height has no significant influence because the values of the vertical dispersion are in most cases lower than H_{mix}.

If we look at the data obtained from the application of the data in Table O-2 and shown in the expert-elicitor tables, we see that the values of the concentration ratio above centerline are low, the 95 percentile being about 0.5: the presence of buildings would undoubtedly enhance the values of σ_z, and in field experiments it would be possible to find higher values for the vertical dispersion than those shown in Table O-2.

Table O-2. Input data for Exercise 2

Distance x (km)	σ_y (m)	σ_z (m)	H_{mix} (m)
0.5	40, 140, 240	13, 30, 47	100-2000
1.0	70, 250, 330	22, 56, 90	150-2000
3.0	200, 750, 1300	55, 138, 221	250-2000
10.0	600, 2250, 3900	—	350-2000
30.0	1500, 6000, 10500	—	500-2000

Exercise 3

The meteorological conditions fixed in this exercise are characteristic of a neutral situation (temperature lapse rate= −1.0 K/100m, and standard deviation of wind direction at 10 m measured over 10 minutes = 10).

Concerning **lateral dispersion** in this case we supposed that the minimum value (the $v_{min}(i)$ of § 1) for σ_y will be that corresponding to a Pasquill category E. in fact, the wind speed of 6 m/s is elevated enough to allow a well defined plume direction, so that a category E might be representative of the minimum lateral dispersion. The mean value for σ_y has been fixed as that single characteristic of a category D, multiplied by the factor $(T/T)^{-05} = (60/10)^{05} =$ 2.5. After the choice of $v_O(i)$ and $v_{min}(i)$, $v_{max}(i)$ is automatically defined, due to the symmetry of the distribution assumed in §1.

For the **vertical dispersion** a maximum value (the $v_{max}(i)$ of § 1) for σ_z has been fixed as a category C with a roughness length of 1 m (for the methodology see § 2), while the minimum value was chosen as for a category E with a roughness length of 1 cm. After the choice of $v_{min}(i)$ and $v_{max}(i)$, $v_O(i)$ is automatically defined, due to the symmetry of the distribution assumed in §1.

As concerns the variability of the boundary layer depth H_{mix}, taking into account the high wind velocity (6 m/s), for the minimum value of H_{mix} we have chosen 400 m at every distance from the source. The maximum value has been fixed at 1200 m, independently of the distance. The mean evaluation suggested by Smith[7] for the depth H_{mix} at the presence of the category D is 800 m.

Table O-3. Input data for Exercise 3

Distance x (km)	σ_y (m)	σ_z (m)	H_{mix} (m)
0.5	30, 95, 160	10, 30, 50	400-1200
1.0	50, 175, 300	16, 53, 90	400-2000
3.0	130, 500, 870	34, 127, 220	400-2000
10.0	400, 1450, 2500	65, 285, 505	400-2000
30.0	1000, 3750, 6500	102, 626, 1150	400-2000

As can be seen, the presence of the boundary layer height has no significant influence because at short distances the values of the vertical dispersion are lower than H_{mix}.

If we look at the data obtained from the application of the above input data and shown in the expert-elicitor tables, we see that here, as in the previous exercise, the values of the concentration ratio above centerline are low, the 95 percentile being about 0.5: the presence of buildings would enhance the values of σ_z, and in field experiments it would be possible to find higher values for the vertical dispersion than those shown in Table O-3.

As said in the previous case, the maximum values of the lateral dispersion actually could be higher than the maximum fixed in Table O-3, but we think that the values proposed are more acceptable for a risk analysis because a situation of variation of the mean direction of the wind every ten minutes is very unusual when the surface mean wind speed is 6 m/s.

Exercise 4

The meteorological conditions fixed in this exercise are characteristic of a moderately stable situation (temperature lapse rate= 2.5 K/100m, and standard deviation of wind direction at 10 m measured over 10 minutes = 2.5).

Concerning **lateral dispersion** in this case we supposed that the minimum value $v_{min}(i)$ for σ_y will be that corresponding to a Pasquill category F: in fact the wind speed of 3 m/s is low enough to allow an uncertainty in the plume direction, so that while a category F might be representative of the minimum lateral dispersion, a category D, multiplied by the factor $(T/T)^{.05} = (60/10)^{.05} = 2.5$, should be fixed for the mean value of σ_y. After the choice of $v_0(i)$ and $v_{min}(i)$, $v_{max}(i)$ is automatically defined, due to the symmetry of the distribution assumed in §1.

For the **vertical dispersion** a maximum value (the $v_{max}(i)$ of § 1) for σ_z has been then fixed as a category D with a roughness length of 1 m (for the methodology see § 2), while the minimum value was chosen as for a category F with a roughness length of 1 cm. After the choice of $v_{min}(i)$ and $v_{max}(i)$, $v_0(i)$ is automatically defined, due to the symmetry of the distribution assumed in §1.

As concerns the variability of the boundary layer depth H_{mix}, no assumption has been made because the diffusivity is very much reduced in stable conditions, and the mixing layer has no further effect in limiting the dispersion.

If we look at the data obtained from the application of the above input data and shown in the expert-elicitor tables, we see that here, contrary to the previous exercise, the values of the concentration ratio above centerline are high for short distances, the mean value being ≈ 0.8. They decrease rapidly for greater distances, reaching ≈ 0.2 for the 95. The presence of buildings would enhance the values of σ_z, and in field experiments it would be possible to find higher values for the vertical dispersion than those shown in Table O-3, when the plume reaches urban areas.

Table O-4. Input data for Exercise 4

Distance x (km)	σ_y (m)	σ_z (m)	H_{mix} (m)
0.5	20, 95, 160	6, 16, 26	—
1.0	35, 175, 315	10, 27, 44	—
3.0	90, 500, 910	22, 40, 58	—
10.0	270, 1450, 2630	42, 111, 180	—
30.0	700, 3750, 6800	50, 170, 290	—

Concerning the lateral dispersion we think that, if the mean wind speed is 3 m/s all over the sampling time of 60 minutes, the values suggested for σ_y would be realistic: for lower wind velocities they would be too low because of the great uncertainty of the wind direction.

Exercise 5

The meteorological conditions fixed in this exercise are characteristic of a neutral situation (wind speed = 6 m/s, and an inverse Monin-Obukhov length negative but near zero give a category neutral to lightly unstable [see Figure O-2]; the standard deviation of wind direction at 10 m measured over 10 minutes = 5 is, however, characteristic of lightly stable conditions).

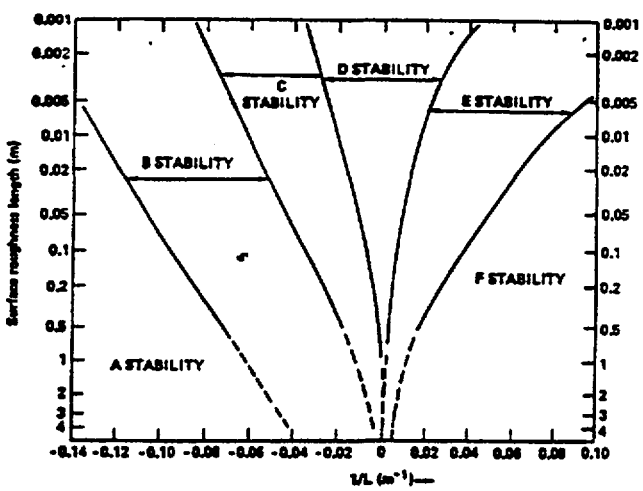

Figure O-2. Relation of Monin-Obukhov length to Pasquill class and roughness length.[8]

Concerning **lateral dispersion** in this case we supposed that the minimum value $v_{min}(i)$ for σ_y will be that corresponding to a Pasquill category E: in fact the wind speed of 6 m/s is too high to allow the establishment of a stability situation, but the lateral dispersion of 5 induces us to think that there is a strong plume direction, probably due to local effects (breeze, valley channelling, etc.).

A category E, multiplied by the factor $(T/T)^{.05} = (60/10)^{.05} = 2.5$, should be fixed for the mean value of σ_y. After the choice of $v_O(i)$ and $v_{min}(i)$, $v_{max}(i)$ is automatically defined, due to the symmetry of the distribution assumed in §1.

For the **vertical dispersion** a maximum value (the $v_{max}(i)$ of § 1) for σ_z has been fixed as a category C with a roughness length of 1 m, while the minimum value was chosen as for a category D with a roughness length of 1 cm; these assumptions are made by considering the extreme values suggested by the graph of Figure O-2. After the choice of $v_{min}(i)$ and $v_{max}(i)$, $v_O(i)$ is automatically defined, due to the symmetry of the distribution assumed in §1.

As concerns the variability of the boundary layer depth H_{mix}, taking into account the high wind velocity (6 m/s), for the minimum value of H_{mix} we have chosen 400 m at every distance from the source. The maximum value has been fixed at 1200 m, independently of the distance. The mean evaluation suggested by Smith for the depth H_{mix} at the presence of category D is 800 m.

Table O-5. Input data for Exercise 5

Distance χ(km)	σ_y (m)	σ_z (m)	H_{mix} (m)
220	11, 28, 45	6, 15, 24	400-1200
315	17, 45, 73	9, 21, 33	400-1200

If we look at the data obtained from the application of the above input data and shown in the expert-elicitor tables, we see that there is a ratio of only one sixth among the 0.05 and the 0.95 percentiles of the ground level concentrations: this is because the lateral standard deviation is very low and the wind speed high, so that the plume mean direction will be very steady. But at short distances like those of Table O-5 the effect of the presence of buildings would be very strong, so that during field experiments the vertical and lateral dispersion would be higher than those shown here.

As said in previous cases, the maximum values of the lateral dispersion actually could be higher than the maximum fixed in Table O-5: the values proposed are acceptable for a risk analysis because a situation of variation of the mean direction of the wind every ten minutes is very unusual when the surface mean wind speed is as high as 6 m/s. Consequently, as concerns the minimum values for the ground level concentration, experimental values could be significantly lower than those shown in the expert-elicitor document in the present report.

Exercise 6

The meteorological conditions fixed in this exercise are characteristic of a neutral to lightly unstable situation (Monin-Obukhov length = -0.01/m gives a category neutral to lightly unstable, see Figure O-2; the standard deviation of wind direction at 10 m measured over 10 minutes = 10 and wind speed = 5 m/s are generally characteristic of neutral conditions).

Concerning the **lateral dispersion** in this case we supposed that the mean value $v_o(i)$ for σ_y will be that corresponding to a Pasquill category D, multiplied by the factor $(T/T)^{.05}$ = $(60/10)^{.05}$ = 2.5. A category C, multiplied by the factor $(T/T)^{.05}$ = $(60/10)^{.05}$ = 2.5, should be fixed for the maximum value of σ_y. After the choice of $v_O(i)$ and $v_{max}(i)$, $v_{min}(i)$ is automatically defined, due to the symmetry of the distribution assumed in §1.

For the **vertical dispersion** a maximum value (the $v_{max}(i)$ of § 1) for σ_z has been then fixed as a category C with a roughness length of 1 m, while the minimum value was chosen as for a category D with a roughness length of 1 cm; these assumptions are made by considering the extreme values suggested by the graph of Figure O-2. After the choice of $v_{min}(i)$ and $v_{max}(i)$, $v_O(i)$ is automatically defined, due to the symmetry of the distribution assumed in §1.

As concerns the variability of the boundary layer depth H_{mix}, taking into account the high wind velocity (5 m/s), for the minimum value of H_{mix} we have chosen 400 m at every distance from the source. The maximum value has been fixed at 1200 m, independently of the distance. The mean evaluation suggested by Smith for the depth H_{mix} at the presence of category D is 800 m.

Table O-6. Input data for Exercise 6

Distance χ(km)	σ_y (m)	σ_z (m)	H_{mix} (m)
220	20, 40, 60	6, 15, 24	400-1200
315	30, 60, 90	9, 21, 33	400-1200

If we look at the data obtained from the application of the above input data and shown in the expert-elicitor tables, we see that there is only a rather light difference within these data and those obtained in the previous exercise 5: this is due to the fact that, while the vertical dispersion does not vary, the lateral dispersion increases 50% against a decreasing of the wind speed of 20%.

As said in previous cases, the maximum values of the lateral dispersion actually could be higher than the maximum fixed in Table O-5: the values proposed are acceptable for a risk analysis, because a situation of variation of the mean direction of the wind every ten minutes is very unusual when the surface mean wind speed is as high as 5 m/s. Consequently, as concerns the minimum values for the ground level concentration, experimental values could be significantly lower than those shown in the expert-elicitor document in the present report.

Exercise 7

The meteorological conditions fixed in this exercise are characteristic of a neutral to lightly unstable situation (the Monin-Obukhov length = -0.02/m gives a category neutral to moderately unstable, depending on the roughness length, see Figure O-2; the standard deviation of wind direction at 10 m measured over 10 minutes = 15 corresponds to a situation slightly unstable, but a wind speed = 8 m/s is generally characteristic of neutral conditions).

Concerning the **lateral dispersion** in this case we supposed that the mean value $v_o(i)$ for σ_y will be that corresponding to a Pasquill category C, multiplied by the factor $(T/T)^{.05} = (60/10)^{.05} = 2.5$. A category D should be fixed for the minimum value of σ_y. After the choice of $v_O(i)$ and $v_{min}(i)$, $v_{max}(i)$ is automatically defined, due to the symmetry of the distribution assumed in §1.

Table O-7. Input data for Exercise 7

Distance χ(km)	σ_y (m)	σ_z (m)	H_{mix} (m)
300	24, 83, 142	15, 30, 45	200-1600
600	44, 163, 282	28, 62, 96	200-1600

For the **vertical dispersion** a minimum value (the $v_{min}(i)$ of § 1) for σ_z has been fixed as for a category C with a roughness length of 1 cm, while the maximum value was chosen as for a category B with a roughness length of 1 m; these assumptions are made by considering the extreme values suggested by the graph of Figure O-2. After the choice of $v_{min}(i)$ and $v_{max}(i)$, $v_O(i)$ is automatically defined, due to the symmetry of the distribution assumed in §1.

As concerns the variability of the boundary layer depth H_{mix}, taking into account the high wind velocity (8 m/s), for the minimum value of H_{mix} we have chosen 200 m at every distance from the source. The maximum value has been fixed at 1600 m, independent of the distance. The mean evaluation suggested by Smith for the depth H_{mix} at the presence of category D is 800 m.

If we look at the data obtained from the application of the above input data and shown in the expert-elicitor tables, we see that there is almost an order of magnitude of difference among these data and those obtained in the previous two exercises (5 and 6), the distances involved being about doubled (300 and 600 m against 220 and 315 m). This is due to the fact that, although the wind speed is increased, the vertical and lateral dispersion are also increased ≈ 200%, due to the greater distance and the more unstable conditions. As concerns the minimum values for the ground level concentration, experimental values would be not significantly lower than those shown in the expert-elicitor document in the present report.

Exercise 8

The meteorological conditions fixed in this exercise are characteristic of a neutral situation (thermal lapse rate = -1.0 K/100 m and standard deviation of wind direction at 10 m measured over 10 minutes = 10 are generally characteristic of neutral conditions).

Concerning the **lateral dispersion** in this case we supposed that the mean value $v_o(i)$ for σ_y will be that corresponding to a Pasquill category D, multiplied by the factor $(T/T)^{.05} = (60/10)^{.05} = 2.5$. A category E has been fixed for the minimum value of σ_y. After the choice of $v_O(i)$ and $v_{min}(i)$, $v_{max}(i)$ is automatically defined, due to the symmetry of the distribution assumed in §1.

For the **vertical dispersion** a maximum value (the $v_{max}(i)$ of § 1) for σ_z has been fixed as a category C with a roughness length of 1 m, while the minimum value was chosen as for a category E with a roughness length of 1 cm: this is possible because of the low value for the wind speed, 3 m/s. After the choice of $v_{min}(i)$ and $v_{max}(i)$, $v_O(i)$ is automatically defined, due to the symmetry of the distribution assumed in §1.

As concerns the variability of the boundary layer depth H_{mix}, for the minimum value of H_{mix} we have chosen 400 m at every distance from the source. The maximum value has been fixed at 1200 m, independently of the distance. The mean evaluation suggested by Smith for the depth H_{mix} at the presence of category D is 800 m.

From the meteorological point of view this situation might also be characteristic of the presence of fog, with an inversion layer based at 100 or 200 m: in this case there will be fumigation, but up to 600 m of distance the value of vertical dispersion σ_z is lower than the value of H_{mix}.

Table O-8. Input data for Exercise 8

Distance χ(km)	σ_y (m)	σ_z (m)	H_{mix} (m)
300	16, 58, 100	6, 19, 32	400-1200
600	30, 110, 190	9, 34, 59	400-1200

If we look at the data obtained from the application of the above input data and shown in the expert-elicitor tables, we see there is a great difference between these data and those obtained in the previous exercise 7: this is due to the fact that the vertical and the lateral dispersion are both decreased here about 50%, and also the wind speed is decreased from 8 to 3 m/s.

As said in previous cases, the maximum values of the lateral and vertical dispersion actually could be higher than the maximum values fixed in Table O-8; thus, as concerns the ground level concentration, experimental values could be significantly lower than the minimum shown in the expert-elicitor document, while the maximum are unlikely to exceed the values of the 0.95 percentiles shown in the same document.

Exercise 9

The meteorological conditions fixed in this exercise are characteristic of a stable situation (thermal lapse rate = +3.0 K/100 m and standard deviation of wind direction at 10 m measured over 10 minutes = 2.5 are generally characteristic of moderately stable conditions).

Concerning the **lateral dispersion** in this case we supposed that the mean value $v_o(i)$ for σ_y will be that corresponding to a Pasquill category D, multiplied by the factor $(T/T)^{-05}$ = $(60/10)^{05}$ = 2.5. A category F has been fixed for the minimum value of σ_y. After the choice of $v_O(i)$ and $v_{min}(i)$, $v_{max}(i)$ is automatically defined, due to the symmetry of the distribution assumed in §1. The justification of such a spread of values is due to the fact that the wind speed is low (3 m/s) and then the plume direction might be very undefined.

For the **vertical dispersion** a maximum value (the $v_{max}(i)$ of § 1) for σ_z has been fixed as a category D with a roughness length of 1 m, while the minimum value was chosen as for a category F with a roughness length of 1 cm. After the choice of $v_{min}(i)$ and $v_{max}(i)$, $v_O(i)$ is automatically defined, due to the symmetry of the distribution assumed in §1.

As concerns the variability of the boundary layer depth H_{mix}, no assumption has been made, as in exercise 4, due to the reduced diffusivity in stable conditions, and the mixing layer has no further effect in limiting the dispersion.

Table O-9. Input data for Exercise 9

Distance χ(km)	σ_y (m)	σ_z (m)	H_{mix} (m)
600	21, 108, 195	6, 19, 32	—

If we look at the data obtained from the application of the above input data and shown in the expert-elicitor tables, we see that the median of the ratio of the air concentration (at y=50 m and z=12 m) over the centerline concentration value is close to one, so that the points considered in this exercise are at a distance from the centerline which is lower than the horizontal and vertical standard deviations σ_y and σ_z, as it can be seen from the data shown in Table O-9.

Exercise 10

The meteorological conditions fixed in this exercise are characteristic of a moderately stable situation (standard deviation of wind direction measured over 10 minutes = 6, average wind speed 1.9 m/s are generally characteristic of stable conditions).

Concerning **lateral dispersion** in this case we supposed that the minimum value $v_{min}(i)$ for σ_y will be that corresponding to a Pasquill category F, multiplied by the factor $(T/T)^{-05}$ = $(60/10)^{05}$ = 2.5 for a sampling time of 60 minutes (= 3.5 for a sampling time of 120 minutes and = 4.9 for a sampling time of 240 minutes). Due to very low wind speed (1.9 m/s), there will be a strong uncertainty in the plume direction, so that while a category F might be representative of the minimum lateral dispersion, a category C, multiplied by the factor $(T/T)^{-05}$, should be fixed for the mean value of σ_y. After the choice of $v_O(i)$ and $v_{min}(i)$, $v_{max}(i)$ is automatically defined, due to the symmetry of the distribution assumed in §1.

For the **vertical dispersion** a maximum value (the $v_{max}(i)$ of § 1) for σ_z has been then fixed considering a category D with a roughness length of 1 m (for the methodology see § 2), while the minimum value was chosen as for a category F with a roughness length of 1 cm. After the choice of $v_{min}(i)$ and $v_{max}(i)$, $v_O(i)$ is automatically defined, due to the symmetry of the distribution assumed in §1.

As concerns the variability of the boundary layer depth H_{mix}, no assumption has been made because the diffusivity is very much reduced in stable conditions, and the mixing layer has no further effect in limiting the dispersion.

If we look at the data obtained from the application of the above input data, and shown in the expert-elicitor tables, we see that the values of the ground concentration increase rapidly when passing from a distance x = 360 m to x = 970 m: this effect is due to the release height (45 m).

The variability with the sampling time is very low because we adopted the law of the square of the sampling time. With such a low wind speed (1.9 m/s) it could be possible to find higher values for the lateral dispersion so that the maximum values for the σ_y might be higher than those shown in Table O-10.

Table O-10. Input data for Exercise 10

Distance X (m) (sampling time, h)	σ_y (m)	σ_z(m)	H_{mix} (m)
360 (1h)	32, 100, 168	6, 13, 20	—
360 (2h)	46, 140, 234	6, 13, 20	—
360 (4h)	64, 196, 328	6, 13, 20	—
970 (1h)	83, 250, 417	10, 27, 44	—
970 (2h)	116, 350, 584	10, 27, 44	—
970 (4h)	162, 490, 818	10, 27, 44	—
1970 (1h)	150, 475, 800	15, 43, 71	—
1970 (2h)	210, 665, 1120	15, 43, 71	—
1970 (4h)	290, 931, 1570	15, 43, 71	—

Also in this case we can say that the maximum values for ground concentration are probably well predicted, while the actual minimum values might be lower than those predicted by a factor of 2-3 (horizontal spread over 360, instead of about 180 as can be deduced from the data of σ_y shown in Table O-10).

Exercise 11

The meteorological conditions are not fixed in this exercise, apart from the wind speed (3.0 m/s). The wind speed is sufficiently high to suppose a constant direction during the sampling time of one minute. We supposed two situations, one moderately stable and another neutral to slightly unstable, considering the data of σ_y given by the literature (extrapolated for such a low distance) as valid for a sampling time of 10 minutes and applying the coefficient of $(T/T)^{.05} = (1/10)^{.05} \approx 3.3$ to obtain the values for one minute. However, it must be emphasized that the data are very subjective.

If we look at the data obtained from the application of the above input data and shown in the expert-elicitor tables, we see a difference of a factor of ≈4 between the median values of the centerline concentration in the two cases.

Table O-11. Input data for Exercise 11

	Distance x (m)	σ_y (m)	σ_z (m)
Case I (stable situation)	60	0.5, 2.5, 4.5	0.5, 1.3, 2
Case II (neutral – slightly unstable situation)	60	2, 6, 10	1, 2, 3

Exercise 12

The meteorological conditions are not fixed in this exercise. We assume that if we know the σ_y, 90% of the material will be contained in an arc of about 3.3 σ_y. The minimum value for σ_y is obtained from Cagnetti and Ferrara,[9] while the mean value is evaluated with the formula σ_y = O.5 T from Heffter and Ferber.[10]

Table O-12. Input data for Exercise 12

Distance x (km)	σ_y (km)	3.3 σ_z (km)	arc length (radians)
80	6, 20, 36	13, 33, 53	0.16, 0.41, 0.66
200	14, 50, 86	46, 165, 284	0.23, 0.82, 1.42
1000	100, 250, 400	330, 825, 1320	0.33, 0.83, 1.32

The last column shows the 0.05, 0.5, and 0.95 percentile of the length of arc crossed by 90% of the material. The evaluations of the lateral dispersion refer to a short release (sampling time ≤1h) and take into account that the distance is meant along the trajectory.

In general, if actual field experiments were carried out, lower values could be experienced. However, if the results of these exercises must be utilized for risk analysis in accident consequence codes, it will be important to adopt an approach which, in a realistic way, must take into account the upper levels of every situation, for safety's sake. What must be said as a comment, taking into account the experience coming from field tests, is that the minimum values will be certainly lower than those chosen here, but the maximum values will not be higher than the maximum found here. If, for example, we suppose the trajectory is twice the value of the distance reached from the source, all the data shown in the Table O-12 will be about doubled; in particular cases, not so unusual, the ratio trajectory/distance might be more than two.

As a conclusion, all the evaluations made in the different exercises are valid as regards the maximum values of air concentration, but in most cases the minimum values may be not well predicted. Does it matter in the case where such data will be handled for a code of risk evaluations?

Dispersion Tables

N/A = not provided by expert

A-1: -2.0 K/100m Temp Lapse Rate Urban & Rural Surface Roughness					
Downwind distance	**Quantile**	**chiC/Q**	**chi(y)/chiC**	**chi(z)/chiC**	**sig-y**
0.5km	**0%**	2.00E-06	1.20E-01	4.70E-01	8.00E+01
	5%	2.70E-06	2.60E-01	6.00E-01	1.56E+02
	50%	6.00E-06	8.70E-01	8.70E-01	2.63E+02
	95%	1.91E-05	9.40E-01	9.50E-01	3.97E+02
	100%	4.70E-05	9.40E-01	9.50E-01	4.80E+02
1.0km	**0%**	3.10E-07	1.20E-01	3.40E-01	1.40E+02
	5%	4.50E-07	2.60E-01	5.40E-01	2.77E+02
	50%	1.00E-06	8.70E-01	9.00E-01	4.69E+02
	95%	3.60E-06	9.40E-01	1.00E+00	7.11E+02
	100%	1.07E-05	9.40E-01	1.00E+00	8.60E+02
3.0km	**0%**	4.20E-08	1.20E-01	6.80E-01	4.00E+02
	5%	6.60E-08	2.60E-01	8.00E-01	7.80E+02
	50%	1.50E-07	8.70E-01	9.90E-01	1.31E+03
	95%	5.00E-07	9.40E-01	1.00E+00	2.00E+03
	100%	1.00E-06	9.40E-01	1.00E+00	2.40E+03
10.0km	**0%**	1.30E-08	1.40E-01	N/A	1.20E+03
	5%	1.90E-08	2.80E-01	N/A	2.38E+03
	50%	4.20E-08	8.80E-01	N/A	4.03E+03
	95%	1.30E-07	9.40E-01	N/A	6.12E+03
	100%	2.60E-07	9.40E-01	N/A	7.40E+03
30.0km	**0%**	6.00E-09	1.40E-01	N/A	3.30E+03
	5%	8.50E-09	2.60E-01	N/A	5.86E+03
	50%	1.80E-08	8.40E-01	N/A	9.42E+03
	95%	5.30E-08	9.20E-01	N/A	1.39E+04
	100%	9.50E-08	9.20E-01	N/A	1.67E+04

A-2: -1.6 K/100m Temp Lapse Rate Urban & Rural Surface Roughness					
Downwind distance	Quantile	chiC/Q	chi(y)/chiC	chi(z)/chiC	sig-y
0.5km	0%	7.20E-06	6.00E-02	0.70E-03	4.00E+01
	5%	9.30E-06	1.40E-01	5.00E-03	7.80E+01
	50%	2.00E-05	8.30E-01	1.90E-01	1.34E+02
	95%	6.40E-05	9.20E-01	5.40E-01	2.05E+02
	100%	1.45E-04	9.20E-01	5.50E-01	2.40E+02
1.0km	0%	2.70E-06	2.00E-02	4.00E-04	7.00E+01
	5%	3.80E-06	6.00E-02	1.00E-03	1.18E+02
	50%	8.10E-06	6.70E-01	1.40E-01	1.84E+02
	95%	2.20E-05	8.20E-01	5.00E-01	2.68E+02
	100%	4.90E-05	8.30E-01	5.20E-01	3.30E+02
3.0km	0%	2.80E-07	6.00E-02	4.00E-04	2.00E+02
	5%	3.80E-07	1.70E-01	8.00E-04	4.10E+02
	50%	8.40E-07	8.50E-01	1.30E-01	7.00E+02
	95%	2.75E-06	9.30E-01	5.00E-01	1.07E+03
	100%	6.80E-06	9.30E-01	5.70E-01	1.30E+03
10.0km	0%	4.10E-08	6.00E-02	N/A	6.00E+02
	5%	5.80E-08	1.70E-01	N/A	1.23E+03
	50%	1.20E-07	8.50E-01	N/A	2.11E+03
	95%	4.00E-07	9.30E-01	N/A	3.22E+03
	100%	1.00E-06	9.30E-01	N/A	3.90E+03
30.0km	0%	7.00E-09	4.00E-02	N/A	1.50E+03
	5%	1.10E-08	1.50E-01	N/A	3.22E+03
	50%	2.40E-08	8.50E-01	N/A	5.60E+03
	95%	8.40E-08	9.30E-01	N/A	8.64E+03
	100%	2.30E-07	9.30E-01	N/A	1.05E+04

A-3: -1.0 K/100m Temp Lapse Rate Urban & Rural Surface Roughness					
Downwind distance	**Quantile**	**chiC/Q**	**chi(y)/chiC**	**chi(z)/chiC**	**sig-y**
0.5km	**0%**	6.80E-06	5.00E-03	5.00E-06	3.00E+01
	5%	9.70E-06	3.00E-02	1.00E-04	5.40E+01
	50%	2.20E-05	6.00E-01	1.40E-01	8.90E+01
	95%	7.30E-05	7.90E-01	5.40E-01	1.34E+02
	100%	1.68E-04	8.10E-01	6.00E-01	1.60E+02
1.0km	**0%**	2.00E-06	1.60E-02	0.00E+00	5.00E+01
	5%	2.80E-06	7.00E-02	1.00E-06	9.80E+01
	50%	6.70E-06	7.60E-01	1.00E-01	1.64E+02
	95%	2.26E-05	8.80E-01	4.90E-01	2.48E+02
	100%	6.20E-05	8.80E-01	5.20E-01	3.00E+02
3.0km	**0%**	2.90E-07	4.00E-02	0.00E+00	1.30E+02
	5%	4.00E-07	1.40E-01	1.00E-06	2.70E+02
	50%	9.60E-07	8.30E-01	8.00E-02	4.70E+02
	95%	3.40E-06	9.20E-01	4.80E-01	7.20E+02
	100%	1.12E-05	9.20E-02	5.10E-01	8.70E+02
10.0km	**0%**	4.30E-08	6.00E-02	N/A	4.00E+02
	5%	6.30E-08	1.70E-01	N/A	8.00E+02
	50%	1.52E-07	8.40E-01	N/A	1.36E+03
	95%	5.40E-07	9.20E-01	N/A	2.07E+03
	100%	1.90E-06	9.20E-01	N/A	2.50E+03
30.0km	**0%**	9.00E-09	6.00E-02	N/A	1.00E+03
	5%	1.50E-08	1.70E-01	N/A	2.05E+03
	50%	3.20E-08	8.50E-01	N/A	3.50E+03
	95%	1.16E-07	9.30E-01	N/A	5.36E+03
	100%	4.80E-07	9.30E-01	N/A	6.50E+03

A-4: 2.5 K/100m Temp Lapse Rate Urban & Rural Surface Roughness					
Downwind distance	Quantile	chiC/Q	chi(y)/chiC	chi(z)/chiC	sig-y
0.5km	0%	2.60E-05	3.60E-01	2.60E-01	2.00E+01
	5%	3.40E-05	5.40E-01	4.00E-01	4.70E+01
	50%	7.70E-05	9.60E-01	7.80E-01	8.80E+01
	95%	3.00E-04	9.80E-01	9.20E-01	1.40E+02
	100%	8.20E-04	9.80E-01	9.20E-01	1.60E+02
1.0km	0%	8.00E-06	2.70E-01	1.20E-02	3.50E+01
	5%	1.10E-05	5.00E-01	5.00E-02	8.80E+01
	50%	2.50E-05	9.60E-01	4.50E-01	1.63E+02
	95%	9.80E-05	9.80E-01	7.60E-01	2.60E+02
	100%	2.80E-04	9.80E-01	7.80E-01	3.15E+02
3.0km	0%	2.00E-06	3.00E-01	0.00E+00	9.00E+01
	5%	2.80E-06	5.60E-01	1.00E-06	2.40E+02
	50%	5.40E-06	9.70E-01	2.00E-02	4.60E+02
	95%	2.20E-05	9.90E-01	1.80E-01	7.40E+02
	100%	4.90E-05	9.90E-01	2.00E-01	9.10E+02
10.0km	0%	1.10E-07	2.20E-01	0.00E+00	2.70E+02
	5%	1.80E-07	4.80E-01	1.00E-06	7.20E+02
	50%	3.50E-07	9.60E-01	4.00E-02	1.35E+03
	95%	1.40E-06	9.80E-01	3.40E-01	2.14E+03
	100%	3.50E-06	9.80E-01	3 60E-01	2.63E+03
30.0km	0%	5.60E-08	2.20E-01	0.00E+00	7.00E+02
	5%	7.80E-08	4.80E-01	1.00E-06	1.86E+03
	50%	1.90E-07	9.60E-01	4.00E-03	3.48E+03
	95%	7.70E-07	9.80E-01	1.90E-01	5.54E+03
	100%	2.77E-06	9.80E-01	2.10E-01	6.80E+03

B-1: Unknown Lapse Rate 6.0 m/s Aver. Wind Speed		
Downwind distance	**Quantile**	**chiC/Q(ground level)**
220. m	**0%**	5.00E-05
	5%	6.70E-05
	50%	1.40E-04
	95%	3.60E-04
	100%	7.70E-04
315. m	**0%**	2.20E-05
	5%	3.10E-05
	50%	6.30E-05
	95%	1.64E-04
	100%	3.30E-04

B-2: Unknown Lapse Rate 5.0 m/s Aver. Wind Speed		
Downwind distance	**Quantile**	**chiC/Q(ground level)**
220. m	**0%**	4.50E-05
	5%	6.00E-05
	50%	1.18E-04
	95%	2 66E-04
	100%	5 10E-04
315. m	**0%**	2.10E-05
	5%	3.00E-05
	50%	5.90E-05
	95%	1.30E-04
	100%	2.20E-04

B-3: Unknown Lapse Rate 8.0 m/s Aver. Wind Speed		
Downwind distance	**Quantile**	**chiC/Q(ground level)**
300. m	**0%**	6.40E-06
	5%	8.50E-06
	50%	1.70E-05
	95%	5.20E-05
	100%	1.05E-04
600. m	**0%**	1.50E-06
	5%	2.00E-06
	50%	4.20E-06
	95%	1.36E-05
	100%	3.00E-05

B-4: -1.0 K/100m Temp Lapse Rate Flat Surface Roughness		
Downwind distance	**Quantile**	**chiC/Q(ground level)**
300. m	**0%**	1.30E-05
	5%	1.80E-05
	50%	4.20E-05
	95%	1.45E-04
	100%	3.80E-04
600. m	**0%**	3.70E-06
	5%	5.20E-06
	50%	1.26E-05
	95%	4.30E-05
	100%	1.38E-04

B-5: 3.0 K/100m Temp Lapse Rate Flat Surface Roughness					
Downwind distance	Quantile	chi(y)/chiC	chi(z)/chiC	sig-y	sig-z
600. m	0%	8.00E-02	2.60E-01	2.10E+01	6.00E+00
	5%	2.80E-01	4.40E-01	5.40E+01	1.10E+01
	50%	9.30E-01	8.40E-01	1.00E+02	1.80E+01
	95%	9.70E-01	9.50E-01	1.59E+02	2.70E+01
	100%	9.70E-01	9.50E-01	1.95E+02	3.20E+01

C: Stable Conditions Urban & Rural Surface Roughness				
Downwind distance	Quantile	60 min	120 min	240 min
360. m	0%	0.00E+00	0.00E+00	0.00E+00
	5%	1.00E-12	1.00E-12	1.00E-12
	50%	4.80E-08	3.40E-08	2.40E-08
	95%	4.90E-06	3.50E-06	2.50E-06
	100%	1.80E-05	1.20E-05	9.10E-06
970. m	0%	0.00E+00	1.20E-08	1.00E-08
	5%	3.70E-08	2.60E-08	1.90E-08
	50%	4.20E-06	3.10E-06	2.10E-06
	95%	1.50E-05	1.10E-05	7.60E-06
	100%	4.50E-05	1.90E-05	1.35E-05
1970. m	0%	2.00E-07	1.30E-07	9.00E-08
	5%	8.40E-07	6.10E-07	4.30E-07
	50%	3.60E-06	2.60E-06	1.80E-06
	95%	1.00E-05	7.50E-06	5.40E-06
	100%	1.50E-05	1.04E-05	7.50E-06

D: Stable Conditions Flat Surface Roughness				
Downwind distance	Quantile	chiC/Q	sig-y	sig-z
60. m	0%	1.20E-02	5.00E-01	5.00E-01
	5%	1.90E-02	1.20E+00	8.00E-01
	50%	4.10E-02	2.10E+00	1.20E+00
	95%	1.50E-03	3.30E+00	1.70E+00
	100%	3.30E-03	4.50E+00	2.00E+00

E: Length of Arc Crossed By 90% of the Material		
Downwind distance	Quantile	90% arc
80.km	0%	N/A
	5%	1.30E+04
	50%	3.30E+04
	95%	5.30E+04
	100%	N/A
200.km	0%	N/A
	5%	4.60E+04
	50%	1.65E+05
	95%	2.84E+05
	100%	N/A
1000.km	0%	N/A
	5%	3.30E+05
	50%	8.25E+05
	95%	1.32E+06
	100%	N/A

References

1. Desiato, F., and R. Lange, "A Sea Breeze Tracer Study with the MATHEW/ADPIC Transport and Diffusion Model," *Emergency Planning and Preparedness for Nuclear Facilities, Proceedings of an International Symposium, 4-8 November 1985*, International Atomic Energy Agency, Vienna, Austria, distributed by Unipub, New York, pp. 271-280, 1986.

2. Doury, A., "Pratique Francaises en Matière de Prevision Quantitative de la Pollution Atmosphérique Potentielle Liée aux Activités Nucléaires," *Radioactive Releases and Their Dispersion in the Atmosphere Following a Hypothetical Reactor Accident, 22-25 April 1980*, Official Publication European Communities L-2985, Commission of the European Communities, Luxembourg, 1:403-448, 1980.

3. Randerson, D., "Temporal Changes in Horizontal Diffusion Parameters of a Single Nuclear Debris Cloud," *Journal of Applied Meteorology*, 11:670-673, 1972.

4. Bassetti, D., et al., "Atmospheric Diffusion Experiments on a Local Scale at a Coastal Site," EUR 10630 EN, Commission of the European Communities, Luxembourg, 1986.

5. Smith, F.B., and R.M. Blackall, "The Application of Field-Experiment Data to the Parameterization of the Dispersion of Plumes from Ground-Level and Elevated Sources," (C.J. Harris, ed.), *Mathematical Modelling of Turbulent Diffusion in the Environment, Proceedings of the Conference, 12-13 September 1978*, Academic Press, New York, pp. 201-236, 1979.

6. Clarke, R.H., "Predicting Atmospheric Dispersion of Radionuclides - A Summary of the First Report of a Working Group in the U.K.," *Seminar on Radioactive Releases and their Dispersion in the Atmosphere Following a Hypothetical Reactor Accident, 22 April 1980*, Commission of the European Communities, Luxembourg, Part I: 465-482, 1980.

7. Smith, F.B., and D.J. Carson, "Some Thoughts on the Specification of the Boundary-Layer Relevant to Numerical Modelling," *Boundary-Layer Meteorology*, 12:307-330, 1977.

8. Golder, D., "Relations Among Stability Parameters in the Surface Layer," *Boundary-Layer Meteorology*, 3:47-58, 1972.

9. Cagnetti, P., and V. Ferrara, "Une Methode Pratique de Calcul pour l'Evaluation des Concentrations Integrées dans le Temps aux Moyennes et Grandes Distances," *Radioactive Releases and Their Dispersion in the Atmosphere Following a Hypothetical Reactor Accident, 22-25 April 1980*, Official Publication European Communities L-2985, Commission of the European Communities, Luxembourg, 2:797-817, 1980.

10. Heffter, L.J., A.D. Taylor, and G.J. Ferber, "A Regional-Continental Scale Transport, Diffusion, and Deposition Model," NOAA/TM-ARL-50, U.S. Department of Commerce, National Oceanic and Atmospheric Administration, Silver Spring, MD, 1975.

Expert P

1. Characterisation of the Dispersion

1.1 Horizontal advection

Horizontal uniformity and quasi stationarity is assumed for most of the questions. The vertical wind profile was assumed to be according to a power law. The wind velocity at release height was taken to be the representative transport velocity.

1.2 Boundary layer characteristics

As far as possible modern parameterisations for the atmospheric boundary layer (ABL) were used, such as Monin-Obukhov (M-O) surface-layer characterisation and convective and stable boundary-layer parameterisations. The horizontal velocity variance can be derived from the derived ABL characteristics and compared with the velocity variance inferred from the wind direction fluctuation measurements. This may serve as a consistency check.

1.3 Terrain features

The characterisation (of the roughness) of the terrain is very important for the dispersion. The available data are marginal and contribute significantly to the uncertainty of the estimates. For flat terrain a roughness of .05 m was assumed. For urban and rural, 0.50 m was assumed.

1.4 Averaging time (short range, long range)

Where necessary, averages taken over specified averaging times were converted to averages over e.g., one hour by simple power law relationships.

2. Dispersion Model

For vertical plume dimensions smaller than the ABL height, a Gaussian distribution was assumed. When the vertical plume dimension exceeds the boundary-layer thickness, a uniform concentration distribution was assumed.

3. A Summary of Used Formula

3.1 *L and u*$_*$

The M-O parameters L and u$_*$ were determined from the temperature lapse rate and the wind velocity at 10 m by an iterative procedure. The lapse rate was assumed to be derived from measurements at 2 and 100 m respectively.

3.2 The boundary layer height *h*

No data on boundary-layer height were available. In unstable to near neutral conditions, the boundary-layer height was therefore estimated, depending on stability in the range of 1200-600 m. In stable conditions the boundary-layer height was estimated from:

$$h = 0.4\left(\frac{u_* L}{f}\right)^{1/2},$$

with f = 1.2E - 4 s^{-1}, the Coriolis parameter at mid-latitude.

3.3 The horizontal velocity variance, σ_v

$$\sigma_v = 2u_*(1 - 0.9z_s/h)^{3/4} \quad (\textit{stable})$$

$$\sigma_v = 2u_* T_{wm} \quad (\textit{neutral})$$

with $$\sigma_v = (0.3w_*^2 + 4T_{wm}^2 u_*^2)^{1/2} \quad (\textit{unstable})$$

$$T_{wm} = 1 - 0.8z_s/h$$

$$w_* = u_*\left(\frac{h}{-kL}\right)^{1/3}$$

3.4 The vertical velocity variance σ_w

$$\sigma_w = 1.3u_*(1 - 0.9z_s/h)^{3/4} \quad (\textit{stable})$$

$$\sigma_w = 1.3u_* T_{wm} \quad (\textit{near neutral})$$

$$\sigma_w = 1.3u_* T_{wm} \quad (\textit{near neutral})$$

$$\sigma_w = w_*\left\{0.4T_{wc}^2 + (1.3T_{wm}u_*/w_*)^2\right\}^{1/2} \quad (\textit{unstable})$$

$$T_{wc} = 2.1\left(\frac{z_s}{h}\right)^{1/3} T_{wm}$$

3.5 The lateral dispersion coefficient σ_y

$$\sigma_y = \frac{\sigma_v t}{1 + 0.9\left(\frac{t}{T}\right)^{1/2}} ,$$

with

t = x/u

and

x ≥ 10 km: T = 15000 s

x < 10 km: T = 1000 s

3.6 The vertical dispersion coefficient σ_z

$$\sigma_z = \frac{\sigma_w t}{1 + \left(\frac{t}{T}\right)^{1/2}} ,$$

T = 60 s (stable)

T = 600 s (neutral and unstable)

3.7 Concentration Estimates

These were based on the general conservation formula

$Q = \iint \chi u \, dy \, dz$

For small distances ($\sigma_z \leq h$), dispersion was assumed to be Gaussian in lateral and vertical directions. For larger distances the vertical distribution was assumed to be uniform in the layer 0-h.

Hence, the centerline concentration:

$$\chi_{cl}/Q = \frac{1}{2\pi\sigma_y\sigma_z u}\left(1 + e^{-1/2\left(\frac{2z_s}{\sigma_z}\right)^2}\right) ,$$

the ground level concentration

$$\chi_{gl}/Q = \frac{1}{\pi\sigma_y\sigma_z u} e^{-1/2\left(\frac{z_s}{\sigma_z}\right)^2} ,$$

The concentration in the vertical plane through the source:

$$\chi_z/Q = \frac{1}{2\pi\sigma_y\sigma_z u}\left(e^{-1/2\left(\frac{z-z_s}{\sigma_z}\right)^2} + e^{-1/2\left(\frac{z+z_s}{\sigma_z}\right)^2}\right) ,$$

the uniform concentration:

$$\chi_h/Q = \frac{1}{\sqrt{2\pi}\sigma_y u h}$$

and the relative lateral concentration

$$\chi_y/\chi_{cl} = e^{1/2\left(\frac{y}{\sigma_y}\right)^2} .$$

3.8 The Wind Velocity

It is unclear at what height the wind velocity is measured. If the height of the source is different from this height the conversion is made through

$$u_{zs} / u_{10} = (z_s / 10)^p,$$

where p is a function of stability. From the 10-minute wind direction fluctuation at release height σ_θ, the horizontal velocity variance can be inferred through

$$\sigma_v = \sigma_\theta u (t / 10)^s ,$$

where t is the sampling time (in minutes) and s is a weak function of stability, here taken constant and equal to 0.19. The wind velocity u is at release height.

4. Case by Case Comments

4.1 Very unstable conditions, good consistency in horizontal variance. Based on (among others) the examples of uncertainties in cross-wind, relative values were estimated to be low (90% within a factor of +/- 5 to 6; the uncertainty in the cross-wind standard deviation was +/- 1.5 to 2.5 and in concentrations 2.5 to 3 depending on consistency). Mixed layer height is 1500 m. Concentrations at 10 and 30 km downwind were assumed to be vertically uniform.

4.2 Unstable, good consistency, mixed-layer height 1000 m.

4.3 Near neutral, medium consistency, mixed-layer height 1000 m.

4.4 Stable, medium consistency, mixed-layer height 150 m.

4.5 Near neutral, medium consistency, mixed-layer height 400 m.

4.6 Near neutral, medium consistency, mixed-layer height 400 m.

4.7 Unstable, poor consistency, mixed-layer height 1500 m.

4.8 Near neutral, medium consistency, mixed-layer height 500 m.

4.9 Stable, good consistency, mixed-layer height 60 m.

4.10 Stable, good consistency, mixed-layer height 170 m. Questions not understood, also not after receipt of fax.

4.11 Stable, mixed-layer height 110 m. The effect of meandering in the 1 minute samples was not taken into account (it was assumed that the sampler was always located at the plume centerline). Standard deviations in plume widths were reduced by approximately 50%; consequently concentrations increased by a factor of 4.

At 80, 200, and 1000 km, downwind travel times were assumed to be respectively 8, 19, and 93 h. Stationary and homogeneous conditions are highly improbable over these times and distances. Estimates are based on the experience and model calculations associated with the Chernobyl reactor accident.

Dispersion Tables

N/A = not provided by expert

A-1: -2.0 K/100m Temp Lapse Rate Urban & Rural Surface Roughness					
Downwind distance	**Quantile**	**chiC/Q**	**chi(y)/chiC**	**chi(z)/chiC**	**sig-y**
0.5km	**0%**	N/A	N/A	N/A	N/A
	5%	4.00E-06	2.00E-01	4.00E-01	1.40E+02
	50%	8.00E-06	7.00E-01	8.00E-01	2.05E+02
	95%	2.50E-05	2.50E+00	2.00E+00	3.00E+02
	100%	N/A	N/A	N/A	N/A
1.0km	**0%**	N/A	N/A	N/A	N/A
	5%	1.00E-06	2.00E-01	2.00E-01	2.50E+02
	50%	2.70E-06	7.00E-01	6.00E-01	3.65E+02
	95%	6.00E-06	2.00E+00	2.00E+00	5.50E+02
	100%	N/A	N/A	N/A	N/A
3.0km	**0%**	N/A	N/A	N/A	N/A
	5%	2.00E-07	1.50E-01	1.50E-01	5.50E+02
	50%	5.20E-07	6.00E-01	3.00E-01	8.50E+02
	95%	1.30E-06	3.00E+00	1.50E+00	1.30E+03
	100%	N/A	N/A	N/A	N/A
10.0km	**0%**	N/A	N/A	N/A	N/A
	5%	1.50E-08	2.00E-01	0.00E+00	1.50E+03
	50%	3.40E-08	8.20E-01	0.00E+00	3.90E+03
	95%	1.00E-07	5.00E+00	0.00E+00	9.00E+03
	100%	N/A	N/A	N/A	N/A
30.0km	**0%**	N/A	N/A	N/A	N/A
	5%	4.00E-09	1.00E-01	0.00E+00	6.00E+03
	50%	1.40E-08	7.70E-01	0.00E+00	9.40E+03
	95%	4.00E-08	5.00E+00	0.00E+00	1.50E+04
	100%	N/A	N/A	N/A	N/A

A-2: -1.6 K/100m Temp Lapse Rate Urban & Rural Surface Roughness					
Downwind distance	Quantile	chiC/Q	chi(y)/chiC	chi(z)/chiC	sig-y
0.5km	0%	N/A	N/A	N/A	N/A
	5%	3.50E-06	2.00E-01	2.00E-01	7.00E+01
	50%	9.00E-06	7.00E-01	7.00E-01	1.25E+02
	95%	2.50E-05	2.00E+00	2.00E+00	1.75E+02
	100%	N/A	N/A	N/A	N/A
1.0km	0%	N/A	N/A	N/A	N/A
	5%	1.00E-06	1.70E-01	1.70E-01	1.50E+02
	50%	3.00E-06	6.70E-01	6.70E-01	2.25E+02
	95%	7.00E-06	2.50E+00	2.50E+00	3.50E+02
	100%	N/A	N/A	N/A	N/A
3.0km	0%	N/A	N/A	N/A	N/A
	5%	3.00E-07	1.50E-01	1.50E-01	3.50E+02
	50%	5.00E-07	6.60E-01	6.60E-01	5.50E+02
	95%	1.30E-06	2.50E+00	2.50E+00	8.00E+02
	100%	N/A	N/A	N/A	N/A
10.0km	0%	N/A	N/A	N/A	N/A
	5%	3.00E-08	2.00E-01	0.00E+00	1.00E+03
	50%	7 40E-08	5.40E-01	0.00E+00	1.35E+03
	95%	1.70E-07	3.00E+00	0.00E+00	2.00E+03
	100%	N/A	N/A	N/A	N/A
30.0km	0%	N/A	N/A	N/A	N/A
	5%	1.50E-08	1.00E-01	0.00E+00	2.00E+03
	50%	3.50E-08	3.70E-01	0.00E+00	2.80E+03
	95%	9.00E-08	3.00E+00	0.00E+00	4.00E+03
	100%	N/A	N/A	N/A	N/A

A-3: -1.0 K/100m Temp Lapse Rate Urban & Rural Surface Roughness					
Downwind distance	**Quantile**	**chiC/Q**	**chi(y)/chiC**	**chi(z)/chiC**	**sig-y**
0.5km	**0%**	N/A	N/A	N/A	N/A
	5%	3.00E-06	1.50E-01	1.50E-01	4.00E+01
	50%	7.90E-06	6.40E-01	6.50E-01	1.05E+02
	95%	2.40E-05	2.00E+00	2.00E+00	2.50E+02
	100%	N/A	N/A	N/A	N/A
1.0km	**0%**	N/A	N/A	N/A	N/A
	5%	8.00E-07	1.50E-01	1.00E-01	1.00E+02
	50%	2.40E-06	7.40E-01	6.30E-01	1.93E+02
	95%	7.50E-06	2.50E+00	2.50E+00	4.00E+02
	100%	N/A	N/A	N/A	N/A
3.0km	**0%**	N/A	N/A	N/A	N/A
	5%	1.50E-07	1.50E-01	1.20E-01	2.50E+02
	50%	4.10E-07	7.70E-01	6.30E-01	4.85E+02
	95%	1.20E-06	3.00E+00	3.00E+00	1.00E+03
	100%	N/A	N/A	N/A	N/A
10.0km	**0%**	N/A	N/A	N/A	N/A
	5%	1.00E-08	2.00E-01	N/A	1.00E+03
	50%	3.30E-08	8.90E-01	N/A	2.05E+03
	95%	1.00E-07	4.00E+00	N/A	4.00E+03
	100%	N/A	N/A	N/A	N/A
30.0km	**0%**	N/A	N/A	N/A	N/A
	5%	5.00E-09	1.00E-01	N/A	2.60E+03
	50%	1.30E-08	8.90E-01	N/A	5.20E+03
	95%	4.00E-08	4.00E+00	N/A	1.00E+04
	100%	N/A	N/A	N/A	N/A

A-4: 2.5 K/100m Temp Lapse Rate Urban & Rural Surface Roughness					
Downwind distance	Quantile	chiC/Q	chi(y)/chiC	chi(z)/chiC	sig-y
0.5km	0%	N/A	N/A	N/A	N/A
	5%	1.70E-05	2.00E-01	2.00E-01	3.50E+01
	50%	5.20E-05	9.20E-01	8.10E-01	7.20E+01
	95%	1.50E-04	5.00E+00	4.00E+00	1.40E+02
	100%	N/A	N/A	N/A	N/A
1.0km	0%	N/A	N/A	N/A	N/A
	5%	7.00E-06	2.00E-01	1.20E-01	6.00E+01
	50%	2.00E-05	9.00E-01	6.20E-01	1.30E+02
	95%	6.00E-05	5.00E+00	4.00E+00	2.00E+02
	100%	N/A	N/A	N/A	N/A
3.0km	0%	N/A	N/A	N/A	N/A
	5%	1.00E-06	2.00E-01	7.00E-02	1.50E+02
	50%	2.90E-06	8.90E-01	3.60E-01	3.10E+02
	95%	9.00E-06	5.00E+00	5.00E+00	4.50E+02
	100%	N/A	N/A	N/A	N/A
10.0km	0%	N/A	N/A	N/A	N/A
	5%	2.00E-07	2.00E-01	1.00E-02	7.00E+02
	50%	6.60E-07	9.40E-01	1.00E-01	1.38E+03
	95%	2.00E-06	6.00E+00	6.00E+00	2.00E+03
	100%	N/A	N/A	N/A	N/A
30.0km	0%	N/A	N/A	N/A	N/A
	5%	7.00E-08	2.00E-01	1.00E-03	1.70E+03
	50%	2.70E-07	9.30E-01	1.00E-02	3.40E+03
	95%	9.00E-07	6.00E+00	6.00E+00	5.00E+03
	100%	N/A	N/A	N/A	N/A

B-1: Unknown Lapse Rate 6.0 m/s Aver. Wind Speed		
Downwind distance	**Quantile**	**chiC/Q(ground level)**
220. m	**0%**	N/A
	5%	2.00E-05
	50%	4.80E-05
	95%	1.00E-04
	100%	N/A
315. m	**0%**	N/A
	5%	1.70E-05
	50%	3.70E-05
	95%	1.00E-04
	100%	N/A

B-2: Unknown Lapse Rate 5.0 m/s Aver. Wind Speed		
Downwind distance	**Quantile**	**chiC/Q(ground level)**
220. m	**0%**	N/A
	5%	2.00E-05
	50%	5.80E-05
	95%	1.80E-04
	100%	N/A
315. m	**0%**	N/A
	5%	1.40E-05
	50%	4.40E-05
	95%	1.20E-04
	100%	N/A

B-3: Unknown Lapse Rate 8.0 m/s Aver. Wind Speed		
Downwind distance	**Quantile**	**chiC/Q(ground level)**
300. m	**0%**	N/A
	5%	5.00E-06
	50%	1.40E-05
	95%	4.00E-05
	100%	N/A
600. m	**0%**	N/A
	5%	1.50E-06
	50%	4.60E-06
	95%	1.30E-05
	100%	N/A

B-4: -1.0 K/100m Temp Lapse Rate Flat Surface Roughness		
Downwind distance	**Quantile**	**chiC/Q(ground level)**
300. m	**0%**	N/A
	5%	2.80E-05
	50%	8.40E-05
	95%	2.50E-04
	100%	N/A
600. m	**0%**	N/A
	5%	1.30E-05
	50%	3.80E-05
	95%	1.10E-04
	100%	N/A

B-5: 3.0 K/100m Temp Lapse Rate Flat Surface Roughness					
Downwind distance	**Quantile**	**chi(y)/chiC**	**chi(z)/chiC**	**sig-y**	**sig-z**
600. m	**0%**	N/A	N/A	N/A	N/A
	5%	7.00E-02	1.20E-01	2.00E+01	7.00E+00
	50%	2.80E-01	6.20E-01	3.10E+01	1.00E+01
	95%	9.00E-01	9.50E-01	4.50E+01	1.50E+01
	100%	N/A	N/A	N/A	N/A

C: Stable Conditions Urban & Rural Surface Roughness				
Downwind distance	**Quantile**	**60 min**	**120 min**	**240 min**
360. m	**0%**	N/A	N/A	N/A
	5%	1.00E-06	8.70E-07	8.00E-07
	50%	4.00E-06	3.48E-06	3.20E-06
	95%	1.20E-05	1.04E-05	9.60E-06
	100%	N/A	N/A	N/A
970. m	**0%**	N/A	N/A	N/A
	5%	6.00E-06	5.22E-06	4.80E-06
	50%	1.70E-05	1.48E-05	1.36E-05
	95%	5.00E-05	4.35E-05	4.00E-05
	100%	N/A	N/A	N/A
1970. m	**0%**	N/A	N/A	N/A
	5%	4.00E-06	3.48E-06	3.20E-06
	50%	1.20E-05	1.04E-05	9.60E-06
	95%	4.00E-05	3.48E-05	3.20E-05
	100%	N/A	N/A	N/A

D: Stable Conditions Flat Surface Roughness				
Downwind distance	Quantile	chiC/Q	sig-y	sig-z
60. m	0%	N/A	N/A	N/A
	5%	6.00E-03	1.00E+00	5.00E-01
	50%	1.20E-02	3.00E+00	2.00E+00
	95%	2.50E-02	8.00E+00	6.00E+00
	100%	N/A	N/A	N/A

E: Length of Arc Crossed By 90% of the Material		
Downwind distance	Quantile	90% arc
80.km	0%	N/A
	5%	1.40E+04
	50%	2.09E+04
	95%	8.37E+04
	100%	N/A
200.km	0%	N/A
	5%	5.24E+04
	50%	2.09E+05
	95%	3.14E+05
	100%	N/A
1000.km	0%	N/A
	5%	5.24E+05
	50%	2.51E+06
	95%	3.35E+06
	100%	N/A

References

Carruthers, D.J., et al., "UK Atmospheric Dispersion Modelling System," (H. van Dop and G. Kallos, eds.), *Air Pollution Modeling and Its Application IX, 29 September–4 October 1991*, Plenum Press, New York, p. 15, 1992.

Crawford, T.V., *Meteorological Measurements for Emergency Response, in Meteorological Aspects of Emergency Response*, A.M.S., Boston, 1990.

Gryning, S.E. et al., "Applied Dispersion Modelling Based on Meteorological Scaling Parameters," *Atmospheric Environment*, 21:79-89, 1987.

Hanna, S.R., "Applications in Air Pollution Modeling," (F.T.M. Nieuwstadt and H. Van Dop, eds.), *Atmospheric Turbulence and Air Pollution Modelling, 21-25 September 1981*, D. Reidel, Boston, MA, pp. 275-310, 1982.

Hanna, S.R., "Lateral Dispersion from Tall Stacks," *Journal of Climate and Applied Meteorology*, 25:1426-1433, 1986.

Holtslag, A.A.M., "Estimates of Diabatic Wind Speed Profiles from Near-Surface Weather Observations," *Boundary-Layer Meteorology*, 29:225-250, 1984.

Holtslag, A.A.M., and H.A.R. de Bruin, "Applied Modelling of the Nighttime Surface Energy Balance Over Land," *Journal of Climate and Applied Meteorology*, 27:689-704, 1988.

Holtslag, A.A.M., and A.P. Van Ulden, "A Simple Scheme for Daytime Estimates of the Surface Fluxes from Routine Weather Data," *Journal of Climate and Applied Meteorology*, 22:517-529, 1983.

Lyons, T.J., and W.D. Scott, *Principles of Air Pollution Meteorology*, Belhaven Press, London, p. 224, 1990.

Nieuwstadt, F.T.M., and C.A. Engeldal, "Application of the Recommended National Air Pollution Model of the Netherlands to the NATO Common Data Base for the Frankfurt Area," KNMI-WR-76-17, Royal Netherlands Meteorological Institute, 1976.

Pasquill, F., and F.B. Smith, *Atmospheric Diffusion*, 3rd ed., Wiley, New York, p. 437, 1983.

Van Dop, H., "Terrain Classification and Derived Meteorological Parameters for Interregional Transport Models," *Atmospheric Environment*, 17:1099-1105, 1983.

Van Dop, H., B.J. de Haan, and C. Engeldal, "The KNMI Mesoscale Air Pollution Model," KNMI-WR-82-6, Royal Netherlands Meteorological Institute, 1982.

APPENDIX B

Short Biographies of Dispersion and Deposition Experts

B. Short Biographies of Dispersion and Deposition Experts

Dispersion Experts

Pietro Cagnetti, Italy

Dr. Cagnetti earned a Ph.D. in Physics (1961) and a Ph.D. in Applied Nuclear Physics (1963) from Rome University, Italy. Since 1967, he has worked in the field of atmospheric diffusion, with the aim of studying mathematical models of diffusion-deposition to evaluate the dose to a population after a release of airborne radioactive material. He is the Italian expert in the field of atmospheric diffusion for the Commission of European Experts (CEE) and charged with the application of Article 37 of the EURATOM Treaty. Since 1970, Dr. Cagnetti has been involved in modeling and experiments in the fluid diffusion field (liquid wastes and related environmental issues). He has also been involved in atmospheric tracer experiments, and was in charge (under the EURATOM Treaty) of elaborating models of diffusion-deposition on regional and continental scales to establish the worst consequences of an accidental airborne release of radioactive material. In 1982, he produced the RAMIC code (Reference Accident Maximum Integrated Concentrations). He carried out several experimental studies for the International Atomic Energy Agency (IAEA, Vienna) and the CEE (such as the 1980 Risoe meeting on radioactive releases and their deposition from the atmosphere). Dr. Cagnetti has been a member of several CEE Working Groups: the Reference Accident Group, the Meteo Group, and the Reactor Safety Research Program. Since 1990 he has been responsible for coordinating the environmental impact evaluations of the Italian Nuclear Energy Committee.

Franklin A. Gifford, U.S.A.

Dr. Gifford is a graduate of New York University, New York, NY (B.S. 1947), and Pennsylvania State University, University Park, PA (M.S. 1954, Ph.D. 1955, Meteorology). He was chief meteorologist at Northwest Airlines until joining the National Oceanic and Atmospheric Administration (NOAA, 1950) as research meteorologist for the U.S. Weather Bureau in its Washington, D.C. office. Dr. Gifford is former director of the NOAA Atmospheric Turbulence and Diffusion Laboratory in Oak Ridge, TN (1955-80). Currently, Dr. Gifford serves as meteorological consultant on atmospheric diffusion and environmental pollution to various clients, including Los Alamos National Laboratory, NOAA, the U.S. Environmental Protection Agency (EPA), National Academy of Engineering (NAE), National Council on Radiation Protection, International Atomic Energy Agency (IAEA), and Sandia National Laboratories. Dr. Gifford received the American Meteorological Society Award for Outstanding Contribution to the Advance of Applied Meteorology, the U.S. Department of Commerce Gold Medal, and other awards; he is the author of over 140 technical publications.

Paul Gudiksen, U.S.A.

Paul Gudiksen is presently Group Leader, Atmospheric and Geophysical Sciences Division, Lawrence Livermore National Laboratory, Livermore, CA. Mr. Gudiksen supervised the development of the ARAC (atmospheric release advisory capability) emergency response service (U.S. Department of Energy–DOE–system for real-time prediction of trajectories of accidental releases and for directing evacuation that is currently in place at all DOE facilities).

Steve Hanna, U.S.A.

Dr. Hanna received his Ph.D. in Meteorology from Pennsylvania State University, University Park, PA. He worked for NOAA's Atmospheric Turbulence and Diffusion Laboratory in Oak Ridge, TN for 14 years. He was a research meteorologist for Environmental Research & Technology in Concord, MA, for four years, and since 1985 has been chief scientist for Sigma Research Corporation, also of Concord, MA. He is the Chief Editor of the *Journal of Applied Meteorology*, a position he has held since 1988. Dr. Hanna has served as former chairman, Atmospheric Turbulence and Diffusion Committee of the American Meteorological Society. He pioneered the use of Monte Carlo models to simulate diffusion. Dr. Hanna has over 80 peer-reviewed publications.

J. G. Kretzschmar, Belgium

Dr. Kretzschmar was graduated in 1965 as an electronic engineer at the Catholic University, Leuven, Belgium, where he went on to receive his certificate (M.S. 1966), and a Ph.D. in Nuclear Physics in 1969. Dr. Kretzschmar was given honorary research associate status at University College, London and then the Esro-NASA post-doctoral research fellowship at the University of California, Berkeley. In 1972, Dr. Kretzschmar joined the Belgian

Nuclear Energy Research Center to begin research on air pollution monitoring, evaluation and modeling (of both nuclear and non-nuclear pollutants). By 1985, Dr. Kretzschmar had shifted his research to artificial intelligence and management information systems. Since 1992, he has chaired the Division of Energy Department of the Flemish Institute for Technological Research (VITO) in Mol. Dr. Kretzschmar is the author of more than 150 peer-reviewed publications, as well as a member of the Royal Society of Flemish Engineers, Institute of Electrical and Electronics Engineers (IEEE), the European Association for the Science of Air Pollution (EURASAP), and the International Microwave Power Institute (IMPI). Dr. Kretzschmar has served as a consultant on air pollution issues to the World Health Organization (WHO), United Nations Environmental Program (UNEP), and other international organizations.

Klaus Nester, Germany

Dr. Nester has a degree in Meteorology from the Technical University of Darnstadt, Germany (1966). After employment at the Swiss Meteorological Service, he worked (1970-1983) in the Environmental Meteorology group of the Safety Department of the Karlsruhe Nuclear Research Centre (KfK), on dispersion experiments carried out at KfK. More than 70 experiments with different tracers have been performed by Dr. Nester, from which came the dispersion parameters that are currently being used in the German Regulatory Guides on atmospheric dispersion. Apart from experiments, Dr. Nester has done dispersion modeling (three dimensional cooling tower plume models). Since 1984, he has been head of the Institute of Meteorology and Climatic Research at KfK, which has since developed the DRAIS model (three dimensional Eulerian grid model for atmospheric dispersion over complex terrain) and TRAVELING model (Lagrangian particle dispersion model). Dr. Nester was also involved in the performance of the mesoscale dispersion experiment with tracers in the TULLA experiment.

Shankar Rao, U.S.A.

Dr. Rao earned his Ph.D. in geophysical fluid mechanics from the University of Notre Dame, Notre Dame, IN (1972), and did post-doctoral work in meteorology at the Air Force Cambridge Research Laboratories (1972-74). Dr. Rao was employed as Senior Scientist at Environmental Research and Technology, Inc. of Concord, MA from 1974 to 1976. Since 1976, Dr. Rao has been Senior Physical Scientist at the Atmospheric Turbulence and Diffusion Division of the NOAA, Oak Ridge, TN. Dr. Rao has been a consultant for the past 22 years on atmospheric boundary layer and turbulence studies, as well as on air pollution modeling. Dr. Rao participated in the DOE U.S. Atmospheric Studies in Complex Terrain program (1979) and developed advanced boundary layer models and several dispersion models which were tested with data from field studies. Dr. Rao has also worked on modeling urban air quality standards for the U.S. EPA, and atmospheric dispersion of UF_6 releases for the U.S. Nuclear Regulatory Agency (NRC). Dr. Rao's current work includes air toxic sampling and data analyses, air pollution model evaluation and uncertainty studies, stochastic dispersion modeling, and parametrization of surface processes for atmospheric models.

Han van Dop, Netherlands

Dr. van Dop received his Ph.D. at the University of Leiden, where he wrote his dissertation on high-energy molecular collisions. From 1974 to 1989, Dr. van Dop was a researcher with the Department of Meteorology of the Netherlands, where he did research primarily on atmospheric turbulence, boundary-layer meteorology, and air pollution diffusion. Dr. van Dop has worked with the University of Cambridge (1983-84) and the World Meteorological Organization (1989-91). Since 1991, Dr. van Dop has been associate professor and researcher with the Institute for Marine and Atmospheric Sciences of the University of Utrecht, conducting research on global modeling of transport and chemistry of atmospheric constituents and atmospheric remote sensing. Among his professional affiliations, Dr. van Dop serves as associate editor of *Atmospheric Environment* and is active as a consultant and peer reviewer.

Deposition Experts

John Brockmann, U.S.A.

John Brockmann is Sandia National Laboratories' premier aerosol scientist, specializing in aerosol source terms arising from severe nuclear reactor accidents. He is chairman of the Nuclear and Radioactive Aerosols Working Group of the American Association for Aerosol Research. He has authored over 65 peer-reviewed publications.

Sheldon Friedlander, U.S.A.

Sheldon Friedlander is Director, Engineering Research Center, Hazardous Substance Control, University of California at Los Angeles (UCLA), and former Chair, Chemical Engineering Department, UCLA. He has received

the Fuchs Memorial Award (International Award for Aerosol Research), the Walker Award from the American Institute of Chemical Engineers (AIChE) for contributions to chemical engineering literature, and many others. He has served on more than 15 national advisory committees, and was chairman of several, including the Subcommittee on Photochemical Oxidants and Ozone (NAS[National Academy of Sciences]/NRC) and the Panel on Particulate Emissions, Committee on Air Quality Management (NRC/NAE). He is the author of *Smoke, Dust, and Haze: Fundamentals of Aerosol Behavior*, and of over 150 peer-reviewed publications.

John Garland, U. K.

John Garland was graduated in Physics at Bristol University in 1960 and joined the United Kingdom Atomic Energy Authority (AEA) in the same year. His research career has included aspects of health physics and occupational hygiene, but since the mid-1960s his work has focused on the environmental behavior of radionuclides and pollutants discharged into the atmosphere. The process of deposition from the atmosphere to the surface of the earth differs for each pollutant-surface combination, and Mr. Garland helped develop an understanding of the deposition of gaseous and particulate pollutants, including I-131, tritium, Cs-137, sulphur dioxide, ozone, and sulphate particles, to various land and aquatic surfaces. He has also quantified the process of resuspension of material deposited on the ground. An additional interest of his has been the influence of pollution on visibility. He is currently Chief Technical Consultant in the National Environmental Technology Centre, AEA Technology, with responsibility for the Environmental Radioactivity Programme, and participates in projects involving sampling, measurement, modeling, and assessment of non-radioactive pollutants in the environment.

Jozef M. Pacyna, Norway

Dr. Pacyna received his M.S. in Chemical Engineering, and did his doctoral work on migration of radionuclides through the environment. Dr. Pacyna has also researched fluxes and transport of air pollutants, and the chemical and physical transformation of particles within air masses and in removal processes. He is working on UV-B impact on human health. Dr. Pacyna is a senior scientist at the Norwegian Institute for Air Research (NILU) in Lillestroem, Norway and an adjunct professor at the School of Public Health, the University of Michigan, Ann Arbor, MI.

Jorn Roed, Denmark

Dr. Jorn Roed is the head of the Contamination Physics Group at Riso National Laboratory in Denmark. One of the tasks of this group for the past few years has been the identification of important parameters concerning deposition of radioactive matter under different conditions. During the last five years, Dr. Roed has participated in the following projects, which have been funded in part or fully by the European Economic Community (EEC) or NKA (Northern Liaison Committee): Recl (NKA), AKTU (NKA), RAD (NKA), Collaboration between Nordic and SNG Countries (NKA), MARIA (EEC), Contamination (EEC), Decontamination (EEC), Ressac (EEC), Deposition and Run-Off (EEC), Reduction in Inhalation Dose (EEC), Indoor Deposition (EEC) and CHECIR (EEC).

Richard Scorer, U. K.

Dr. Scorer lectured in meteorology at Imperial College, London, and became Professor of Theoretical Mechanics in 1962 at this institution, where he served with distinction until retirement. He was awarded title of Senior Research Fellow in Environmental Technology and became one of the founders of the *International Journal on Air Pollution*, which later changed its name to *The International Journal of Atmospheric Environment*. Dr. Scorer has done research and published on the topics of atmospheric waves, convection, and physical and mechanical mechanisms in clouds. Dr. Scorer is past president of the Royal Meteorological Society. His present research deals with the use of satellite pictures to study the physics and mechanics of clouds, as well as pollutant effects on the environment.

George Sehmel, U.S.A.

George Sehmel, presently of Pacific Northwest Laboratories, has 30 years of experience in the field of aerosol deposition related to smoke/obscurant theory, testing in the field and in wind tunnels, pollutant plume depletion by dry deposition removal, and wind resuspension of surface contaminants into the air. He is the author of over 290 peer-reviewed publications.

Sean Twomey, U.S.A.

Presently a consultant, Mr. Twomey is a retired professor of Atmospheric Sciences, University of Arizona, Tucson, AZ. He has received a citation from the U.S. Secretary of Commerce for his contribution to the satellite remote sensing program for the U. S. Weather Service, and the Rossby Medal of the American Meteorological Society. He is the author of *Atmospheric Aerosols*, and over 100 peer-reviewed publications.

DISTRIBUTION

Pietro Cagnetti
Indirrizzo Postalc
Post Address
C.P.2400
00100 ROMA
(ITALIA)

Frank Gifford
109 Gorgas Lane
Oak Ridge, TN 37830

Paul Gudiksen
L.L. National Laboratory
P.O. Box 808 L-262
Livermore, CA 94550

Steve Hanna
Sigma Research Corporation
196 Baker Avenue
Concord, MA 01742

Jan Kretzschmar
Vareselaan 13
B-2400 Mol
Belgium

Klaus Nester
Institut fur Meteorologie
& Klimaforschung
Kernforschungszentrum
GmbH Postfach 3640
D-76021 Karlsruhe
GERMANY

Shankar Rao
NOAA/ERL/Air Resources
Laboratory
456 South Illinois Avenue
P.O. Box 2456
Oak Ridge, TN 37831

Han van Dop
Princetonplein 5 3584 CC
P.O. Box 80.005 3508 TA Utrecht
The NETHERLANDS

John Brockmann
Sandia National Laboratories
Department 6422
P.O. Box 5800
Albuquerque, NM 87185

Sheldon Friedlander
5531 Boelter Hall
University of California
Los Angeles, CA 90024

John Garland
AEA Technology
Culham
Abingdon
Oxfordshire OX14 3DB
United Kingdom

Jozef Pacyna
Norwegian Institute for
Air Research
Lillestrom
Norway

Joern Roed
RISO National Laboratory
P.O. Box 49
DK-4000 Roskilda
Denmark

Richard Scorer
2 Stanton Road
London SW20 8RL
United Kingdom

George Sehmel
Battelle
Battelle Blvd.
LSL2 Building
Richland, WA 99352

Sean Twomey
11280 E. Escalante Rd.
Tuscon, AZ 85730

Roger Cooke
Delft University of Technology
Julianalaan 132
P.O. Box 356
2600 AJ Delft
The Netherlands

Louis Goossens (50)
Delft University of Technology
Kanaalweg 2
2628 EB Delft
The Netherlands

Steve Hora
University of Hawaii
Dept. Business & Economics
P.O. Box 5622
Hilo, HI 96720

Bernd Krann
Kloosterkade 171
2628 JA Delf
the Netherlands

Juergen Paesler-Saur
Nuclear Research Center
INR, Bldg. 433
Postfach 3640
D-7500 Karlsruhe
West Germany

Oak Ridge National Laboratory(2)
Attn: Steve Fisher
Sherrel Greene
MS-8057
P.O. Box 2009
Oak Ridge, TN 37831

Westinghouse Savannah River Co. (2)
Attn: Kevin O'Kula
Jackie East
Safety Technology Section
1991 S. Centennial Ave. Bldg. 1
Aiken, SC 29803

Vern Peterson
Bldg. T886B
EG&G Rocky Flats
P.O. Box 464
Golden, CO 80402

Brookhaven National Laboratory (3)
Attn: Lev Neymotin
Arthur Tingle
Trevor Pratt
Bldg. 130
Uptown, NY 11973

EG&G Idaho, Inc. (2)
Attn: Doug Brownson
Darrel Knudson
MS-2508
P.O. Box 1625
Idaho Falls, ID 83415

EG&G Idaho, Inc.(2)
Attn: Art Rood
Mike Abbott
MS-2110
P.O. Box 1625
Idaho Falls, ID 83415

Judy Rollstin
GRAM Inc.
8500 Menaul Blvd. NE
Albuquerque, NM 87112

Los Alamos National Labs (2)
Attn: Desmond Stack
Kent Sasser
N-6, K-557
Los Alamos, NM 87545

Technadyne Engineering Consultants(3)
Attn: David Chanin
Jeffery Foster
Walt Murfin
Suite A225
8500 Menaul Blvd. NE
Albuquerque, NM 87112

David M. Brown
Paul C. Rizzo Associates, Inc.
300 Oxford Drive
Monroeville, PA 15146-2347

Westinghouse Electric Company(3)
Attn: John Iacovino
Burt Morris
Griff Holmes
Energy Center East, Bldg. 371
P.O. Box 355
Pittsburgh, PA 15230

Marc Rothschild
Halliburton NUS
1303 S. Central Ave.
Suite 202
Kent, WA 98032

Knolls Atomic Power Laboratory(2)
Attn: Ken McDonough
Dominic Sciaudone
Box 1072
Schenectady, NY 12301

Mr. Dennis Strenge
Pacific Northwest Laboratory
RTO/125 P.O. Box 999
Richland, WA 99352

Mr. Fred Mann
Westinghouse Hanford Co.
W/A-53
P.O. Box 1970
Richland, WA 99352

Chuck Dobbe
EG&G Idaho
Technical Support Annex
1580 Sawtelle
Idaho Falls, ID 83402

Kamiar Jamili
DP-62/FTN
Department of Energy
Washington, DC 20585

Sarbes Acharya
Department of Energy
NS-1/FORS
Washington, DC 20585

Lawrence Livermore National Lab(4)
Attn: George Greenly
Marvin Dickerson
Rolf Lange
Sandra Brereton
Livermore, CA 94550

Mr. Terry Foppe
Safety Analysis Engineering
Rocky Flats Plant
Energy Systems Group
Rockwell International Corp.
P.O. Box 464
Golden, CO 80401

U.S. Environmental Protection Agency(2)
Attn: Allen Richardson
Joe Logsdon
Office of Radiation Programs
Environmental Analysis Division
Washington, DC 20460

U.S. Department of Energy(2)
Attn: Ken Murphy (EH351)
Ed Branagan (EH332)
Washington, DC 20545

Michael McKay
Los Alamos National Labs
A-1, MS F600
P.O. Box 1663
Los Alamos, NM 87544

Mr. Robert Ostmeyer
U.S. Department of Energy
Rocky Flats Area Office
P.O. Box 928
Golden, CO 80402

Mr. Bruce Burnett
CDRH (HFZ-60)
U.S. Department of Health
& Human Services
Food & Drug Administration
5600 Fishers Lane
Rockville, MD 20857

Mr. Scott Bigelow
S-CUBED
2501 Yale, SE, Suite 300
Albuquerque, NM 87106

David Black
American Electric Power
1 Riverside Plaza
Columbus, OH 43215

Gerald Davidson
Fauske & Associates, Inc.
16 W 070 West 83rd Street
Burr Ridge, IL 60521

Keith Woodard
Pickard, Lower, and Garrick
Suite 730
1615 M. Street
Washington, DC 20056

Jim Mayberry
Ebasco Services
160 Chubb Ave.
Lyndhurst, NJ 07071

Mr. Mike Cheok
NUS
910 Clopper Road
Gaithersburg, MD 20878

Ken O'Brien
University of Wisconsin
Nuclear Engineering Dept.
153 Engineering Research Blvd.
Madison, WI 53706

Mr. Harold Careway
General Electric Co., M/C 754
175 Curtner Ave.
San Jose, CA 95129

Zen Mendoza
SAIC
5150 El Camino Real
Suite C31
Los Altos, CA 94022

Roger Blond
SAIC
20030 Century Blvd.
Suite 201
Germantown, MD 20874

John Luke
Florida Power & Light
P.O. Box 14000
Juno Beach, FL 33408

Duke Power Co. (2)
Attn: Duncan Brewer
Steve Deskevich
422 South Church Street
Charlotte, NC 28242

Mr. Griff Holmes
Westinghouse Electric Co.
Energy Center East
Bldg. 371
P.O. Box 355
Pittsburgh, PA 15230

Mr. Edward Warman
Stone & Webster Engineering Corp.
P.O. Box 2325
Boston, MA 02107

Mr. William Hopkins
Bechtel Power Corporation
15740 Shady Grove Road
Gaithersburg, MD 20877

R. Toossi
Physical Research, Inc.
25500 Hawthorn Blvd.
Torrance, CA 90505

Bill Eakin
Northeast Utilities
Box 270
Hartford, CT 06141

Ian Wall
Electric Power Research Institute
3412 Hillview Avenue
Palo Alto, CA 94304

Jim Meyer
Scientech
11821 Parklawn Dr.
Suite 100
Rockville, MD 20852

Ray Ng
NUMARC
1776 Eye St. NW
Suite 300
Washington, DC 20006-2496

Robert Gobel
Clark University
Center for Technology, Environment
and Development
950 Main St.
Worcester, MA 01610-1477

Ken Keith
TVA
W 20 D 201
400 West Summit Hill
Knoxville, TN 37092

Shengdar Lee
Yankee Atomic Electric Co.
580 Main St.
Bolton, MA 01740

Paul Govaerts
Studiecentrum voor Kernenergie
(SCK/CEN)
Boeretang, 200
B-2400 Mol
BELGIUM

S. Daggupaty
Environment Canada
4905 Dufferin Street
Downsview
Ontario, M3H 5T4
CANADA

Soren Thykier-Nielsen
Riso National Laboratory
Postbox 49
DK-4000 Roskile
DENMARK

Seppo Vuori
Technical Research Centre
of Finland
Nuclear Engineering Lab
Lonnrotinkatu 37
P.O. Box 169
SF-00181 Helsinki 18
FINLAND

Daniel Manesse
IPSN
Voite Postale 6
F-92265 Fontenay-auz-Roses CEDEX
FRANCE

Dr. J. Papazoglou
National Center for Scientific
Research
"DEMOKRITOS" Institute of
Nuclear Technology
P.O. Box 60228
GR-153 10 Aghia Paraskevi
Attikis
GREECE

ENEA/DISP (2)
Attn: Alvaro Valeri
Alfredo Bottino
Via Vitaliano Brancati, 48
00144 Roma EUR
ITALY

Mr. Hideo Matsuzuru
Tokai Research Establishment
Tokai-mur
Maka-gun
Ibaraki-ken, 319-11
JAPAN

Mr. Jan Van de Steen
KEMA Laboratories
Utrechtseweg, 310
Postbus 9035
NL-6800 ET Arnhem
THE NETHERLANDS

D. Eugenio Gil Lopez
Consejo de Seguridad Nuclear
Calle Justo Dorado, 11
e-28040 Madrid
SPAIN

Lennart Devell
Studsvik Nuclear
Studsvik Energiteknik AB
S-611 82 Nykoping
SWEDEN

Hanspeter Isaak
Abteilung Strahlenschutz
Hauptabeilung fur die Dicherheit
der Kernanlagen (HSK)
CH-5303 Wurenlingen
SWITZERLAND

M. Crick
Division of Nuclear Safety
IAEA
P.O. Box 100
A-1400 Vienna
AUSTRIA

Ulf Tveten
Environmental Physics Section
Institutt for Energiteknikk
Postboks 40
N-2007 Kjeller
NORWAY

M. K. Yeung
University of Hong Kong
Mechanical Engineering Dept.
Polfulam, HONG KONG

Leonel Canelas
New University of Lisbon
Quinta de Torre
2825 Monte de Caparica
PORTUGAL

Stephen Boult
Electrowatt Engineering Services (UK) Ltd.
Grandford House
16 Carfax, Horsham
West. Sussex RH12 1UP
ENGLAND

Nadia Soido Falcao Martins
Comissao Nacional de Energia Nuclear
R General Severianao 90 S/408-1
Rio de Janeiro
BRAZIL

Eli Stern
Isreal AEC Licensing Div.
P.O. Box 7061
Tel-Aviv 61070
ISRAEL

Der-Yu Hsia
Atomic Energy Council
67, Lane 144
Keelung Road, Section 4
Taipei, Taiwan 10772
TAIWAN

J. Western
Nuclear Electric plc
Barnett Way, Barnwood
GB-Gloucester GL4 7RS
UK

Dr. E. Lazo
OECD Nuclear Energy Agency
Le Seine Saint-Germain Bldg.
12, boulevard des Iles
F-92130 Issy-les-Moulineaux

Mr. Toshimitsu HOMMA
Environmental Assessment Lab.
JAERI - Tokai Research Establishment
Tokai-mura, Naka-gun
Ibaraki ken, 319-11 JAPAN

G.N. Kelly (150)
Commission of the European Communities
(DG XII/F/6 -ARTS 3/53
200, rue de la Loi
B-1049 Brussels
BELGIUM

S. Cole
Commission of the European Communities
(DG XII/D1 - SDME 3/49)
200, rue de la Loi
B-1049 Brussels
BELGIUM

G. Fraser
Commission of the European Communities
(DG XI/A/1 - WAG C3-353)
Bat Jean Monnet, Rue Alcide De Gasperi
L-2920 LUXEMBOURG

E. Lopez-Menchero
Commission of the Eureopean Communities
(DG XI - Safety in Nuclear Installations)
(DG XI - BU-5 6/140)
200, rue de la Loi
B-1049 Brussels
BELGIUM

F. Girardi, Head of Unit
Institute for the Environment
EC Joint Research Centre
I-21020 Ispra (Varese)

A. Besi
Institute for Systems Engineering
& Information Technology
EC Joint Research Centre
I-21020 Ispra (Varese)

Dr. Torben Mikkelsen
Dept. of Meteorology & Wind Energy
RISO National Laboratory
DK-4000 Roskilde
DENMARK

Dr. J. Ehrhardt
Kernforschungszentrum
Karlsruhe (KfK)
Institut fur Neutonenphysik
u. Reaktortechnik
Postfach 3640
D-76021 Karlsruhe 1,
GERMANY

Dr. E. Hofer
Gesellschaft fur Reaktorsicherheit
(GRS) mbH
Forschungsgelande
D-85764 OberschleiBheim

Dr. Peter Jacob
GSF - ISAR
Forschungszentrum fur
Umwelt und Gesundheit GmbH
Institut fur Strahlenschutz
Ingolstradter Landstr.1
D-85764 OberschleiBheim
GERMANY

Ir P.M. Roelsfsen
Netherlands Energy Research
Foundation, ECN
Westerduinweg 3
P.O. Box 1
NL-1755 LE Petten
The NETHERLANDS

Prof. Eduardo Gallego
Departamento de Ingenieria Nuclear
E.T.S. Ingenieros Industriales
Universidad Poltecnica de Madrid
C/Jose Gutierrez Abascal 2
F-28006 Madrid, SPAIN

Dr. U. Baverstam
Swedish National Institute of Radiation
Protection
Box 60204
S-10401 Stockholm, SWEDEN

Dr. Jacqueline Boardman
Safety & Reliability Directorate (SRD)
Environmental Risk Assessment Dept.
AEA Technology
Wigshaw Lane, Culchet
GB-Cheshire WA3 4NE
UNITED KINGDOM

Mrs. S. Haywood
National Radiological Protection Board
(NRPB)
Chilton, Didcot
GB-Oxon OX11 ORQ
UNITED KINGDOM

Mr. M. Herzeele
CEC Commission of the European
Communities
DG for the Environment
Nuclear Safety & Civil Protection
Centre Wagner C354
L-2920 Luxembourg
Luxembourg

Dr. R. Serro
Commission of the European Communities
DG XI - Environment & Nuclear Safety
Building Wagner
L-2920 Luxembourg
Luxembourg

M. J-L. Lamy
CEC Commission of the European
Communities
DG XI, BU-5 6/148
Rue de la Loi 200
Brussels 1049
Belgium

Mr. S.P. Arsenis
Industry Enviroment Unit,
Joint Research Centre
Institute for Systems,
Engineering & Informatics
I 21020 ISPRA (Va)
Italy

Mr. E. Lyck
C/O Dr. Torbin Mikkelsen
RISO National Laboratory
DK-4000 Roskilde
Denmark

Mr. P. Lofstrom
C/O Dr. Torbin Mikkelsen
RISO National Laboratory
DK-4000 Roskilde
Denmark

Mr. H.E. Jorgensen
C/O Dr. Torbin Mikkelsen
RISO National Laboratory
DK-4000 Roskilde
Denmark

dr. M. G. Delfini
VROM/DGMilieubeheer
Directie Stoffen, Veiligheid,
Straling/655
Afdeling Straling en Nucleaire
Veiligheid
Postbus 30945
2500 GX Den Haag
the NETHERLANDS

Dr. R. Brown
British Gas plc
Research & Technology Division
Group Leader Combustion Science Division
Midlands Reseach Station
Wharf Lane, Solihull
West Midlands B91 2JW
U.K.

Dr. J.A. Jones
NRPB National Radiological
Protection Board
Assessments Department
Chilton, Didcot
Oxon OX11 0RQ
U.K.

Dr. B. Joliffe
National Physical Laboratory
DQM
Queens Road
Teddington, Middlesex
U.K. TW11 0LW

Dr. Y. Belot
Commissariat a l'Energie Atomique
Institut de Protection et
Surete Nucleaire
DPEI/SERGD
BP 6
F-92265 Fontenay aux Roses Cedex
Frankrijk

Dr. K. Shrader-Frenchette
Environmental Sciences and Policy Program
Department of Philosophy
University of South Florida
4202 East Fowler Avenue, CPR 259
TAMPA, Florida 33620

dr. J. Slanina
Group Environmental Research Fossil Fuels
ECN
Postbus 1
1755 ZG Petten NH
the NETHERLANDS

dr. J. H. Duijzer
TNO/IMW
P.O. Box 6011
2600 JA DELFT
the NETHERLANDS

dr. G. Deville-Carelin
IPSN/CE
bat 159
13108 Saint Paul les Durance Cedex
la France

Mr. Ph. Berne
IPSN
DPEI/SERAC/LESI
38041 GRENOBLE Cedex
la France

Dr. W. Biesiot
IVEM/Energie en Milieukunde
RUGroningen
Nijenborgh 4
9747 AG GRONINGEN
the Netherlands

<u>USNRC</u>

Denwood Ross, AEOD
MS-MNBB 3701

Themis Speis, RES
MS-NL/S 007

Brian Sheron, RES/DSR
MS-NL/S 008

Joseph Murphy, RES/DSIR
MS-NL/S 007

Mark Cunningham, RES/PRAB
MS-NL/S 372

Mat Taylor, EDO
MS-17G21

Bill Morris, RES/DRA
MS-NL/S 007

Zoltan Rosztoczy, RES/ARB
MS-NL/S 169

Donald Cool, RES/RPHEB
MS-NL/S 139

Warren Minners, RES/DSIR
MS-NL/S 007

Thomas King, RES/DSR
MS-NL/S 007

William Beckner, NRR/PRAB
MS-10E4

Frank Congel, NRR/DREP
MS-10E2

Charles Willis, NRR/DREP
MS-10E2

Richard Barrett, NRR/PD3-2
MS-13D1

Lemoine Cunningham, NRR/PRPB
MS-10DR

Ashok Thadani, NRR/DST
MS-8E2

William Russell, NRR/ADT
MS-12G18

Stewart Ebneter
Regional Administrator, RGN II
U.S.N.R.C.
101 Marietta St., Suite 2900
Atlanta, GA 30323

John Martin
Regional Administrator, RGN III
U.S.N.R.C.
801 Warrenville Rd.
Lisle, IL 60532-4351

James Glynn, RES/PRAB
MS-NL/S372

Thomas Martin
Regional Administrator RGN I
U.S.N.R.C.
475 Allendale Rd.
King Prussia, PA 19406-1415

Harold VanderMolen, RES/PRAB
MS T9F31

Christiana Lui (10), RES/PRAB
MS T9F31

Les Lancaster, RES/PRAB
MS T9F31

Chris Ryder, RES/PRAB
MS T9F31

Michael Jamgochia, RES/SAIB
MS-NL/S 324

Leonard Soffer, RES/SAIB
MS-NL/S 324

John Ridgely, RES/SAIB
MS-NL/S 324

Shlomo Yaniv, RES/RPHEB
MS-NL/S 139

Robert Kornasiewicz, RES/DE
MS-NL/S 007

Joe Levine, NRR/PRPB
MS-10D4

Robert Palla, NRR/PRAB
MS-10E4

Tom McKenna, AEOD/IRB
MS-MNBB 3206

Internal

MS0491 Norm Grandjean, 12333
MS0736 N. R. Ortiz, 6400
MS0747 A. L. Camp, 6412
MS0748 L. A. Miller, 6413
MS0748 M. L. Young, 6413
MS0748 F. T. Harper, 6413
MS0748 T. D. Brown, 6413
MS1141 L. F. Restrepo, 6453
MS1093 Hong-Nian Jow, 7714
MS9018 Central Technical Files, 8523-2
MS0899 Technical Library, 13414 (7)
MS0619 Technical Publications, 13416 (1)

NRC FORM 335
(2-89)
NRCM 1102,
3201, 3202

U.S. NUCLEAR REGULATORY COMMISSION

BIBLIOGRAPHIC DATA SHEET

(See instructions on the reverse)

1. REPORT NUMBER (Assigned by NRC, Add Vol., Supp., Rev., and Addendum Numbers, if any.)

NUREG/CR-6244
EUR 15855EN
SAND94-1453
Vol. 2

2. TITLE AND SUBTITLE

Probabilistic Accident Consequence Uncertainty Analysis

Dispersion and Deposition Uncertainty Assessment

Appendices A and B

3. DATE REPORT PUBLISHED

MONTH	YEAR
January	1995

4. FIN OR GRANT NUMBER

L2294

5. AUTHOR(S)

F. T. Harper (SNL), L. H. J. Goossens (TUD), R. M. Cooke (TUD), S. C. Hora (UHH), M. L. Young (SNL), J. Päsler-Sauer (KfK), L. A. Miller (SNL), B. Kraan (TUD), C. H. Lui (USNRC), M. D. McKay (LANL), J. C. Helton (ASU), J. A. Jones (NRPB)

6. TYPE OF REPORT

Technical

7. PERIOD COVERED (Inclusive Dates)

8. PERFORMING ORGANIZATION - NAME AND ADDRESS (If NRC, provide Division, Office or Region, U.S. Nuclear Regulatory Commission, and mailing address; if contractor, provide name and mailing address.)

Sandia National Laboratories
Albuquerque, NM 87185-0748

9. SPONSORING ORGANIZATION - NAME AND ADDRESS (If NRC, type "Same as above"; if contractor, provide NRC Division, Office or Region, U.S. Nuclear Regulatory Commission, and mailing address.)

Division of Systems Technology
Office of Nuclear Regulatory Research
U.S. Nuclear Regulatory Commission
Washington, DC 20555-0001

Commission of the European Communities
DG XII and XI
200, rue de la Loi
B-1049 Brussels

10. SUPPLEMENTARY NOTES

11. ABSTRACT (200 words or less)

The development of two new probabilistic accident consequence codes, MACCS and COSYMA, was completed in 1990. These codes estimate the consequences from the accidental releases of radiological material from hypothesized accidents at nuclear installations. In 1991, the U.S. Nuclear Regulatory Commission and the Commission of the European Communities began co-sponsoring a joint uncertainty analysis of the two codes. The ultimate objective of this joint effort was to systematically develop credible and traceable uncertainty distributions for the respective code input variables. Because of the magnitude and expense required to complete a full-scale consequence uncertainty analysis, a trial study was performed to evaluate the feasibility of such a joint study by initially limiting efforts to the dispersion and deposition code input variables. A formal expert judgment elicitation and evaluation process was identified as the best technology available for developing a library of uncertainty distributions for these consequence parameters. This report focuses on the methods used in and results of this trial study.

12. KEY WORDS/DESCRIPTORS (List words or phrases that will assist researchers in locating the report.)

uncertainty analysis, atmospheric dispersion, atmospheric deposition, accident consequence analysis, nuclear accident analysis, probabilistic analysis, expert elicitation, MACCS, COSYMA, consequence uncertainty analysis

13. AVAILABILITY STATEMENT

Unlimited

14. SECURITY CLASSIFICATION

(This Page)

Unclassified

(This Report)

Unclassified

15. NUMBER OF PAGES

16. PRICE